

1987

Part I Total Synthesis Of (+,-)-hirsutene Part Ii Photochemical And Photophysical Properties Of N-benzoylindoles

Bimsara Wijesekara Disanayaka

Follow this and additional works at: <https://ir.lib.uwo.ca/digitizedtheses>

Recommended Citation

Disanayaka, Bimsara Wijesekara, "Part I Total Synthesis Of (+,-)-hirsutene Part Ii Photochemical And Photophysical Properties Of N-benzoylindoles" (1987). *Digitized Theses*. 1593.
<https://ir.lib.uwo.ca/digitizedtheses/1593>

This Dissertation is brought to you for free and open access by the Digitized Special Collections at Scholarship@Western. It has been accepted for inclusion in Digitized Theses by an authorized administrator of Scholarship@Western. For more information, please contact tadam@uwo.ca, wlsadmin@uwo.ca.



National Library
of Canada

Bibliothèque nationale
du Canada

Canadian Theses Service

Services des thèses canadiennes

Ottawa, Canada
K1A 0N4

CANADIAN THESES

THÈSES CANADIENNES

NOTICE

The quality of this microfiche is heavily dependent upon the quality of the original thesis submitted for microfilming. Every effort has been made to ensure the highest quality of reproduction possible.

If pages are missing, contact the university which granted the degree.

Some pages may have indistinct print especially if the original pages were typed with a poor typewriter ribbon or if the university sent us an inferior photocopy.

Previously copyrighted materials (journal articles, published tests, etc.) are not filmed.

Reproduction in full or in part of this film is governed by the Canadian Copyright Act, R.S.C. 1970, c. C-30.

AVIS

La qualité de cette microfiche dépend grandement de la qualité de la thèse soumise au microfilmage. Nous avons tout fait pour assurer une qualité supérieure de reproduction.

S'il manque des pages, veuillez communiquer avec l'université qui a conféré le grade.

La qualité d'impression de certaines pages peut laisser à désirer, surtout si les pages originales ont été dactylographiées à l'aide d'un ruban usé ou si l'université nous a fait parvenir une photocopie de qualité inférieure.

Les documents qui font déjà l'objet d'un droit d'auteur (articles de revue, examens publiés, etc.) ne sont pas microfilmés.

La reproduction, même partielle, de ce microfilm est soumise à la Loi canadienne sur le droit d'auteur, SRC 1970, c. C-30.

**THIS DISSERTATION
HAS BEEN MICROFILMED
EXACTLY AS RECEIVED**

**LA THÈSE A ÉTÉ
MICROFILMÉE TELLE QUE
NOUS L'AVONS REÇUE**

PART I

TOTAL SYNTHESIS OF (±)-HIRSUTENE

PART II

PHOTOCHEMICAL AND PHOTOPHYSICAL PROPERTIES OF
N-BENZOYLINDOLES

by

Bimsara W. Disanayaka

Department of Chemistry

Submitted in partial fulfillment
of the requirements for the degree of
Doctor of Philosophy

Faculty of Graduate Studies
The University of Western Ontario
London, Canada

February 1987

© Bimsara W. Disanayaka 1987

Permission has been granted to the National Library of Canada to microfilm this thesis and to lend or sell copies of the film.

The author (copyright owner) has reserved other publication rights, and neither the thesis nor extensive extracts from it may be printed or otherwise reproduced without his/her written permission.

L'autorisation a été accordée à la Bibliothèque nationale du Canada de microfilmer cette thèse et de prêter ou de vendre des exemplaires du film.

L'auteur (titulaire du droit d'auteur) se réserve les autres droits de publication; ni la thèse ni de longs extraits de celle-ci ne doivent être imprimés ou autrement reproduits sans son autorisation écrite.

ISBN 0-315-36061-5

ABSTRACT

PART ONE

The synthesis of polycyclic compounds usually requires various synthetic approaches to construct the required carbon skeletons. This thesis describes a sequence which leads to the preparation of the tricyclo[6.3.0.0^{2,6}]undecane skeleton found in a number of physiological fungal metabolites. The key steps in this sequence are photochemical cycloaddition of the enol of 5,5-dimethylcyclohexane-1,3-dione to a cyclopentene, followed by intramolecular reductive coupling of the dione with a low valence titanium compound. A formal synthesis of the fungal metabolite hirsutene is described using this procedure. The route involves the photochemical [2 + 2] cycloaddition of 5,5-dimethylcyclohexane-1,3-dione to 2-methyl-2-cyclopentenol, followed by the treatment of the silylated photoadducts with a low valence titanium reagent resulting in intramolecular reductive coupling to give the hirsutene carbon skeleton with the desired regiochemistry. Desilylation with fluoride ion, followed by sequential catalytic hydrogenation and Jones' oxidation completed the formal synthesis by yielding the norketone, obtained by ozonolysis of hirsutene.

PART TWO

This part of the thesis describes the studies performed to determine the nature, and the reactive species in the photoannulation reaction of N-benzoylindole with cyclopentene which was found to proceed via a triplet state. The existence of a solvent polarity dependent charge-transfer triplet excited state, in addition to a solvent polarity independent triplet state, was proposed to rationalize the rate constant values obtained for N-benzoylindole from a combination of dilution, quenching and triplet counting experiments.

The fluorescence properties of various N-carbonyl substituted indoles 142a and 156-162 were examined. The N-benzoylindole derivatives 142a and 158-160 were shown to fluoresce weakly at anomalously long wavelengths and were dependent on the polarity of the solvent used. It was concluded that the initially formed singlet excited state is non-emissive and can relax to an intramolecular charge-transfer state which is weakly fluorescent. The solvent induced shifts in the wavelength of the fluorescence emission correlate well with Lippert equation. A poor correlation with the empirical $E_T(30)$ solvent polarity parameter was observed.

ACKNOWLEDGEMENTS

The author wishes to express his sincere gratitude and appreciation to Dr. A.C. Weedon for his endless encouragement, assistance and direction provided throughout the course of this work. Many thanks are also in order to the other members of the faculty, especially to Professor P. de Mayo and Dr. A. Siemiarczuk for their expert advice and assistance. Dr. T. Hudlicky is thanked for providing the spectral data of (\pm)-hirsutene.

Many thanks are also extended to the staff and my fellow colleagues for their assistance, companionship and friendship, in and out of the laboratory; most notably, K. Roach, D. Wong, D. Lombardo and D. Hastings.

The author also wishes to thank Mrs. Anne Leait and D. Fraser for their invaluable assistance in the preparation of this thesis.

This Work is Dedicated

to My

Dear Mother and Father

TABLE OF CONTENTS

	Page
CERTIFICATE OF EXAMINATION	ii
ABSTRACT	111
ACKNOWLEDGEMENTS	v
TABLE OF CONTENTS	vii
LIST OF TABLES	ix
LIST OF FIGURES	xi
LIST OF SCHEMES	xiv
PART I: TOTAL SYNTHESIS OF (±)-HIRSUTENE	1
CHAPTER 1: INTRODUCTION	2
1.1 Introduction	2
1.2 Structural Elucidation of Hirsutene	4
1.3 Biosynthesis of Hirsutene	8
1.4 Synthesis of Hirsutene	13
CHAPTER 2: MODEL STUDIES LEADING TO THE TOTAL SYNTHESIS OF (±)-HIRSUTENE	35
2.1 Proposed Synthetic Route	35
2.2 Model Study with the Use of Cyclopentene as the Alkene	46
2.3 Model Study with the Use of 2-Cyclopentene-1-ol as the Alkene	50
CHAPTER 3: TOTAL SYNTHESIS OF (±)-HIRSUTENE	69
3.1 Synthesis of 2-Methyl-2-cyclopentene-1-one ...	69
3.2 Formal Synthesis of (±)-Hirsutene	78
CHAPTER 4: EXPERIMENTAL	94
4.1 EXPERIMENTAL	94
PART II: PHOTOCHEMICAL AND PHOTOPHYSICAL PROPERTIES OF N-BENZOYLINDOLES	115
CHAPTER 5: MECHANISM OF PHOTOANNEALING REACTION OF N-BENZOYLINDOLE WITH CYCLOPENTENE	116
5.1 Introduction	116
5.2 General Properties of N-Benzoylindole	127
5.3 Structure and Stereochemistry of Cycloadduct Products	133

	Page
CHAPTER 5 (Cont'd):	
5.4 Multiplicity of the Excited State Involved in the Cycloaddition Reaction of N-Benzoylindole with Alkenes	138
5.5 Derivation of the Kinetic Equations	141
5.6 Quenching Studies	145
5.7 Stern-Volmer Quenching Experiments	146
5.8 Variation of Quantum Yield of Cycloaddition with Substrate Concentration	149
5.9 Evaluation of the Rate Constant for Self-Quenching	157
5.10 Consideration of the Possibility of Involvement of an Exciplex in the Cycloaddition Mechanism	161
5.11 Possibility of the Existence of a Charge-Transfer Triplet State	170
5.12 Measurement of the Intersystem Crossing Quantum Yields of N-Benzoylindoles	183
CHAPTER 6: CHARGE-TRANSFER FLUORESCENCE OF SOME N-BENZOYLINDOLES	192
6.1 Introduction	192
6.2 Charge-Transfer Fluorescence	204
6.3 Intramolecular Charge-Transfer Model	205
6.4 Fluorescence Properties of 6H-Indole[2,1-a]	207
6.5 Fluorescence Quantum Yields	208
6.6 Correlation of the Fluorescence Emission with the Lippert Equation	210
6.7 Correlation of Fluorescence Emission of NBI with $E_T(30)$ Values	218
CHAPTER 7: EXPERIMENTAL	223
REFERENCES	243
VITA	255

LIST OF TABLES

Table	Description	Page
PART I		
I	^{13}C nmr chemical shifts of C-1 and C-8 of compounds (82), (83) and (90)	54
II	^{13}C nmr chemical shifts of C-1 and C-8 of compounds (82), (102) and (103)	64
III	^{13}C nmr chemical shifts of methine, carbons of compounds (104a), (105a) and (105b)	66
IV	^{13}C nmr chemical shifts of compounds (102), (103), (120) and (121)	81
V	^{13}C nmr chemical shifts of compounds (104), (105), (122) and (123)	85
PART II		
VI	^1H nmr and ^{13}C nmr chemical shifts of the cyclobutane ring of compound (152)	136
VII	Rate constants for the reactivity of radicals with alkenes	161
VIII	Photophysical properties of compounds (142a) and (157-162)	177
IX	Wavelengths of absorption and fluorescence emission for compounds (142a) and (157-162) in various solvents	202
X	Substitution effect on N-benzoylindole charge separation	206
XI	Quantum yields of fluorescence for compounds (142a) and (157-162) in various solvents	211

Table	Description	Page
XII	Dipole moment changes derived from the Lippert plots for compounds (142a), (158) and (160)	214
XIII	Stern-Volmer quenching data for the NBI-cyclopentene reaction	234
XIV	Quantum yields of photooxidation of NBI at various cyclopentene concentrations	235
XV	Triplet counting experimental data for the compounds (142a) and (157-161)	238

LIST OF FIGURES

Figure	Description	Page
PART II		
1	Absorption spectra of compounds (142a), (159) and indole	128
2a	Absorption spectra of compounds (158), (159) and (160)	129
2b	Absorption spectra of compounds (161) and (162)	130
3	Phosphorescence spectrum of NBI	134
4	Quenching of NBI-cyclopentene reaction with 1,3-cyclohexadiene	147
5	Plot of the reciprocal of Stern-Volmer gradients of Figure 4 against the cyclopentene concentration	148
6	Effect of cyclopentene concentration on the quantum yield of photoaddition of NBI and cyclopentene	151
7	Plot of the reciprocal of quantum yield of photoaddition of NBI and cyclopentene vs the reciprocal of cyclopentene concentration	152
8	Plot of the reciprocal of quantum yield of photoaddition of NBI and cyclopentene vs the NBI concentration	160
9	Energy levels of the singlet excited states of NBI	174
10	Energy levels of excited states of NBI in polar and non-polar solvents	174
11	Variation of the T_1 (C.T.) state of NBI in solvents of different polarity	179

Figure	Description	Page
12	Variation of S_1 (C.T.) state of NBI in polar and non-polar solvents	181
13	Variation in quantum yield of sensitized trans-cis isomerization of piperylene as a function of pentadiene concentration for sensitizers (142a), (157), (158) and (160)	186
14	Variation in quantum yield of 0.027 M NBI sensitized trans-cis isomerization of piperylene in acetonitrile as a function of pentadiene concentration	187
15	Variation in quantum yield of 0.027 M NBI sensitized trans-cis isomerization of piperylene in methylene chloride as a function of pentadiene concentration	188
16	Variation in quantum yield of sensitized trans-cis isomerization of piperylene in benzene as a function of pentadiene concentration for sensitizers (159) and (161)	189
17	Absorption and double fluorescence of 3-methyl-4-cyano-N,N-dimethylaniline in several solvents	196
18	Corrected and normalized fluorescence quantum spectra of (167) and (168) in n-hexane and acetonitrile	196
19	Normalized fluorescence spectra of compound (142a) (10^{-5} M)	203
20	Energy levels of excited NBI	209
21	Lippert plot for compound (142a) in non-chlorinated solvents	215
22	Lippert plot for compound (142a) in chlorinated solvents	216
23	Plot of energy of the $S_0 \rightarrow S_1$ transition in kcal/mol of NBI against the solvent $E_T(30)$ value	219

Figure

Description

Page

24

Plots of energy of the $S_0 \rightarrow S_1$ transition in kcal/mol of NBI against the solvent $E_T(30)$ value (full circles) and solvent $E_T(30)$ value against the Lippert Δf_n (open circles)

220

LIST OF SCHEMES

Scheme	Description	Page
PART I		
1	Biogenesis of humulene-derived sesquiterpenoids	3
2	Transformation of protoilluden into hirsutene	7
3	Biogenesis of hirsutic acid through rearrangement of a farnesyl precursor	9
4	^{13}C labelling patterns of hirsutic acid	10
5	The use of doubly-labelled [1,2- ^{13}C]-acetate to establish the biosynthetic pathway to the hirsutene skeleton	12
6	Synthesis of hirsutene using the Cope rearrangement as the key step	14
7	Synthesis of hirsutene using the Claisen rearrangement as the key step	15
8	Synthesis of hirsutene using a β -enolate rearrangement as the key step	17
9	Synthesis of hirsutene using intramolecular cyclopropanation rearrangement of dienic diazo ketones	18
10	Skeletal rearrangement of a tricyclic 6-4-5 fused ring system	19
11	Synthesis of hirsutene using photochemical cycloaddition as the key step	20
12	Synthesis of hirsutene utilizing an arene-olefin photochemical cycloaddition as the main step	21
13	Synthesis of hirsutene using a stepwise metathesis of Diels-Alder adducts	23

Scheme	Description	Page
14	Electrochemical transformation of (48) to hirsutene	24
15	Conversion of (51) to hirsutene	25
16	Retro-synthetic analysis of hirsutene	27
17	Synthesis of hirsutene using an intramolecular nitron-olefin cycloaddition as the key step	28
18	Synthesis of optically pure hirsutene	28
19	Synthesis of hirsutene using an organoselenium mediated cyclization reaction as the key step	31
20	Synthesis of hirsutene using a tandem radical cyclization method	32
21	Synthesis of hirsutene using an organosilicon mediated reaction as the key step	33
22	Proposed route to hirsutene	36
23	Photochemical cycloaddition of an enolized 1,3-diketone to an alkene	37
24	A generalized mechanistic scheme	39
25	Reductive dimerization of (80)	43
26	Generation of pinacol from acetone	44
27	Mechanism of deoxygenation of pinacols	45
28	Model study with cyclopentene as the alkene	48
29	Model study with cyclopentene-2-ol as the alkene	51
30	Retro-aldol ring opening of (89)	53
31	Conversion of compounds (90) and (89) to (104) and (105)	63
32	Conversion of compound (104) to (107)	68

Scheme	Description	Page
33	Schematic representation of the synthesis of 2-methyl-2-cyclopentene-1-one starting from diethyladipate	70
34	Formation of allylic hydroperoxides	72
35	Synthesis of 2-methyl-2-cyclopentene-1-ol using a photo-oxygenation method	73
36	Proposed synthetic route to 2-methyl-2-cyclopentene-1-one	72
37	The catalytic effect of N-methylaniliniumtrifluoroacetate	76
38	Attempted synthesis of compounds (118) and (119)	78
39	Retro-aldol ring opening of compound (116)	80
40	Synthesis of compounds (122) and (123)	82
41	Acid catalyzed migration of the methyl group in compound (124)	89
42	Conversion of compound (124) to (\pm)-hirsutene	91
PART II		
43	Mechanism of photocyanoethylation of indole derivatives	119
44	Synthesis of benzazepine derived from N-benzoylindole	122
45	Regio- and stereoselectivities in the photocycloaddition reaction of N-benzoylindole derivatives	123
46	Structural elucidation of N-benzoylindole photocycloaddition products	124
47	Photoreaction of N-methylindole to dimethyl acetylenedicarboxylate	125

Scheme	Description	Page
48	Schematic representation of N-benzoylindole photocycloaddition with an alkene	140
49	General scheme for decay of the triplet biradical	156
50	Schematic representation of N-benzoylindole photocycloaddition with an alkene, involving an exciplex	162

The author of this thesis has granted The University of Western Ontario a non-exclusive license to reproduce and distribute copies of this thesis to users of Western Libraries. Copyright remains with the author.

Electronic theses and dissertations available in The University of Western Ontario's institutional repository (Scholarship@Western) are solely for the purpose of private study and research. They may not be copied or reproduced, except as permitted by copyright laws, without written authority of the copyright owner. Any commercial use or publication is strictly prohibited.

The original copyright license attesting to these terms and signed by the author of this thesis may be found in the original print version of the thesis, held by Western Libraries.

The thesis approval page signed by the examining committee may also be found in the original print version of the thesis held in Western Libraries.

Please contact Western Libraries for further information:

E-mail: libadmin@uwo.ca

Telephone: (519) 661-2111 Ext. 84796

Web site: <http://www.lib.uwo.ca/>

PART I

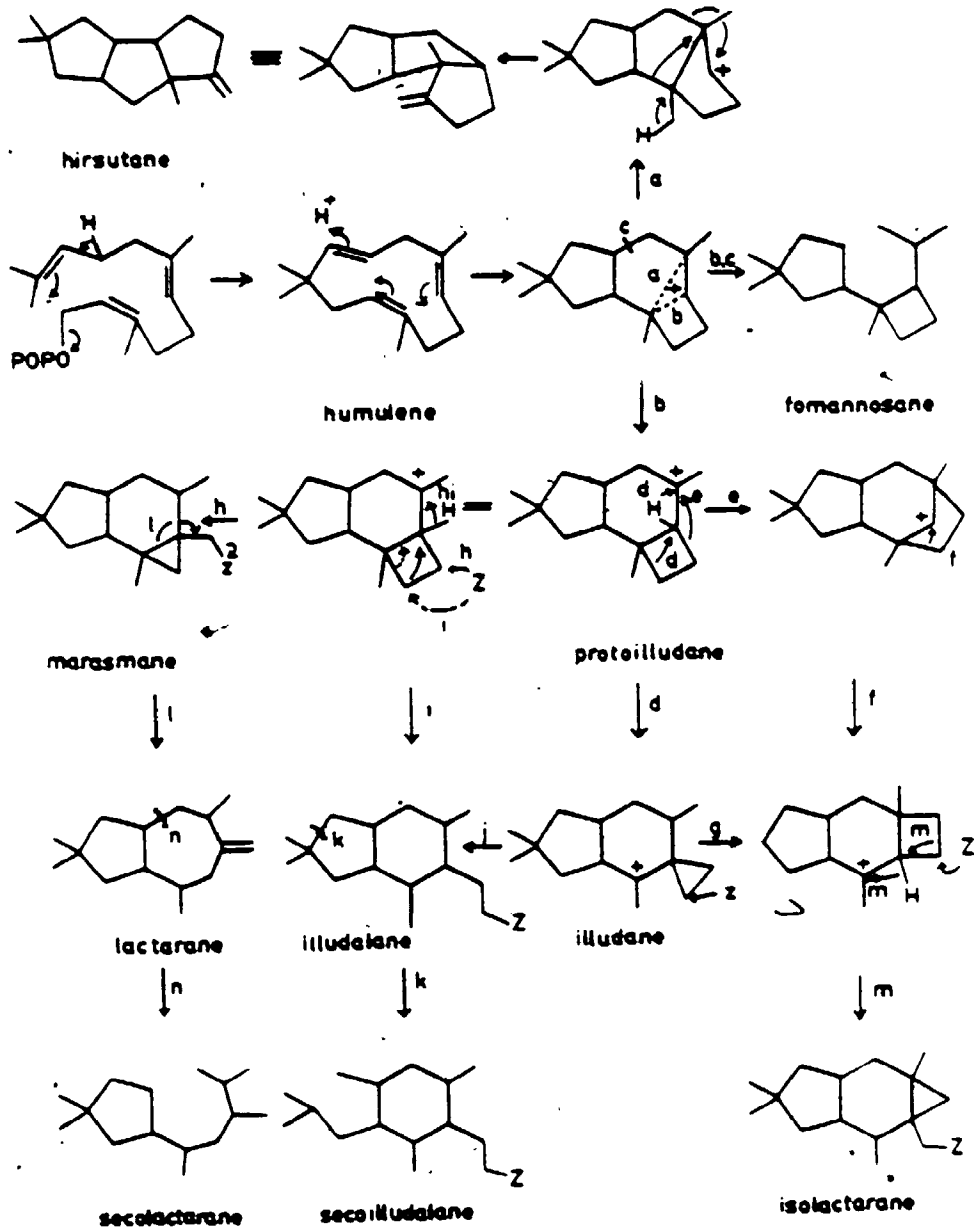
TOTAL SYNTHESIS OF (±)-HIRSUTENE

CHAPTER 1
INTRODUCTION

1.1 INTRODUCTION

Sesquiterpenoids are defined as the group of C_{15} compounds derived by the assembly of three isoprenoid units and they are found in many forms of living systems of which higher plants are the principal member. The historical background to sesquiterpenoids can be traced back to the early nineteenth century, but the foundation stone of terpenoid chemistry in general was laid by Ruzicka with the proposal of the Biogenetic Isoprene Rule. There has been a considerable amount of work done in the field of sesquiterpenoids during the past 25 years and undoubtedly one of the major highlights has been the development of outstanding syntheses.

In dealing with the difficult problems of skeletal construction and stereochemical control associated with some of these syntheses, new methods have been used which have equipped the synthetic organic chemist with a new array of armaments for future use. Hirsutene, shown in Scheme 1, possesses a tricyclo[6.3.0.0^{2,6}]undecane carbon skeleton with cis-anti-cis stereochemistry, and is a sesquiterpene which is derived from humulene.



SCHEME 1

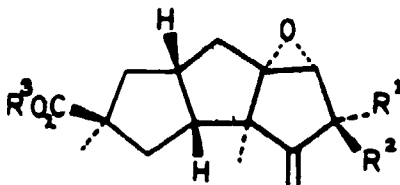
The biogenesis of the humulene-derived sesquiterpenoids comprises 11 different skeleton types which are shown in Scheme 1. Humulene, which arises by cyclization of farnesyl pyrophosphate, can be further cyclized to the hirsutane skeleton (path a) or to the protoilludane skeleton (path b). Rearrangement of a protoilludane cation may give rise to the illudane skeleton (path d), the sterpurane skeleton (paths e, f or d, g) or the marasmane skeleton (path h). Bond cleavage of a suitable protoilludane intermediate leads to the formannosane skeleton (path b, c) or to the illudalane skeleton (paths i or d, j), whereas further bond cleavage of an illudalane gives the secoilludalane skeleton (path k). Rearrangement of a marasmane leads to the lactarane skeleton (path l), while rearrangement of a sterpurane gives rise to an isolactarane skeleton (path m). Bond cleavage of a lactarane (path n) gives the secolactaranes. The results of several biosynthetic investigations are consistent with this general scheme.¹

1.2 STRUCTURAL ELUCIDATION OF HIRSUTENE

In 1947, Heatley² reported that a fungus, first encountered as a chance contaminant on an agar plate and identified as *stereum hirsutum*, produced a number of acidic metabolites, some of which had antibiotic properties. In 1965 Scott et al^{3a-c} re-examined these products and by a

combination of x-ray and chemical studies established the structure of the major metabolite, hirsutic acid.

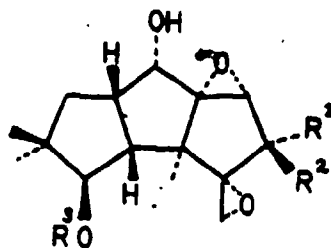
Ir and nmr analysis of hirsutic acid ($C_{15}H_{20}O_4$) (1) showed the presence of $CH-OH$, $C=CH_2$, $-COOH$ and $2CH_3$ groups. Oxidation of methyl hirsutate (2) with manganese dioxide in chloroform afforded an α,β -unsaturated ketone which proved to be an *exo*-methylene cyclopentanone. Reduction of methyl hirsutate by lithium aluminum hydride gave a triol in which two hydrogen atoms had been added, in addition to those required for reduction of the ester function. Acetylation of the triol formed a diacetate. From this information it was concluded that the fourth oxygen of hirsutic acid was present as an epoxide which was reduced to yield a tertiary alcohol.



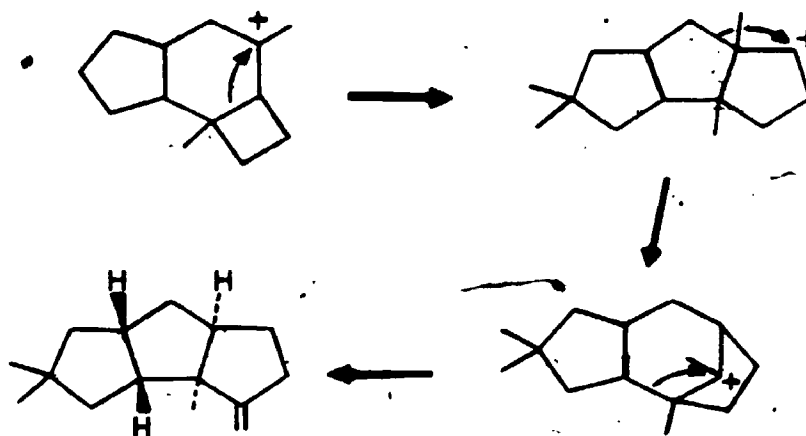
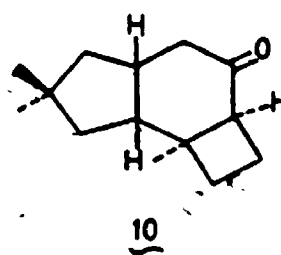
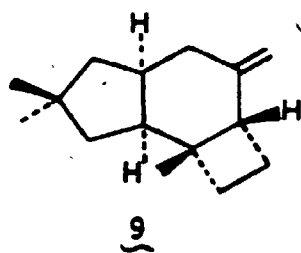
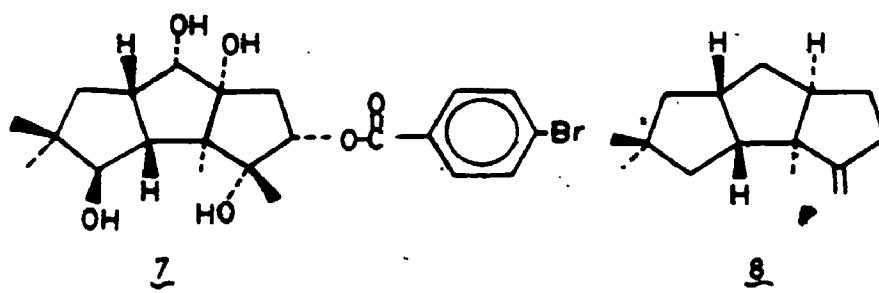
- (1) $R^1 = OH, R^2 = R^3 = H$
 (2) $R^1 = OH, R^2 = H, R^3 = CH_3$
 (3) $R^1 = OH, R^2 = H, R^3 = pBrC_6H_4COCH_2$
 (11) $R^1, R^2 = O, R^3 = H$

The complete structure of hirsutic acid (1) was established by x-ray diffraction studies of its *p*-bromophenacyl ester (3).^{3c}

Japanese mushrooms, *Coriolus consors*, produce the sesquiterpenes coriolin (4),^{4,5} coriolin B (5) and coriolin C (6). These sesquiterpenes possess a hirsutane-type carbon skeleton and exhibit antibiotic and antitumor activity. The structures of these compounds were assigned based upon the results of chemical degradation, spectroscopic analysis and biogenetic considerations. The absolute configuration of coriolin (4) was determined by x-ray analysis of its hexahydro-*p*-bromobenzoate derivative (7).



- | | | |
|---|----------------------------|-------------------------|
| 4 | $R^1, R^2 = O,$ | $R^3 = H$ |
| 5 | $R^1 = OH, \quad R^2 = H,$ | $R^3 = COC_7H_{15}$ |
| 6 | $R^1, R^2 = O,$ | $R^3 = COCHOHC_6H_{13}$ |



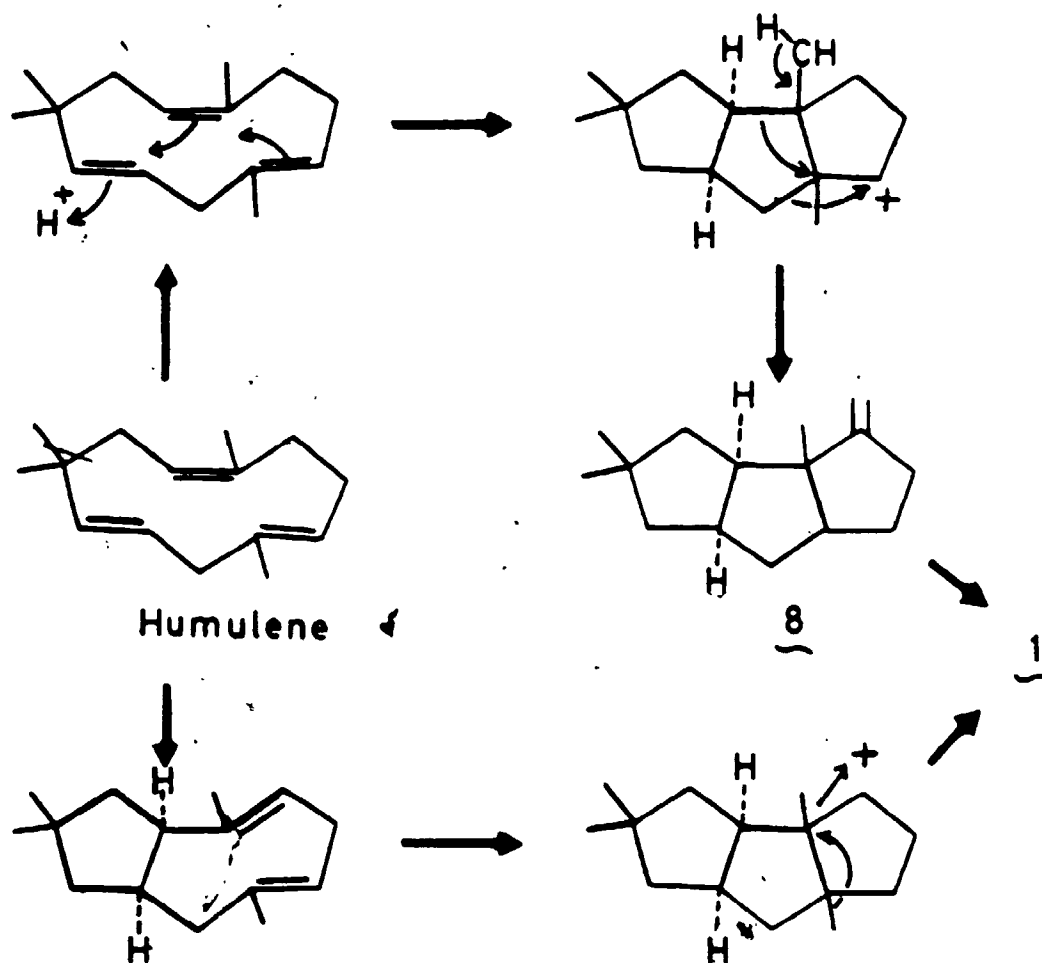
SCHEME 2

In 1976 Nozoe et al⁶ isolated hirsutene (8) from the extract of *Coriolus consors*. Hirsutene has been proposed as a biogenetic precursor of coriolin (4),⁷ and the presence of humulene and caryophyllene in trace amounts in the hirsutene containing extracts of *C. consors* further supports the hypothesis that the hirsutane-type sesquiterpenes arise via a farnesyl precursor.^{7,8}

Matsumoto et al^{9,10} have described the involvement of a sequence of rearrangements depicted in Scheme 2 in the transformation of Δ^7 -protoilludene (9) and 7-keto-13-norprotoilludane (10) into compounds possessing the hirsutene (8) skeleton. This process involved a triple skeletal rearrangement (Scheme 2) as the key step.

1.3 BIOSYNTHESIS OF HIRSUTENE

Early work on the biosynthesis of the hirsutene sesquiterpenes was hindered by the inability of subsequent workers to isolate hirsutic acid from cultures of *S. hirsutum* using the procedure originally reported by Heatley et al² in 1947. However, the isolation of hirsutanes from *Stereum complicatum*¹¹ and *C. consors*¹² removed this obstacle. In 1967 Scott et al¹³ put forward a scheme (Scheme 3) for the biogenesis of hirsutic acid (1) through a rearrangement of a farnesyl precursor via humulene and hirsutene (8).



SCHEME 3

The terpenoid nature of these metabolites was demonstrated by the incorporation of [2- ^{14}C]-mevalonic acid into [^{14}C]-hirsutic acid. In 1974 Mellows et al.¹⁴ put forward experimental evidence to support the theory of enzymic construction of the hirsutene skeleton from

farnesyl pyrophosphate. He used ^{13}C labelling patterns of hirsutic acid⁷ and complicatic acid¹¹ as evidence for the biosynthetic pathway. In this study sodium [1- ^{13}C]-acetate and sodium [2- ^{13}C]-acetate were fed in parallel to cultures of *S. complicatum*. The proton decoupled ^{13}C nmr of the compounds isolated from the cultures exhibited the labelling pattern as shown in Scheme 4.

The results show consistency with a mechanism involving an initial formation of a humulene-type precursor (12) from farnesyl pyrophosphate and proceeding through the carbonium ion intermediate (14). Several routes for the formation of (14) from (12) satisfy the labelling pattern in hirsutic acid (1); pathway (a) involves an abridged form of route (b) as suggested by Scott et al,¹³ and (c) involves intermediacy of the protoilludane precursor (19) which was shown to be involved in the biosynthesis of the illudins¹⁵ and marasmic acid.¹⁶

In another study doubly-labelled [1,2- ^{13}C]-acetate¹⁷ was used to establish the biosynthetic pathway to the hirsutane skeleton. The ^{13}C nmr spectrum of coriolins obtained from [1,2- ^{13}C]-acetate fed *C. consors* showed the presence of six intact acetate units in the hirsutane carbon skeleton (Scheme 5).

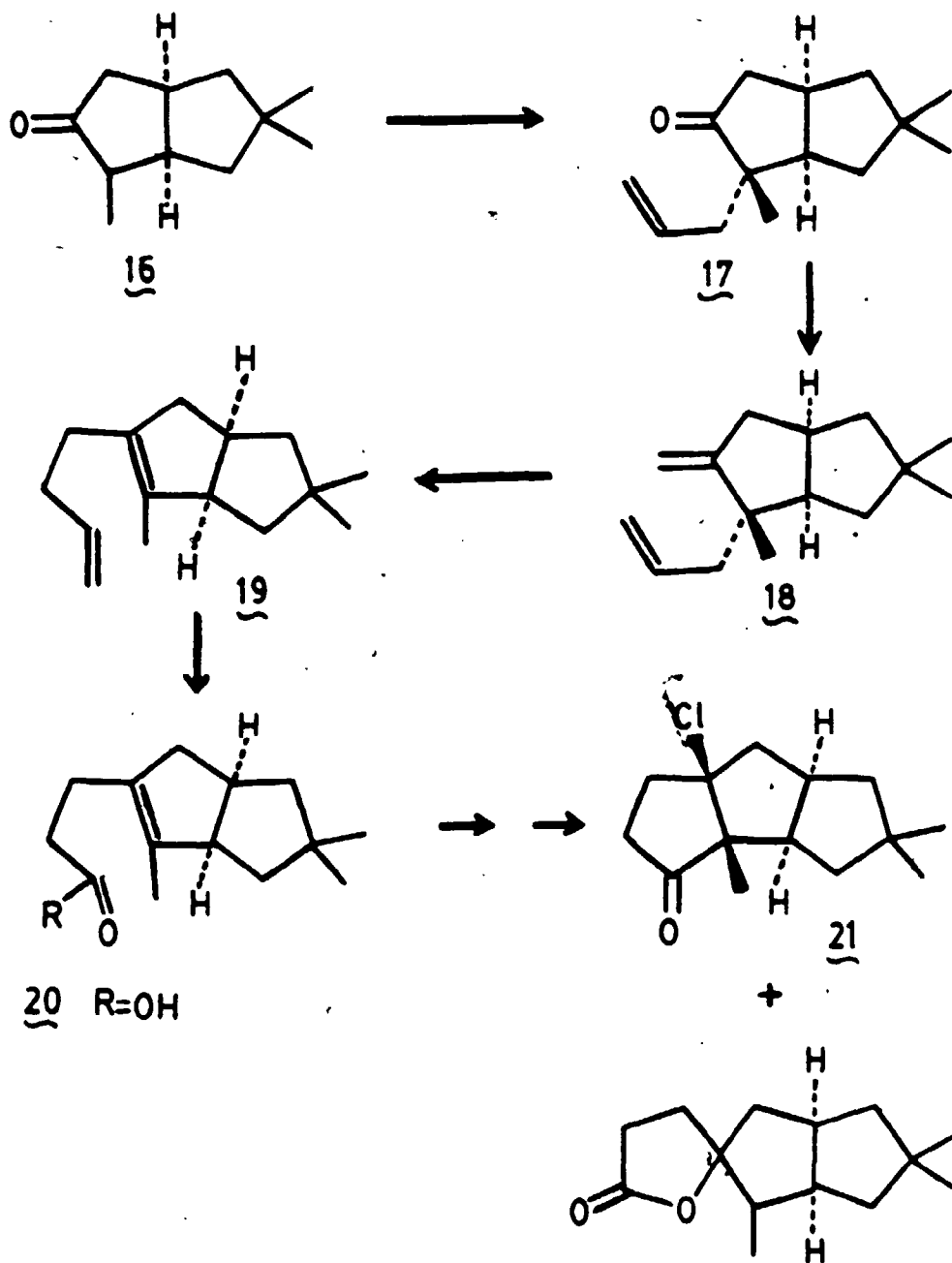
From humulene to the tricyclic coriolin metabolites three cyclization routes are possible. Each involves the initial protonation of humulene at C-10 followed by formation of the C-2-C-9 and C-3-C-7 bonds.

The resulting C-3 cationic species could then react further by one of these pathways to give, after a series of Wagner-Meerwein shifts, the coriolin ring system. The only route with [1,2-¹³C]-acetate as a substrate that retains the six intact acetate units is path a (Scheme 5), which clearly established the biosynthetic pathway for coriolin.

1.4 SYNTHESIS OF HIRSUTENE

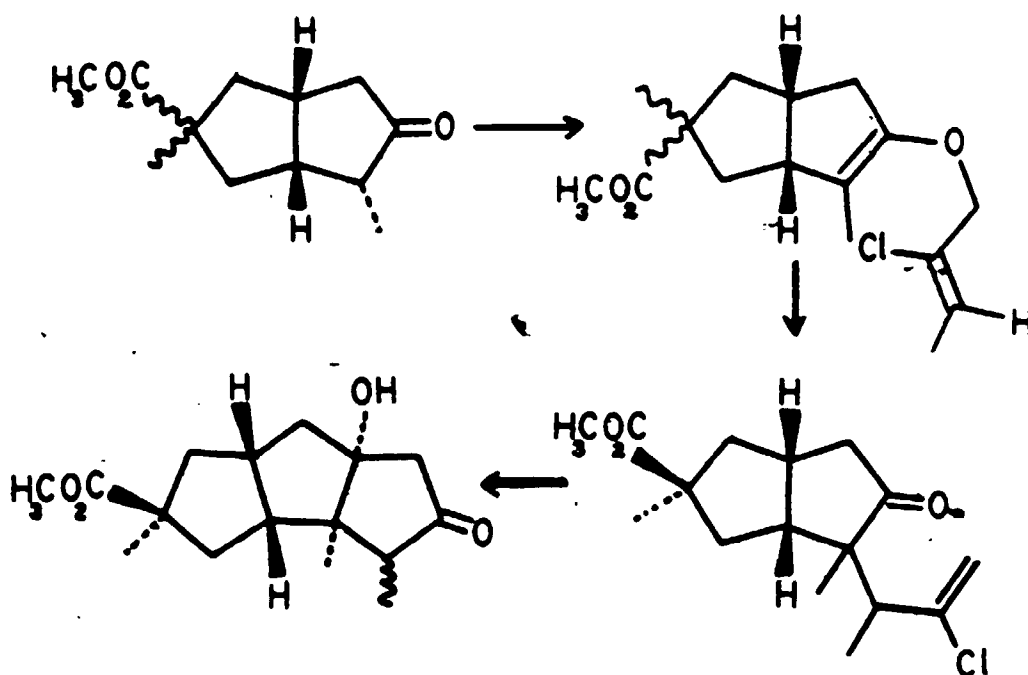
Since the discovery of the linearly fused tricyclopentanoid carbon skeleton of hirsutanes by Scott et al^{3a-c} in 1965, synthetic chemists around the world have shown a keen interest in synthesizing hirsutanes and their efforts have resulted in development of a wide variety of interesting new synthetic methods.

One of the key problems in the synthesis of hirsutene is the creation of the tricyclopentanoid carbon skeleton with the correct stereochemistry. Several successful methods which involve different approaches have been reported. Nozoe et al⁶ used the Cope rearrangement (Scheme 6) of the bicyclooctane derivative (18) to give (19); selective cleavage of the terminal olefin of (19) yielded (20), and subsequent cyclization of the acid chloride derivative of (20) gave the chloroketone (21) with the desired carbon skeleton and stereochemistry. Reductive removal of chlorine and Wittig methylenation then provided hirsutene (8). Lansbury et al^{18,19} have reported two synthetic approaches leading to hirsutic acid (1) using the



SCHEME 6

Claisen rearrangement as a key step. Both syntheses lead to a known degradation product of hirsutic acid and involve alkylation of a suitably functionalized bicyclic octanone, Claisen rearrangement, hydrolysis and aldol cyclization (e.g. Scheme 7).

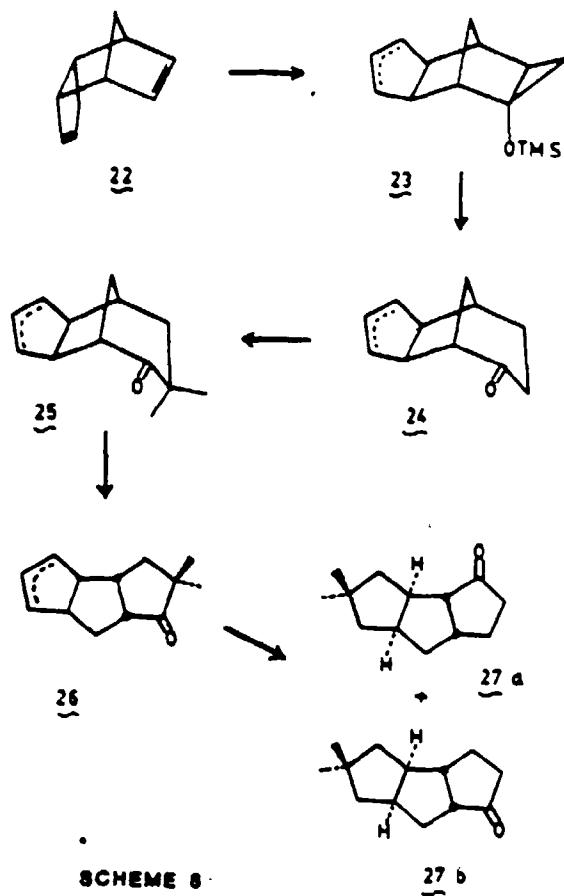


SCHEME 7

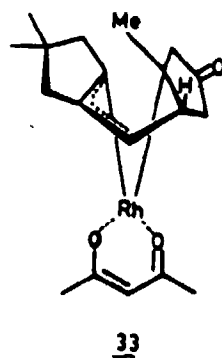
Stothers et al^{20a,b} used a β -enolate rearrangement as the key step to generate the ring system and the desired stereochemistry of hirsutene. A major feature of this synthesis is that the stereochemistry at three of the four chiral centers is established essentially at the outset of the sequence and the constraints are such that the

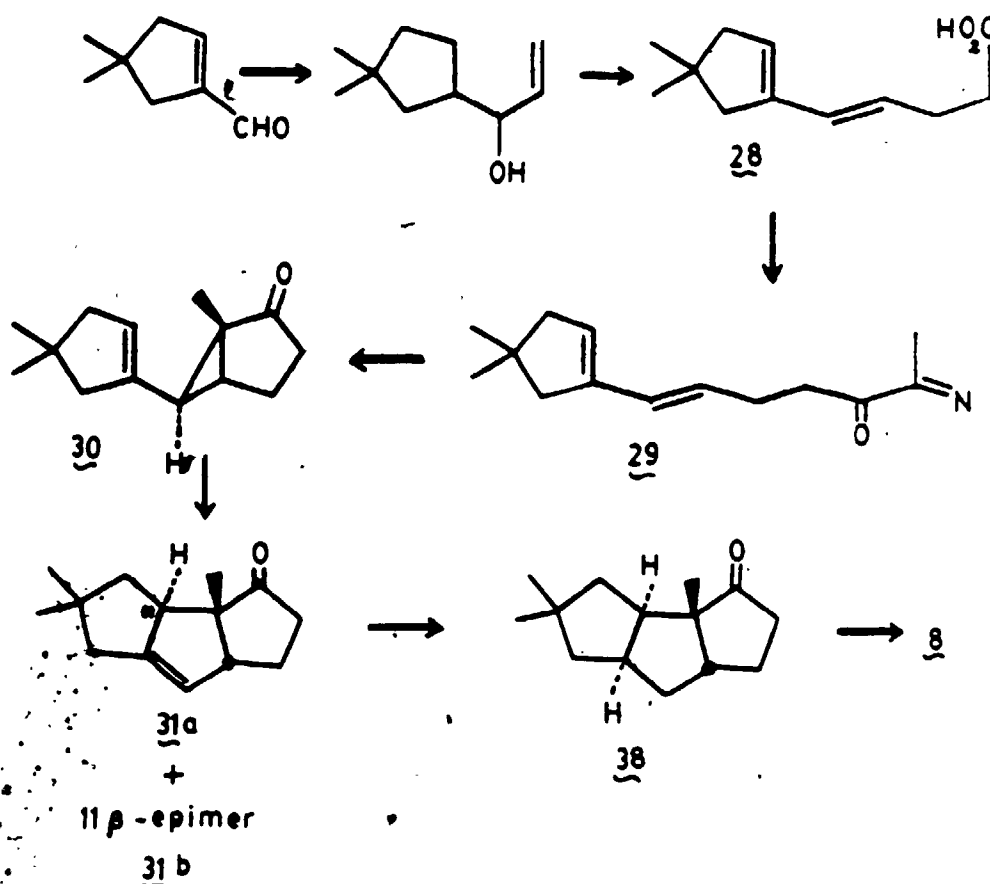
β -enolate rearrangement specifically generates the correct configuration at the fourth center exclusively (Scheme 8). The ring expansion of the starting material, dicyclopentadiene (22), was achieved by ketonization of the cyclopropoxide derived from (23) and this was followed by the skeletal rearrangement of (25) through a β -enolate to yield (26), which was eventually converted to (27), an intermediate in a published synthesis of hirsutene.^{21a-c} Hudlicky et al.^{22a,b} have described an intermolecular cyclopropanation rearrangement sequence of dienic diazo ketones which provides facile access to bicyclo[3.3.0]octanes, and this has been applied to the synthesis of hirsutene (Scheme 9).

The cyclopropane (30) was generated as a single stereoisomer by refluxing a dilute solution of (29) in benzene containing 10 mol % of $\text{Ca}(\text{acac})_2$. Pyrolysis of (30) by flash evaporation of the sample through a properly conditioned Vycor tube at reduced pressure gave (31b). This rearrangement was found to be sensitive to slight variations in pyrolytic conditions which could alter the ratio of diastereoisomers (31a) and (31b). Enhanced stereoselectivity was observed using $(\text{C}_2\text{H}_4)_2\text{Rh}(\text{acac})$; this catalyzed the bond reorganization of (30) to the *cis-anti-cis* fused epimer (31a) preferentially, which suggests an intermediate of type (33) is involved and determines final stereochemical outcome.



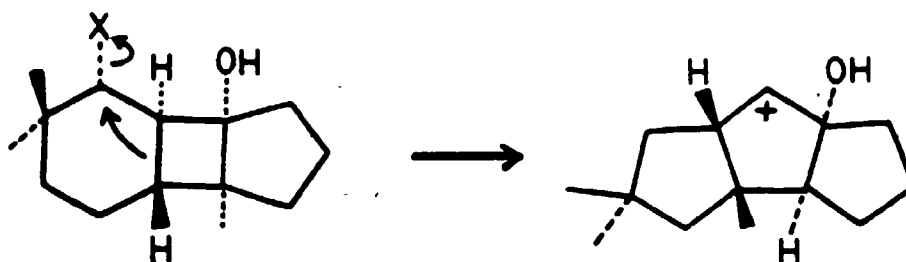
SCHEME 8





SCHEME 9

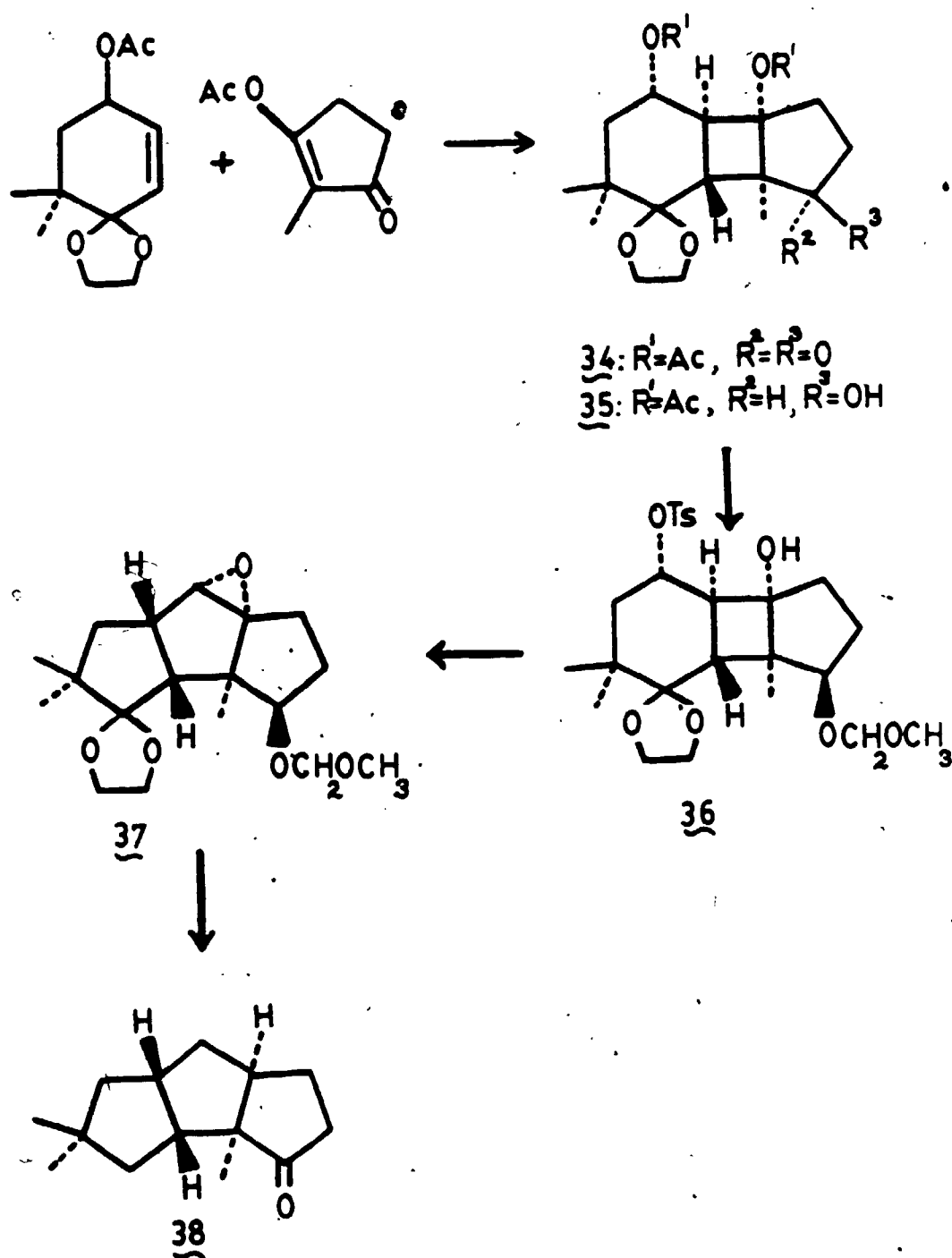
Photochemistry is another discipline organic chemists have applied to obtain carbon skeletons and stereochemistries which are not easily accessible by ground state organic synthetic methods. Tatsuta et al^{23a,b} have reported a stereocontrolled synthesis of hirsutene and coriolin which provides a new entry to the *cis-anti-cis*-tricyclo[6.3.0.0^{2,6}]undecane series. The key step in this approach is a skeletal rearrangement of a tricyclic 6-4-5 fused ring to a *cis-anti-cis*-tricyclic 5-5-5 fused ring (Scheme 10).



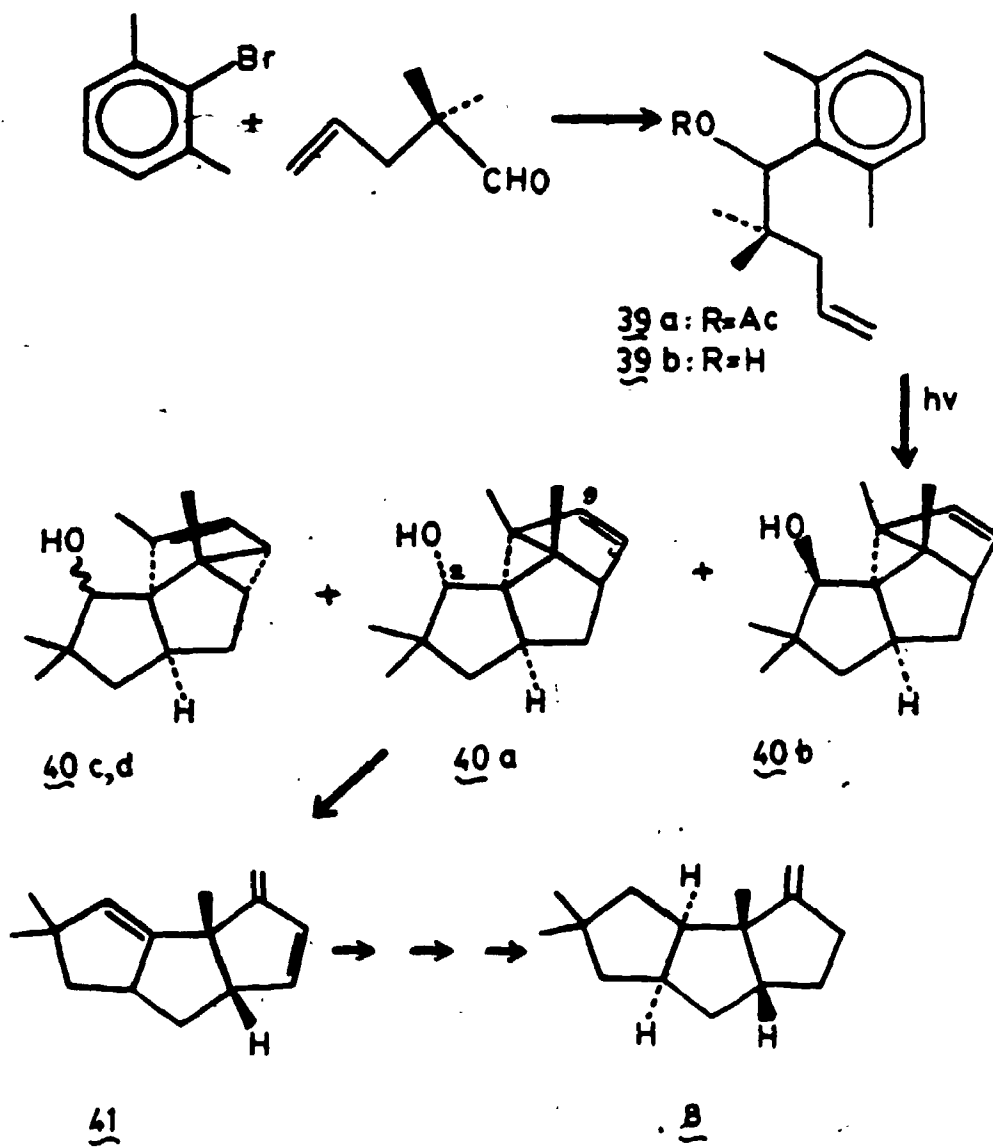
SCHEME 10

Photochemical cycloaddition of the ethylene ketal of 4-acetoxy-6,6-dimethyl-2-cyclohexanone with 2-methylcyclopentane-1,3-dione enol acetate (Scheme 11) gave the starting tricyclic compound (34). This was shown to be a head-to-head adduct of *cis,trans* stereochemistry which was determined by x-ray crystallographic analysis of the *p*-bromobenzoate of the corresponding alcohol (35). Heating compound (36) with potassium carbonate in aqueous acetone resulted in the skeletal rearrangement to give (37), which had the desired *cis-anti-cis* stereochemistry confirmed by x-ray analysis. The synthesis of hirsutene was completed by functional group modification of (37) to form norketone (38) which had previously been transformed to hirsutene.⁶

Wender et al^{24a,b} have utilized arene-olefin photochemical cycloaddition to provide a facile entry into the linear tricyclopentanoid skeleton (Scheme 12). Photolysis of (39a) gave, after deacetylation of the crude



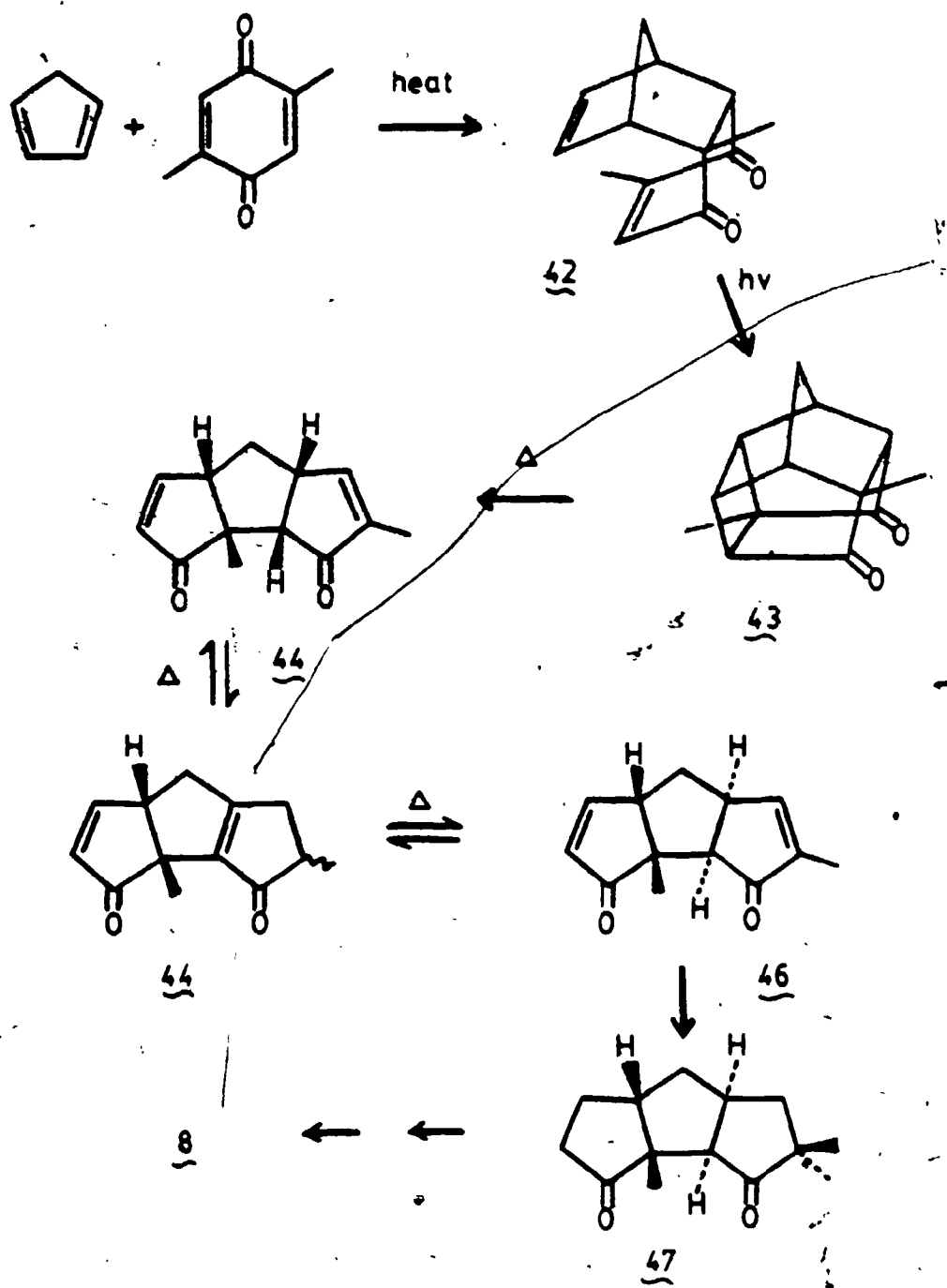
SCHEME 11



SCHEME 12

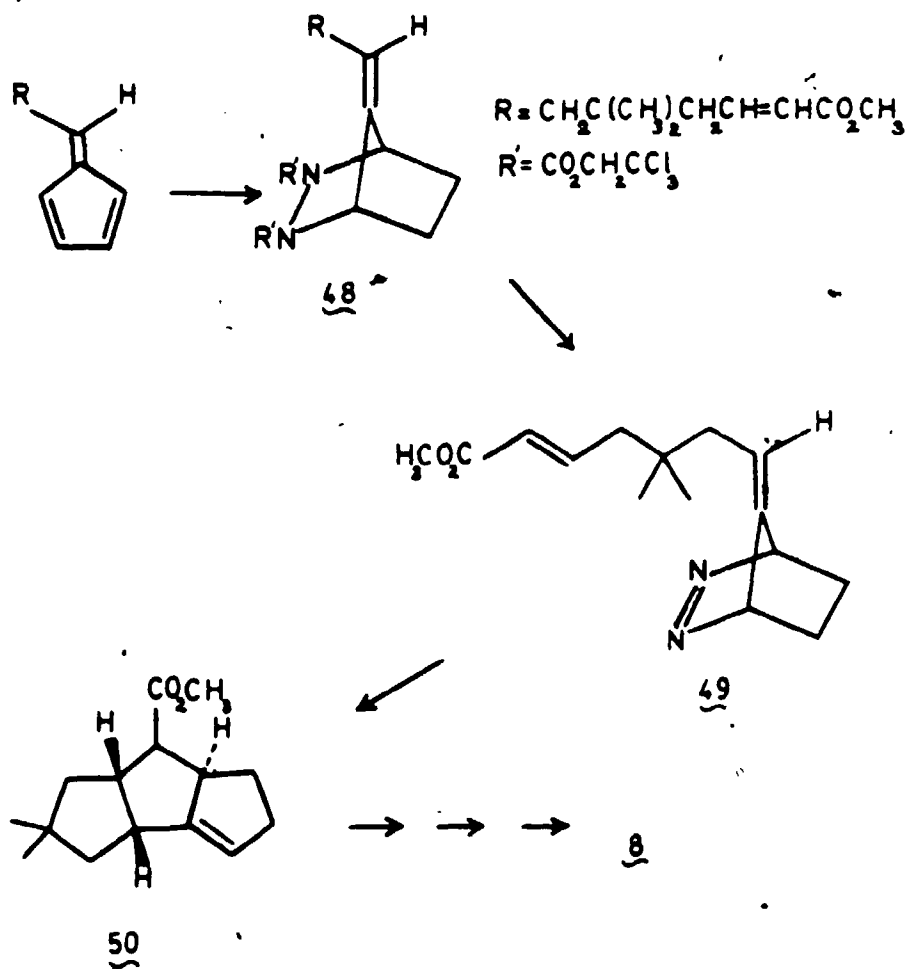
mixture, four identifiable cycloadducts (40a-d) resulting from "meta" cycloaddition of the alkene to the benzene ring. Photolysis of the unprotected alcohol precursor (39b) gave identified products but in somewhat reduced yield. The next step in this synthesis is cyclopropane cleavage which could be induced by development of electron deficiency at C-2 or C-9 (see 40a). One might also expect allylic stabilization involving the olefin at C-8,C-9 to provide a bias towards the desired cleavage of bond a, which indeed was the case. Thus acid catalyzed dehydration and rearrangement of (40a) gave (41). Suitable manipulation of (41) completed the synthesis of hirsutene.

Mehta et al^{25a,b} have proposed a general protocol for the synthesis of linear triquinane natural products. The key element in this approach was a stepwise (photothermal) metathesis of Diels-Alder adducts derived from 1,3-cyclopentadiene and a p-benzoquinone (Scheme 13). This methodology was applied to the total synthesis of hirsutene, capnellene and coriolin. Diels-Alder reaction of cyclopentadiene and 2,5-dimethyl-p-benzoquinone gives (42) in high yields, which acquires the cis-syn-cis-tricyclopentanoid frame (44) by employing light and heat as the reagents. Thermal equilibration of (44) by refluxing in benzylbenzoate gives the required cis-anti-cis system (46); catalytic hydrogenation followed by regioselective alkylation furnished (47) which was eventually converted to hirsutene.



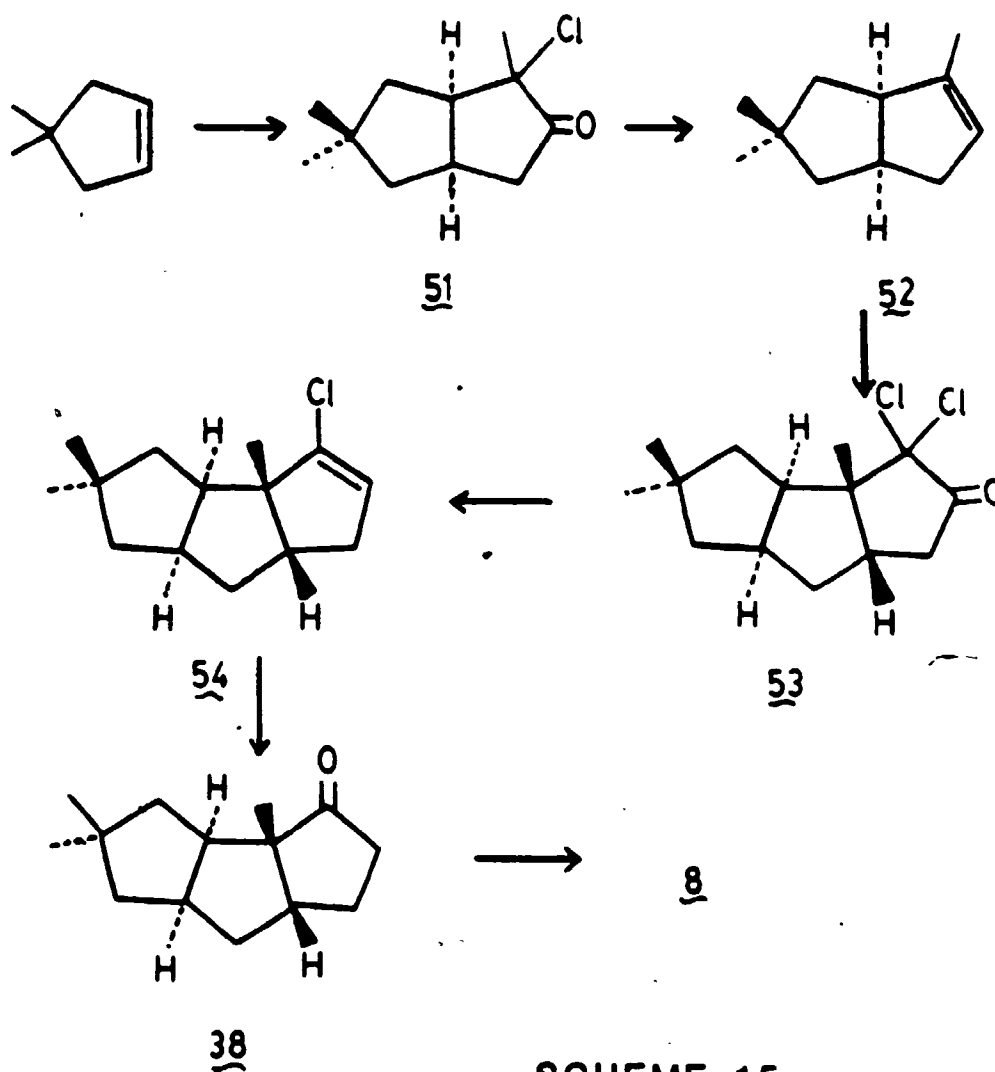
SCHEME 13

Little et al^{21a-c} employed a regiospecific and highly stereoselective intramolecular diyl trapping reaction to construct the required linearly fused tricyclopentanoid ring system of hirsutene. In this process two new carbon-carbon bonds are formed with creation of two five-membered rings, and the stereoselective generation of four asymmetric centers with proper relative stereochemistry for further elaboration to hirsutene (Scheme 14).



SCHEME 14

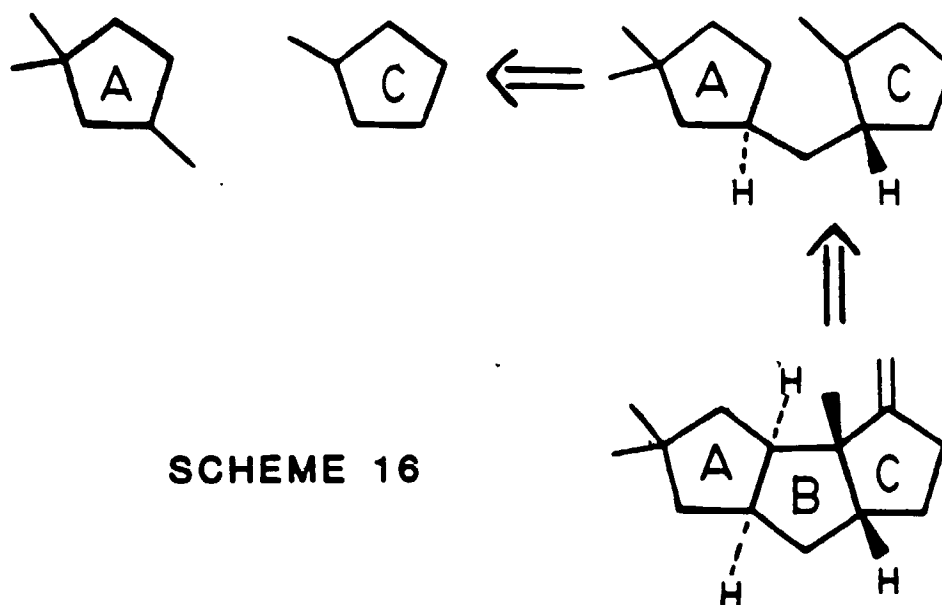
The bicyclic azo compound (49) was prepared by a Diels-Alder addition of a fulvene and bis-trichloroethylazodicarboxylate, followed by selective hydrogenation to give the bicyclic bis-carbamate (48). Electrochemical transformation of (48) gives the bicyclo azo compound (49), and thermolysis gives the tricyclopentanoid ring-containing system (50), which is then converted to hirsutene by a series of steps.



SCHEME 15

Greene²⁶ has reported a three carbon annulation procedure which has been applied to the synthesis of hirsutene (Scheme 15). Bicyclochloroketone (51) was prepared by thermal (2+2) cycloaddition of dimethylcyclopentene with methylchloroketene followed by ring expansion with diazomethane. Compound (51) was then reduced to chlorohydrin followed by transformation to an olefin (52) utilizing chromous perchlorate. The third ring was stereo- and regioselectively joined to (52) using dichloroketene to produce a dichlorocyclobutanone. Sequential treatment with diazomethane, sodium borohydride and chromous perchlorate gave the vinyl chloride (54). Acid hydrolysis gave the known ketone (38) which has previously been transformed to hirsutene.⁶ Funk et al^{27a} used a strategy to synthesize hirsutene, in which two substituted cyclopentanes were joined together to create the central five-membered ring and thus complete the triquinane skeleton ($A + C \rightarrow AC \rightarrow ABC$) (Scheme 16).

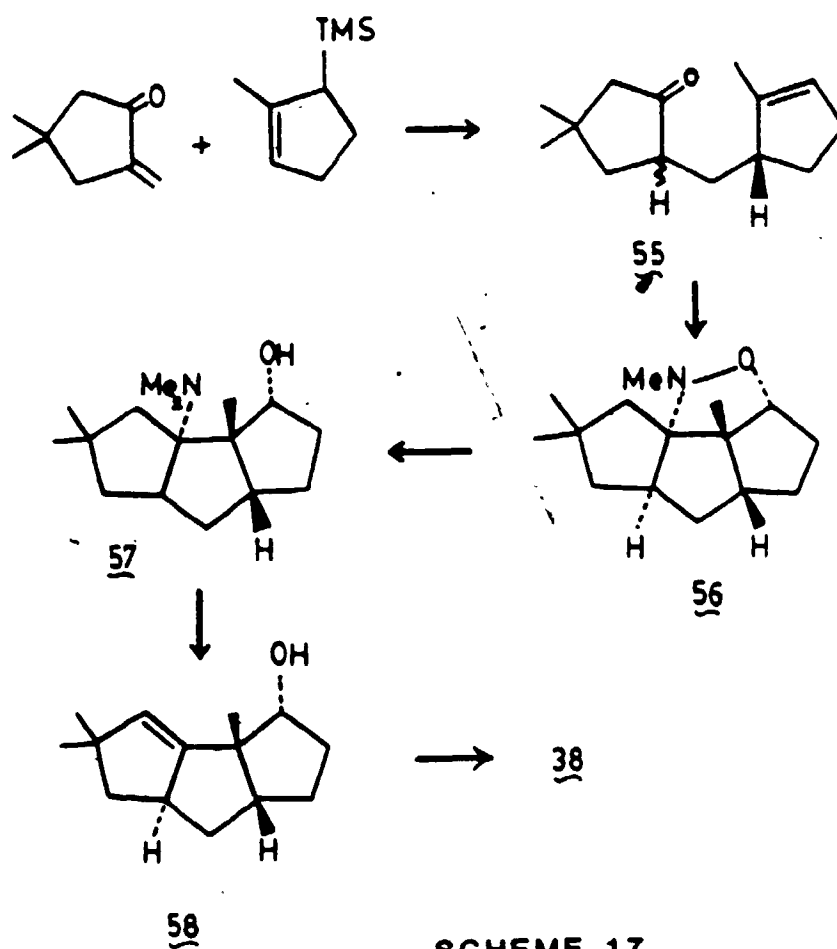
The correct stereochemistry of the hirsutene skeleton is obtained by an intramolecular nitron-olefin cycloaddition which gives exclusively the anti isomer. The nitron precursor (55) was prepared by inverse addition of a mixture of 4,4-dimethyl-2-methylenecyclopentanone and $TiCl_3$ to 3-trimethylsilyl-2-methylcyclopentene in CH_2Cl_2 (Scheme 17). Treatment of (55) with $MeNH_2$ and sodium ethoxide gave (56) via cycloaddition of the intermediate nitron.



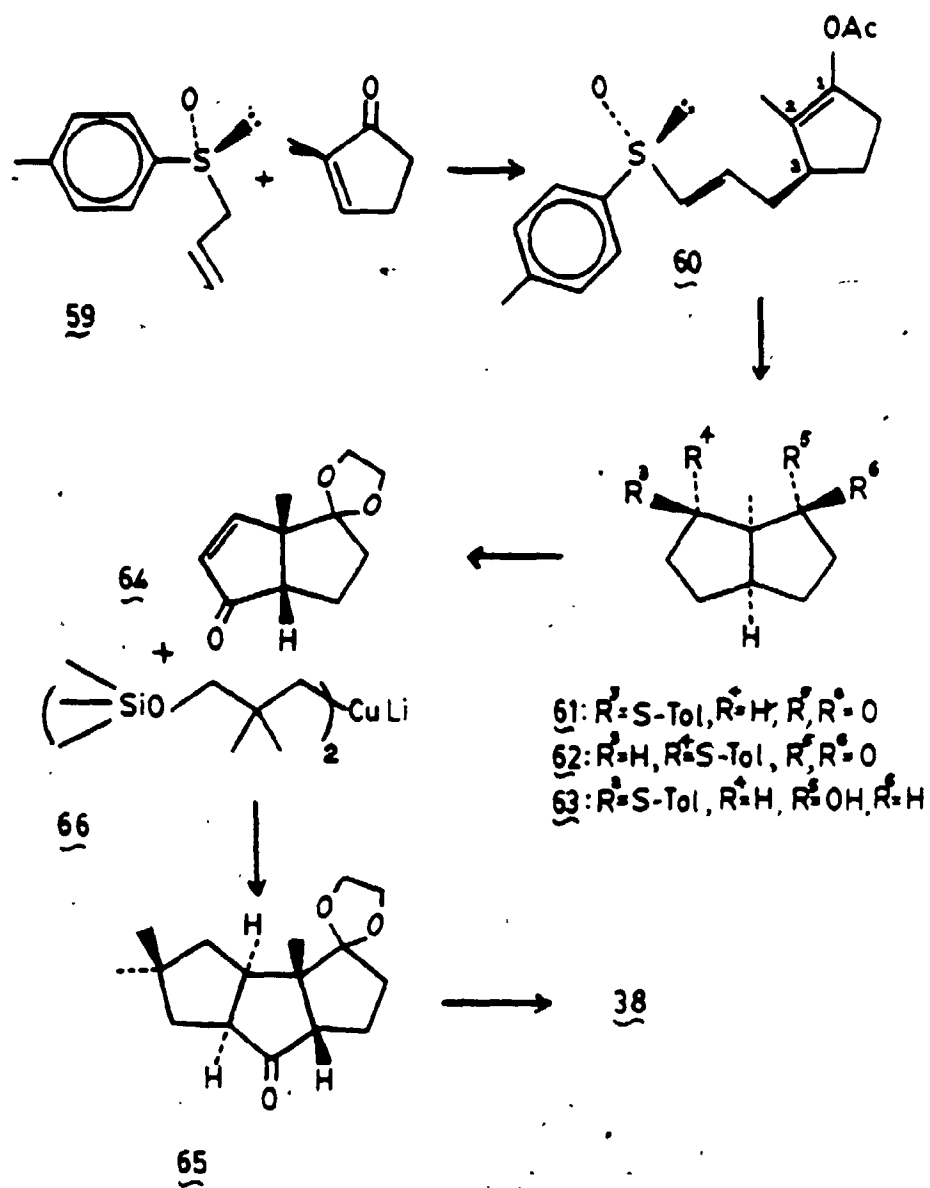
SCHEME 16

Methylation, hydrogenation and oxidation to the corresponding amine oxide of (57) followed by Cope elimination yielded (58) as the only product. The synthesis was concluded by oxidation of alcohol (58) followed by stereospecific hydrogenation to furnish the ketone (38), a known precursor to hirsutene.⁶

Although several total syntheses⁶ of (±)-hirsutene have been reported, the absolute configuration of (+)-hirsutene remained unknown, until Hua et al^{27b} reported the synthesis of (+)-hirsutene. This was achieved by a route involving a chiral sulfinylallyl anion and a facile ring closure of enol thioether and enol acetate moieties (Scheme 18). Treatment of (+)-(R)-allyl-*p*-tolyl sulfoxide (59) with LDA at -78°C followed by 2-methyl-cyclopentenone



SCHEME 17

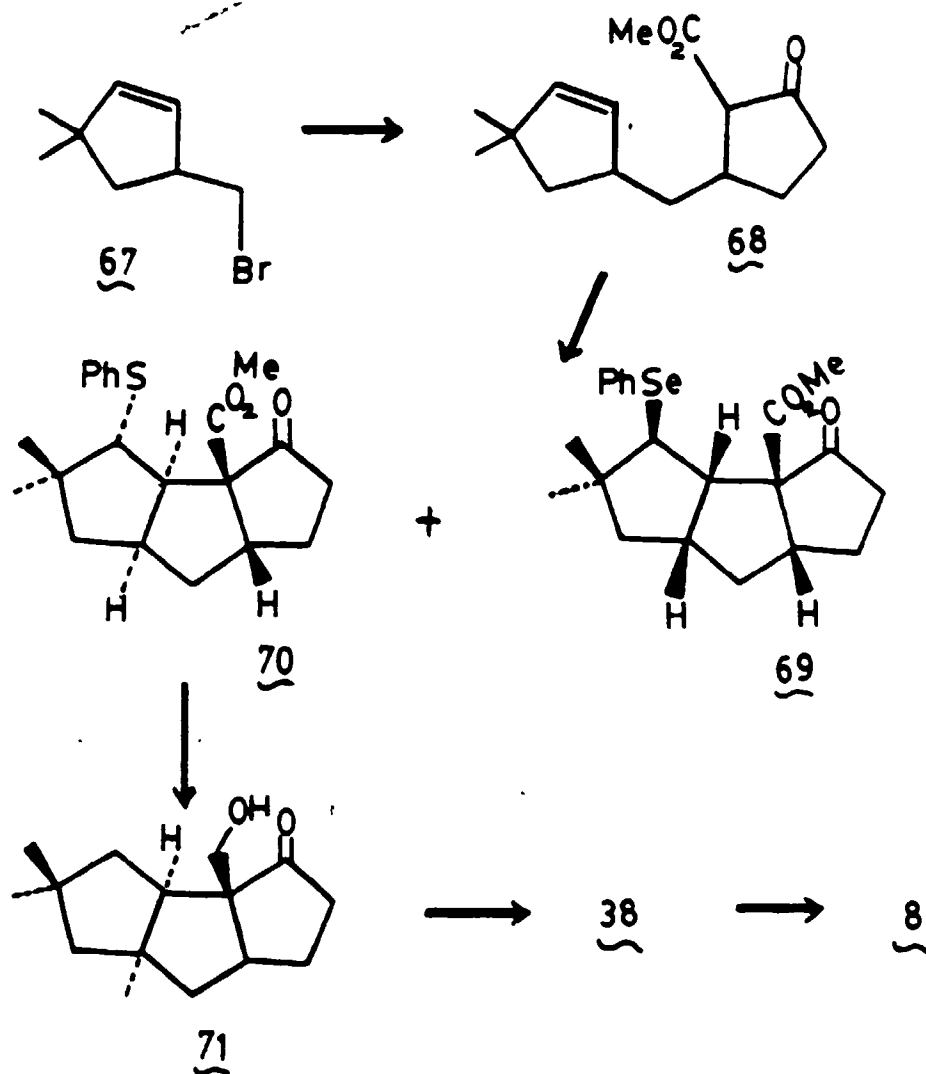


SCHEME 18

HMPA provided the 1,4-adduct (60). The absolute configuration and optical purity of (60) was determined by transforming it into bicyclo[3.3.0]octanol (63), where a ^{19}F nmr method was applied. The diastereoisomers (61) and (62) were then obtained from (-)-(S)-allyl-p-tolylsulfonide (59) and were transformed to the enone (64) by oxidation and desulfenylation followed by allylic oxidation. 1,4-addition of cuprate (66) to (64) gave the ketone (65). Deoxygenation of (65) to the corresponding tricycloundecane followed by deprotection yielded the norketone (38), a known precursor of hirsutene.⁶

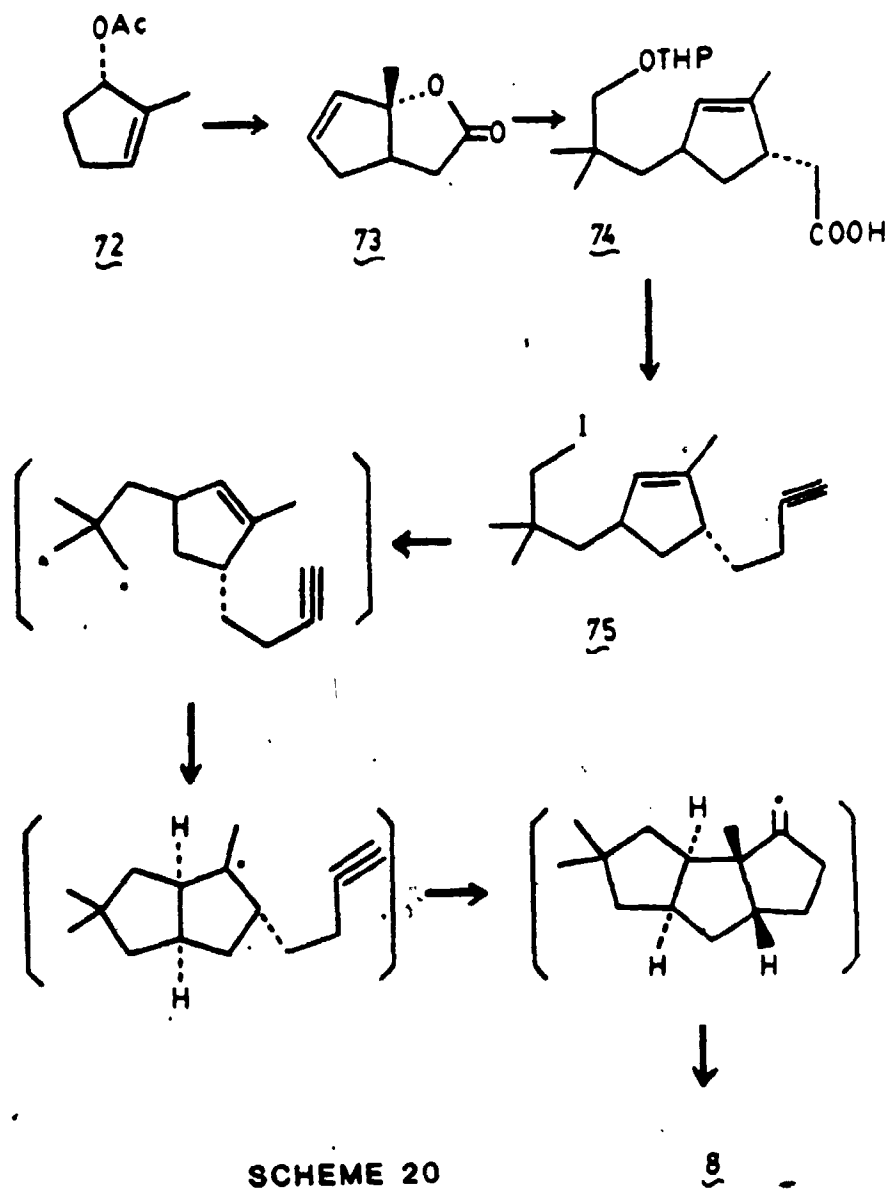
Ley et al²⁸ have reported a short synthesis of (\pm)-hirsutene utilizing an organoselenium mediated cyclization reaction as the key synthetic step. Addition of unsaturated bromide (67) via its cuprate to methyl 2-oxocyclopentanecarboxylate gave (68) (Scheme 19) which was smoothly cyclized to a readily separable mixture of syn (69) and anti (70) stereoisomers using N-phenylselenophthalimide and SnCl_4 . Reduction of (70) followed by protection of the ketone as its enolate and reduction gave (71). Final elaboration of (71) to the known ketone (38) was performed by conversion of the primary hydroxy-group to the corresponding phenylselenide followed by reduction.

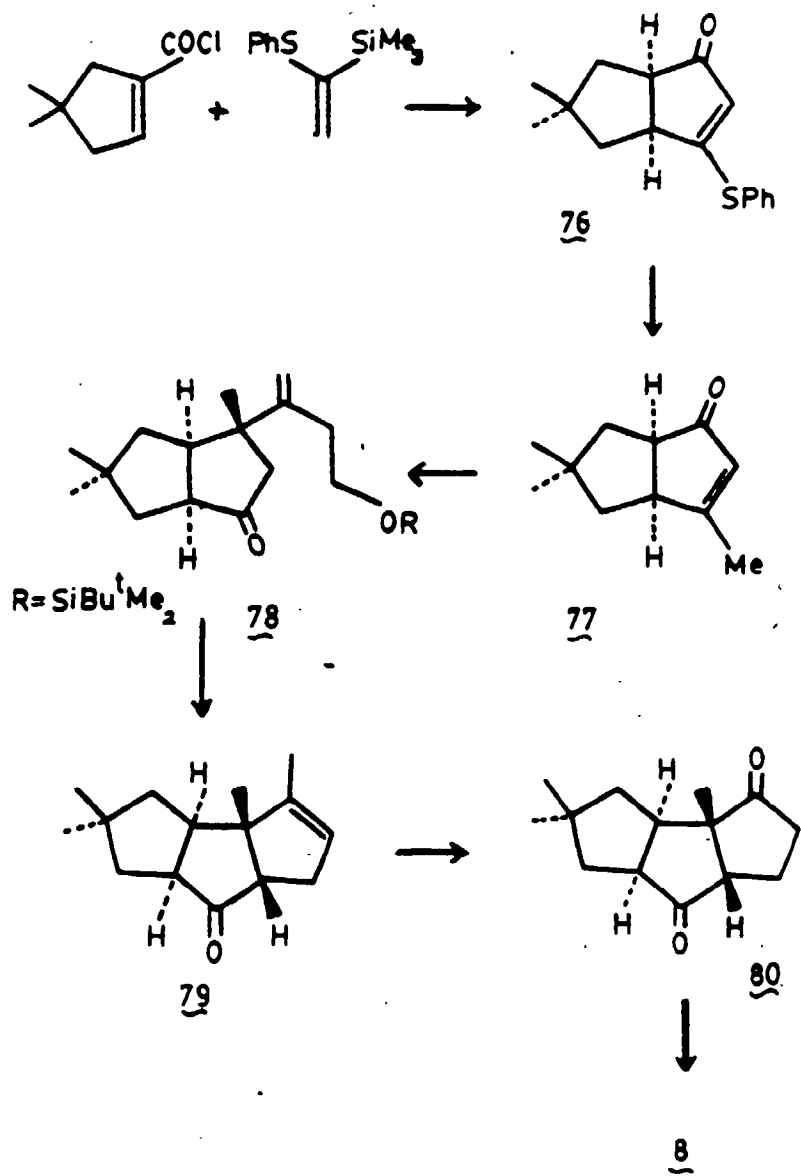
Curran et al²⁹ reported total synthesis of (\pm)-hirsutene via a tandem radical cyclization (Scheme 29).



SCHEME 19

The vinyl lactone (73) was easily prepared from acetylated 2-methylcyclopentanol (72). Subsequent S_N2' addition to the vinyl lactone (73) gave the acid product (74) which was reduced to the corresponding diol and converted to the diiodide (75). Since both hexenyl radical cyclizations (Scheme 20) must proceed in a *cis* fashion, the S_N2'-anti





SCHEME 21

opening of (73) effectively ensures the cis-anti-cis stereochemistry present in hirsutene. Treatment of (75) with tri-n-butyltinhydride gave hirsutene as the single major non-tin containing product.

Magnus et al^{30a,b} have synthesized hirsutene using organosilicon-mediated reactions as the key steps.

1-(trimethylsilyl)-1-(phenylthio)ethylene results in a regiospecific electrophilic substitution in the presence of silver tetrafluoroborate to give the bicyclic enone (76) (Scheme 21). The incorporation of the required four-carbon unit to make (78) was achieved by the reaction of (77) with the cuprate derivative of 1-tert-butyldimethylsilyl-3-bromo-3-butene. Treatment of the p-toluenesulfonate ester of (78) with lithiohexamethyldisilazane gave the tricyclic ketone (79) which was then converted to hirsutene.

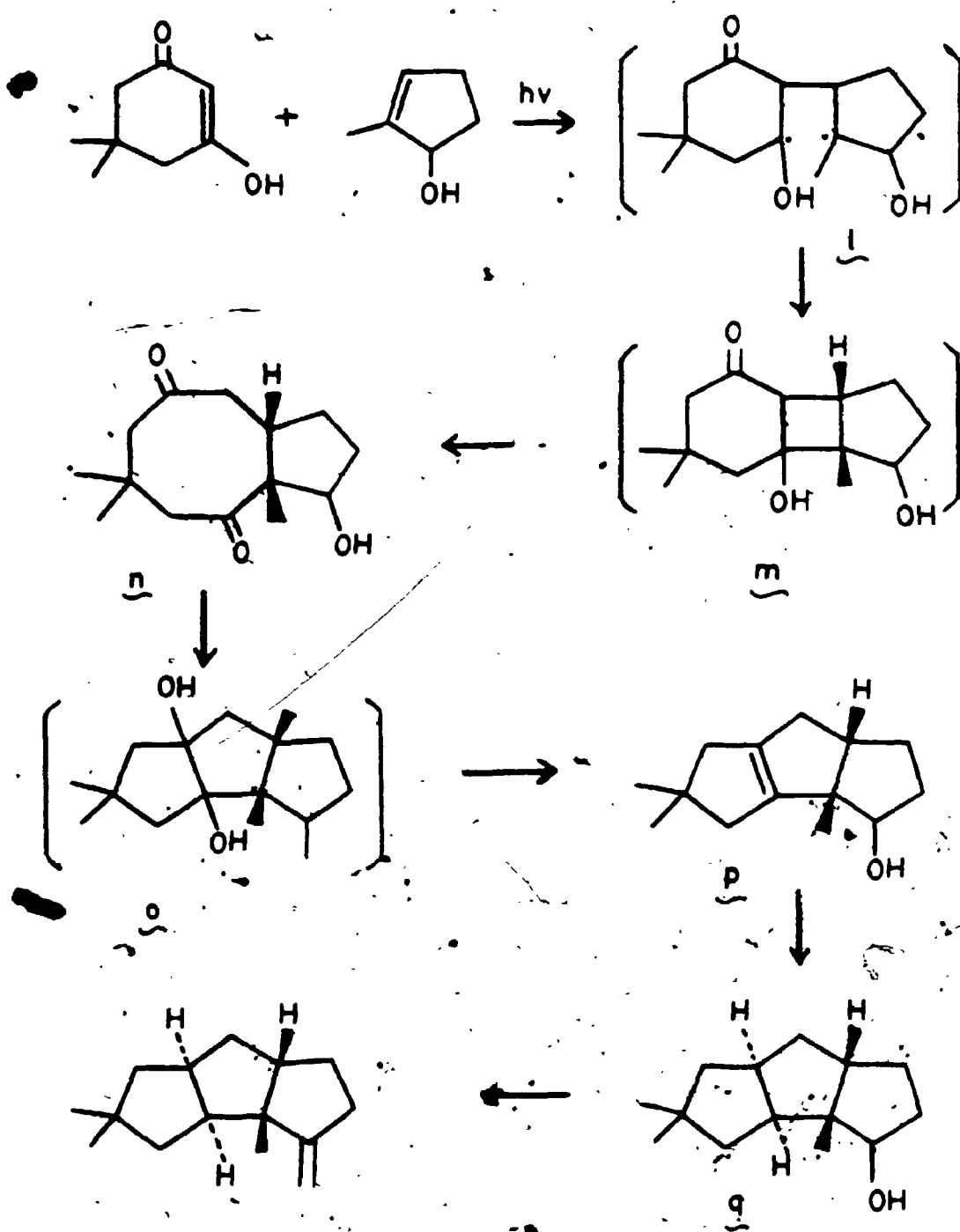
CHAPTER 2

MODEL STUDIES LEADING TO THE TOTAL SYNTHESIS OF (±)-HIRSUTENE

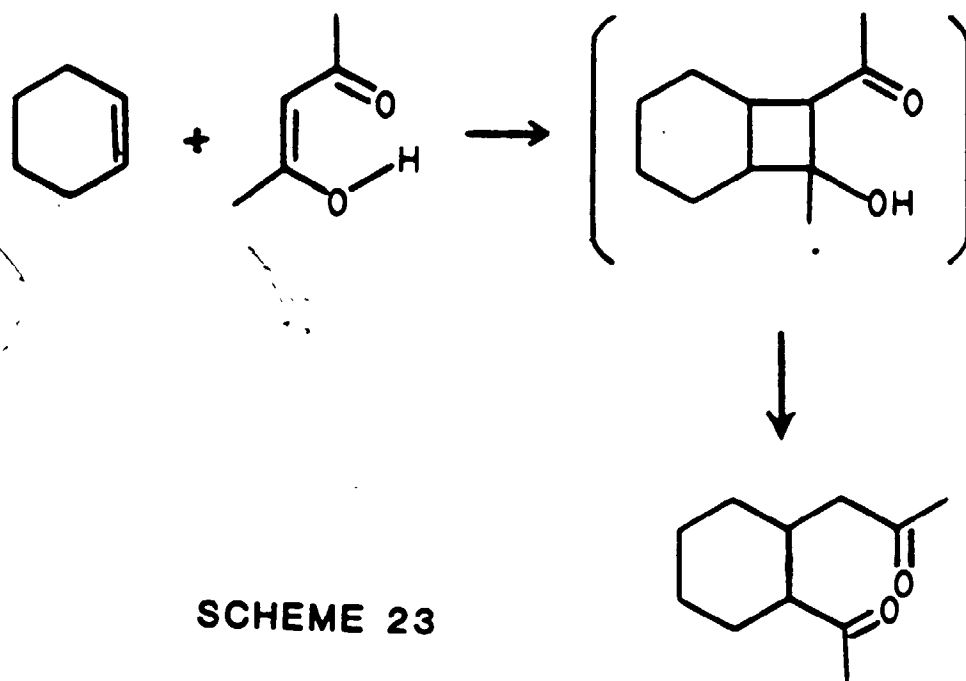
2.1 PROPOSED SYNTHETIC ROUTE

The different synthetic approaches directed towards the total synthesis of (+)-hirsutene which have appeared in the literature were discussed in Chapter 1. The main objective of the work described here was to develop a short stereospecific and regiospecific synthetic route leading to (±)-hirsutene.

The proposed route to the tricyclo[6.3.0.0^{2,6}]-undecane skeleton utilized photochemical cycloaddition of 2-methyl-2-cyclopentenol to an enolized cyclohexane-1,3-dione (the de Mayo Reaction) followed by intramolecular reductive coupling of the diketone photoproduct with a low valence titanium species (McMurry's reagent), as shown in Scheme 22. The first key step in the reaction pathway proposed for the total synthesis of hirsutene is photochemical cycloaddition. Subsequent to the first report of the photochemical cycloaddition of an enolized 1,3-diketone to an alkene³¹ (Scheme 23), numerous examples have appeared in the literature of the use of such reactions in synthesis.^{32a-c}



SCHEME 22



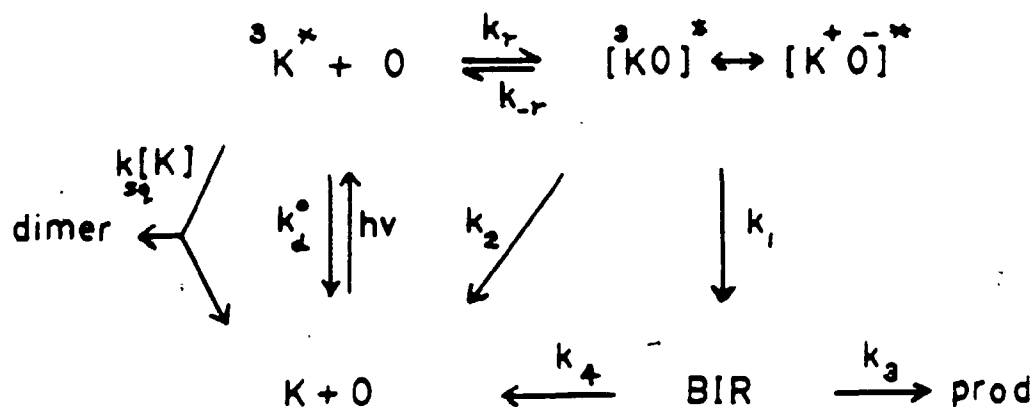
SCHEME 23

In this reaction an excited α,β -unsaturated ketone reacts with a ground state alkene to form a cyclobutane ring, which collapses under the reaction conditions to a 1,5-dione via a retro-aldol process. The reactive excited states involved in the cycloaddition of cyclic enones are triplets³³ with very short lifetimes.³⁴ The lifetimes are short because the excited state can relax to the ground state by twisting around the carbon-carbon double bond of the enone. In the case of acyclic enones this twisting mode of decay is not constrained by the presence of a ring and the excited state lifetimes become sufficiently short that no intermolecular photochemical cycloaddition occurs. In the case of acyclic enolized 1,3-diketones such as

acetylacetone it is believed that intramolecular hydrogen-bonding prevents rotation around the carbon-carbon double bond and lengthens the lifetime so that photochemical cycloaddition could occur. The cis-trans isomerization of cyclic α,β -unsaturated ketones is apparently not an effective path for deactivation of the excited state, whereas excited acyclic α,β -unsaturated ketones are deactivated by cis-trans isomerization with a near unity quantum yield.³⁵

Cyclic α,β -unsaturated ketones exhibit two electronic transitions in the ultra-violet region, a weak band at 325 nm region, assigned to an $n \rightarrow \pi^*$ transition and intense band at 225 nm assigned to a $\pi \rightarrow \pi^*$ transition. It is the excitation of the $n\pi^*$ band which is most frequently used in synthetic photochemistry. Following excitation, the ketone can decay via several reaction pathways: (a) 2+2 cycloaddition either at the carbonyl group or at the double bond to yield 1:1 adducts; (b) reaction with solvent molecules; (c) skeletal rearrangement to an isomer; (d) cleavage of the molecule.

The use of inert solvents and dilute solutions combined with the slow quantum efficiency of skeletal rearrangement of cyclic enones leave (a) as the major mode of decay of excited state. A generalized mechanistic scheme for α,β -unsaturated ketone cycloaddition to alkenes has been proposed by de Mayo³⁴ and is presented below (Scheme 24) where K, O and BIR are the enone, olefin and



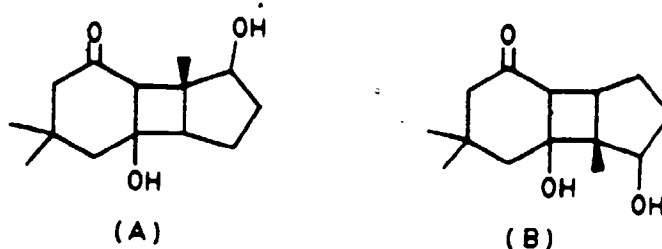
→ SCHEME 24

biradical, respectively. There are different fates proposed for the triplet excited enone molecule: (a) decay back to the starting material (including cis-trans isomerization) represented by k_d ; (b) self-quenching by enone molecules possibly leading to dimer formation; (c) excited complexes (exciplex) formation with alkenes.

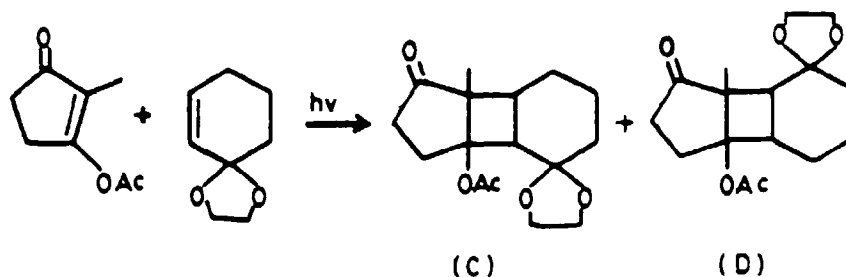
The exciplex intermediate (3KO) can decay back to the ground state components or to a triplet biradical intermediate (BIR), which then undergoes spin inversion and bonding to give the cyclobutane products or the starting enone and olefin. The enolized form of dimedone undergoes photochemical $n\pi^*$ excitation at a wavelength of 254 nm in ethanol. The resulting singlet excited state is then assumed to undergo intersystem crossing to yield the triplet excited state. The photochemical cycloaddition is thought to proceed from the triplet via a diradical intermediate such as **1** to yield the cyclobutane adduct **2** as

intermediate such as **1** to yield the cyclobutane adduct **m** as shown in Scheme 22.

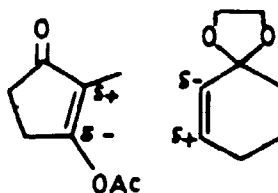
In the photochemical cycloaddition of an unsaturated ketone to an unsymmetrical olefin two types of adducts may be obtained; the head-to-head or the head-to-tail product.³⁶ In the head-to-tail adduct the polar substituent originally present on the alkene is situated on the newly formed cyclobutane ring diagonally opposite to the carbonyl function of the enone, whereas in the head-to-head adduct it is adjacent to the carbonyl function. In the proposed synthesis of hirsutene two regioisomeric sets of photoadducts are possible; (A) having the head-to-head configuration and (B) having the head-to-tail configuration.



It is the head-to-tail adduct (B) which is required for the synthesis of hirsutene. It was reported by de Mayo^{37a,b} that the ratio of the regioisomeric adducts formed in enone cycloaddition was solvent dependent.



In a system analogous to that proposed in Scheme 24 for the synthesis of hirsutene, the enol acetate of 2-methylcyclopentan-1,3-dione was photochemically added to the ethylene ketal of cyclohexanone to give both the head-to-tail adduct (C) and the head-to-head adduct (D). de Mayo's studies showed that irradiation in hydrocarbon solvents gave isomer (D) almost exclusively. Irradiation in polar solvents such as methanol or acetonitrile yielded approximately equal amounts of both isomers (C) and (D).

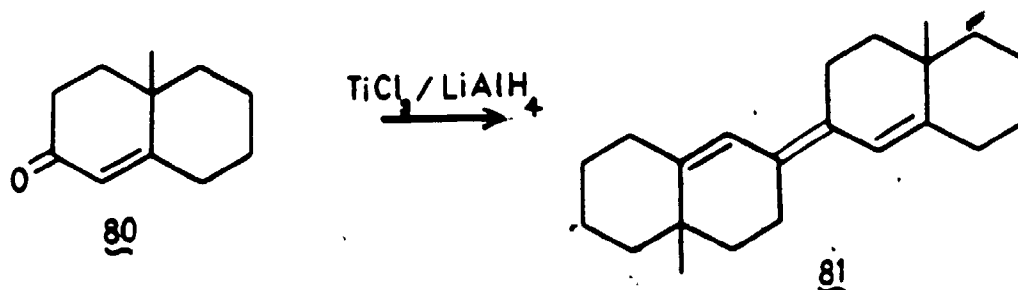


The explanation for the observed orientation involves the idea originally proposed by Corey et al³⁸ that the preferred orientation of an intermediate complex in the reaction is that in which oppositely polarized ends of the reacting double bonds are closest together. Thus considering only the dipoles of the two interacting species the head-to-head adduct should predominate, as seen with hydrocarbon solvents. By changing the solvent to ones of increasing dielectric constant the solvent can exert an insulating effect on the dipole interactions so that both adducts are obtained. Based upon these arguments the solvent to be used in the hirsutene synthesis should be one of high dielectric constant in order to obtain the required head-to-tail adduct in maximum yield, and it is to be expected that it will most probably require separation from the undesired head-to-head adduct.

The three rings of hirsutene have a *cis-anti-cis* stereochemistry. Cyclopentene yields photoadducts in which the ring junction is always *cis*,³⁶ and thus the stereochemistry of one of the ring junctions of hirsutene is determined in this step. The initially formed cyclobutane adduct obtained from the β -diketone and the olefin spontaneously rearranges by a retro-aldol opening of the cyclobutane ring to give the 1,5-diketone,^{32a,37a} conserving the *cis* fused ring junction, as will be discussed below.

Reductive coupling of the 1,5-diketone can be brought about in a number of ways. The method proposed in this scheme involves coupling via "McMurry's reagent".^{39a,b,40}

In 1974 McMurry et al.^{39a,b,40} reported a reductive dimerization of an α,β -unsaturated ketone (80) in the presence of $\text{TiCl}_3/\text{LiAlH}_4$ (Scheme 25), which he discovered unexpectedly while trying to transform (80) to the corresponding alkene without the migration of the double bond.



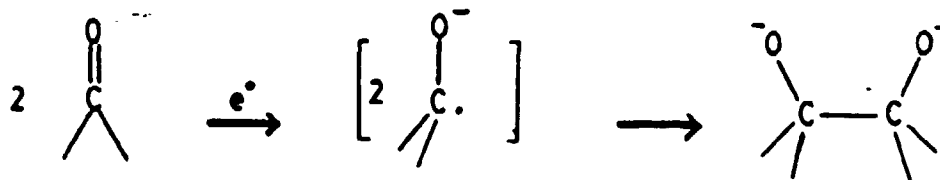
SCHEME 25

In the approach towards the total synthesis of (\pm)-hirsutene described here, the intramolecular coupling of a 1,5-diketone plays a crucial role, and it was hoped to achieve the transformation using McMurry's reagent (TiCl_3/K).

Active titanium metal, produced in a finely divided form by reduction of TiCl_3 with either potassium or LAH reductively couples ketones and aldehydes to olefins. This

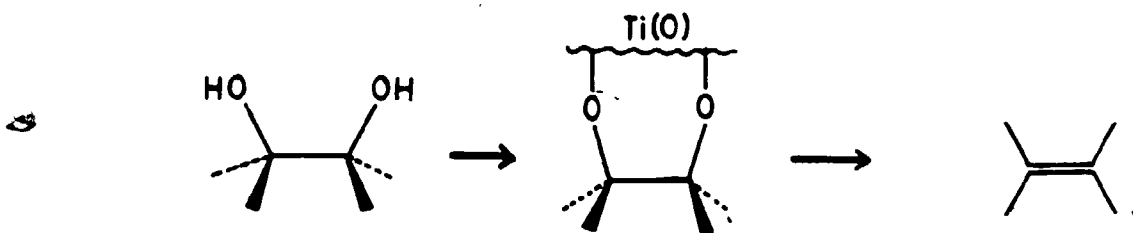
type of coupling occurs intermolecularly as well as intramolecularly. The intermolecular coupling works best when two identical carbonyls are coupled to a symmetrical product, but selective unsymmetrical coupling can also be carried out in certain cases. The nature of the active titanium metal has been studied by scanning electronic microscopy, and it is believed that the coupling reaction occurs on the surface of the active titanium particle. These types of coupling reactions have also been observed with systems such as $\text{TiCl}_3/\text{Zn}^{41}$ and $\text{TiCl}_3/\text{Mg}^{42}$

The overall coupling reaction takes place in two steps: an initial carbon-carbon bond forming step, which is followed by a deoxygenation step. The carbon-carbon bond forming step is simply a pinacol reaction.⁴³ The Titanium reagent donates one electron to the ketone to generate a ketyl radical anion, which dimerizes, yielding the intermediate pinacol following protonation (Scheme 26).



SCHEME 26

Pinacols have been isolated from titanium-induced couplings if the reactions are carried out below room temperature and are quenched after a sufficiently brief period of time that deoxygenation has not yet occurred. Treatment of pinacols with the titanium reagent yields the deoxygenation products which confirm this. However the deoxygenation process is not concerted; mixtures of geometrical isomers are produced starting from stereochemically pure 1,2-diols, although some of the stereochemistry is preserved. Hence the second step can be postulated as given below (Scheme 27), which involves coordination of the diol of the surface of a heterogeneous titanium particle.



SCHEME 27

Cleavage of the two carbon-oxygen bonds then occurs stepwise, yielding the olefin and an oxide-coated titanium surface.

The intramolecular coupling of the diketone (n) was expected to proceed via the cis diol intermediate (o)

(Scheme 24) to yield the olefin (p). Photochemically produced 1,5-diketones have been shown to undergo reductive coupling photochemically^{31,32a-c,37a} to yield a diol such as intermediate (o), but the synthetic efficiency of the reaction has not been examined. Vicinal diols may be converted to olefins by a number of methods of reduction.⁴⁴

The olefin (126) has been reported in the literature, and is claimed to be readily hydrogenated by hydrogen gas and platinum oxide from the more hindered side.^{22a} The olefin (p) has a hydroxyl group on the more hindered side of the molecule, hence we could also expect the hydroxyl group to hold the platinum surface on the more hindered side resulting in "cis" hydrogenation from that side. Therefore the reduction of the olefin (p) with hydrogen gas and platinum oxide yields the cis-anti-cis-tricyclo[6.3.0.0^{2,6}]undecane carbon skeleton of the hirsutene family.

2.2 MODEL STUDY WITH THE USE OF CYCLOPENTENE AS THE ALKENE

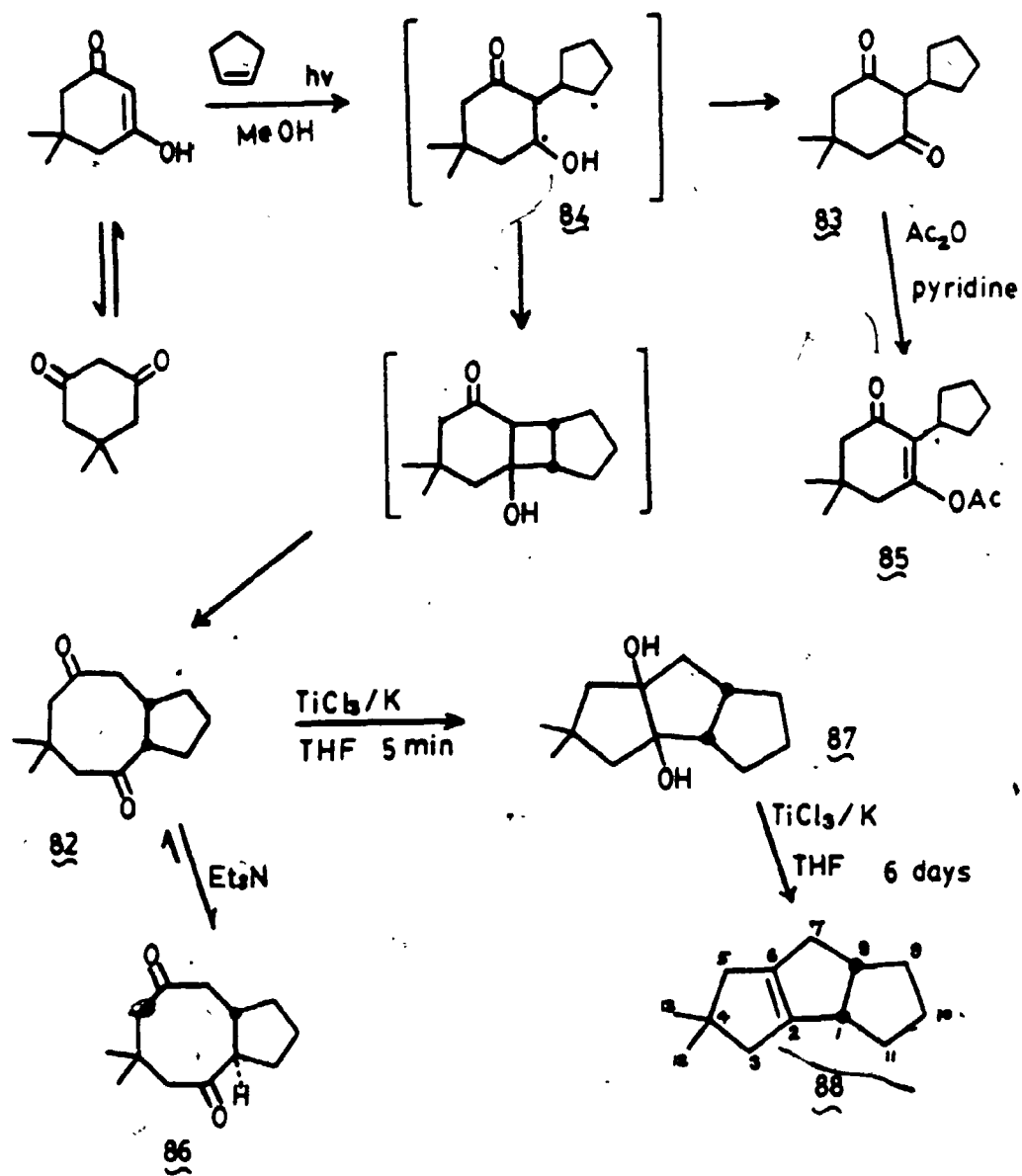
The viability of the proposed route to obtain the tricyclic undecane skeleton through an intramolecular 1,5-diketone coupling was initially examined by Weedon et al.⁴⁵ Irradiation of a 1% methanolic solution of 5,5-dimethylcyclohexane-1,3-dione (dimedone) and cyclopentene using uv light of wavelength 254 nm resulted in complete conversion of the diketone to a mixture of two

products, the cyclooctanedione (82) (90%) and the cyclohexanedione (83) (10%) (Scheme 28).

The separation of the two compounds was achieved by removal of the solvent under reduced pressure followed by the extraction of (83) into aqueous base. The compound (83) was characterized as its enol acetate. The removal of (83) with base resulted in partial epimerization of (82) to (86).

The cyclooctadione (82) was isolated as a white crystalline solid (m.p. 114-115°C). The structure was assigned from the ^1H nmr, ^{13}C nmr, ir and mass spectra and by analogy with the products of photoaddition between dimedone and cyclohexene and between cyclopentene and cyclohexane-1,3-dione.^{32b,46} The cis stereochemistry of cyclooctane-cyclopentane ring fusion of (82) was confirmed by epimerization (triethylamine or p-toluenesulfonic acid in refluxing benzene) to the more stable⁴⁰ trans-fused system (86) (m.p. 62.5-63°C).

Refluxing of a solution of anhydrous titanium trichloride in dry THF with potassium metal under dry nitrogen gave a black air-sensitive mixture which rapidly converted the diketone (82) to the diol (87) as the only product. The exact stereochemistry of this compound could not be deduced from the available data. Further refluxing of the above reaction mixture (6 days) resulted in the clean conversion of the diol (87) to the olefin (88) as the only product. This was purified by preparative gas



SCHEME 28

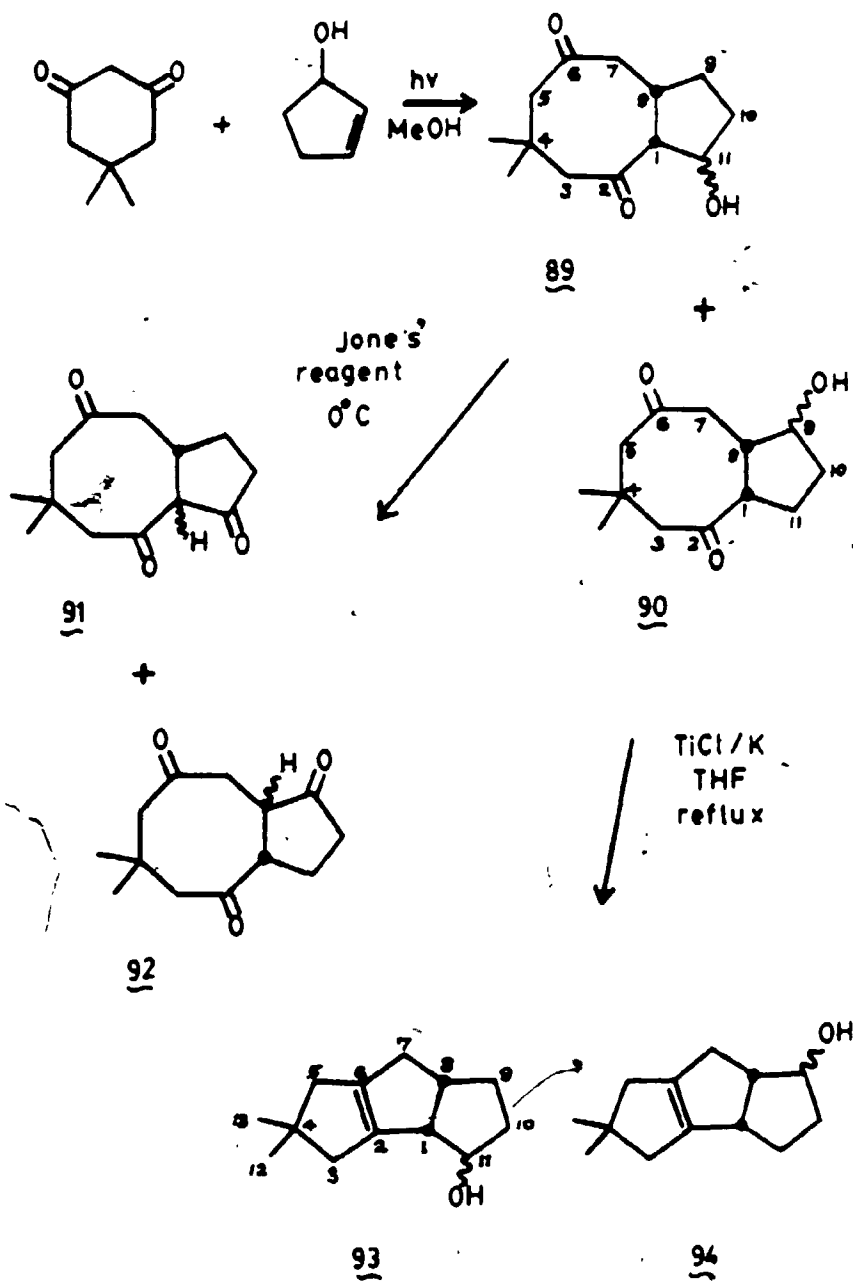
chromatography and the structure was confirmed by ^1H nmr, ^{13}C nmr, ir and mass spectral data.

These transformations provide a new entry into the tricyclo[6.3.0.0^{2,6}]undecane system. As part of the work described in this thesis, repeated attempts to obtain the desired tricyclo[6.3.0.0^{2,6}]undecane system using initial photoaddition of 2-methyl-2-cyclopenten-1-ol to cyclohexane-1,3-dione followed by TiCl_3 induced coupling of the 1,5-dione formed proved unsuccessful. This is discussed in detail in Chapter 3. The preliminary conclusion drawn was that the synthesis of the target molecule (\pm)-hirsutene required further investigation of the effects of the hydroxy and methyl groups of the cyclopentene on the regiochemistry of the photochemical cycloaddition. In addition, it was concluded that the ring opening of the photoproduct in the basic titanium trichloride/potassium reaction mixture, by a retro-aldol process might be interfering with the desired course of the reaction. Consequently it was decided to examine a model system in which 2-cyclopentene-1-ol was used as the alkene rather than 2-methylcyclopent-2-en-1-ol. This model study will be discussed in this chapter. As will be seen in Chapter 3, the model study became essential for the assignment of the stereochemistries of the intermediates in the hirsutene synthesis.

2.3 MODEL STUDY WITH THE USE OF 2-CYCLOPENTENE-1-OL AS THE ALKENE

In solution, cyclohexane-1,3-dione is in equilibrium with its enolized form 3-hydroxycyclohex-2-ene-1-one and the use of polar solvents such as methanol increases the amount of the latter present in the equilibrium. The non-enolized dione possesses a saturated carbonyl chromophore ($\lambda_{\text{max}} \sim 290 \text{ nm}$) whereas the enolized form absorbs at $\sim 250 \text{ nm}$ ($n \rightarrow \pi^*$ transition) and at $\sim 310 \text{ nm}$ ($n \rightarrow \pi^*$ transition). Thus, irradiation of dimedone in methanol at 254 nm (in a Rayonet apparatus) results in efficient excitation of the enolized form selectively. If an alkene is present then adduct formation^{32b,47,48} occurs via interaction of the alkene with the triplet excited state of dimedone. Unless the enol is stabilized by derivatization, the initial adduct undergoes spontaneous retro-aldol ring opening under the reaction conditions to give a cyclooctanedione as the isolated product^{32b,37} (Scheme 24).

When a 1% methanolic solution of 5,5-dimethylcyclohexane-1,3-dione and 2-cyclopentene-1-ol was irradiated using uv light of wavelength 254 nm , gas chromatographic analysis indicated 98% conversion of the diketone to a mixture containing approximately equal amounts of two products which were subsequently assigned the structures (89) and (90) (Scheme 29). Removal of the solvent under reduced pressure followed by column chromatographic separation using silica gel resulted in the isolation of pure crystalline (89) (38%) (m.p. $91-94^\circ\text{C}$,

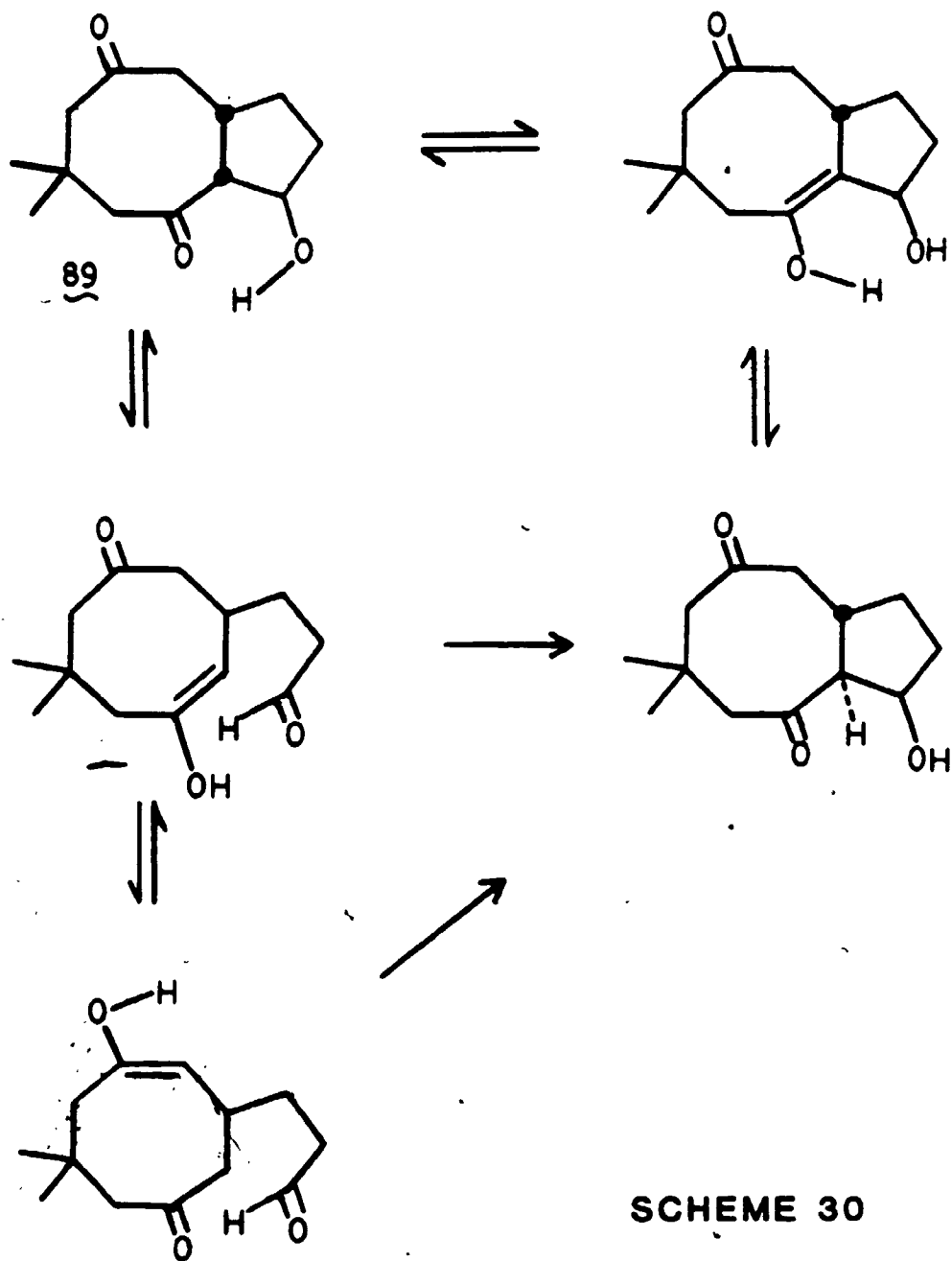


SCHEME 29

diethyl ether/hexane), and (90) (49%) (m.p. 103°C, diethyl ether/hexane). Comparison of the ^{13}C nmr spectrum of the crude reaction mixture with the spectra of isolated (89) and (90) suggested that partial loss of compound (89) had occurred during the process of separation. This may be due to either retro-aldol ring opening on the occurrence of enolization-epimerization of the species (89) on the silica gel surface (Scheme 30).

Mass spectroscopic analysis of both of these compounds indicated a precise mass of 224.141 which corresponds to species with the formula of (89) and (90). Ir data indicated the presence of a saturated ketone group and a non-hydrogen bonded -OH group. The ^{13}C nmr spectra indicated that each compound possessed 18 carbon atoms and comparison with the APT^{63a} and DEPT^{63b} spectra indicated that these comprised 2 -CH₃, 5 -CH₂-, 3 -CH-, 1 C and 2 C=O in (90). This is consistent with the expected structures.

The stereochemistries of the ring fusion positions of compounds (89) and (90) were assigned as cis on the basis of the known course of the cycloaddition reaction in closely related analogues.^{39,45,49,50} The regiochemistries of adducts (89) and (90) were determined by comparison of their ^{13}C nmr spectra with that of the non-hydroxylated analogue (82), and by ^1H nmr decoupling experiments. The ^{13}C nmr chemical shifts of the methines at position 1, which is α to a carbonyl group, and position 8 of compound (82) appeared at 58.8 and 38.4 ppm, respectively. In



SCHEME 30

cycloalkanols the hydroxyl group deshields the α carbons (β -effect) and shields the β carbon atom (γ -effect);⁵¹ this effect was taken into account to determine the regiochemistries of the two species (89) and (90). The presence of an -OH group at position 11 would cause the chemical shift of methine carbon 1 to move downfield and the methine carbon 8 to move upfield whereas a -OH group at position 9 will shift the methine carbon 8 downfield and carbon 1 to high field (Table I).

	82	89	90
C-1	58.8 ppm	65.8 ppm	56.1 ppm
C-8	38.4 ppm	36.6 ppm	46.8 ppm

TABLE I: ^{13}C nmr chemical shifts of C-1 and C-8 of compounds (82), (89) and (90)

These changes in chemical shifts were observed in compounds (89) and (90). Hence unambiguously the dione with methine carbons at 65.8 and 36.6 ppm was assigned as compound (89) and the compound with methine carbons at 56.1 and 46.1 ppm was assigned (90). These assignments were further confirmed by ^1H nmr decoupling experiments; irradiation of the hydroxymethine (i.e. the hydrogen at position 11 in (89) and position 9 in (90)) revealed the chemical shift and splitting pattern of the ring fusion methine at

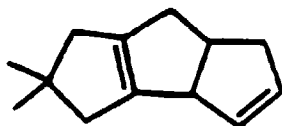
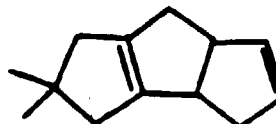
position 1 in (89) and position 8 in (90). The methine hydrogen at position 8 in the isomer assigned as (90) appeared at δ 2.95 as a multiplet ($J = 1.5, 4, 6$ and 10 Hz) split by the four adjacent hydrogen atoms; only compound (90) can have a methine hydrogen α to the hydroxymethine with four adjacent hydrogen atoms. The methine at position 1 in the isomer assigned structure (89) appeared at δ 2.85 and was split into three lines ($J = 8$ Hz) by the adjacent hydrogen atoms; only species (89) can have a methine hydrogen atom α to the hydroxymethine with only two adjacent hydrogen atoms.

Oxidation of the product mixture of (89) and (90) with Jones' reagent at 0°C gave a mixture of products with one component predominating, as determined by gas chromatography. The column chromatographic separation of the crude reaction mixture using silica gel and hexane/diethyl ether as the solvent gave only one isolated component, a white crystalline solid (m.p. $130.5\text{--}131^\circ\text{C}$ hexane/diethyl ether). This compound showed a precise mass which corresponds to either compound (91) or (92). Ir data indicated the presence of a saturated ketone and the absence of a hydroxyl group. The ^{13}C nmr spectrum indicated the presence of 2 CH_3 , 5 CH_2 , 2 CH , and 1 C , along with 3 $\text{C}=\text{O}$ at 214.07, 209.8 and 209.3 ppm. The carbonyl group shows a stronger α effect and a stronger β effect than a hydroxymethine. Oxidation of the hydroxyl group of compound (89) to a carbonyl group will shift the

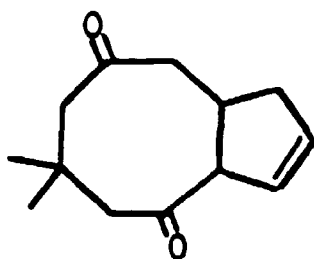
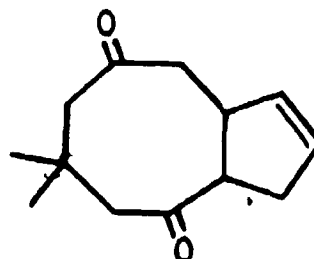
methine carbon 1 downfield and the methine carbon at position 8 to high field whereas oxidation of (90) will move the methine carbon at position 8 to low field and the carbon at position 1 to high field. The triketone obtained has two methine carbons, one at 56.7 ppm and one at 49.7 ppm. This indicates that the crystalline oxidation product is (92), and not (91), since the chemical shift of the methine carbon at position 8 has been moved downfield following oxidation. This was further confirmed by ^1H nmr decoupling experiments. The ^1H nmr spectrum of (92) shows the methine proton at position 1 as a multiplet at 2.5 ppm ($J = 12, 10$ and 7.5 Hz) and the methine proton at position 8 as a double triplet at 2.87 ppm ($J = 12, 12$ and 3 Hz). Both are coupled to each other (12 Hz) and no doublet is observed, which would be expected for the methine proton at position 1 of compound (91). These spectral data prove the absence of compound (91) and confirm the structure of the crystalline oxidation product as (92). The failure to observe or isolate compound (91) could be due to retro-aldol ring opening of (89) under the conditions of the oxidation reaction, or due to a hydrolytic cleavage process in the triketone.

With the photoadducts in hand, and their regiochemistries known, the intramolecular diketone coupling reaction with McMurry's reagent was performed on a mixture of the cycloadducts using the conditions found to be successful for (82). This involved refluxing the

photoadducts (89) and (90) with a suspension of McMurry's reagent in dry tetrahydrofuran under N_2 for 6 days. But, contrary to expectations, the desired products could not be isolated in good yield from the reaction mixture. Further investigation of the reaction suggested initial formation of the desired products (93) and (94) along with the disappearance of starting materials, with the yield of the products reaching a maximum after 4 days; however, further refluxing of the reaction mixture apparently led to a decrease in the yield of the products. This could be explained by the possibility of dehydration of products (93) and (94) to give hydrocarbons (97) and (98) which were isolated in small amounts and confirmed by mass spectral data.

9798

The possibility of dehydration is further confirmed by the isolation of dehydrated starting materials (99) and (100) from the reaction mixture.

99100

The reaction was repeated; the mixture of (89) and (90) was refluxed with McMurry's reagent in dry tetrahydrofuran under dry N_2 for 4 days only in order to avoid secondary reactions of the desired products. The reaction mixture was concentrated and extracted with ether; the concentrated ether extract was then separated by column chromatography. One product predominated as determined by glc. This compound showed a precise mass which corresponded to either compound (93) or (94). Ir data indicated the presence of a hydroxy group. The ^{13}C nmr spectrum indicated the presence of 2 CH_3 , 5 CH_2 , 3 CH and 3 C . The ^{13}C nmr spectra of species (88) (Scheme 28) showed two methine carbons, one at 47.12 and the other at 46.55 ppm which were assigned to carbons at positions 1 and 8. The α -effect arising from the presence of a hydroxyl group at the 11 or 9 positions will move the methine carbon α to the hydroxyl group downfield. The ^{13}C nmr spectra of the compound obtained from reduction of the mixture of (89) + (90) showed the hydroxy methine at 79.9 ppm and two

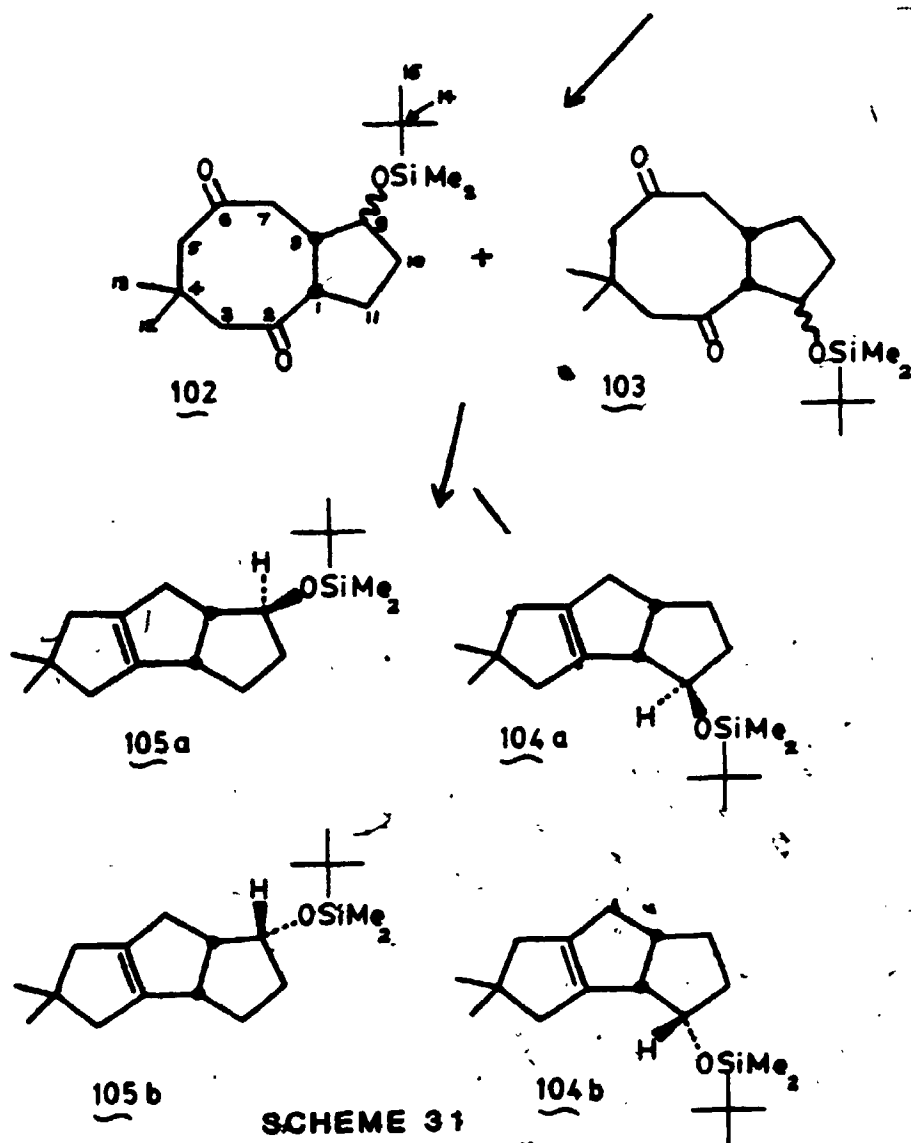
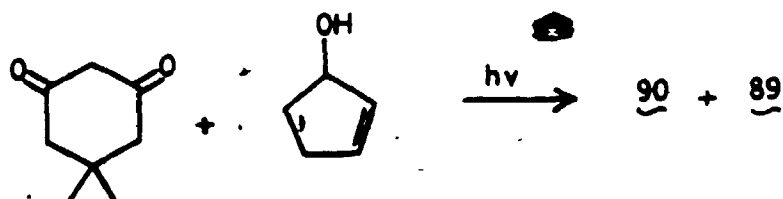
other methine carbon atoms at 45.2 and 56.3 ppm (methine carbon α to hydroxy group). Because the chemical shift difference of methine carbons 1 and 8 in compound (88) is so small, it is difficult to assign the structure of the compound derived from the mixture of (89) and (90) on the basis of the ^{13}C spectrum. Hence ^1H nmr decoupling experiments were used to deduce the structure. Irradiation of the hydroxy methine (3.95 δ , m, 4, 4 and 2 Hz) revealed the chemical shift and splitting pattern of the ring fusion methine α to the hydroxy group, which appeared at 2.85 δ (m, 8, 8, 2 and 4 Hz). The splitting pattern indicated that it was coupled to four adjacent hydrogen atoms. If this compound were species (93) then the methine hydrogen at position 1 should appear as a double doublet, whereas in (94) it should split by four adjacent hydrogen atoms. Thus the observed coupling pattern for the methine adjacent to the hydroxymethine indicates structure (94) for the product of reductive coupling of (89) and (90). This was supported by the observation of the second ring junction methine at 3.6 ppm, which appeared as a double triplet ($J = 8, 8$ and 2 Hz). This methine would be coupled to four protons in (93). The spectral data indicated the product as the regioisomer (94), which is not the regioisomer required for the synthesis of hirsutene. The absence of the regioisomer (93) is consistent with retro-aldol ring opening of the diketone (89) in the basic potassium/titanium trichloride/ tetrahydrofuran reaction

mixture.⁵² This led us to the conclusion that protection of the hydroxy group was necessary in order to inhibit the retro-aldol ring opening. 060

There have been several useful methods published for the protection of hydroxyl groups.⁵³ The silylation of organic compounds has been recognized as an important method in both organic chemistry and biochemistry, because of the resulting protection afforded functional groups, and also because of increased thermal stability, solubility in non-polar solvents and reactivity towards attacking reagents, whether at the site of the newly introduced silyl substituent or in adjacent positions.⁵⁴ Many excellent general purpose reagents and procedures have been developed (e.g. trimethylchlorosilane (TMCS), trimethylsilylimidazole (TMSI), hexamethyldisilazane (HMDZ), and other silylamines, N,O-bis(trimethylsilyl)acetamide (BSA) and the corresponding monosilylated derivative (MTSA), bis(trimethylsilyl)trifluoroacetamide, bis(trimethylsilyl)-urea (BSU) and trimethylsilyldiphenylurea (TDFU)) and are widely used to introduce the trimethylsilyl group.⁵⁵ Mitscher et al⁵⁶ have reported the use of trimethylsilyl enol ethers of acetyl acetone (101) to prepare trimethylsilyl ethers of allylic alcohols.⁵⁶ Cyclopent-2-ene-1-ol is an allylic alcohol and so Mitscher's procedure using the trimethylsilyl ether of acetyl acetone (101) was used to prepare the corresponding trimethylsilyl ether of cyclopent-2-ene-1-ol.

used, are frequently too susceptible to solvolysis in protic media (either in the presence of acid or base) to be broadly useful in synthesis. The dimethyl-tert-butylsiloxy group is 10^4 times more stable⁵⁴ than the trimethylsiloxy group, and yet can be cleaved rapidly with tert-n-butylammonium fluoride in tetrahydrofuran at 25°C. These characteristics convinced us to investigate the use of the dimethyl-tert-butylsiloxy group as the protector of the -OH group in (89) + (90).

The mixture of hydroxy diketones (89) and (90) in methylene chloride gave, upon treatment with dimethyl-tert-butylsilyl chloride and imidazole in dimethyl formamide at 25°C for 12 hr, a mixture of silyl ethers (83%) (Scheme 31). Separation by column chromatography gave two major products, as indicated by glc. Both these compounds exhibited a precise mass m/e of 338.228 which corresponds to species (102) and (103). The ^{13}C nmr spectra indicated the presence of 19 carbon atoms in each compound consisting of 7 CH_3 , 5 CH_2 , 3 CH , 2 C and 2 carbonyl carbons. The stereochemistries of the ring fusion positions of both these compounds were assigned as *cis* on the basis of the known course of the cycloaddition reaction in closely related analogues.^{49,45,50} The regiochemistries were determined by comparison of the ^{13}C nmr spectra with those of (89) and (90). The ^{13}C nmr chemical shifts of methines at positions 1 and 8 of compound (82) appeared at 58.8 and 38.4 ppm. The presence of a $-\text{OSiMe}_2^t\text{Bu}$ group at



SCHEME 31

position 11 would cause the chemical shift of the methine carbon at position 1 to move downfield due to the β effect, and the methine carbon at position 8 to move upfield due to the γ effect; conversely, a $-\text{OSiMe}_2^t\text{Bu}$ at position 9 will shift the methine carbon at position 8 downfield and carbon 1 to high field.⁵¹ These changes in chemical shifts were observed in the silylated compounds and allowed their assignment as regioisomers (102) and (103) (Table II).

	82	102	103
C-1	58.8 ppm	55.9 ppm	65.9 ppm
C-8	38.4 ppm	47.3 ppm	37.4 ppm

TABLE II: ^{13}C nmr chemical shifts of C-1 and C-8 of compounds (82), (102) and (103)

Hence the dione with methine carbons at 65.9 and 37.4 ppm was assigned as compound (103) and was obtained in 39%, while the regioisomer with methine carbons at 55.9 and 47.3 ppm was assigned as (102) and was obtained in 43% yield. Similar changes in chemical shifts were observed in the corresponding regioisomers (89) and (90). The close similarity of the chemical shifts of the C-1 and C-8 methines of (89) and (103) suggests that they possess the same stereochemistries at the ring junction and argues against the occurrence of any epimerization at C-H during the silylation process.

Refluxing the mixture of (102) and (103) with McMurry's reagent in dry tetrahydrofuran under dry N_2 for 48 hrs gave a mixture of dimethyl-tert-butylsiloxy olefins (59%) which were subsequently assigned the structures (104) and (105) (Scheme 31). The time required for the complete conversion to olefins in this instance seems much shorter than for other cases (2 days as opposed to 4 and 6 days for (89), (90) and (82), respectively). Extended exposure of the reaction mixture to the reaction conditions (more than 2 days) resulted in desilylation of the dimethyl-tert-butylsiloxy olefin. The desilylated products proved to be difficult to separate from the polar reaction mixture; however, with the dimethyl-tert-butylsiloxy group still present the products were of much reduced polarity and were readily separated from the polar reaction mixture. Column chromatographic separation of the dimethyl-tert-butylsiloxy olefin mixture gave three compounds.

These compounds showed a precise mass which corresponded to either species (104) or (105). The ^{13}C nmr data were consistent with this and showed that each compound contained 19 carbon atoms, comprising 7 CH_3 , 5 CH_2 , 3 CH , 2 C and two alkene carbon atoms. The ^{13}C nmr spectrum of hydrocarbon (88) showed two methine carbons, one at 47.12 ppm and the other at 46.55 ppm, which correspond to C-1 and C-8 in (104) or (105). Although the presence of a $-OSiMe_2^tBu$ group at either of positions 11 and 9 will move the α methine carbon downfield and the

β methine carbon upfield, the difference in ^{13}C nmr chemical shifts of the methine carbons of the model (88) is too small to identify which position has changed its chemical shift in the products assigned at (104) and (105). The methine carbons of the three compounds (identified as X, Y and Z) are given in Table III.

	Siloxy Methine (ppm)	Methine α to -OSiMe ₂ ^t Bu (ppm)	CH (ppm)
X	81.3	56.3	45.7
Y	76.0	57.9	45.4
Z	75.5	50.5	45.5

TABLE III: ^{13}C nmr chemical shifts of methine carbons of compounds (104a), (105a) and (105b)

Hence it was decided to use the ^1H nmr decoupling experiments to determine the regiochemistry of these three compounds. Irradiation of the siloxy methine (4.0 ppm, 3, 3 and 3 Hz) of compound X revealed the chemical shifts and the splitting pattern of the ring fusion methine α to the -OSiMe₂^tBu group, which appeared at 2.9 ppm (3, 8, 8 and 3.5 Hz). The observation of 4 coupling constants indicates that this methine is split by four adjacent hydrogen atoms. The other methine proton appeared at 3.1 ppm (m). Only species (105) can have a methine hydrogen α to the siloxy group with four adjacent hydrogen atoms; and hence species X is assigned as regioisomer (105). The coupling

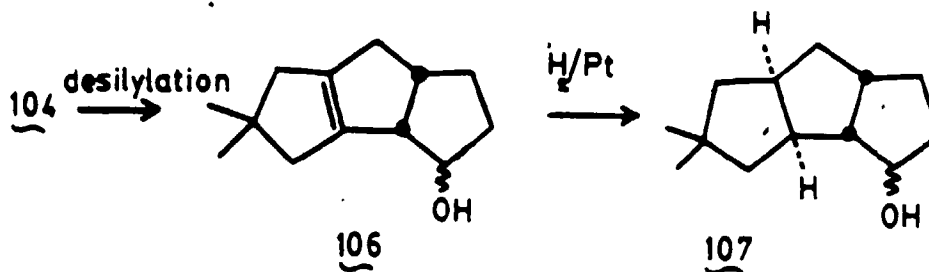
constant between the siloxy methine and the methine hydrogen α to the siloxy group is 3 Hz which indicates that the two hydrogens are trans to each other. Thus the structure of X is assigned as (105a), which is not the regioisomer required in the hirsutene synthesis.

The irradiation of the siloxy methine (4.05 ppm, 3, 3 and 2 Hz) of compound Y showed the chemical shifts and splitting pattern of the ring fusion methine α to the $-\text{OSiMe}_2^t\text{Bu}$ group. It appeared at 2.95 ppm (2 and 8 Hz) and so is coupled to two adjacent H-atoms. Only species (104) can have a methine hydrogen α to the siloxy group with two adjacent hydrogen atoms, disclosing the structure of Y as (104). The coupling constant between the siloxy methine and the methine hydrogen α to the siloxy group is 2 Hz which suggests that the two hydrogens are trans to each other. Hence the structure of Y is assigned as (104a). The other methine proton appeared at 3.25 ppm (tq 8, 8, 8, 3 and 3 Hz).

Similarly, the irradiation of the siloxy methine (4.6 ppm; 5, 3 and 8 Hz) of compound Z showed the chemical shift and splitting pattern of the ring fusion methine α to the $-\text{OSiMe}_2^t\text{Bu}$ group which appeared at 3.05 ppm (8, 8, 4 and 7 Hz) showing it as being coupled to four adjacent hydrogen atoms. The coupling constant between the siloxy methine and the methine hydrogen α to the siloxy group is 8 Hz which confirms that the two hydrogens are cis to each other. The other methine proton appeared at 2.95 ppm (m).

These spectral data support the assignment of compound 2 as the regioisomer (105b).

Desilylation of (104), followed by hydrogenation will give the corresponding alcohol (107) (Scheme 32) (both of these steps are described in Chapter 3).



SCHEME 32

The species (107) is an intermediate in published synthesis of hirsutene.²¹ These results clearly demonstrate that the protection of the hydroxyl group by the dimethyl-tert-butylsilyloxy group effectively inhibited the presumed retro-aldol isomerization of the regioisomer (103), and the reduced polarity of the olefin mixture following treatment with McMurry's reagent made it easily separable from the polar reaction mixture.

The above model study clearly demonstrated that the photochemical cycloaddition/reductive cyclization sequence can be effectively utilized to synthesize the hirsutene skeleton. It also suggests that this methodology could be applied to the synthesis of more complex naturally occurring tricyclic undecane systems.

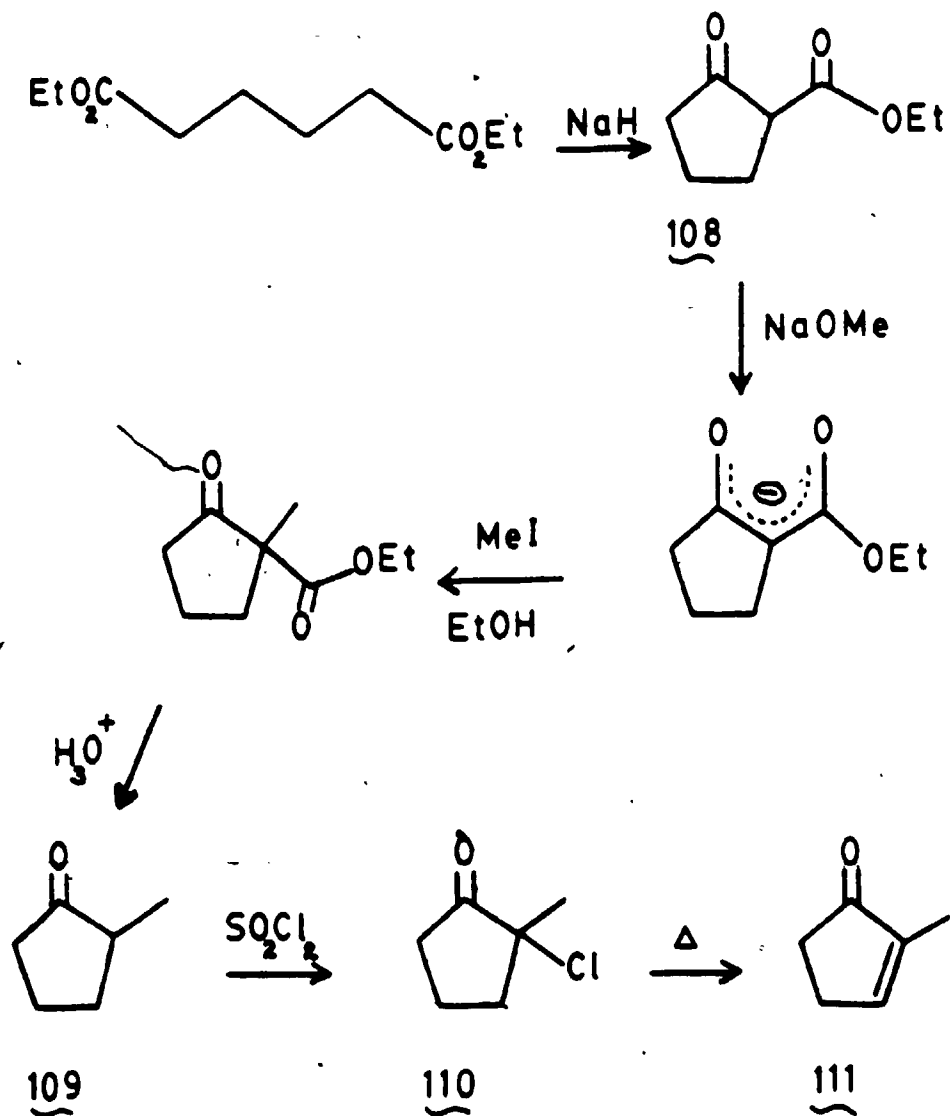
CHAPTER 3

TOTAL SYNTHESIS OF (±)-HIRSUTENE

3.1 SYNTHESIS OF 2-METHYL-2-CYCLOPENTENE-1-ONE

2-Methyl-2-cyclopentene-1-one (111) is a useful synthetic starting material and many routes for its preparation have been reported.^{27a,57} However, the majority of these routes are inconvenient in terms of time or expense, especially if large quantities are required. Perhaps the simplest and most economic route described hitherto involves mono-epoxidation of methylcyclopentadiene followed by hydrolysis, dehydration, and rearrangement to give a mixture of 2-methyl-2-cyclopentene-1-one and 3-methyl-2-cyclopentenone in the ratio 9:1.⁵⁷

Gassman et al⁵⁸ reported a method which involves chlorination-dehydrochlorination of 2-methylcyclopentanone (Scheme 33) and proceeds in 79% yield. This route requires condensation of diethyladipate to yield 2-carboethoxycyclopentanone (108), Methylation of (108) using NaOMe and MeI gives 2-methylcyclopentanone (109). Introduction of the α,β -unsaturation was brought about through chlorination with sulfuryl chloride followed by dehydrochlorination. The α -chloroketone is thermally unstable and the unsaturation is introduced during distillation with evolution of hydrochloric acid.



SCHEME 33

Attempted repetition of this method gave low yields, possibly due to the problem of nucleophilic ring opening of the five-membered ring during the methylation step, and due also to polymerization of the α,β -unsaturated ketone during the dehydrochlorination step. The alternative published routes also proved to be somewhat troublesome and time-consuming. This led us to attempt to develop a new simple, fast and inexpensive route to 2-methyl-2-cyclopentene-1-one (III).

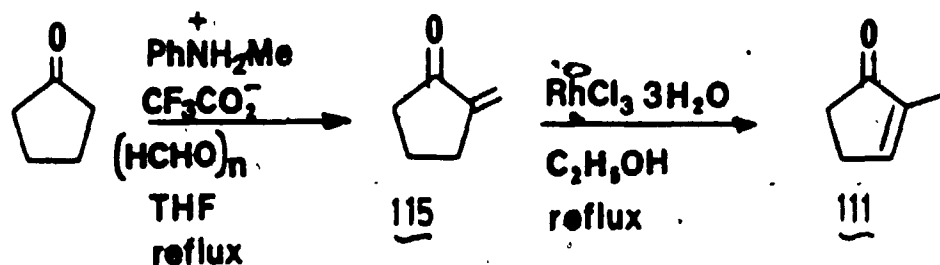
The dye-sensitized photo-oxygenation of mono-olefins results in formation of a dioxetane or a hydroperoxide. The reduction of the hydroperoxide yields an allylic alcohol. The reaction between an olefin and singlet oxygen can follow two distinct courses. Singlet oxygen can attack either the double bond directly to give a dioxetane, or the allylic C-H bond, whereupon an allylically rearranged hydroperoxide is formed via the so-called "ene reaction". Dioxetanes are usually formed from strained or electron-rich double bonds.^{59a,b} However, the production of hydroperoxides requires not only the presence of an allylic C-H bond, but that it effectively conjugates with the adjacent double bond. The formation of the allylic hydroperoxides involves a mechanism where the singlet oxygen approaches the allylic hydrogen and the terminal vinyl carbon atoms simultaneously and concerted formation of the C-O and O-H bonds occurs (Scheme 34). The reaction was proposed as the main step in a new synthetic



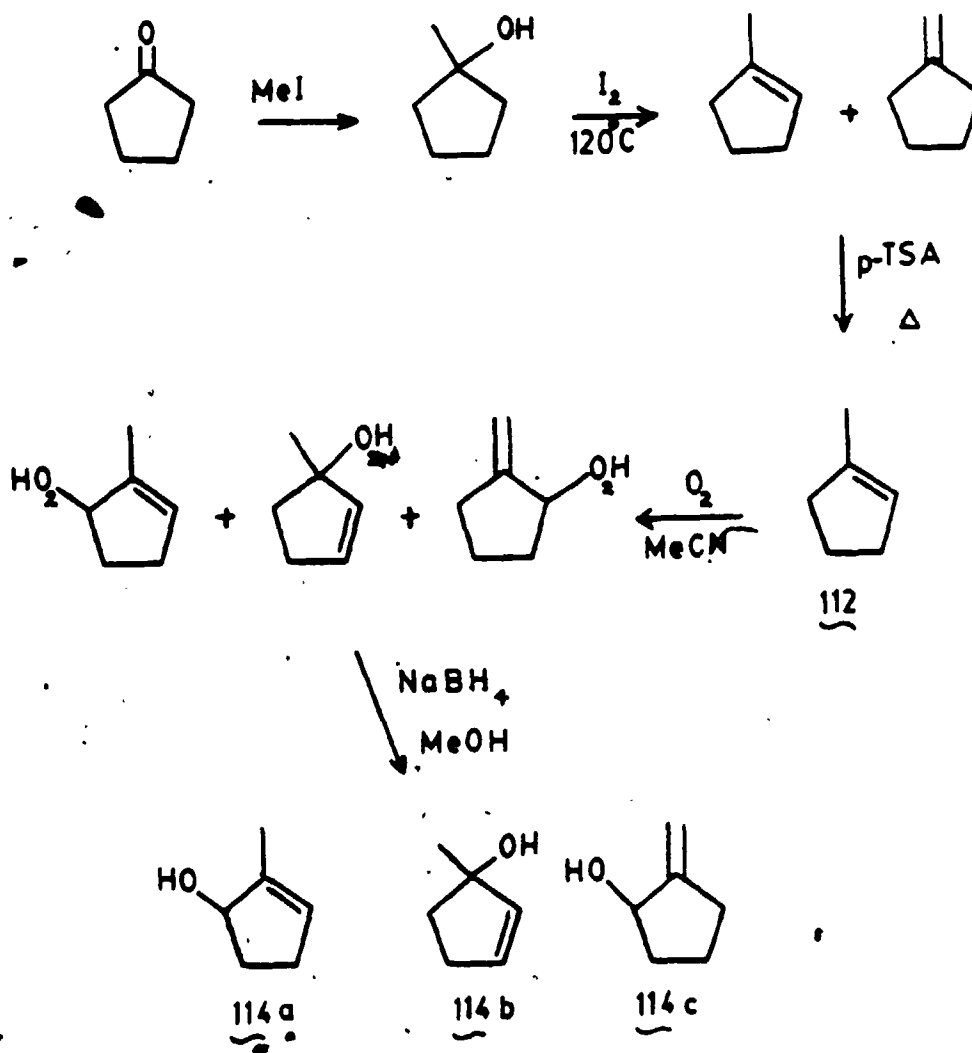
SCHEME 34

route to 2-methyl-2-cyclopentene-1-one.

1-Methylcyclopentene (112) was prepared by the Grignard reaction of cyclopentanone with methyl iodide followed by dehydration in the presence of I_2 and subsequent isomerization in the presence of *p*-toluenesulfonic acid (Scheme 35). 1-Methylcyclopentene (112) was then reacted with singlet oxygen to give a mixture of hydroperoxides which was reduced to give three alcohols (114a, 114b and 114c). Although the required alcohol (114a) was formed, the yield was found to be low and the separation of the mixture of alcohols was proved difficult, which made this method unsatisfactory. An alternative two-step synthetic route to 2-methyl-2-cyclopentene-1-one⁶⁰ is shown in the scheme below (Scheme 36).



SCHEME 36



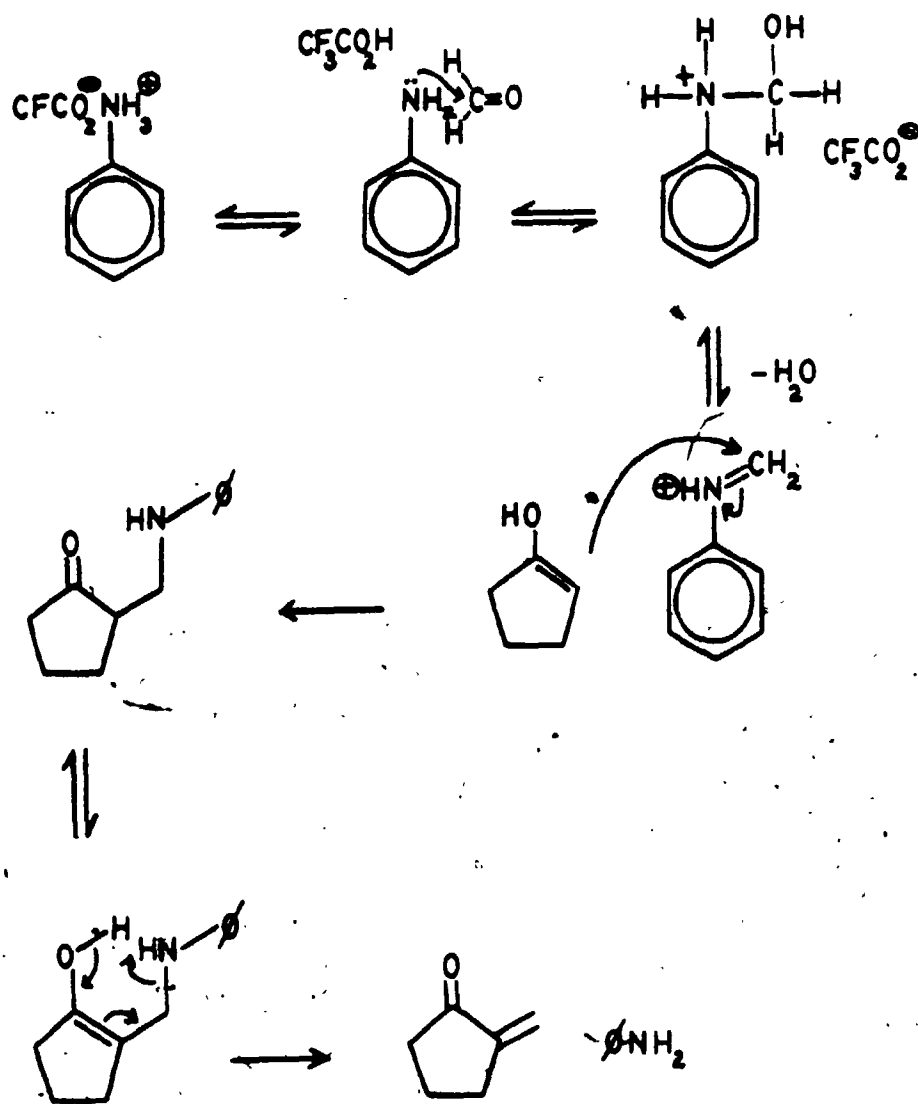
SCHEME 35

The scheme consists of the condensation of formaldehyde with cyclopentanone to give 2-methylenecyclopentanone, followed by $\text{RhCl}_3 \cdot 3\text{H}_2\text{O}$ catalyzed rearrangement of the endocyclic isomer.

Gras has reported⁶¹ that 2-methylenecyclopentanone can be prepared in quantitative yields by treatment of cyclopentanone with trioxane in tetrahydrofuran in the presence of the trifluoroacetic acid salt of N-methylaniline (TAMA). Unfortunately, this reaction could not be reproduced; all attempts resulted in no reaction. However, substitution of paraformaldehyde for trioxane did result in the formation of 2-methylenecyclopentanone (115) as the major product. This suggests that the report by Gras that trioxane is suitable as a source of formaldehyde in this reaction is in error. 2-Methylenecyclopentanone is a very labile species and undergoes polymerization under acidic conditions at higher temperatures and at higher concentrations. 2-Methylenecyclopentanone was prepared under an acidic environment at 67°C (boiling point of tetrahydrofuran) which was the ideal situation for polymerization. Longer reaction times lead to higher conversion of the starting materials to products with the expense of product polymerization. Hence it was necessary to obtain the optimum conditions which were instituted as 14 min of refluxing time or 60% conversion. Increase of cyclopentanone concentration, too, led to higher product formation but again had to encounter the problem of

polymerization. After further experimentation the optimum formation (as indicated by gas-liquid chromatography) of the product 2-methylenecyclopentanone could be obtained at a molar ratio of 0.288:0.119 of N-methylanilinium-trifluoroacetate and cyclopentanone. Another obstacle was the low solubility of paraformaldehyde (the source of formaldehyde) in tetrahydrofuran. This could be done either by increasing the temperature, which is out of the question, or by changing the solvent. Replacement of THF by dimethylformamide and dimethylsulfoxide (in both these solvents the solubility of paraformaldehyde was higher compared to THF) gave either no or very low 2-methylenecyclopentanone formation. Increasing the volume of tetrahydrofuran also increased the yield of the product, which may be due to the enhanced solubility of paraformaldehyde and slower polymerization of the product due to low concentration of 2-methylenecyclopentanone. However the volume of tetrahydrofuran was limited to 250 mL for 10 g of cyclopentanone due to the difficulty of handling large volumes in making large quantities of 2-methylenecyclopentanone.

The role of N-methylaniliniumtrifluoroacetate is catalytic (Scheme 37) and both aniline and trifluoroacetic acid are retained at the end of the reaction. Following 14 min of refluxing the reaction mixture was diluted with diethyl ether, followed by cooling in ice and successive washing with 50% aqueous hydrochloric acid and saturated

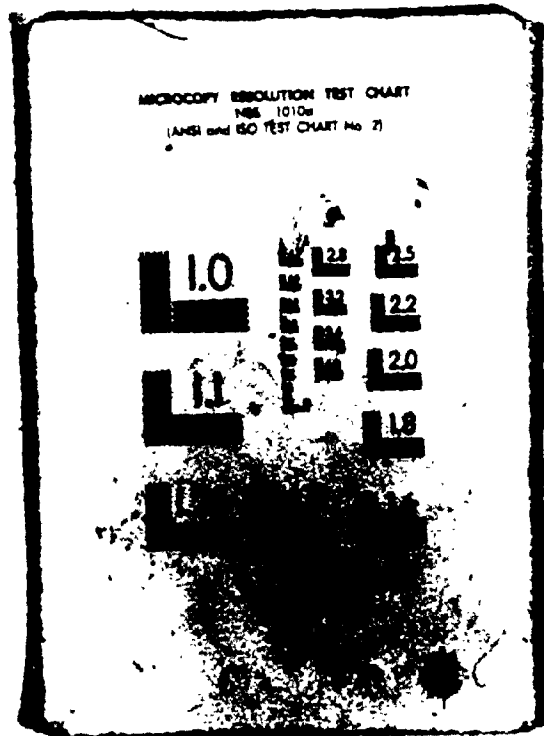


SCHEME 37

aqueous sodium hydrogen carbonate to which excess solid sodium hydrogen carbonate was added in portions to ensure complete neutralization of acid and to inhibit any polymerization. Following the aqueous work-up the crude 2-methylenecyclopentanone (contaminated with unconverted cyclopentanone) was smoothly converted to 2-methyl-2-cyclopentenone by refluxing an ethanolic solution with a catalytic quantity of rhodium trichloride. The catalyst, which is moderately expensive, can be recovered by simple filtration at the end of the reaction. The use of Al_2O_3 as the catalyst instead of rhodium trichloride did not lead to the desired products. Andrieux et al⁶² have reported this procedure for the conversion of 2-alkylidenecyclopentanone to 2-alkylcyclopent-2-en-1-ones in less than one day. The overall yield of isolated product (107) following distillation was 15-20%, and is higher if allowance is made for recovered cyclopentanone. The reaction can also be performed in "one pot" if desired by adding rhodium trichloride to the reaction mixture after condensation of formaldehyde with cyclopentanone, but yields are lower and the catalyst is less easily recovered.

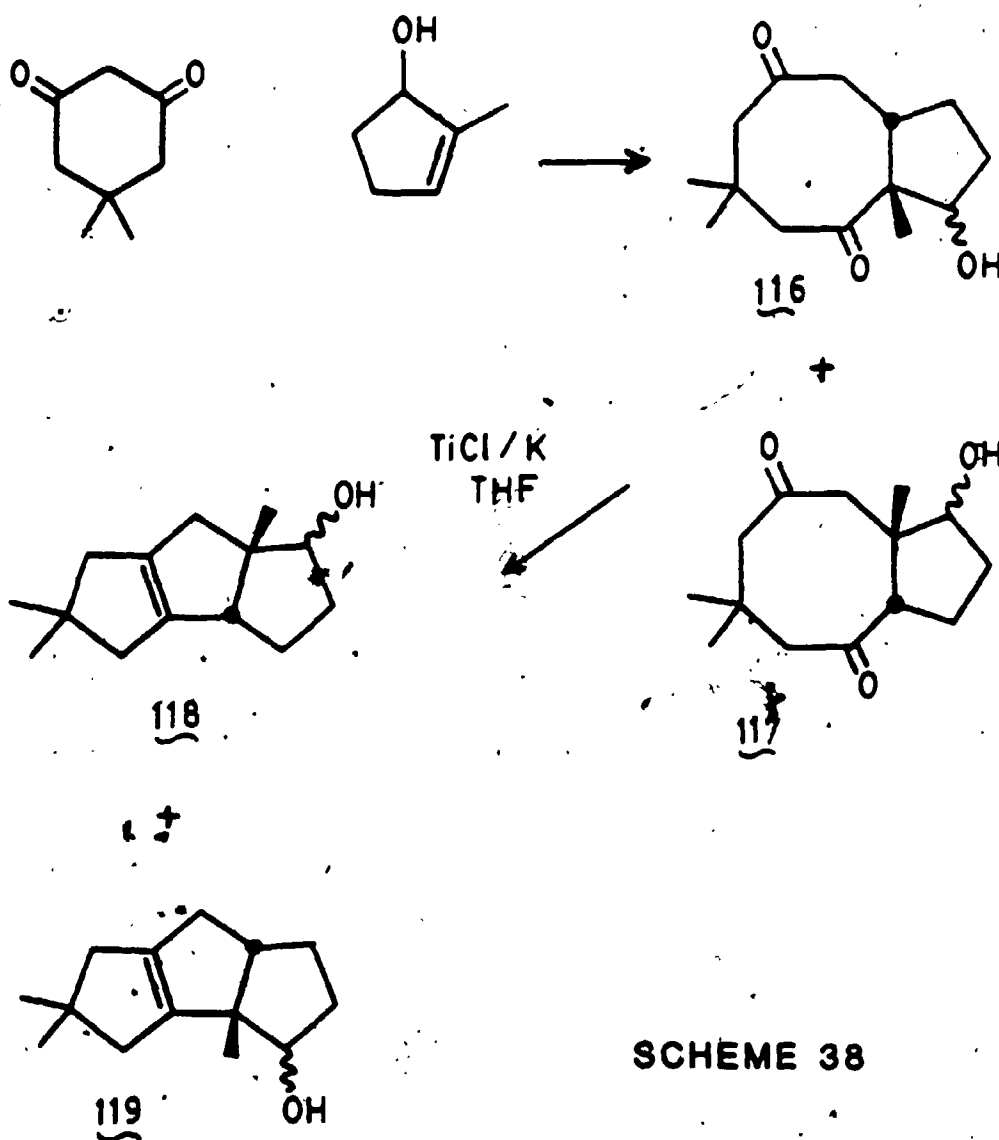
2-Methyl-2-cyclopentenone was reduced with lithium aluminium hydride to give the corresponding alcohol 2-methyl-2-cyclopentene-1-ol in quantitative yields.

2



3.2 FORMAL SYNTHESIS OF (±)-HIRSUTENE

Irradiation of a 1% solution of 5,5-dimethylcyclohexane-1,3-dione and 2-methyl-2-cyclopentene-1-ol using uv light of wavelength 254 nm gave a mixture of two products as analyzed by glc (Scheme 38).

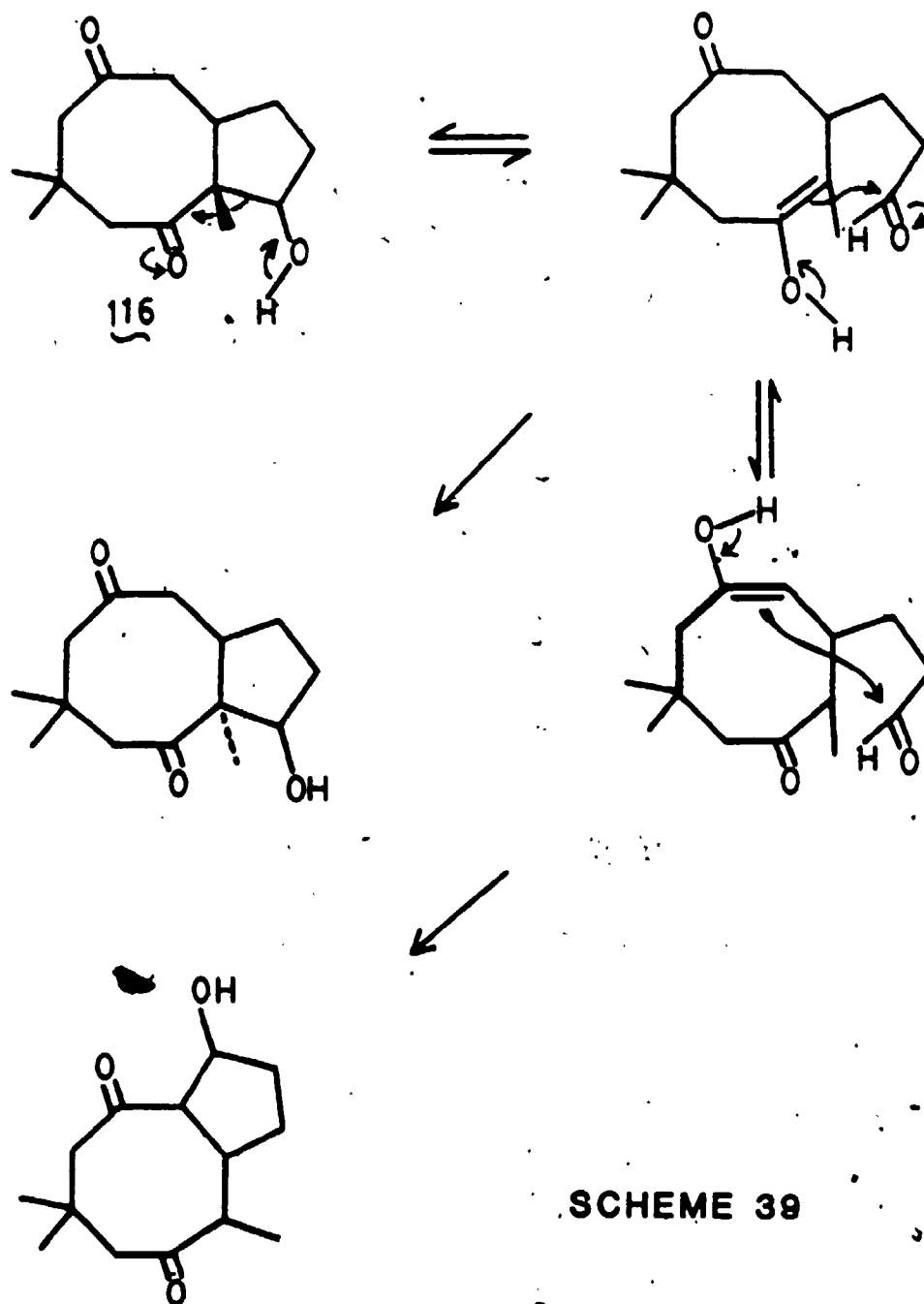


SCHEME 38

Gas-liquid chromatographic/mass spectral coupled analysis showed that the majority of products had masses corresponding to species (116) and (117); but attempts to separate these products were unsuccessful.

Comparison of the ^{13}C nmr spectra of the crude reaction mixture with that of the separated products showed a marked difference in the ^{13}C nmr chemical shifts. As explained in Chapter 2, the cyclobutane adduct obtained from the light-induced cycloaddition of the β -diketone and the olefin, rearranges spontaneously by a retro-aldol opening of the cyclobutane ring to give a 1,5-diketone, retaining the cis-fused ring junction. Although the stereochemistry could be conserved due to the presence of the angular methyl group at the ring junction preventing enolization and epimerization there is the possibility of retro-aldol ring opening leading to undesired products (Scheme 39). This type of ring opening could easily occur and is known to occur on the silica gel surface.

Treatment of the crude mixture of cycloadducts with McMurry's reagent did not lead to the products expected. McMurry's reaction was carried out under basic conditions known to induce isomerization⁵² and ring opening. With the loss of cis stereochemistry at the ring junction the 1,5-diketone is not accessible for the reductive coupling. These results clearly demonstrated the necessity to protect the -OH group to inhibit the loss of stereochemistry at the ring junction. (This was discussed in detail in

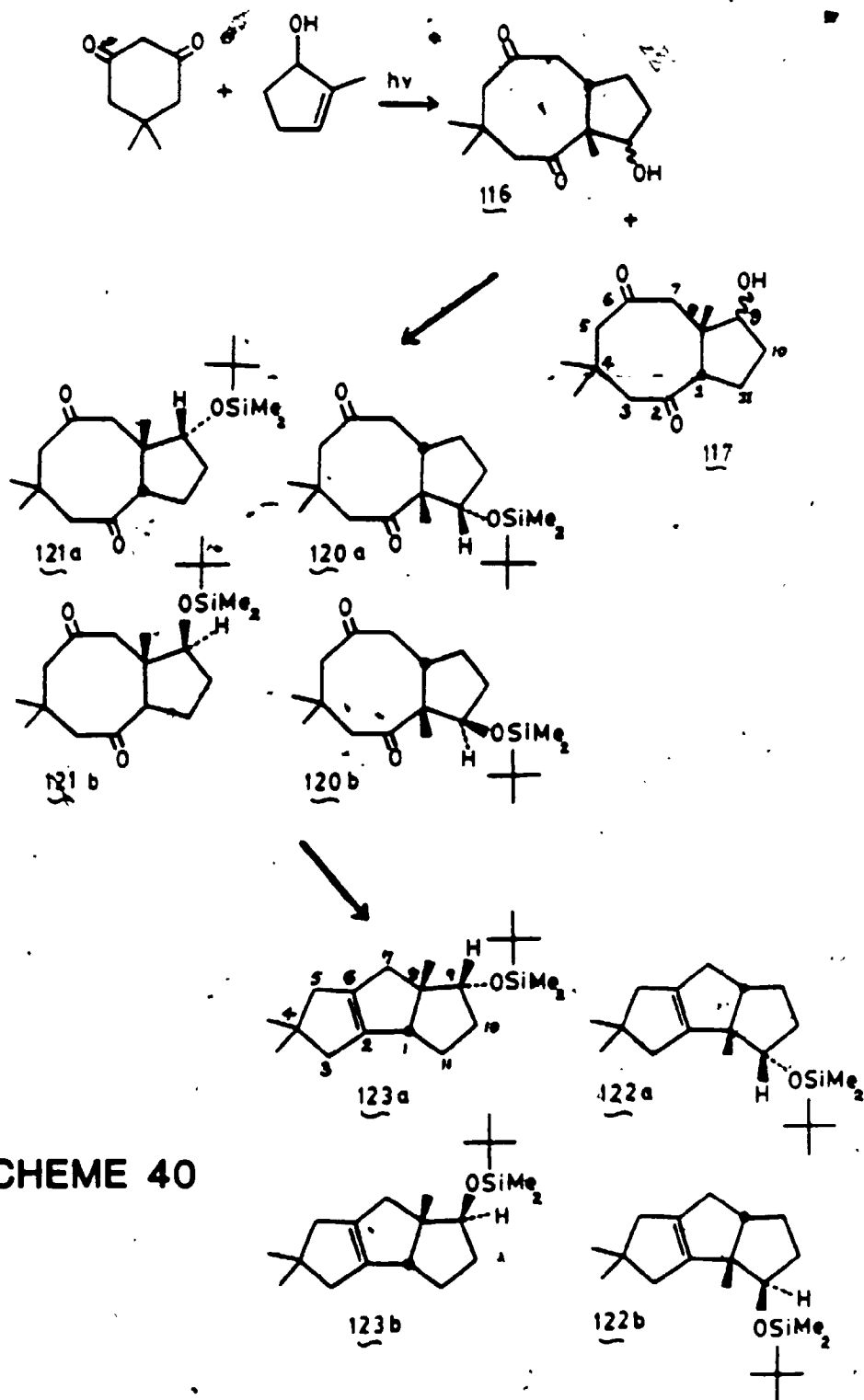


Chapter 2. It was at this point we decided to do a model study to examine the feasibility of the proposed route.)

The crude cycloadduct product mixture which consisted of the hydroxy diketones (116) and (117) was silylated with tert-butyldimethylsilyl chloride to produce a mixture of tert-butyldimethylsilyl derivatives in a combined yield of 89% (Scheme 40); separation by column chromatography gave three major compounds as analyzed by glc (the three compounds were named L, M and N for simplicity). Mass spectral data showed all three compounds having a precise mass which corresponded to the regioisomers (120) and (121). The ^{13}C nmr spectra of the three compounds indicated each compound contained 20 carbon atoms including 8CH_2 , 5CH_2 , 2CH , 3C and 2 carbonyl carbon atoms. The regiochemistries of these compounds were determined by comparing the ^{13}C nmr spectra with those of (102) and (103). The ^{13}C nmr chemical shifts of the methine carbons and the quaternary carbon α to the siloxy methine are given in Table IV.

	L	M	N	103	102
Siloxy Methine	81.1	82.5	80.6	72.6	79.9
Quaternary Carbon α to Siloxy CH	70.65	47.5	47.9	65.9	47.3
CH β to Siloxy CH	53.4	60.3	58.9	37.4	55.9

TABLE IV: ^{13}C nmr chemical shifts of compounds (102), (103), (120) and (121)



SCHEME 40

^{13}C nmr chemical shifts of methine carbons at positions 1 and 8 of compound (103) appeared at 65.9 ppm and 37.4 ppm. Having a methyl group at position 1 will, make the chemical shifts of methine carbons 1 and 8 move downfield.⁵¹ The chemical shift shown by compound L with a quaternary carbon at 70.65 ppm and a methine at 53.4 ppm agrees with the change in chemical shifts predicted by having an angular methyl group at position 1 of compound (103). Hence compound L was assigned the structure (120) (29%). The ^1H nmr shows the siloxy methine proton at 4.05 ppm (dd, 6 and 8.5 Hz) and another methine proton at 3.23 ppm (m, 1 and 1.5 Hz). But from these data the exact stereochemistry of the tert-butyldimethylsiloxy group could not be identified. ^{13}C nmr chemical shifts of methine carbons at positions 8 and 1 of compound (102) appeared at 47.3 ppm and 55.9 ppm. Since compound (103) has an angular methyl group at position 8, the chemical shifts of methine carbons 1 and 8 will move downfield.⁵² The chemical shifts shown by compound M (quaternary carbon at 47.5 ppm and a methine carbon at 60.3 ppm) agree with the changes in chemical shifts predicted. Hence compound M was assigned the structure (121) (29%). The ^1H nmr shows the siloxy methine proton at 3.75 ppm (dd, 8.5 and 6.5 Hz) and the methine at position 1 appears at 3.05 ppm (dd, 8.5 and 6.4 Hz); but these spectral data did not provide sufficient information to determine the exact stereochemistry of the tert-butyldimethylsiloxy group.

Although both epimers of the regioisomer (121) (59%) were isolated, only one could be isolated for the regioisomer (120) (29%). By comparison with the model study, (102) and (103) did not show a difference in the ^{13}C nmr chemical shifts for the epimers, which could be seen in the compounds, (104) and (105), which are rigid molecules. These results show that compound (121) is a relatively rigid molecule. Hence the presence of only one epimer isolated in the regioisomer (120) could be due to:

- a) a more flexible molecule compared to the species (121);
- b) only one epimer is obtained in the initial cycloaddition step;
- c) steric effects present in the silylation step.

The chemical shifts shown by compound N, with a quaternary carbon at 47.9 ppm and a methine carbon at 58.9 ppm, agree with the changes in chemical shifts predicted by having an angular methyl group at position 8 of compound (102).

Hence compound N was assigned the structure (121) (29%).

The ^1H nmr shows the siloxy methine proton at 3.7 ppm (dd, 8 and 6 Hz) and another methine proton at 3.0 ppm (dd, 9 and 4.5 Hz). Again from these data the exact stereochemistry of the tert-butyl dimethylsiloxy group could not be identified. Both compounds M and N have the same regioisomeric structure. This shows that M and N are the two epimers of the regioisomer (121). Refluxing the

mixture of (121) and (120) with McMurry's reagent in dry tetrahydrofuran under dry N₂ positive pressure for 24 h resulted in complete conversion to a product mixture. Comparison with the model studies (Chapter 2) revealed that the time required for the coupling step is much shorter (24 h as compared to 6 days and 2 days). As reasoned earlier this may be due to enhanced steric effects. Separation of the product mixture revealed that it consisted of two compounds (the two compounds were named S and T for convenience). Mass spectral studies of both compounds showed a precise mass which corresponded to species (122) or (123). The ¹³C nmr spectra revealed both species having 20 carbon atoms consisting of 8CH₃, 5CH₂, 2CH, 3C and two alkene carbon atoms. ¹³C nmr chemical shifts of the methine carbons and the quaternary carbon α to the siloxymethine are given in Table V. In the case of

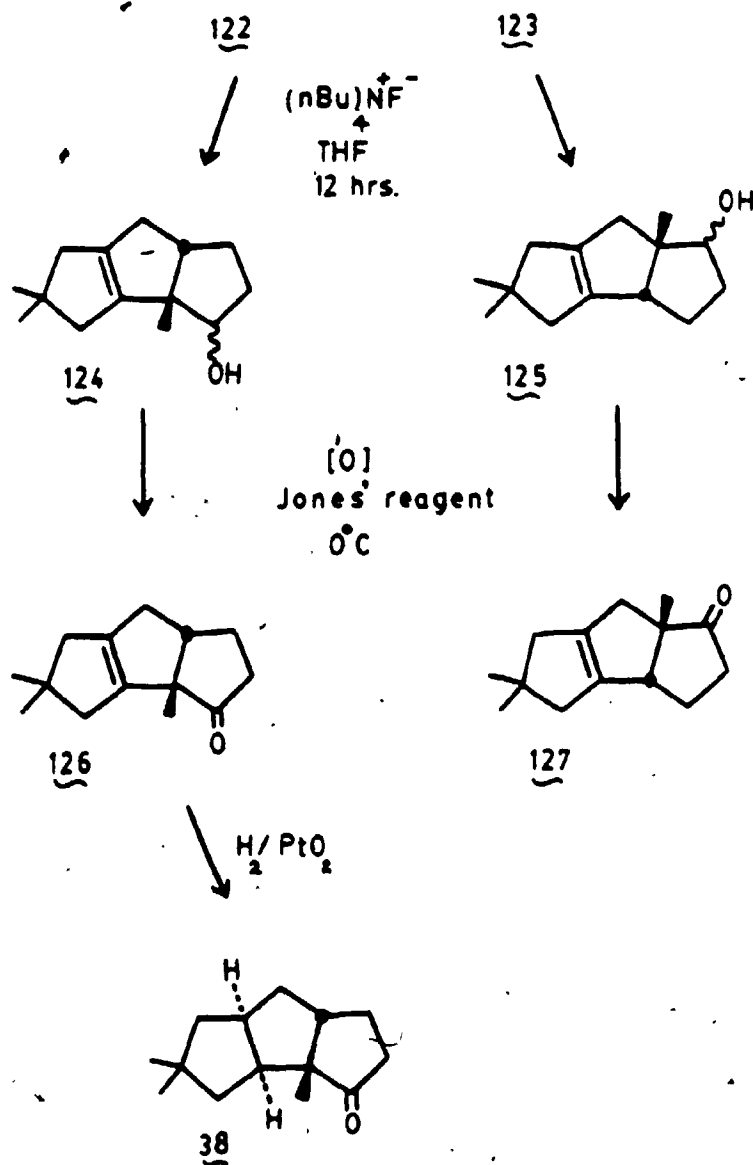
	S	T	104a	105a	105b
Siloxy Methine	81.29	81.57	76.0	81.3	75.5
Carbon α to Siloxy CH	59.2	57.2	57.9	56.3	50.5
CH β to Siloxy CH	53.2	52.6	45.4	45.7	45.5

TABLE V: ¹³C nmr chemical shifts of compounds (104), (105), (122) and (123)

compound (105) the presence of a methyl group at position 8 will move the chemical shift of the siloxy methine 9 and

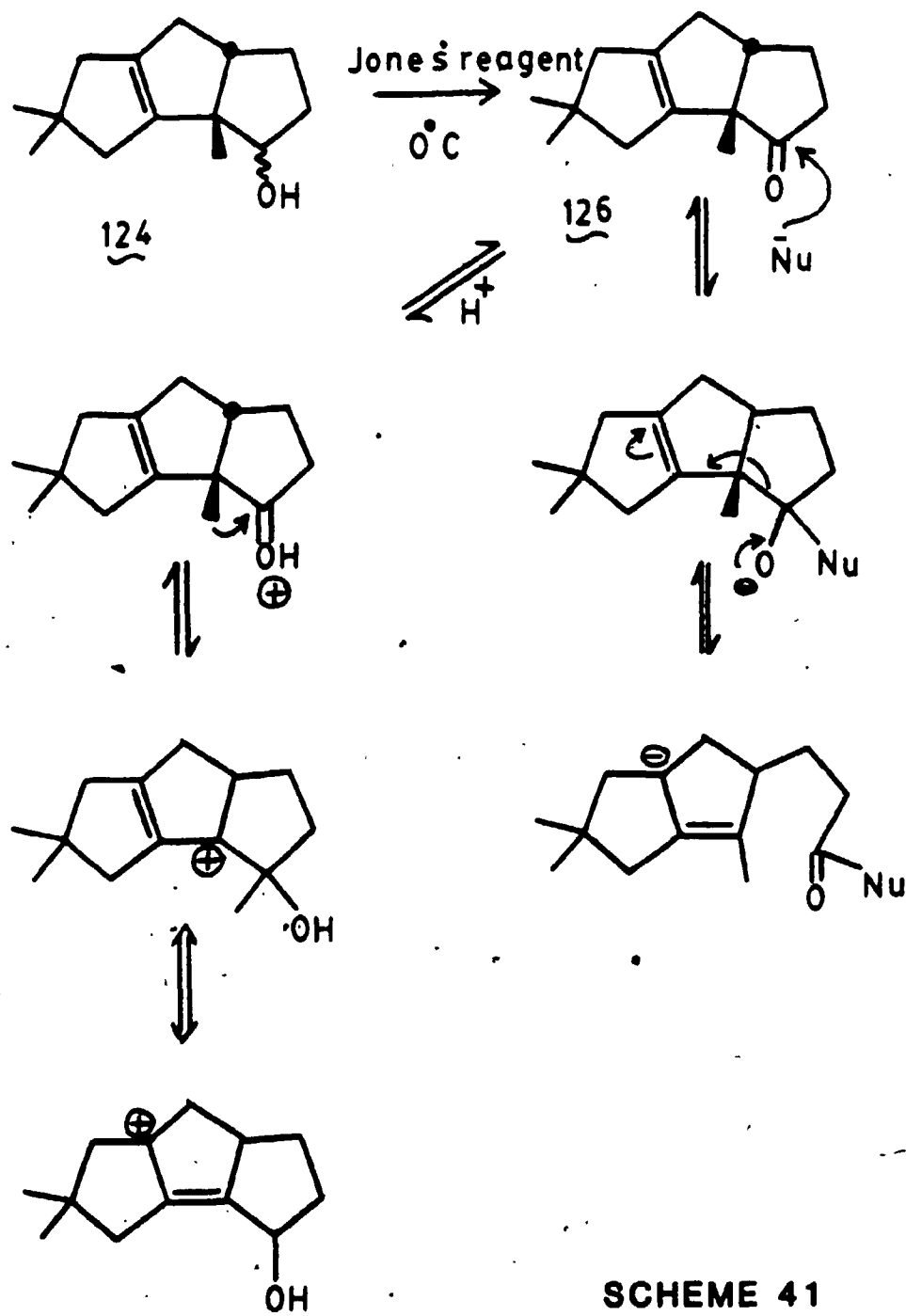
the methine carbon 1 downfield. Similarly in compound (104), having an angular methyl group at position 1 will move the siloxy methine 11 and the methine 8 downfield. But in these compounds, especially in (104a) and (105a), the chemical shift differences of both methine carbons are too small to predict the regiochemistries of species S and T. ^1H nmr decoupling experiments of compound S showed the siloxy methine proton at 3.69 ppm (t, 4 and 4 Hz) and the 1 methine proton at 2.25 ppm (3.5, 9 and 1 Hz). Compound T showed the siloxy methine proton at 3.7 ppm (5, 5 and 0.5 Hz) and the 1 methine proton at 2.6 ppm (2.7, 1.5, 3 and 3 Hz). None of this information could distinguish the regiochemistries of the two compounds. Hence it was decided to regenerate the starting material (the siloxy diketone) by the ozonolysis of the siloxy alkenes.

The siloxy alkene S was dissolved in methylene chloride and ozone was passed through it at -5°C . Subsequent treatment with Zn dust and acetic acid gave a single compound. The ^{13}C nmr and ^1H nmr spectra of this compound were identical with those of (121). This shows that compound S is obtained from the head-tail cycloaddition product and is assigned as (123) (38%). Compound T was therefore assigned the regioisomeric structure (122) (17%). In both these regioisomers the stereochemistry of the tert-butyldimethylsiloxy group could not be determined from the available data.

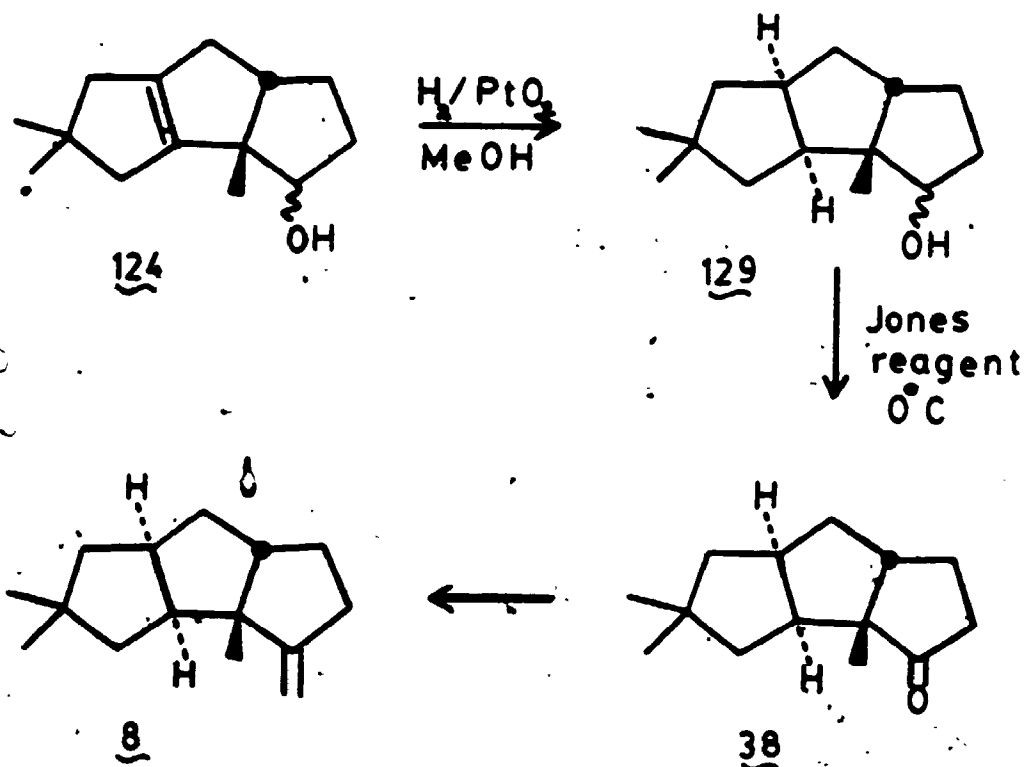


To reach the objective of synthesizing *dl*-hirsutene the siloxy alkene (122) had to be desilylated. Several desilylating agents were used; but the use of tetra-*n*-butylammonium fluoride in dry tetrahydrofuran⁵⁶ gave almost complete desilylation⁵⁶ to give a single compound as analyzed by glc. But the separation of this from the rest of the reaction mixture proved quite difficult and resulted in a low recovery percentage (53%). Mass spectral studies showed the product to have a precise mass of 206.1668 corresponding to compound (124). The ¹³C nmr spectrum showed 14 carbon atoms including 3CH₃, 5CH₂, 2CH, 2C and two alkene carbons. The ¹³C nmr chemical shifts were quite similar to (122) and included a quaternary carbon at 57.5 ppm and a methine carbon at 53.3 ppm. As the reactant was compound (122) the structure of the product was undoubtedly assigned as (124). Similarly desilylation of (123) gave a compound which had a precise mass corresponding to species (125). The ¹³C nmr spectrum showed 14 carbon atoms including 3CH₃, 5CH₂, 2CH, 2C and two alkene carbons. The ¹³C nmr chemical shifts were similar to (123). Hence the product was assigned as (125).

Oxidation of (124) with Jones' reagent at 0°C gave a single compound as analyzed by glc. The isolation of this compound proved difficult and was found to be unstable on silica gel and at room temperature. Glc coupled with mass spectral studies showed that the compound, which has a precise mass of 204.1516, corresponded to species (126).



All attempts to isolate this compound proved unsuccessful. 090
This could be reasoned due to the possibility of nucleophile-initiated ring opening to give an allylic anion, or the acid catalyzed migration of the CH₃ group leading to the allylic cation resulting in undesired products (Scheme 41). Similarly oxidation of (125) gave a yellow-coloured reaction mixture which was separated and purified using a silica gel column to give a single product. Mass spectral studies indicated a precise mass corresponding to species (127). ¹³C nmr spectral studies showed the presence of 14 carbons including a carbonyl carbon at 226.0 ppm. Oxidation of (125) will give a carbonyl carbon at position 9; this will make the quaternary carbon 8 shift downfield and the methine carbon 1 shift upfield.⁵² These chemical shifts were observed in the compound, where the quaternary carbon has shifted from 58.69 ppm to 65.8 ppm and the methine carbon 1 was shifted from 53.1 ppm to 51.6 ppm. These spectral data confirm the structure of the product as (127). The difficulty in obtaining the regioisomer (126) shows the instability of it (Scheme 41) as compared to (127). But it is the regioisomer (126) which is required for the synthesis of hirsutene. The difficulties experienced in isolating the desired isomer (126) resulted in the synthetic scheme being altered, as shown in Scheme 42.



SCHEME 42

As stated earlier the presence of the quaternary carbon in between two sp^2 carbon atoms may make it susceptible to rearrangements (Scheme 41). One approach to overcoming this problem was to reduce the double bond C_2-C_6 prior to the oxidation of the hydroxyl group. Reduction of the double bond utilizing PtO_2/H_2 may then give *cis* hydrogenation²² resulting in the stereochemically more stable *cis-anti-cis* carbon skeleton (129).

Oxidation of (129) will produce the norketone (38) which is an intermediate in a previous published synthesis of hirsutene.

Reduction of compound (124) in methanol in the presence of PtO_2 under a positive hydrogen pressure gave one major compound as analyzed by glc. The ^{13}C nmr data of the crude reaction mixture confirmed the reduction of the $\text{C}_2\text{-C}_6$ double bond, with the disappearance of the quaternary carbons at 145.3 ppm and 142.0 ppm of compound (124). Mass spectral analysis showed this compound to have a precise mass corresponding to compound (129). Neither the ^1H nmr nor ^{13}C nmr chemical shifts could unambiguously prove the stereochemistry of the two methine protons at 2 and 6 positions, although literature precedent predicts that the reduction should give the *cis-anti-cis* products.⁶² Hence, it was decided to oxidize the crude reaction mixture containing (129) to obtain the norketone (38) since the spectral data of (38) has been reported in the literature.^{21b}

Oxidation of the crude reaction mixture containing (129) with Jones' reagent at 0°C gave a single compound as analyzed by glc. Purification and isolation of this proved difficult and hence resulted in a low yield. Mass spectral studies of the product showed a precise mass corresponding to (38). The ^{13}C nmr spectral data indicated the presence of 14 carbon atoms including a carbonyl carbon at 224.5 ppm and a quaternary carbon at 59.4 ppm. The ^{13}C nmr

nmr and ^1H nmr spectral data of this compound were identical to those of the norketone (38) which were provided to us by Professor T. Hudlicky. This confirms that oxidation product was indeed (38) and also the cis-anti-cis stereochemistry in (129). The formal synthesis of hirsutene is completed with this step since norketone (38) is an intermediate in a previously published synthesis of hirsutene.

CHAPTER 4
EXPERIMENTAL

4.1 **EXPERIMENTAL**

Melting points and boiling points are uncorrected. Melting points were determined on a Koffler hot stage melting point apparatus. Ir spectra were recorded with a Beckmann 4250 spectrometer. Ultra-violet spectra were recorded on a Cary 118 uv-visible spectrometer and on a Hewlett Packard 8450A diode array spectrophotometer. Mass spectra were obtained on a Varian MAT-311A spectrometer at 70 eV (direct inlet). Determined exact masses are reported for molecular ions. Routine proton magnetic resonance spectra (^1H nmr) were obtained on a Varian T-60 instrument, and those of pure samples were obtained with Varian XL-200 and XL-300 spectrometers. Both of these instruments were used to obtain the ^{13}C nmr spectra. Methyl, methylene, methine and quaternary signals were identified by comparing the fully decoupled spectra with the APT^{63a} and DEPT.^{63b} The chemical shifts are given in parts per million (ppm) downfield from tetramethylsilane (Me_4Si) in δ units and coupling constants are given in cycles per second (Hz): The data is reported as: chemical shift, multiplicity (s = singlet, d = doublet, t = triplet, q = quartet, m = multiplet, dd = double doublet, dt = double triplet,

etc.), number of protons, coupling constants and assignments.

Gas-liquid chromatography (glc) analyses were done using 0.2' x 6" glass and copper columns packed with 5% S.E. 30 on Chemisorb W columns with Varian 2400, Varian 90-P and Aerograph A90-P3 instruments, and with a Hewlett Packard 3390A integrator. All retention times were recorded with a flow rate of 30 mL min⁻¹. Thin layer chromatography (tlc) was done on Kiesel gel 50 F₂₅₄ plates. Thick layer chromatography (plc) was performed using Kiesel gel F₂₅₄ on glass plates. Open-column chromatography was performed using Kiesel gel. All irradiations were performed using a Rayonet reactor equipped with a low pressure mercury lamp. Solutions were degassed with dry nitrogen gas before irradiation and were irradiated in quartz tubes and the course of the reaction was followed by gas-liquid chromatography (glc).

Reagent grade solvents were used for all reactions. Tetrahydrofuran was freshly distilled before use from sodium and benzophenone. Anhydrous ethyl ether was Baker reagent grade and was used without further purification. All anhydrous reactions were performed under a dry nitrogen atmosphere with all glassware being dried overnight in a drying oven at 150°C prior to use. Assembly of the reaction apparatus was conducted under a flow of dry nitrogen with the glassware being heated with a hot gun before being closed to the atmosphere. The drying agent

used in all reactions was potassium carbonate anhydrous (K_2CO_3 , an) 'Baker Analyzed' reagents.

2-Cyclopentenol

2-Cyclopentenone was prepared by the reaction of cyclopentene with singlet oxygen in the presence of acetic anhydride and pyridine in methylene chloride utilizing tetratolylporphyrin as the sensitizer instead of 4-(dimethylamino)pyridin as reported in the literature.^{59b} 2-Cyclopentenone was reduced with $LiAlH_4$ in dry diethyl ether under positive dry nitrogen pressure to give 2-cyclopentenol.

Bicyclo[6.3.0]-4,4-dimethyl-11-hydroxyundecane-2,6-dione (89) and Bicyclo[6.3.0]-4,4-dimethyl-9-hydroxyundecane-2,6-dione (90)

Irradiation of a solution of 5,5-dimethylcyclohexane-1,3-dione (dimedone) (250 mg, 1.78 mmol) in methanol in the presence of excess 2-cyclopentenol (1.9 g, 1.9 mmol) using uv light of wavelength 254 nm resulted in complete conversion (72 h) of the diketone to a mixture of products as analyzed by glc; retention times 7.49 and 8.01 at program temperature 130-200°C (10°C/min) in the column 5% S.E. 30 on Chemisorb W. The reaction mixture was concentrated at reduced pressure at room temperature to give a yellow-coloured oil. ^{13}C nmr of this showed the presence of two major compounds. These (235 mg) were separated using 50 g of

silica gel (60-200 mesh, Baker Analyzed reagent) using hexane/diethyl ether/methanol as solvents, to give 89 (72 mg) and 90 (92 mg).

89; a crystalline white solid (recrystallized from n-hexane). M.p. 91-94°C. ¹H nmr (CDCl₃): 4.6 ppm (q, 1H, 8 Hz, ¹CH.OH), 3.1 (m, 1H, ⁸CH), 2.85 ppm (t, 1H, J = 8 Hz, ¹CH), 2.75 ppm (d, 1H, J = 12 Hz, ⁵CH₂), 2.45 ppm (d, 1H, J = 12 Hz, ⁵CH₂), 2.4 ppm (d, 1H, J = 12 Hz, ³CH₂), 2.6 ppm (d, 1H, J = 12 Hz, ³CH₂), 1.05 ppm (s, 3H, CH₃), 2.5 ppm (m, 2H, CH₂), 1.4-1.5 ppm (m, 4H, CH₂). Ir (NaCl, film) 1680 cm⁻¹, 3550 cm⁻¹. ¹³C nmr (CDCl₃), 71.4 (CH.OH), 65.8 (¹CH), 53.0, 52.4 and 49.9 (CH₂ α to C=O), 36.6 (⁸CH), 35.4 (⁴C), 30.6 and 30.1 (CH₂), 32.5 and 27.6 (CH₃), 211.5 and 210.5 (C=O); exact mass m/e 224.14101.

90; crystalline white solid (recrystallized from n-hexane). M.p. 100-103°C. ¹H nmr (CDCl₃): 4.0 ppm (dt, 1H, J = 1.57, 5.75 Hz, ⁹CH), 3.45 ppm (dt, 1H, J = 6, 8 Hz, ¹CH), 2.95 ppm (m, 1H, J = 6, 1.57, 4 and 10, ⁸CH), 2.7 ppm (d, 1H, J = 12, CH₂ α to C=O), 2.6 ppm (d, 1H, J = 12, CH₂ α to C=O), 1.1 ppm (s, 6H, CH₃), 2.0-2.2 (4H, CH₂ α to C=O), 1.5-1.8 ppm (m, 4H, CH₂). Ir (NaCl, film) 1690 cm⁻¹, 3580 cm⁻¹; ¹³C nmr (CDCl₃), 56.1 (¹CH), 211.1 and 210.2 (C=O), 52.2, 52.6 and 45.3 (CH₂ α to C=O), 35.3 (⁴C), 46.8 (⁸CH), 79.4 (CH.OH), 20.5 and 32.0 (CH₂), 32.8 and 27.3 (CH₃); exact mass m/e 224.14098.

Bicyclo[6.3.0]-4,4-dimethylundecane-2,6,11-trione (91) and
Bicyclo[6.3.0]-4,4-dimethylundecane-2,6,9-trione (92)

A mixture of 89 and 90 (350 mg) was dissolved in 15 mL of acetone at 0°C, 4 mL of Jones' reagent (6.7 g of CrO₃ in 15.5 mL of H₂O and 5.8 mL of H₂SO₄) was added slowly, maintaining the temperature until the reaction mixture became orange. Stirring continued for 1/2 h, added a few drops of 2-propanol until the reaction mixture became green, which was then diluted with diethyl ether, filtered, and concentrated under reduced pressure. This was again extracted with ether, several times; combined ether extracts were dried over K₂CO₃ (an) and concentrated under reduced pressure (506 mg). The reaction was followed by glc on a 5% S.E. 30 on Chemisorb W column, with a retention time of 6.67 min at program temperature 130-200°C [10°C/min]. Column chromatographic separation of the crude reaction mixture using 50 g of silica gel and hexane/diethyl ether as the solvent system, gave one major compound as analyzed by glc.

92; crystalline white solid (recrystallized by hexane/diethyl ether). M.p. 130.5-131°C. ¹H nmr (CDCl₃): 3.05 ppm (dd, 1H, J = 16 and 3 Hz, ⁷CH₂), 2.76 ppm (m, 1H, J = 12, 10, 7.5 Hz, ¹CH), 2.48 ppm (d, 1H, J = 12 Hz, ⁵CH₂), 2.39 ppm (d, 1H, J = 12 Hz, ⁴CH₂), 2.26 ppm (dd, 1H, J = 12 and 12 Hz, ⁷CH₂), 2.24 ppm (dd, 1H, J = 12 and 9.5 Hz, ¹⁰CH₂), 2.19 ppm (m, 1H, ¹⁰CH₂), 2.12 ppm (d, 1H, J = 12 Hz, ⁵CH₂), 2.06 ppm (m, 2H, ¹¹CH₂), 1.12 ppm (s, 3H,

CH₃), 1.09 ppm (s, 3H, CH₃). Ir (NaCl, film); 1690 cm⁻¹, 1730 cm⁻¹. ¹³C NMR (CDCl₃): 214.07, 209.9 and 209.29 (C=O), 56.7 (¹CH), 49.7 (²CH), 52.3, 50.47, 45.1 and 36.0 (CH₂ α to C=O), 36.1 (C), 22.6 (CH₂), 30.7 and 29.3 (CH₃).

4,4-Dimethyl-2,6-dehydro-11-hydroxytricyclo[6.3.0.0^{2,6}]-undecane (93) and 4,4-Dimethyl-2,6-dehydro-9-hydroxytricyclo[6.3.0.0^{2,6}]-undecane (94)

Potassium metal washed with dry tetrahydrofuran (3.3 g) was added to a stirred slurry of TiCl₃ (3.6 g) in 150 mL of dry tetrahydrofuran at room temperature under dry nitrogen. After refluxing for 1 h the black reaction mixture was cooled to room temperature and a crude reaction mixture of cycloadducts consisting of 89 and 90 (323 mg) in 5 mL of dry tetrahydrofuran was added; the mixture was refluxed under dry nitrogen for 4 x 24 h and was monitored by glc; cooled in ice, added methanol (75 mL) to quench the reaction, filtered through celite, concentrated under reduced pressure and the concentrated reaction mixture was extracted with 3 x 50 mL of dry diethyl ether. The ether extracts were concentrated under reduced pressure to give a yellow oil (252 mg). Glc analysis shows predominantly one compound with a retention time of 3.7 min on program temperature 130-200°C [10°C/min] in the column 5% S.E. 30 on Chemisorb W. Column chromatographic separation, using 10 g of silica gel and 10% diethyl ether/hexane as the solvent gave one major compound, 94.

94; ^1H nmr (CDCl_3): 3.95 ppm (dt, 1H, $J = 4$ and 2 Hz, ^9CH), 3.6 ppm (dt, 1H, $J = 8$ and 2 Hz, ^1CH), 2.85 ppm (ddt, 1H, $J = 8, 2$ and 4 Hz, ^8CH), 2.5 ppm (dd, 1H, $J = 16$ and 8 Hz, $^7\text{CH}_2$), 1.95-1.85 ppm (m, 5H, CH_2), 1.55-1.3 ppm (m, 4H, CH_2), 1.1 ppm (s, 3H, CH_3), 1.05 ppm (s, 3H, CH_3).

Ir (NaCl, film); 3610 cm^{-1} . ^{13}C nmr (CDCl_3): 146.0 and 141.1 (C=O), 81.3 ($^9\text{CH.OH}$), 56.2 (^1CH), 46.4 (^8CH), 45.4 (C), 45.8, 44.5, 35.6, 34.2 and 27.1 (CH_2), 31.3 and 31.1 (CH_3); exact mass m/e 192.15182.

Bicyclo[6.3.0]-4,4-dimethyl-11-(tert-butyldimethylsiloxy)-undecane-2,6-dione (103) and Bicyclo[6.3.0]-4,4(dimethyl)-(tert-butyldimethylsiloxy)-undecane-2,6-dion (102)

Tert-butyldimethylsilyl chloride (1.6 g, 1.8 eq) and imidazole (1.5 g, 3.6 eq) was dissolved in dimethylformamide (1 mL) at room temperature; after 10 min this was added to the cycloadduct product mixture consisting of 89 and 90 (244 mg) in methylene chloride (5 mL) at 0°C , stirred for 12 h at room temperature, diluted with diethyl ether (50 mL), washed with H_2O (3 x 10 mL), dried the ether layer with K_2CO_3 (an), concentrated under reduced pressure at room temperature to give a yellow oil. Glc analysis showed this as a mixture of two major compounds (1.16 g); retention times of 9.8 and 10.5 min at program temperature $130\text{-}200^\circ\text{C}$ [$10^\circ\text{C}/\text{min}$] in the column 5% S.E. 30 on Chemisorb W. This was separated using 150 g of silica gel (60-200 mesh) and 50% diethyl

ether/ n-pentane as the solvent to give 103 (140 mg, 39.5%)
and 102 (156 mg, 43%).

103; ^1H nmr (CDCl_3): 4.55 ppm (dt, 1H, $J = 6.5, 6$ Hz, $\text{CH}_2\text{OSi}^t\text{BuMe}_2$), 3.0 δ (m, 1H, ^9CH), 2.8 ppm (dd, 1H, $J = 6$ and 8 Hz, ^1CH), 2.85 ppm (d, 1H, $J = 12.5$ Hz, CH_2 α to C=O), 2.4 ppm (d, 1H, $J = 12.5$ Hz, CH_2 α to C=O), 2.35 ppm (d, 1H, $J = 12.5$ Hz, CH_2 α to C=O), 2.25 ppm (d, 1H, $J = 12.5$ Hz, CH_2 α to C=O), 2.1 ppm (d, 2H, $J = 12.5$ Hz, $^7\text{CH}_2$), 1.7-1.5 ppm (m, 4H, CH_2), 1.05 ppm (s, 6H, CH_3), 0.85 ppm (s, 9H, t-Bu), 0.05 ppm (s, 6H, CH_3). ^{13}C nmr (CDCl_3): 65.9 (^1CH), 215.9 and 210.8 (C=O), 51.7, 54.2 and 50.4 (CH_2 α to C=O), 37.4 (^9CH), 30.9 and 32.4 (CH_2), 72.6 (^{11}CH), 27.5 and 32.6 (CH_3), 17.9 (C), 25.7 (t-Bu), -4.4 and -4.6 (Si- CH_2), 35.6 (^4C).

102; ^1H nmr (CDCl_3): 3.9 ppm (dt, 1H, $J = 1.5$ and 4 Hz, ^9CH), 3.3 ppm (dt, 1H, $J = 8$ and 6 Hz, ^1CH), 2.9 ppm (m, 1H, $J = 9, 1.5, 6$ and 4 Hz, ^8CH), 2.6 ppm (d, 2H, $J = 12.5$ Hz, CH_2 α to C=O), 2.3-2.1 ppm (4H, CH_2 α to C=O), 1.6-1.2 ppm (m, 4H, CH_2), 1.05 ppm (s, 6H, CH_3), 0.85 ppm (s, 9H, t-Bu), 0.05 ppm (s, 6H, CH_3). ^{13}C nmr (CDCl_3): 55.9 (^1CH), 212.9 and 211.7 (C=O), 35.1 (C), 47.3 (^9CH), 79.9 (^8CH), 32.3 and 20.5 (CH_2), 27.5 and 32.5 (CH_3), 17.9 (C), 25.7 (t-Bu), -4.7 and -4.8 (Si- CH_3).

4,4-Dimethyl-2,6-dehydro-1 β ,8 β -dihydro-11 β -(tert-butyl-dimethylsiloxy)-tricyclo[6.3.0.0^{2,6}]undecane, (104a);
4,4-Dimethyl-2,6-dehydro-1 β -8 β -dihydro-11 α -
(tert-butyl-dimethylsiloxy)-tricyclo[6.3.0.0^{2,6}]undecane,
(104b); 4,4-dimethyl-2,6-dehydro-1 β ,8 β -dihydro-9 β -
(tert-butyl-dimethylsiloxy)-tricyclo[6.3.0.0^{2,6}]undecane,
(105a); and 4,4-Dimethyl-2,6-dehydro-1 β ,8 β -dihydro-9 α -
(tert-butyl-dimethylsiloxy)-tricyclo[6.3.0.0^{2,6}]undecane,
(105b)

Potassium metal (3.3 g) was washed with dry tetrahydrofuran to remove oil and was added to a stirred slurry of TiCl₃ (3.6 g) in dry tetrahydrofuran (200 mL) at room temperature under dry nitrogen gas. After refluxing for 1 h the black reaction mixture was cooled to room temperature and a mixture of silylated cycloadduct products consisting of 102 and 103 (872 mg) in dry tetrahydrofuran (5 mL) was added. After refluxing for 48 h under dry nitrogen, the reaction mixture was cooled to room temperature, added methanol (50 mL) to quench the reaction, filtered through Celite, concentrated under reduced pressure and the concentrated product was extracted with dry diethyl ether (3 x 50 mL). The combined ether extracts were concentrated under reduced pressure to give a yellow oil (414 mg). Glc analysis shows this as a mixture of two compounds with retention times of 7.05 and 7.8 min on program temperature 130-200°C [10°C/min] in the column 5% S.E. 30 on Chemisorb W. Column chromatographic separation using 40 g of silica gel and hexane as the solvent gave three compounds, 105a, 105b and 104a in the ratio 21:28:10 (combined yield of 59%).

104a; ^1H nmr (CDCl_3): 4.05 ppm (dt, 1H, $J = 3$ and 2, CH-OSi^tBuMe₂), 2.95 ppm (dd, 1H, $J = 2$ and 8 Hz, ^1CH), 9.25 ppm (tq, 1H, $J = 8$ and 3 Hz, ^8CH), 2.05-1.9 ppm (m, 6H, CH₂), 1.7-1.5 ppm (m, 4H, CH₂), 1.24-1.20 ppm (s, 6H, CH₃), 0.9 ppm (s, 9H, -Bu^t), 0.05 ppm (s, 6H, CH₃).

^{13}C nmr (CDCl_3): 144.4 and 143.3 (C=C), 76.0 (CH-OSi^tBuMe₂), 57.9 (^1CH), 45.4 (^8CH), 44.1 (^4C), 45.2, 38.0, 34.5, 32.3 and 26.6 (CH₂), 30.8 and 30.6 (CH₃), 26.0 (t-Bu), 18.3 (C), -4.3 and -4.5 (Si-CH₃); exact mass m/e 306.2379.

105a; ^1H nmr (CDCl_3): 4.0 ppm (q, $J = 3$ Hz, CH-OSi^tBuMe₂), 2.9 ppm (m, 1H, $J = 3, 8$ and 3.5 Hz, ^8CH), 3.1 ppm (m, 1H, ^1CH), 1.85-1.75 ppm (m, 5H, CH₂), 1.7-1.45 ppm (m, 4H, CH₂), 1.18-1.1 ppm (s, 6H, CH₃), 0.9 ppm (s, 9H, t-Bu), 0.05 ppm (s, 6H, Si-CH₃). ^{13}C nmr (CDCl_3): 146.0 and 141.1 (C=C), 81.3 (CH-OSi^tBuMe₂), 56.3 (^8CH), 45.7 (^1CH), 45.2 (^4C), 45.4, 43.7, 34.8, 34.0 and 26.7 (CH₂), 30.9 and 30.6 (CH₃), 26.0 (t-Bu), 18.3 (C), -4.3 and -4.4 (Si-CH₃), exact mass m/e 306.2379.0

105b; ^1H nmr (CDCl_3): 4.1 ppm (m, 1H, $J = 5, 3$ and 8 Hz, CH-OSi^tBuMe₂), 3.0 ppm (m, 1H, ^1CH), 2.05-1.85 ppm (m, 6H, CH₂), 1.6-1.45 ppm (m, 4H, CH₂), 1.1 ppm (s, 6H, CH₃), 0.9 ppm (s, 9H, t-Bu), 0.05 ppm (s, 6H, Si-CH₃). ^{13}C nmr (CDCl_3): 144.8 and 143.5 (C=C), 75.5 (CH-OSi^tBuMe₂), 50.5 (^8CH), 45.5 (^1CH), 45.3 (C), 44.5, 43.4, 32.9, 29.2

and 27.3 (CH₂), 30.9 and 30.6 (CH₃), 26.0 (t-Bu), 18.3 (C),
-4.5 and -4.7 (Si-CH₃); exact mass m/e 306.2379.

1-Methylcyclopent-1-ene

The reaction of cyclopentanone with methyl iodide and magnesium turnings in dry diethyl ether gave 1-methylcyclopent-1-ol (Grignard reaction).

1-Methylcyclopent-1-ol (86.2 g) and iodine (0.36 g) were placed in a 250 mL flask fitted with a Claisen distilling head and a condenser. The flask was heated at 120°C and the suspected olefin-water distillate (73.2 g) was collected in a receiver cooled in ice. This was dried by sending through a Na₂SO₄ (an) column to give a crude reaction mixture of olefins (44.8 g). The ¹H nmr spectra of the crude mixture indicated a major compound and an 8% impurity; ¹H nmr showed a proton at 5.2 ppm which is due to the methylene hydrogen of the endo-cyclic 1-methylcyclopent-1-ene and a small peak at 4.7 ppm due to the exo-cyclic isomer methylenecyclopentene.

1-Methylcyclopent-1-ene (44.5 g) (contaminated with 8% methylenecyclopentene), glacial acetic acid (57 mL) and p-toluenesulfonic acid (1.18 g) were heated under reflux for 1 h, cooled and washed with H₂O (3 x 100 mL) and saturated aqueous sodium bicarbonate solution (3 x 75 mL) and dried over anhydrous magnesium sulphate. The dried solution (27.9 g) was distilled through a 15 inch vigreux

column to give pure 1-methylcyclopent-1-ene (24.6 g) as analyzed by glc.

2-Methyl-2-cyclopenten-1-ol

1-Methylcyclopent-1-ene (5.0 g) and methyleneblue sensitizer (0.0128 g) were dissolved in acetonitrile (40mL) (the concentration of the methyleneblue sensitizer was 10^{-3} M) and placed in an irradiation cell. Air was replaced by O_2 and allowed to come to thermal equilibrium. The reaction mixture was photo-oxygenated using a 500 W tungsten filament lamp (Sylvania) as the light source. The lamp was turned on and the reaction was carried out at a positive O_2 pressure of 1 cm Hg higher than the atmospheric pressure. The amount of O_2 absorbed (cm^3) was measured with respect to time. The reaction cell was cooled continuously by air. The photo-oxygenation was stopped after 97% completion of the reaction determined by the amount of O_2 absorbed. The reaction mixture was treated with sodium borohydride (5.0 g) in methanol (40 mL) and was kept at room temperature. After 30 min water (75 mL) was added and extracted with diethyl ether (3 x 75 mL), washed the combined ether extracts with H_2O (50 mL), dried over $MgSO_4$ (an) and was concentrated under reduced pressure to give a mixture of products (4.6 g) as analyzed by 1H nmr. The 1H nmr spectrum of the alcohol mixture indicated a peak at 5.7 ppm and at 4.6 ppm which are due to the hydroxy methine proton and the olefinic proton of compound 114a,

respectively. The ^1H nmr also indicated peaks at 4.4 ppm and 4.8 ppm (olefinic protons of compound 114c) and at 4.5 ppm and 5.9 ppm which are due to the two olefinic protons of compound 114b. Integration of the ^1H nmr spectrum of the vinyl alcohol mixture indicated the ratio of 114a:114b:114c = 33%:44%:22%. Several attempts were made to separate the three alcohols by distillation and by glc, which proved unsuccessful. Hence this method of preparation was abandoned as pure alcohol 114a is needed for the cycloaddition and contamination of others could lead to undesirable products and complications in the separation of cycloadduct products.

2-Methyl-2-cyclopenten-1-one

Cyclopentanone (10 g, 0.119 mol), N-methylanilinium-trifluoroacetate (63.7 g, 0.288 mol) and paraformaldehyde (9.8 g) were refluxed together with stirring in dry tetrahydrofuran (250 mL) for 14 min. The reaction was followed by glc (10% OV 101 at 70°C). At the end of 14 min the glc analysis indicated 60% conversion of cyclopentanone and further reaction time resulted in substantial polymerization of the product. After 14 min of refluxing the reaction mixture was cooled in ice, diluted with diethyl ether (200 mL), and successively washed with 50% aqueous hydrochloric acid (75 mL), and saturated aqueous sodium hydrogen carbonate (50 mL) to which excess solid sodium hydrogen carbonate (59 g) was added. The aqueous

phases were back extracted with diethyl ether (3 x 25 mL), combined ether extracts, were dried with magnesium sulphate, and concentrated under reduced pressure at room temperature. To the crude 2-methylenecyclopentanone 95% ethanol (10 mL) and rhodium trichloride (0.090 g of the trihydrate, 0.34 mmol) was added and the mixture was refluxed for 90 min during which time glc analysis indicated complete conversion to 2-methyl-2-cyclopenten-1-one. Ether (100 mL) was added to the cooled reaction mixture, filtered, dried with magnesium sulphate, and concentrated under reduced pressure (30% yield). Distillation through a short vigreux column gives 2-methyl-2-cyclopentene-1-one (14-20% yield).

B.p. 59°C/16 torr. ^1H nmr (CDCl_3): 7.30 ppm (m, 1H, olefin proton), 2.2-2.7 ppm (m, 4H, CH_2), 1.7 ppm (s, 3H, CH_3).

Bicyclo[6.3.0]-4,4,1-trimethyl-11-hydroxyundecane-2,6-dione (116) and Bicyclo[6.3.0]-4,4,8-trimethyl-9-hydroxyundecane-2,6-dione (117)

Irradiation of a solution of 5,5-dimethylcyclohexane-1,3-dione (250 mg) in methanol in the presence of excess 2-methyl-2-cyclopentene-1-ol (1 g, 11.9 mmol) using uv light of wavelength 254 nm resulted in conversion of the diketone to a mixture of products (the irradiation was stopped at 70% conversion as analyzed by glc to stop secondary irradiation of the products; 5 x 24 h); retention times of 7.85 and 8.55 min at program

temperature 130-200°C [10°C/min] in the column 5% S.E. 30 on Chemisorb W. The reaction mixture was concentrated at room temperature under reduced pressure to give a yellow-coloured oil. Glc/mass spectra analysis showed the majority of products having the desired carbon skeleton; exact mass m/e, 238.1569.

Bicyclo[6.3.0]-4,4,8 β -trimethyl-9-(tert-butylidimethylsiloxy)- β -hydroundecane-2,6-dione (121) and Bicyclo[6.3.0]-4,4,1 β -trimethyl-11-(tert-butylidimethylsiloxy)-8 β -hydroundecane-2,6-dione (120)

Tert-butylidimethylsilylation of a mixture of 116 and 117 was performed in the same procedure as reported earlier (for compounds 100 and 101). Gas-liquid chromatographic analysis of the product mixture (1.3 g) showed the presence of three compounds; retention times of 11.09, 12.20 and 12.92 min at program temperature 130-200°C [10°C/min] in the column 5% S.E. 30 on Chemisorb W. This was separated using 150 g of silica gel (60-200 mesh) and 40% diethyl ether/hexane as the solvent to give 121 [M], 121 [N] and 120.

120; ^1H nmr (CDCl_3): 3.7 ppm (dd, 1H, $J = 6$ and 8.5 Hz, $^1\text{CH}-\text{OSi}^t\text{BuMe}_2$), 2.95 ppm (m, 1H, ^6CH), 2.35-2.25 ppm (m, 2H, $^7\text{CH}_2$), 2.15-1.77 ppm (m, 4H, CH_2 α to $\text{C}=\text{O}$), 1.8-1.55 ppm (m, 4H, CH_2), 1.15-1.0 ppm (s, 9H, CH_3), 0.9 ppm (s, 9H, $t\text{-Bu}$), 0.05 ppm (s, 6H, $\text{Si}-\text{CH}_3$). ^{13}C nmr (CDCl_3): 210.99 and 216.2 ($\text{C}=\text{O}$), 81.1 ($\text{CH}-\text{OSiMe}_2^t\text{Bu}$), 70.65 (^1C), 53.4 (^6CH), 32.8 (^4C), 55.2, 51.3, 46.1, 33.9 and 21.1 (CH_2).

31.6, 27.2 and 20.3 (CH₃), 25.7 (t-Bu), 18.0 (C), -4.3 and -4.9 (CH₃).

121 [M]: ¹H nmr (CDCl₃): 3.75 ppm (dd, 1H, J = 6.5 and 8.5 Hz, ⁹CH-OSiMe₂^tBu), 3.05 ppm (dd, 1H, J = 8.5 and 6.5 Hz, ¹CH); 2.7-2.25 ppm (m, 6H, CH₂ α to C=O), 2.05-1.9 ppm (m, 4H, CH₂), 1.1-1.0 ppm (s, 9H, CH₃), 0.9 ppm (s, 9H, t-Bu), 0.05 ppm (s, 6H, Si-CH₃). ¹³C nmr (CDCl₃): 211.7 and 212.7 (C=O), 60.3 (¹CH), 82.5 (CH-OSi^tBuMe₂), 47.5 (°C), 54.5, 50.3, 45.6, 30.3 and 21.1 (CH₂), 35.6 (°C), 31.2, 29.8 and 25.6 (CH₃), 25.8 (t-Bu), -4.39 and -4.49 (Si-CH₃), 18.0 (C).

121 [N]: ¹H nmr (CDCl₃): 3.7 ppm (dd, 1H, J = 8 and 6 Hz, ⁹CH-OSiMe₂^tBu), 3.0 ppm (dd, 1H, J = 9 and 4.5 Hz, ¹CH), 2.77 ppm (d, 1H, J = 13.5 Hz, ^{3,5}CH₂), 2.5 ppm (s, 2H ⁷CH₂), 2.35 ppm (d, 1H, J = 13.5 Hz, ^{3,5}CH₃), 2.3-2.2 ppm (d, 2H, J = 13.5 Hz, ^{3,5}CH₂), 1.85 ppm (m, 2H, CH₂), 1.5 ppm (m, 2H, CH₂), 1.1-1.0 ppm (s, 9H, CH₃), 0.9 ppm (s, 9H, t-Bu), 0.05 ppm (s, 6H, Si-CH₃). ¹³C nmr (CDCl₃): 210.65 and 214.66 (C=O), 80.6 (⁹CH-OSiMe₂^tBu), 58.89 (¹CH), 47.9 (°C), 55.4, 55.2, 51.5, 30.7 and 22.85 (CH₂), 34.4 (°C), 32.5, 28.7 and 21.1 (CH₃), 25.79 (t-Bu), 17.79 (C), -4.3 and -4.9 (Si-CH₃).

4,4,1 β -Trimethyl-2,6-dehydro-8 β -hydro-11-(tert-butylidimethylsiloxy)-tricyclo[6.3.0.0^{2,6}]undecane (122) and 4,4,8 β -Trimethyl-2,6-dehydro-1 β -hydro-9-(tert-butylidimethylsiloxy)-tricyclo[6.3.0.0^{2,6}]undecane (123)

Coupling of the diketone reaction mixture of 120 and 121 (266 mg) with McMurry's reagent was performed in the same procedure as reported earlier (for compounds 103 and 102) except the time of reflux, 24 h as opposed to 48 h. (Further refluxing leads to undesired products.) Glc analysis of the product mixture shows the presence of two compounds, with retention times of 7.03 and 7.95 min on program temperature 130-200°C [10°C/min] in the column 5% S.E. 30 on Chemisorb W. Chromatographic separation using 50 g of silica gel and hexane as solvent gave two compounds 122 and 123.

122; ¹H nmr (CDCl₃): 3.7 ppm (m, 1H, J = 5 Hz, 0.5 Hz, CH-OSi^tBuMe₂), 2.6 ppm (ddt, J = 2.75, 1.5 and 3 Hz, ^oCH), 2.0-1.8 ppm (m, 6H, CH₂), 1.7-1.35 ppm (m, 4H, CH₂), 1.15-1.1 ppm (s, 9H, CH₃), 0.9 ppm (s, 9H, t-Bu), 0.05 ppm (s, 6H, Si-CH₃). ¹³C nmr (CDCl₃): 144.2 and 142.6 (C=C), 81.5 (CH-OSi^tBuMe₂), 57.12 (¹C), 52.59 (^oCH), 43.6, 37.9, 33.3, 29.7, 27.8 (CH₂), 30.8, 30.5 and 25.1 (CH₃), 25.9 (t-Bu), 18.2 (C), -4.4 and -4.8 (Si-CH₃), 44.3 (^oC).

123; ¹H nmr (CDCl₃): 3.69 ppm (t, 1H, J = 4 Hz, CH-OSi^tBuMe₂), 2.25 ppm (m, 1H, J = 3.5, 9 and 1 Hz, ¹CH), 1.95-1.9 ppm (m, 4H, CH₂), 1.85-1.75 ppm (m, 2H, J = 16 Hz, CH₂), 1.65-1.15 ppm (m, 4H, CH₂), 1.15-1.1 ppm (s, 9H,

CH₃), 0.9 ppm (s, 9H, t-Bu), 0.05 ppm (s, 6H, Si-CH₃).

¹³C nmr (CDCl₃): 145.9 and 139.7 (C=C), 81.3

(³CH-OSi^tBuMe₂), 59.2 (²C), 53.2 (¹CH), 44.4 (⁴C), 45.4,

44.07, 44.05, 34.04 and 26.4 (CH₂), 30.8, 30.5 and 23.3

(CH₃), 25.9 (t-Bu), 18.2 (C), -4.4 and -4.8 (Si-CH₃).

Ozonolysis of (123)

Compound 123 (20 mg) was dissolved in methylene chloride (5 mL) and O₃ was sent through it at -5°C (dry ice/acetone) which gave a purple coloured solution. After 30 min O₂ was sent through it to degass the dissolved O₃ which made the decolourization of the solution. Zn dust (500 mg) and glacial acetic acid (4 mL) was added to the reaction mixture, after 10 min chloroform (50 mL) was added, filtered, extracted the reaction mixture with H₂O, dried over K₂CO₃ (an) and concentrated under reduced pressure to give a yellow coloured oil (19 mg). This was purified by a silica gel column (4 g) and diethyl ether/hexane solvent. Gas-liquid chromatographic analysis of the product shows a retention time of 12.15 min on program temperature 130-200°C [10°C/min] in the column 5% S.E. 30 on Chemisorb W. Mass spectral, ¹H nmr and ¹³C nmr analyses of this compound agree with-121.

4,4,1 β -Trimethyl-2,6-dehydro-8 β -hydro-11-hydroxy-
tricyclo[6.3.0.0^{2,6}]undecane (124) and
4,4,8 β -Trimethyl-2,6-dehydro-1 β -hydro-9-hydroxytricyclo-
[6.3.0.0^{2,6}]undecane (125)

Compound 122 (57 mg) was dissolved in dry tetrahydrofuran (2 mL) and 0.1 M tert-butylammoniumfluoride (1.5 mL) was added and stirred for 12 h, diluted with methylene chloride (10 mL) and extracted with H₂O (2 x 3 mL). The H₂O layer was extracted with methylene chloride (2 mL) and was combined with the CH₂Cl₂ layer, dried over K₂CO₃ (an) and concentrated under reduced pressure. Glc analysis showed a retention time of 2.69 min on program temperature 130-200°C [10°C/min] in the column 5% S.E. 30 on Chemisorb W. Purification of the product was performed by using thick layer plates and 30% diethylether/hexane solvent.

124; ¹H nmr (CDCl₃): 3.95 ppm (broad dd, 1H, J = 5 and 2.5 Hz, CH.OH), 2.6 ppm (m, 1H, ⁸CH), 2.05-1.30 ppm (m, 11H, CH₂ and OH), 1.15-1.05 ppm (s, 9H, CH₃). ¹³C nmr (CDCl₃): 145.3 and 142.0 (C=C), 81.5 (CH.OH), 57.3 (¹C), 53.2 (⁸CH), 44.3 (⁴C), 43.5, 37.5, 33.2, 29.3 and 27.5 (CH₂), 30.8, 30.6 and 25.2 (CH₃).

125; ¹H nmr (CCl₄): 3.9 ppm (t, 1H, J = 4 Hz, CH.OH), 2.5 ppm (m, 1H, J = 8.5, 2.5 and 1 Hz, ¹CH), 2.0-1.4 ppm (m, 11H, CH₂ and OH), 1.15-1.05 ppm (s, 9H, CH₃). ¹³C nmr (CDCl₃): 145.6 and 139.8 (C=C), 81.1 (CH.OH),

58.69 ($^{\circ}\text{C}$), 53.1 (^1CH), 45.3, 44.2, 43.9, 33.5 and 26.3 (CH_2), 44.1 (^4C), 30.7, 30.5 and 22.1 (CH_3).

4,4,8-Trimethyl-2,6-dehydro-9-oxotricyclo[6.3.0.0^{2,6}]-undecane (127)

Compound 125 (41 mg) was dissolved in acetone (5 mL) and was kept at 0°C in an ice bath. Jones' reagent (1.5 mL) (6.7 g of CrO_3 in 15.5 mL of H_2O and 5.8 mL of CH_2SO_4) was added slowly at 0°C to maintain the temperature, until the reaction mixture became orange in colour. The stirring continued for 80 min and the green coloured CrO_2 precipitated, added few drops of 2-propanol until the orange colour disappeared, extracted with acetone, dried over K_2CO_3 an, concentrated under reduced pressure to give a yellow oil. This was re-extracted with methylene chloride (2 x 10 mL) and concentrated under reduced pressure. Purification of this was performed using silica gel, thick layer plate and 35% diethyl ether/hexane solvent which gave compound 127.

127; ^1H nmr (CDCl_3): 2.3-1.35 ppm (m, 11H, CH_2 and ^1CH), 1.15-1.0 ppm (s, 9H, CH_3). ^{13}C nmr (CDCl_3): 226.0 ($\text{C}=\text{O}$), 65.8 ($^{\circ}\text{C}$), 51.6 (CH), 144.7 and 143.7 ($\text{C}=\text{C}$), 45.3, 43.5, 41.9, 36.4 and 21.9 (CH_2), 30.9, 30.3 and 20.8 (CH_3).

4,4,1 β -Trimethyl-2 α ,6 α ,8 β -trihydro-11-oxotricyclo-
[6.3.0.0^{2,6}]undecane (38)

Compound 124 (52 mg) was dissolved in methanol (20 mL) and PtO₂ (12 mg) was added. This was stirred for 10 h under positive hydrogen pressure, filtered the reaction mixture, dried over K₂CO₃ (an) and concentrated at room temperature under reduced pressure to give an oil. The oxidation of this oil with Jones' reagent yielded a single compound followed by glc. This was purified by thick layer chromatography to give compound 38. The spectral data of 38 matched that of norketone which was provided to us by Professor T. Hudlicky.

38; ¹H nmr (CDCl₃): 1.2-2.6 ppm (m, 13H), 1.05-.095 ppm (s, 9H, CH₃). ¹³C nmr (CDCl₃): 224.5 (C=O), 59.3 (¹C), 46.8, 41.9, and 43.4 (CH), 34.2, 37.7, 29.7, 22.4 and 48.9 (CH₂), 29.3, 26.6 and 17.3 (CH₃), 41.2 (⁴C).

PART II

PHOTOCHEMICAL AND PHOTOPHYSICAL PROPERTIES OF
N-BENZOYLINDOLES

PART II

CHAPTER 5

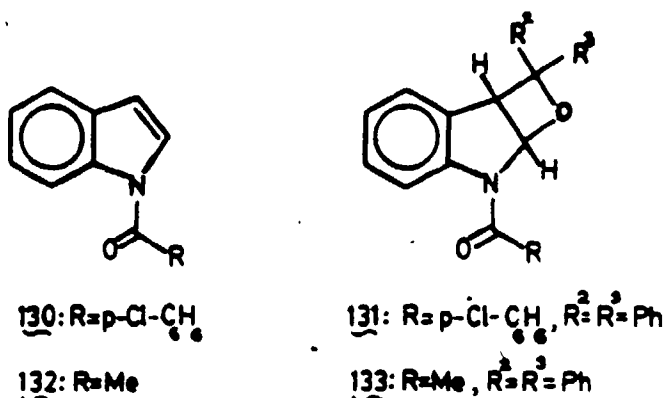
MECHANISM OF PHOTOANNELATION REACTION OF N-BENZOYLINDOLE WITH CYCLOPENTENE

5.1 INTRODUCTION

The subject of this chapter is the photocycloaddition reactions of N-derivatized indoles, specifically the photochemical reactions of N-benzoylindoles with cyclopentene. The first investigation of the photocycloaddition reactions of N-derivatized indoles was reported by Julian et al.⁶⁴ Irradiation of benzophenone in the presence of N-p-chlorobenzoylindole (130) gave the corresponding oxetane (131). These types of oxetanes are also obtained from the photochemical reaction of aromatic heterocycles such as furans⁶⁵ and 2,5-dimethylthiophene with benzophenone. Similarly N-acetylindole (132) gave the oxetane (133).⁶⁶

Thiophene, pyrrole, oxazole, indole and isoxazole do not undergo such cycloadditions.⁶⁷ Their failure to react may reflect greater resonance energy in the heterocyclic π -system, or possibly quenching of the excited ketone by the non-bonded electrons on the hetero-atom. Thus an unreactive aromatic heterocycle such as indole appears to

be rendered more reactive by placing an electron withdrawing group on the nitrogen atom to interact with the non-bonding pair and make it less available for donation or delocalization through the aromatic system.

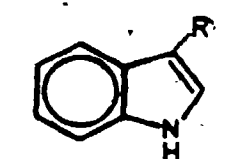


No oxetane formation was observed when acetophenone, benzaldehyde, acetone or propionaldehyde were irradiated with N-benzoylindole. However, benzoylformamide and methyl benzoylformate gave oxetanes. These results suggest that only ketones with triplet energies of less than 68 kcal/mol add to (130). This implies that the triplet energy of (130) is greater than 68 kcal/mol and that the triplet excited ketones add to the ground state indole. Thus those ketones with higher triplet energies are unreactive because they are quenched by the indole derivative. Sato et al⁶⁸ reported that irradiation of indoles in the presence of acrylonitrile yields the corresponding cyanoethylated

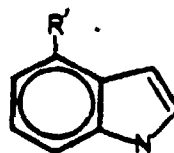
products via complex intermediates. Thus irradiation of indole with acrylonitrile in methanol yielded 3-(2-cyanoethyl) indole (134) and 4-(2-cyanoethyl)indole (135). Noteworthy characteristics of this photochemical reaction are

- (a) NH-indoles undergo photocyanoethylation in both methanol and acetonitrile, whereas N-methylindoles react with acrylonitrile only in protic solvents such as methanol, indicating that proton transfer either from the solvent or from the NH group of indoles of acrylonitrile may be involved in the formation of the products.
- (b) Addition of piperylene had no significant effect on the photocyanoethylations.
- (c) The fluorescence emission of indole was strongly quenched by acrylonitrile at room temperature.

These observations were used to draw the conclusions that this photochemical reaction may proceed via singlet exciplexes as intermediates and that an important step in the decay of the exciplexes may involve proton transfer to the acrylonitrile group. Observed reactivities of the 3- and 4-positions of the indole nucleus in the

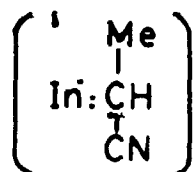
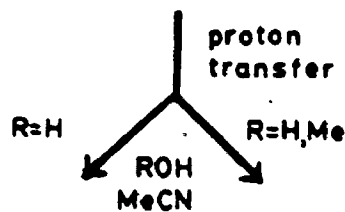


134: R=CHCNMe-

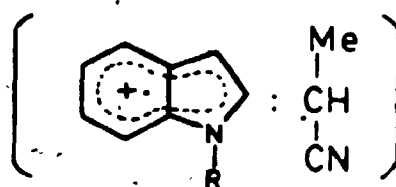


135: R=CHCNMe

photocynoethylation reactions are interpreted in terms of the calculated spin densities of indole cation radical⁶⁹—(Scheme 43).

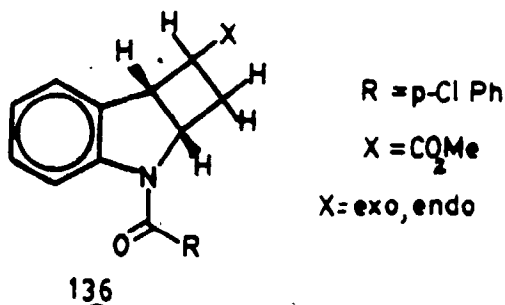


products

products + H⁺

SCHEME 43

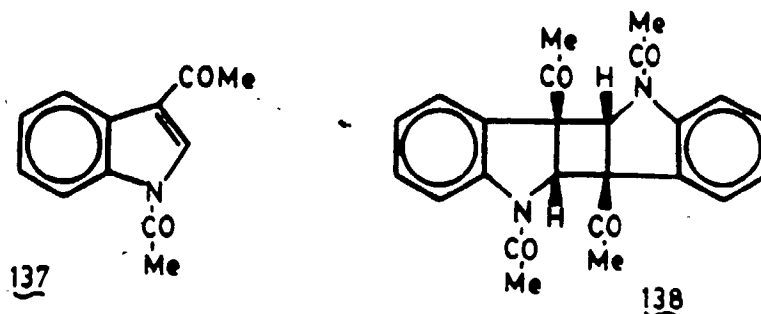
Julian et al⁷⁰ also reported the photochemical cycloaddition of olefins to the 2,3-double bond of N-derivatized-indoles to produce a cyclobutane ring. For example, irradiation of N-p-chlorobenzoylindole (130) and methylacrylate in acetonitrile using acetophenone as sensitizer yielded *exo*- and *endo*-adducts (136). Direct irradiation gave similar results. No reaction was observed when methylacrylate was irradiated with indole or N-methylindole in benzene, either directly or sensitized by acetophenone; therefore, the N-acyl protecting group is critical.



Acrylonitrile, acrylamide and ethyl vinyl ether also added to (130), yielding the corresponding *exo*- and *endo*-adducts. In a competitive reaction between ethyl vinyl ether and acrylonitrile, compound (130) added almost entirely to the nitrile, which suggests that the photoaddition is more efficient with electron-deficient olefins. The fact that the reaction was capable of being

sensitized, along with the observation that product formation could be quenched by naphthalene addition led to the suggestion that the triplet excited state of indole is involved.

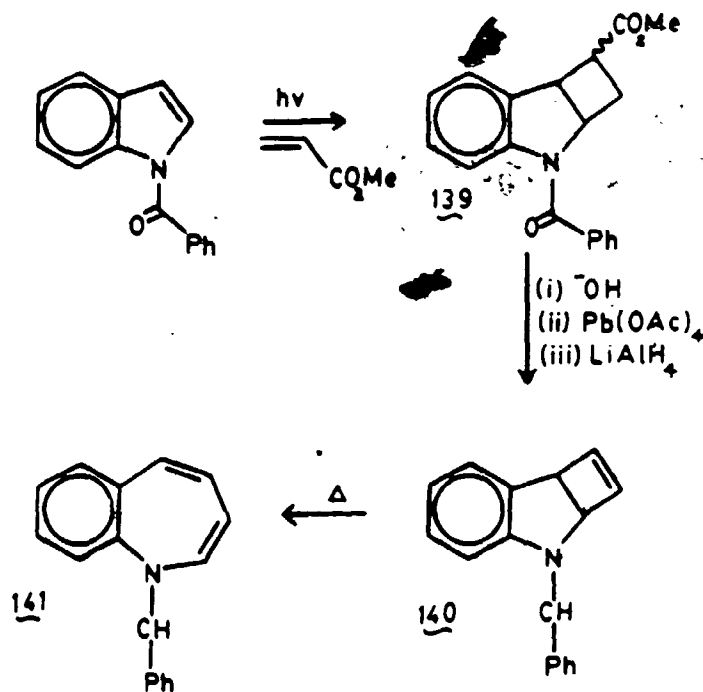
Hino et al⁷¹ reported the photodimerization of 1,3-diacetylindole (137) to give the cyclobutane derivative (138). The analogous photodimerization of indene, benzofuran and benzothiophene 1,1-dioxide⁷² with or without a sensitizer to form cyclobutane derivatives, has also been reported. Irradiation of 1,3-diacetylindole (137) in ethanol precipitated the dimer (138) and the molecular structure was determined by x-ray analysis.



No other isomeric dimers were isolated, even when benzophenone was used as a sensitizer or when the solvent was changed to methanol, tert-butanol, benzene or acetone. Also, 3-acetyl, 1-acetyl or 1-benzenesulfonylindoles did not give the corresponding dimers under similar conditions.

Ikeda et al⁷³⁻⁷⁵ used the cycloadduct product (139), derived from N-benzoylindole and methylacrylate, as the

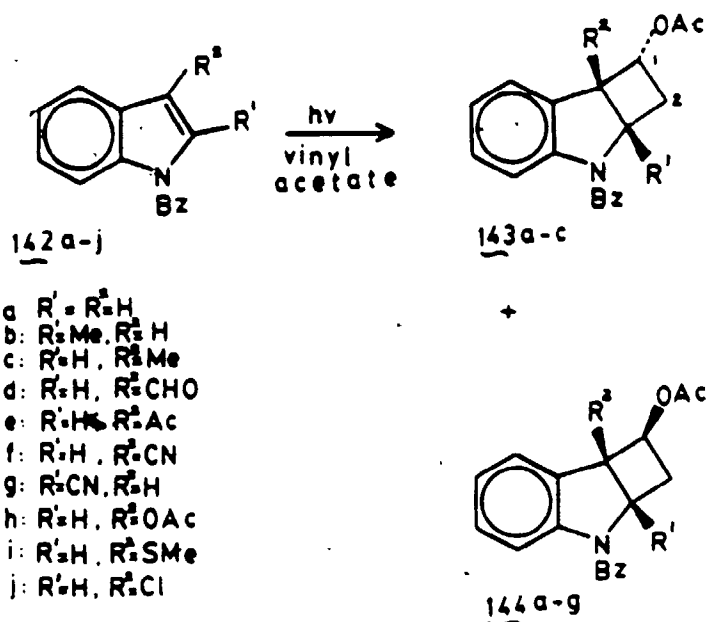
initial species in the synthesis of 1H-1-benzazepines (Scheme 44). Alkaline hydrolysis of (139) followed by oxidative decarboxylation with lead tetra-acetate and reduction with lithium aluminium hydride at room temperature gave (140). Thermal ring opening of (140) yielded 1H-1-benzazepine (141).



SCHEME 44

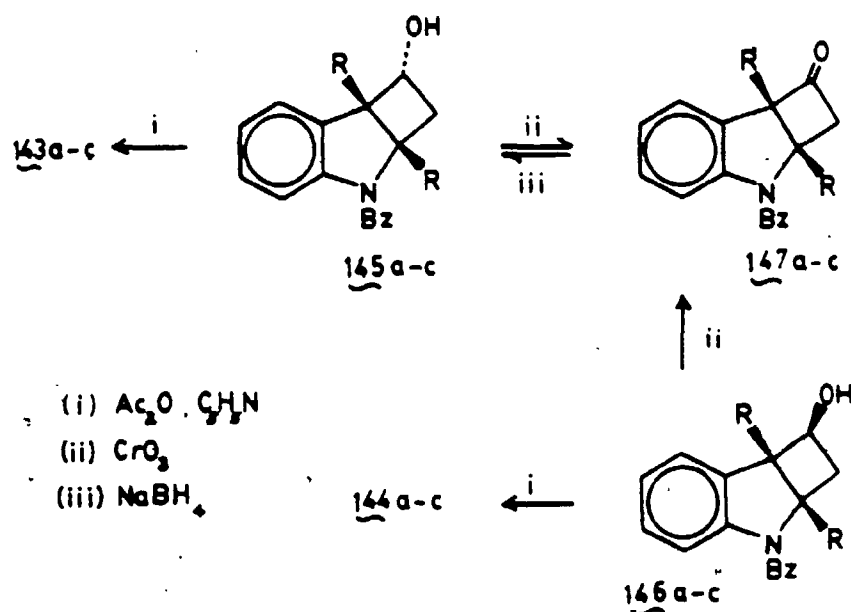
Ikeda et al⁷⁶ also investigated the regio- and stereoselectivities in the (2+2) photocycloaddition of a series of N-benzylindoles with vinyl acetate and methylacrylate. Irradiation of a solution of the

N-benzoylindoles (142a-j) and an excess of olefin in degassed benzene, in the presence of acetophenone as a triplet sensitizer in the case of vinyl acetate, or without acetophenone in the case of methyl acrylate, with a 350 W high-pressure mercury lamp in a Pyrex tube afforded a mixture of products (143a-c and 144a-c), which were not separable (Scheme 45).



SCHEME 45

Pure samples of the acetates were obtained by alkaline hydrolysis of the crude mixture, separation of the resulting alcohols (145a-c and 146a-c) by column chromatography and reacetylation (Scheme 46).



SCHEME 46

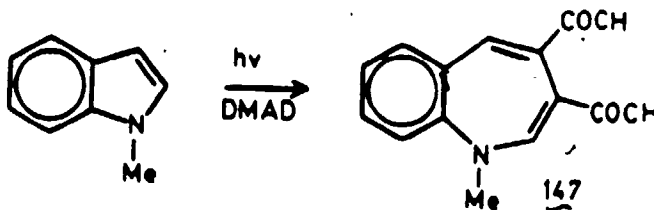
The structures of the acetates were elucidated by oxidation of each alcohol to the corresponding cyclobutanone (147a-c). The yields and ratios of the adducts showed that the addition of vinyl acetate to the N-benzylindoles, particularly those with an electron withdrawing group at the 3-position, proceeded in high yield, with high regioselectivity (formation of the 1-substituted isomers only) but low stereoselectivity (formation of 1:1 mixture of endo and exo-isomers); on the other hand, methyl acrylate added to N-benzylindoles in moderate yields only, but with high regioselectivity (formation of the 1-substituted isomers as the major products) and high

stereoselectivity (formation of the 1-exo-isomers as the major products).

125

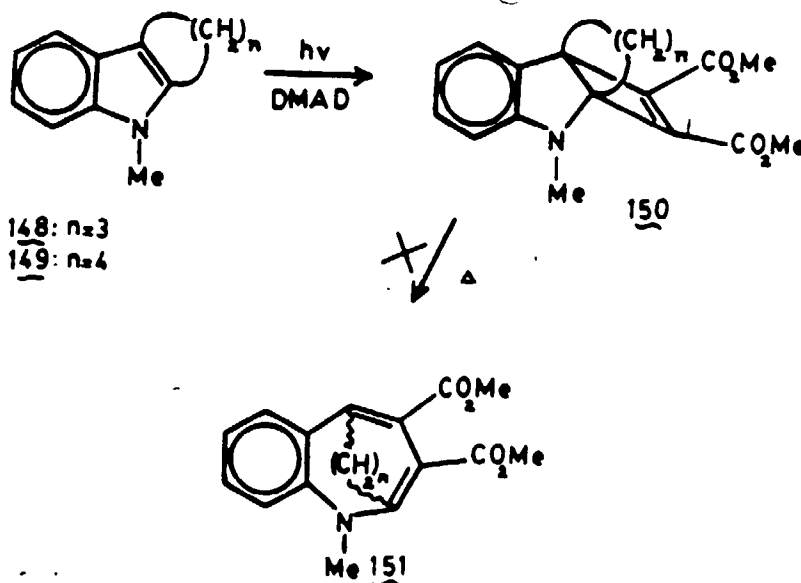
These regiochemical selectivities are similar to those-observed in the photocycloaddition of 2-quinolones,⁷⁷ 1-isoquinolones,⁷⁸ coumarins,⁷⁹ indenes⁸⁰ and thionaphthene-1,1-dioxides⁸¹ to unsymmetrical olefins (which all give one regioisomer predominantly, regardless of the nature of the olefin) and is in contrast to the results of the photocycloaddition of cyclic α,β -unsaturated ketones to unsymmetrical olefins.⁸²

Neckers et al⁸³ have reported the photochemical reaction of N-methylindole to dimethyl acetylenedicarboxylate (DMAD) which results in direct formation of N-methyl-3,4-dicarbomethoxybenzoazepine (147) (Scheme 47). The product is derived from a $\pi^2s + \pi^2s$ cycloaddition process and subsequent thermal ring opening at room temperature.



SCHEME 47

The isolation of the initial cyclobutane adducts in the N-alkylindole systems has been accomplished by using fused indoles to prevent cyclobutane ring opening. The photoreactions of 1-methyl-2,3-trimethyleneindole (148, $n = 3$) and 6,7,8,9-tetrahydro-1-methylcarbazole (149, $n = 4$) demonstrate this point. Direct cycloaddition to produce the cyclic adduct (150) would not likely be followed by ring opening to the benzazepines (151) since in these cases the derived benzazepine would have two bridgehead double bonds.



The photochemical cycloaddition of N-derivatized indoles to alkenes has potential synthetic applications. In view of this potential it was decided to investigate the mechanism of photochemical cycloaddition of N-derivatized indoles to alkenes so that synthetic limitations could be predicted.

5.2 GENERAL PROPERTIES OF N-BENZOYLINDOLE

In all solvents indole shows principal absorption maxima at circa 225 nm ($\epsilon = 25000$) and 270 nm ($\epsilon = 6000$); vibrational structure in these bands is also observed. The appearance of the absorption spectrum of indole is quite characteristic and is used to identify indole alkaloids. The absorption spectrum of tryptophan is the most intense of the three natural aromatic amino acids, tryptophan, tyrosine and phenylalanine,⁸⁴ and the spectra of proteins are largely the result of their tryptophan content.

The absorption spectra of N-benzoylindoles are quite different from that of indole. N-Benzoylindole exhibits two characteristic absorption bands in the ultra-violet spectrum; an intense band ($\epsilon = 24000$) in the region of 247 nm, and a weaker band ($\epsilon = 8000$) in the region of 302 nm (Fig. 1). In addition, there is no pronounced vibrational structure.

It is the excitation of the weaker band at 302 nm which has been used in the photochemical cycloaddition reactions employing a medium pressure mercury lamp.⁶⁴

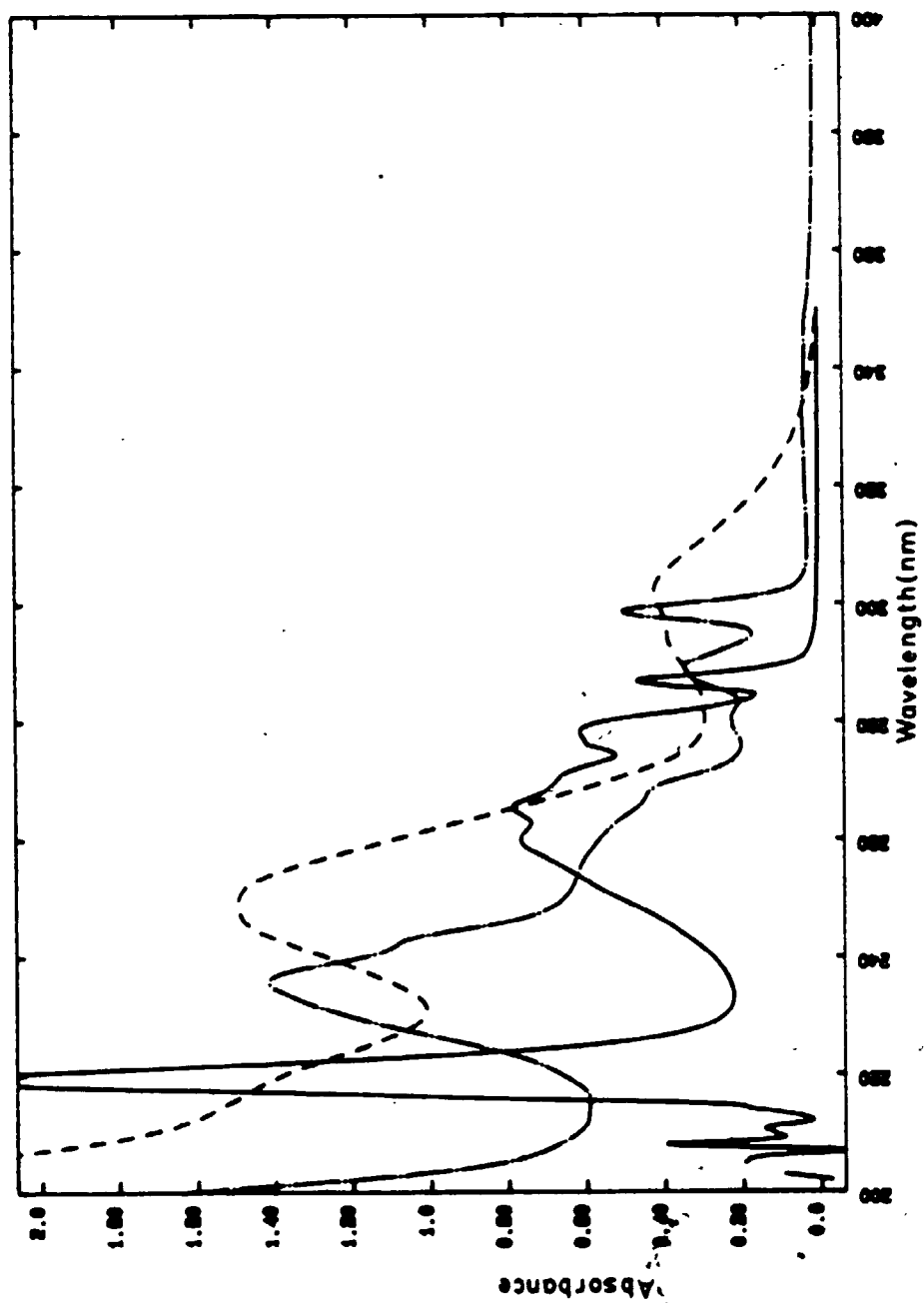


FIGURE 1: Absorption spectra of compounds (142a) (-----), (159) (-.-.-.-) and indole (———)

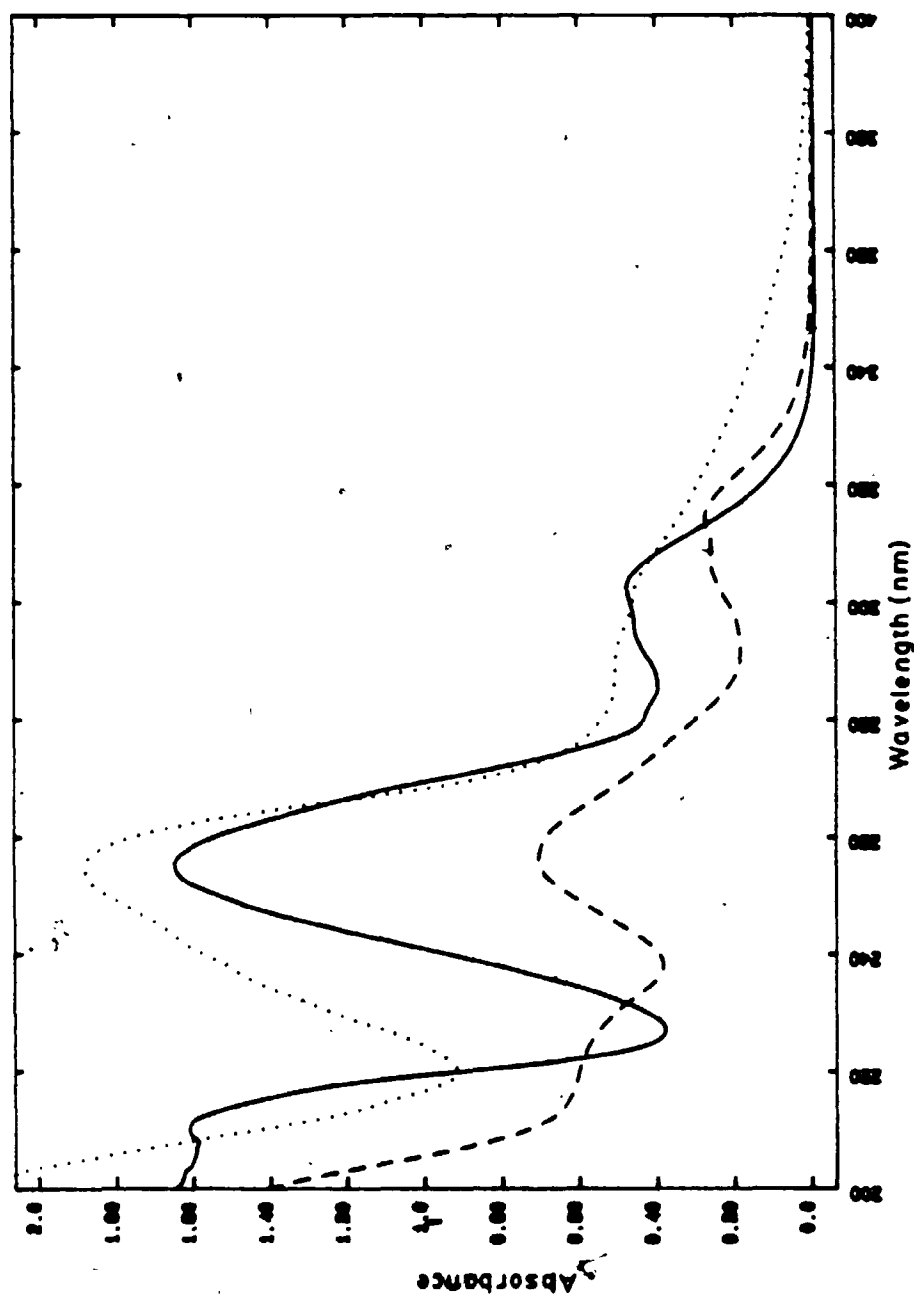


FIGURE 2a: Absorption spectra of compounds (158) (—), (159) (.....) and (160) (---)

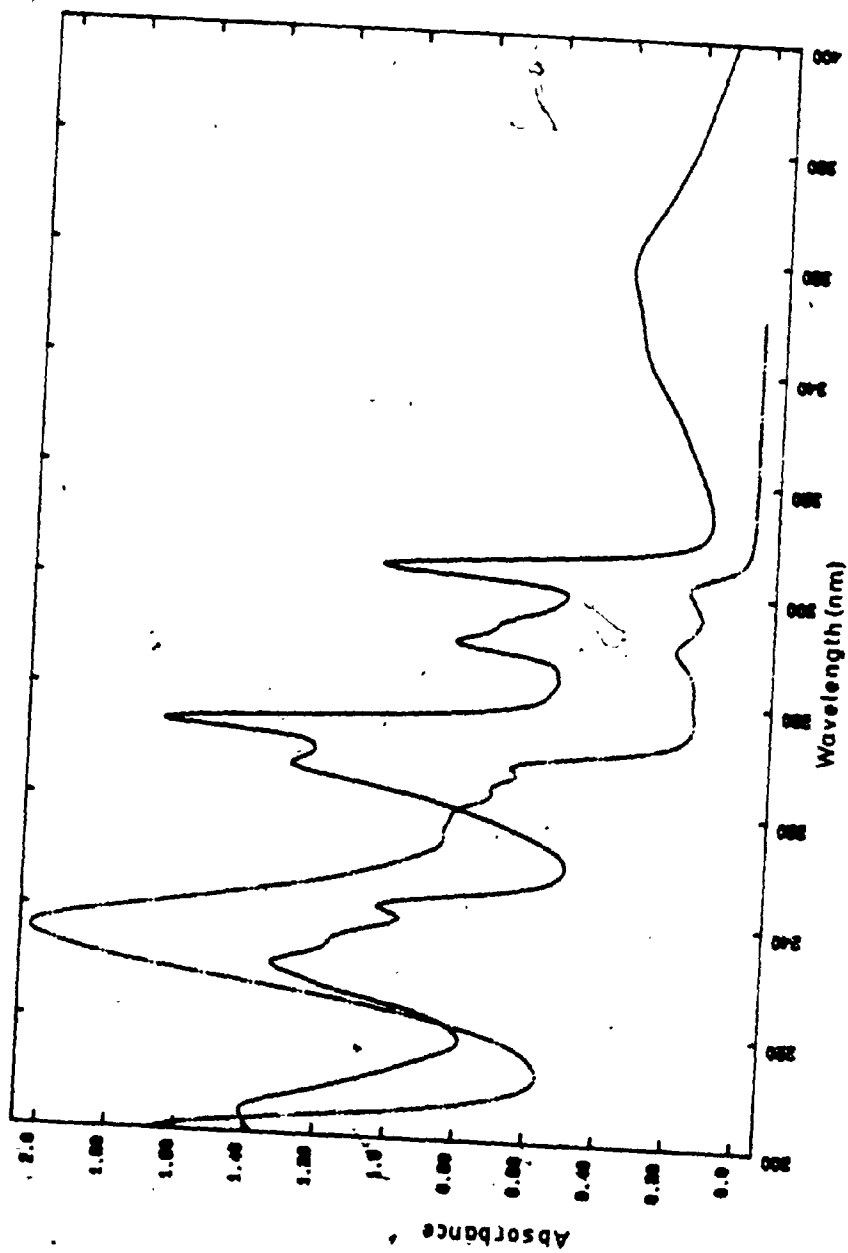


FIGURE 2b: Absorption spectra of compounds (161) (-----) and (162) (———)

Changing the solvent from non-polar hexane to polar acetonitrile results in virtually no shift in the wavelengths of the absorption maxima. This suggests that the absorption maxima do not correspond to a simple $n \rightarrow \pi^*$ transition localized on the benzoyl carbonyl group. The absorption maxima of N-benzoylindole in different solvents are given in Table VIII.

Several pathways are potentially available for the excited N-benzoylindole (NBI) molecule to undergo deactivation to the ground state;

- (i) cycloaddition reactions, either to the c_3-c_2 double bond or to the carbonyl group, to yield 1:1 adducts. In principle this could proceed from either the singlet or triplet excited state.
- (ii) reaction with solvent molecules;
- (iii) radiative decay to the ground state;
- (iv) non-radiative decay to the ground state.
- (v) dimerization with a ground state N-benzoylindole molecule.

The solvent generally used in this work was spectral grade, doubly-distilled benzene purged with dry nitrogen gas. This solvent was found to be inert with respect to

addition to photochemically excited N-benzoylindoles, so that mode (ii) of deactivation is unimportant.

Hino et al⁷¹ have observed photochemical dimerization of 1,3-diacetylindoles as described above; no such reaction occurred with N-acetylindoles and N-benzenesulfonylindoles. In the work which will be described in this thesis evidence was found to indicate that inefficient quenching of the N-benzoylindole triplet excited state by the ground state N-benzoylindole molecule occurred, but no dimerization products were detected. That inefficient self-quenching occurred was determined by measuring the change in the quantum yield of cycloaddition of NBI with cyclopentene as a function of the NBI concentration (this is discussed in detail later in this chapter). It can be concluded, therefore, that dimerization processes do not represent a major pathway for decay of the excited NBI molecule.

It was observed during the work described in this thesis that N-benzoylindole exhibited fluorescence at room temperature; however, it was very much weaker (the fluorescence quantum yield was determined to be 4.1×10^{-2} in hexane) than that of indole itself, and was observed at anomalously long wavelength. It was also observed that the position and intensity of the emission was exceedingly solvent dependent (this is discussed in detail in Chapter 6). The intensity of the fluorescence was unaffected by the presence of alkenes (cyclopentene,

1,3-cyclohexadiene and 1,3-pentadiene) and it was thus concluded that the emitting state was not involved in cycloaddition and that radiative decay is not a major mode of deactivation of the NBI singlet state.

N-benzoylindole was also found to exhibit phosphorescence in frozen solutions at 77°K which from the position of the 0-0 band of the emission indicated the presence of a triplet state of energy 67 kcal/mol (Figure 3). Triplet counting experiments, which will be described in detail later, indicated that the NBI triplet state is populated efficiently. The quantum yield of intersystem crossing was solvent dependent, and was of the order of 10^{-1} or greater.

In addition to the various normal modes of radiationless decay open to NBI, the presence of the conjugated, but conformationally mobile benzoyl group, suggested that rotation of the latter might provide an additional mode of decay. Evidence for this process is discussed later in this chapter.

The first step taken to deduce the mechanism of the photoaddition reaction of NBI was to identify the reacting state. In order to do this the addition of cyclopentene to NBI was chosen as the reaction to be studied.

5.3 STRUCTURE AND STEREOCHEMISTRY OF CYCLOADDUCT PRODUCTS

Cyclopentene was chosen as the alkene partner because of its symmetrical structure and the relative

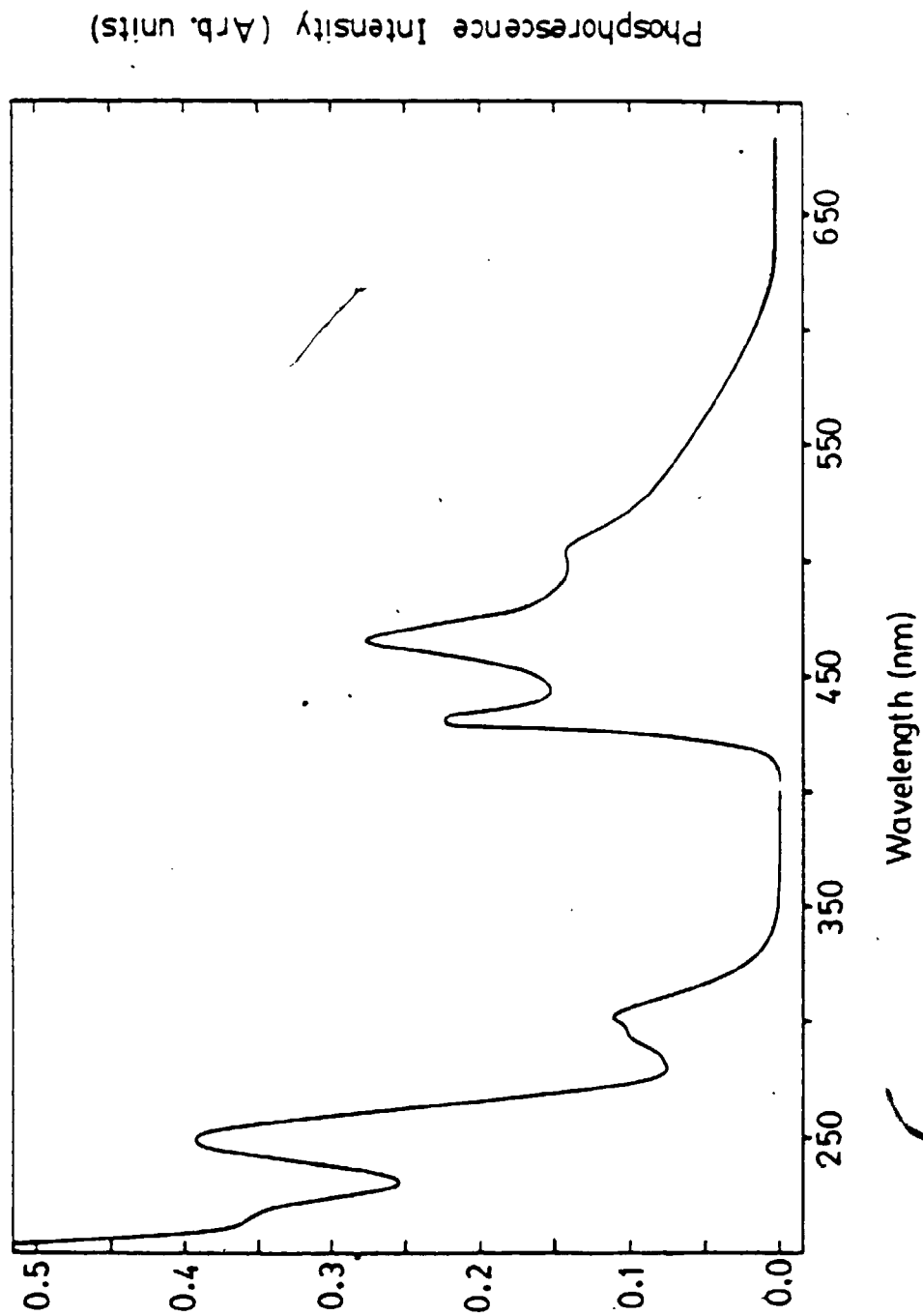


FIGURE 3: Phosphorescence spectrum of NBI

simplicity of the cycloadduct products. Non-symmetrically substituted alkenes can yield regioisomeric cycloadducts (i.e. head-tail or head-head adducts), whereas no regioisomerism is possible with cyclopentene.

N-Benzoylindole and cyclopentene were irradiated in nitrogen purged benzene using a Pyrex filtered medium pressure mercury lamp. Gas chromatographic analysis indicated the apparent conversion of NBI to a single product. Column chromatographic separation using silica gel resulted in the isolation of a pure crystalline compound. The molecular ion in the mass spectrum of this compound showed a precise mass of 289.1464 which corresponds to the cycloadduct products (152) and (153). The ^{13}C nmr spectrum of the crystalline product in deuteriochloroform indicated the presence of 20 carbon atoms including four methine carbon atoms at 63.6, 45.0, 46.2 and 47.9 ppm. The ^1H nmr spectrum of this compound in CDCl_3 showed four peaks distinctly separated from the rest of the spectrum; at 4.0, 3.35, 2.84 and 2.70 ppm. Each of these peaks corresponded to one hydrogen atom, and they were assigned to the four methine protons of structures (152) or (153).

Of these four protons the lowest chemical shift appeared at 4.0 ppm as a broad unstructured signal and was assigned as H_a (see structures (152) and (153)) since the proton adjacent to the nitrogen atom would be expected to appear at lowest chemical shift compared to H_b , H_c and H_d .

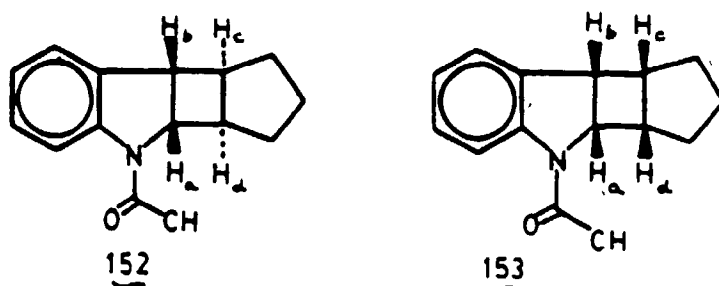
The broadness of the signal is ascribed to the longer relaxation time of the nitrogen atom. Irradiation of H_a decoupled the peak at 3.35 ppm which collapsed to a doublet and revealed its coupling constants (dd, $J = 7.5$ and 3 Hz). Irradiation of H_a also decoupled the peak at 2.84 ppm which collapsed to a broad triplet (bdt, $J = 3$ and 7 Hz). Hence the peak at 3.35 ppm was assigned as H_b since only H_b would appear as a doublet on irradiation of H_a . The signal at 2.84 ppm was accordingly assigned as H_d . Irradiation of H_b and H_d indicated that the peak at 2.7 ppm (bdt, $J = 3$ and 7 Hz) could be assigned as H_c . The 1H and ^{13}C nmr chemical shifts relative to TMS and the proton-proton coupling constants of each of the methine carbons and protons are given in Table VI.

	1H nmr	^{13}C nmr	J, Jz
H_a	4.0 ppm	63.6 ppm	$J_{a,b} = 7.5$
H_b	3.35 ppm	45.0 ppm	$J_{b,c} = 3.0$
H_c	2.7 ppm	46.0 ppm	$J_{c,d} = 7.0$
H_d	2.84 ppm	47.8 ppm	$J_{d,a} = 3.0$

TABLE VI: 1H nmr and ^{13}C nmr chemical shifts of the cyclobutane ring of compound (152)

Comparison of the above coupling constants with those obtained from the Karplus equations using dihedral

angles estimated from models of structures (152) and (153) indicated that both H_a and H_b , and H_c and H_d are *cis* to each other. The similar coupling constants observed between H_a and H_d , and H_c and H_b indicated them to be *trans* to each other and hence the stereochemistry of the crystalline adduct was assigned as *cis-anti-cis* and has structure (152).



Comparison of the ^{13}C nmr spectrum of the crude reaction mixture with the spectrum of the isolated crystalline adduct (152) suggested the existence of another adduct with the same retention time on gas-liquid chromatographic column as that of 152, but which failed to crystallize out of the mixture. Two-dimensional nmr spectral analysis of the non-crystalline compound indicated this to be the *cis-syn-cis* adduct^a (153).

[^a: D. Hastings and A.C. Weedon, unpublished work.]

5.4 MULTIPLICITY OF THE EXCITED STATE INVOLVED IN THE CYCLOADDITION REACTION OF N-BENZOYLINDOLE WITH ALKENES

The cycloaddition could, in principle, occur from either a singlet state or a triplet excited state. Direct excitation of NBI (long wavelength maxima at 302 nm) should yield the S_1 state with an energy of 94.7 kcal/mol. The observed fluorescence of NBI (discussed in detail in Chapter 6) is from a lower-lying charge-transfer state whose energy is solvent dependent (65 kcal/mol in hexane, 52.9 kcal/mol in CH_3CH). The phosphorescence emission of NBI at 77 K was not solvent dependent, and from the position of the O-O band, a triplet energy of 67.7 kcal/mol was indicated. A typical phosphorescence spectrum is shown in Figure 3.

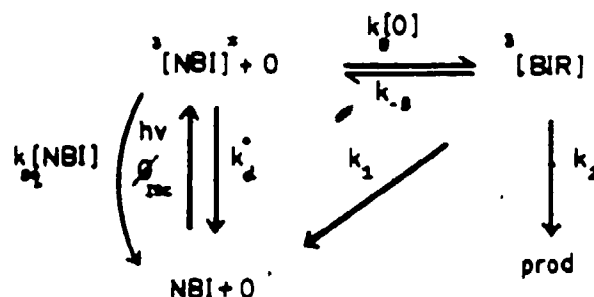
Ikeda et al⁷³⁻⁷⁵ observed the cycloaddition of NBI and methyl acrylate in the presence and absence of acetophenone triplet sensitizer, which enabled us to speculate that the cycloaddition reaction occurs from the triplet excited state. Preliminary quenching experiments indicated that the cycloaddition of cyclopentene to NBI was quenched by typical triplet quenchers (piperylene $E_T = 56$ kcal/mol, isoprene $E_T = 59$ kcal/mol) and sensitized by sensitizers having triplet energies above 73 kcal/mol. These facts led us to conclude that the triplet excited state of NBI is involved in the cycloaddition reaction but did not rule out the possibility that the singlet excited states were also reactive. Triplet-counting experiments

(described in detail at the end of this chapter) using trans-piperylene indicated that the yield of triplet NBI (i.e. $\Phi_{T.S.C.}$) is higher than its quantum yield of cycloaddition with cyclopentene. This is consistent with the exclusive involvement of the triplet state in the cycloaddition process but does not rule out a parallel singlet excited state pathway.

The fluorescence of NBI was not quenched in the presence of alkenes such as cyclopentene, piperylene and isoprene; this eliminated the possibility of the involvement of the fluorescing singlet state in the cycloaddition reaction. However as mentioned above, this state appears to be a charge-transfer state produced by the relaxation of the initially formed singlet excited state; the fact that it is not quenched by alkenes does not rule out the possibility that the first formed singlet excited state is reactive. As will be described below, more conclusive evidence for non-involvement of the singlet excited state is given by the observation of a linear Stern-Volmer plot obtained from quenching of the photochemical cycloaddition of NBI and cyclopentene.

If it is assumed that the singlet excited state of NBI is unreactive, then a simple form of cycloaddition mechanism involving NBI and cyclopentene can be proposed and is summarized in Scheme 48. This proposes direct formation of a triplet biradical (BIR) resulting from the interaction of triplet excited NBI with ground state

alkene. The biradical will eventually result in the formation of the products following spin inversion. The biradical intermediate is included so as to provide a means for the system to proceed from the triplet surface to the singlet surface. The structure of the biradical will be considered further below. This scheme is similar to that for enone cycloaddition, and by analogy allowance is made for the biradical to collapse to the starting alkene and the ground state indole.



SCHEME 48

where NBI, O and [BIR] are NBI, olefin and biradical, respectively.

$$k_d^* = k_p + k_d + k_q [Q]$$

where k_p = rate constant for phosphorescence

k_d = rate constant for radiationless decay

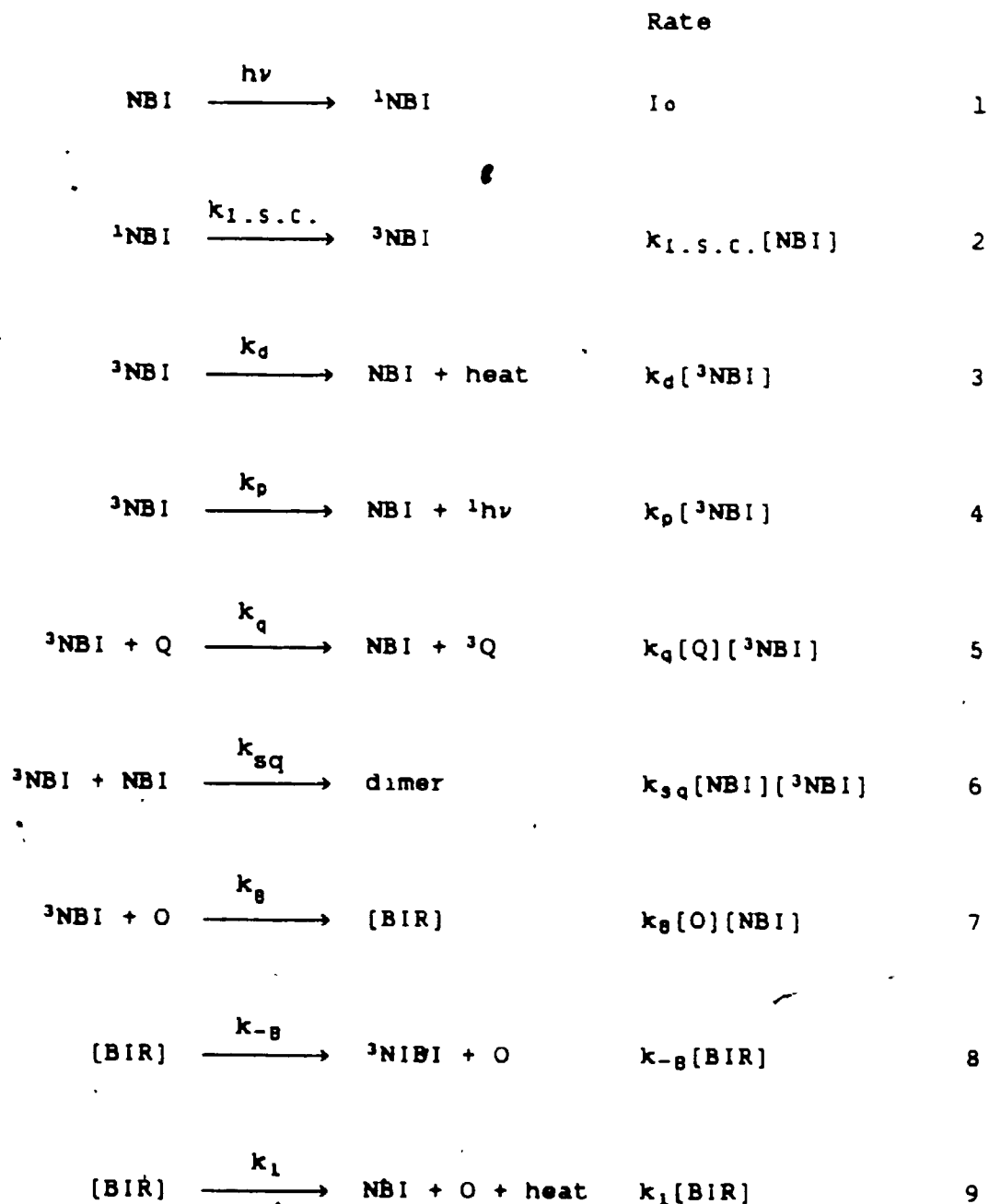
k_q = rate constant for quenching

$k_{2,q}$ = rate constant for bimolecular self-quenching.

5.5 DERIVATION OF THE KINETIC EQUATIONS

141

The simple scheme for cycloaddition from the triplet state only can be rewritten as follows:





The symbols NBI, O, Q, $\Phi_{\text{I.S.C.}}$ and [BIR] refer to NBI, olefin, quencher, intersystem crossing quantum yield and the biradical, respectively.

If it is assumed that the ^3NBI and BIR each achieve a steady state concentration, then an expression for the quantum yield of product formation in absence of quencher (Φ_p°) can be derived, and has the form:

$$\Phi_p^\circ = \frac{k_2 k_B [\text{O}] \Phi_{\text{I.S.C.}}}{(k_1 + k_2 + k_{-B})(k_d + k_p + k_{sq}[\text{NBI}]) + k_B [\text{O}](k_1 + k_2)} \quad 11$$

inversion of this equation results in the more useful form:

$$\frac{1}{\Phi_p^\circ} = \frac{(k_1 + k_2 + k_{-B})(k_d + k_p + k_{sq}[\text{NBI}])}{k_2} \cdot \frac{1}{\Phi_{\text{I.S.C.}}} \cdot \frac{1}{[\text{O}]} + \frac{(k_1 + k_2)}{k_2} \cdot \frac{1}{\Phi_{\text{I.S.C.}}} \quad 12$$

$$= \left[\frac{k_2}{k_1 + k_2 + k_{-B}} \quad \frac{k_B}{k_d + k_p + k_{sq}[\text{NBI}]} \right]^{-1} \cdot \frac{1}{\Phi_{\text{I.S.C.}}} \cdot \frac{1}{[\text{O}]} + \frac{(k_1 + k_2)}{k_2} \cdot \frac{1}{\Phi_{\text{I.S.C.}}} \quad 13$$

where $\frac{k_2}{(k_1+k_2+k_{-8})}$ represents the fraction of the

intermediate biradicals giving the observed products and $k_8/(k_d+k_p+k_{sq}[NBI])$ represents the efficiency of formation of the intermediate biradical from the triplet NBI. Thus a linear relationship should be observed between $1/\Phi_p^\circ$ and $1/[O]$. If a quencher is introduced which can selectively quench the triplet excited NBI, then an expression for the quantum yield of product formation, Φ_p , in the presence of the quencher can be derived, and has the form:

$$\Phi_p = \frac{k_2 k_8 [O] \Phi_{i.s.c.}}{(k_1+k_2+k_{-8})(k_d+k_p+k_{sq}[NBI]+k_q[Q]) + k_8 [O](k_1+k_2)} \quad 14$$

Division of Equation 11 by Equation 14 leads to the Stern-Volmer expression:

$$\frac{\Phi_p^\circ}{\Phi_p} = \frac{(k_1+k_2+k_{-8})k_q[Q]}{(k_1+k_2+k_{-8})(k_d+k_p+k_{sq}[NBI]) + k_8(k_1+k_2)[O]} \quad 15$$

The slope (M) of the Stern-Volmer equation is

$$M = \frac{(k_1+k_2+k_{-8})k_q}{(k_1+k_2+k_{-8})(k_d+k_p+k_{sq}[NBI]) + k_8(k_1+k_2)[O]} \quad 16$$

where

$$\frac{1}{M} = \frac{(k_d + k_p + k_{sq}[NBI])}{k_q} + \frac{k_B(k_1 + k_2)[O]}{(k_1 + k_2 + k_B)k_q} \quad 17$$

Examination of Equation 17 reveals that a plot of $1/M$ vs $[O]$ should have an intercept equal to $(k_d + k_p + k_{sq}[NBI])/k_q$, where the expression $(k_d + k_p + k_{sq}[NBI])$, which describes the decay of the triplet state, should be a function of NBI only and independent of the olefin concentrations. For exo-thermic quenching, the value of k_q , the rate constant for quenching, can be assumed to be approximately equal to the diffusion rate constant, k_{diff} .

This can be calculated approximately by means of the Debye equation:

$$k_q = k_{diff} = \frac{8RT}{3 \times 10^3 \eta} \quad 18$$

where η is the viscosity in Poise, $R = 8.31 \times 10^7$ erg/mol K, T is the temperature in degrees Kelvin. Using this expression k_q was found to be $1.1 \times 10^{-10} \text{ M}^{-1} \text{ s}^{-1}$ in benzene at 25°C . The intercept of Equation 17 can be determined experimentally by measurement of the gradients of the Stern-Volmer plots (described by Equation 15) obtained for the reaction of NBI with cyclopentene in the presence of a quencher at a variety of different values of

[O]. If the Stern-Volmer gradients are also measured for various values of [NBI] at constant [O], then values of $k_{s,q}$ and the triplet lifetime τ ($= 1/k_p + k_d$) can also be determined. Experimental measurement of the gradient of Equation 17 will also give the rate of formation of the biradical from the triplet excited state (i.e. k_B), if it is assumed that there is no reversal of the biradical intermediate to the triplet state (i.e. assuming $k_{-B} = 0$; this assumption will be discussed further below).

5.6 QUENCHING STUDIES

The phosphorescence spectrum of NBI indicated that it has a triplet state energy of 67.7 kcal/mol at 77 K. Assuming a similar value at room temperature, then the readily available dienes with triplet energies in the range 53-60 kcal/mol should be convenient and efficient quenchers for the cycloaddition of NBI with an alkene. Dienes which fulfill this criterion are 1,3-pentadiene, 1,3-cyclohexadiene and isoprene. These have been widely used as quantitative quenchers of excited triplet states. Care must be exercised in using these quenchers, however, because they can also quench singlet excited states. For example, Cantrell et al.^{85,86} have found that 2-cyclopentenone and 2-cyclohexenone undergo (2+2) photochemical cycloaddition to conjugated dienes with moderate efficiency in competition with diffusion controlled quenching of the enone triplet excited states by

the dienes. The products are mainly cyclobutanes resulting from (2+2) cycloaddition of one of the diene double bonds to the enone C-C double bond. However, these results were obtained at very high concentrations of the diene, and the reactions possibly result from interactions with the enone singlet excited states; by using low concentrations of the diene this problem can easily be overcome. Interactions of diene quenchers with the singlet excited state, as well as the triplet, can be readily detected by the observation of curvature in the Stern-Volmer plots.

5.7 STERN-VOLMER QUENCHING EXPERIMENTS

Stern-Volmer quenching experiments were performed by measuring the relative quantum yield of adduct formation when N-benzoylindole was irradiated with varying cyclopentene concentrations in both the absence and the presence of various concentrations of the quencher 1,3-cyclohexadiene. The results are shown in Figure 4. The Stern-Volmer expression is given by Equation 15. If the slope of the Stern-Volmer plot is represented by M (Equation 16), then the reciprocal of the gradient (1/M) will give the more useful form shown in Equation 17. The plot of 1/M against alkene concentration, [O] (Fig. 5), gives the value of the intercept $(k_d + k_p + k_{sq}[NBI])/k_q$. By taking k_q to be $1.1 \times 10^{10} \text{ M}^{-1} \text{ s}^{-1}$ in benzene at room temperature (Equation 18) the expression $(k_d + k_p + k_{sq}[NBI])$ was calculated to have the value $(6.0 \pm 0.6) \times 10^6 \text{ s}^{-1}$.

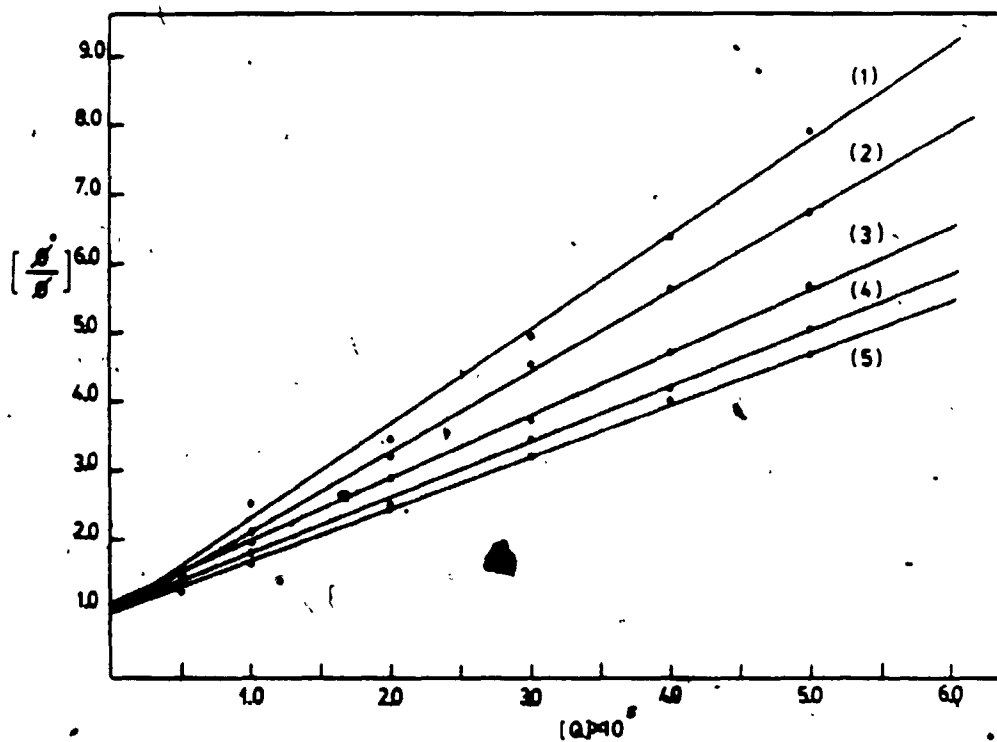


FIGURE 4: Quenching of NBI-cyclopentene reaction with 1,3-cyclohexadiene. Lines 1 to 5 are for cyclopentene concentrations of 0.35 M, 0.53 M, 0.82 M, 1.12 M and 1.41 M, respectively.

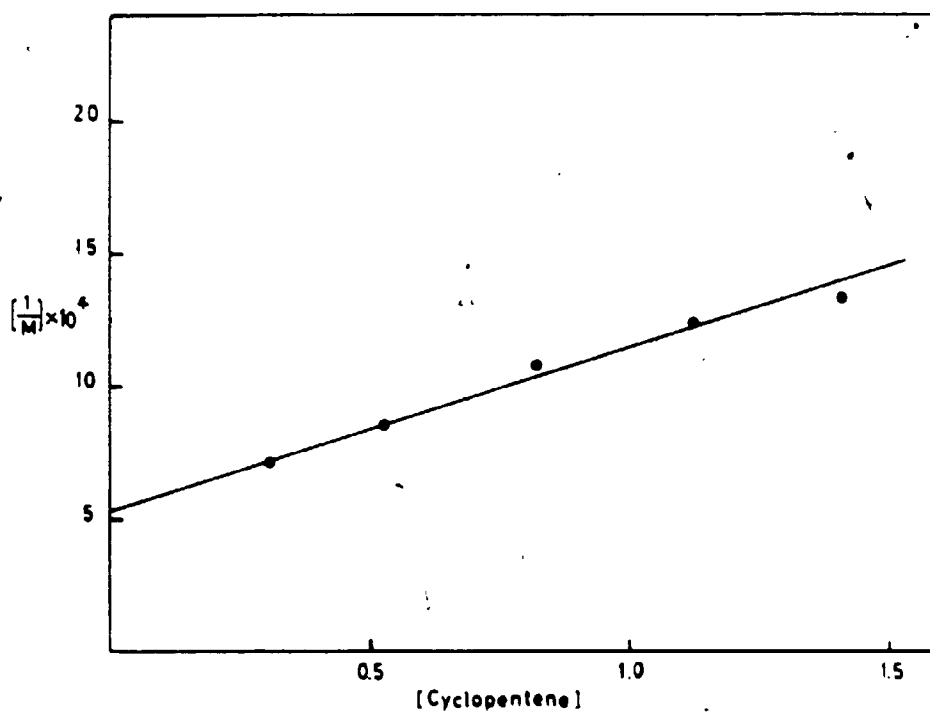


FIGURE 5: Plot of the reciprocal of Stern-Volmer gradients of Figure 4 against the cyclopentene concentration.

By independent measurements (discussed later in the chapter), k_{3q} was estimated to be $(1.21 \pm 0.18) \times 10^7 \text{ M}^{-1} \text{ s}^{-1}$, and hence $k_{3q}[\text{NBI}]$ is $(2.4 \pm 0.3) \times 10^5 \text{ s}^{-1}$ which is only 4.0% of the term $(k_c + k_p + k_{3q}[\text{NBI}])$. Hence the lifetime of triplet excited state of NBI was estimated to be $(1.74 \pm 0.15) \times 10^{-7} \text{ s}$. The slope of the plot of $1/M$ against $[O]$ (i.e. Equation 17) was found to be $(5.8 \pm 0.5) \times 10^{-6}$ and represents $k_B(k_1 + k_2) / (k_1 + k_2 + k_{-B})k_q$; hence, it was estimated that

$$\frac{k_B(k_1 + k_2)}{(k_1 + k_2 + k_{-B})} = (6.4 \pm 0.5) \times 10^6 \text{ s}^{-1}$$

If no reversal of the biradical is assumed, then $k_{-B} = 0$ and the above expression reduces to k_B , the rate constant for formation of the biradical. Using this assumption, k_B is therefore estimated to be $(6.4 \pm 0.5) \times 10^6 \text{ M}^{-1} \text{ s}^{-1}$. This is the minimum rate k_B could have; if there were reversal of the biradical to the triplet state (i.e. $k_{-B} > 0$) then k_B would be larger than this value by the factor $k_{-B} / (k_1 + k_2)$.

5.8 VARIATION OF QUANTUM YIELD OF CYCLOADDITION WITH SUBSTRATE CONCENTRATION

If the kinetic scheme shown in Scheme 48 is correct, then a linear relationship should be observed between the reciprocal of the quantum yield of adduct formation between

NBI and cyclopentene, and the reciprocal of cyclopentene concentration, as predicted by Equation 12.

The absolute quantum yield of the reaction was measured at various alkene concentrations. The direct plot of the quantum yield of cycloaddition for NBI with cyclopentene against the substrate concentration in benzene at room temperature should follow Equation 11, and show a curve. This is observed, as can be seen in Figure 6. Similarly, a plot of $1/\Phi$ vs $1/[O]$ shows the straight line expected if Equation 12 holds, as can be seen in Figure 7. The slope of the plot was found to be equal to 149 ± 2 and corresponds to

$$\frac{(k_1+k_2k_g)}{k_2} \frac{(k_d+k_p k_{sq}[\text{NBI}])}{k_B} \cdot \frac{1}{\Phi_{\text{I.S.C.}}}$$

The intercept corresponds to

$$\frac{(k_1+k_2)}{k_2} \cdot \frac{1}{\Phi_{\text{I.S.C.}}}$$

and was found to be 16.0 ± 0.8 . From triplet counting experiments the value of $\Phi_{\text{I.S.C.}}$ for NBI in benzene was found to be equal to $0.39 \pm .01$ at room temperature (this will be discussed later in this chapter). The value of $\Phi_{\text{I.S.C.}}$ is independent of the substrate, and the value measured by other means such as triplet counting can be

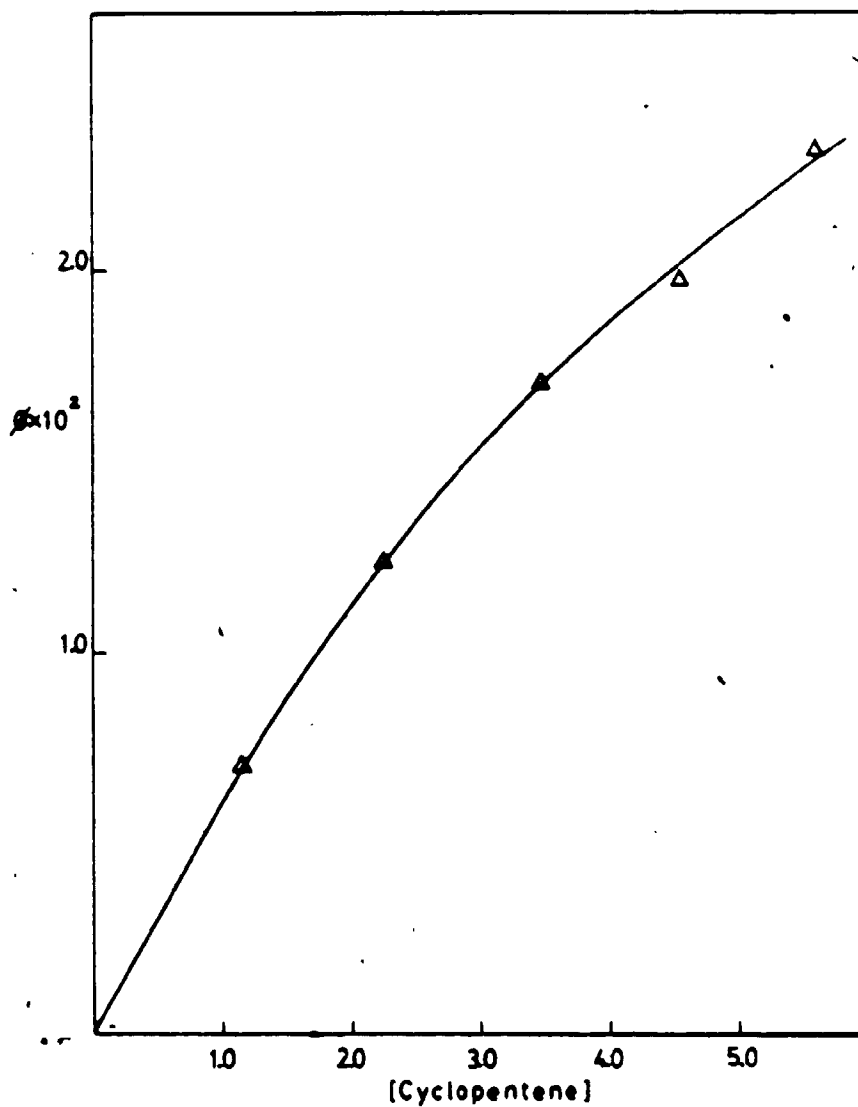


FIGURE 6: Effect of cyclopentene concentration on the quantum yield of photoaddition of NBI and cyclopentene

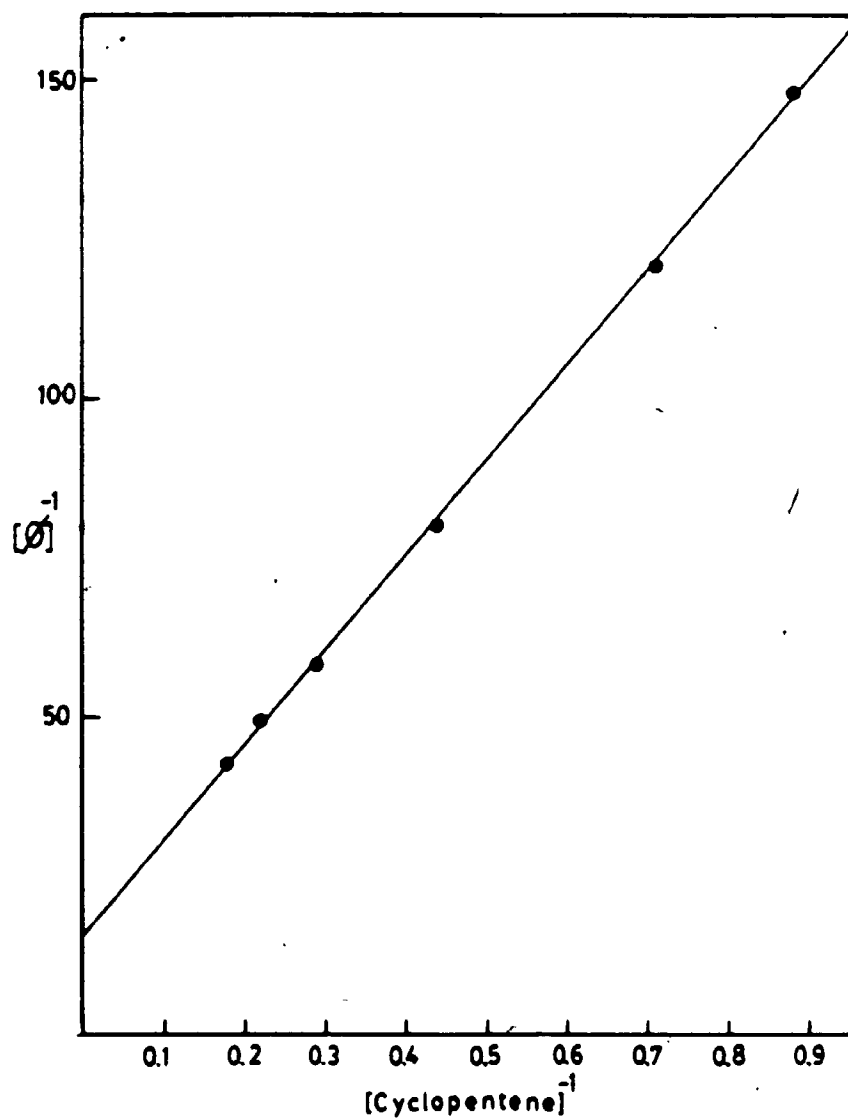


FIGURE 7: Plot of the reciprocal of quantum yield of photoaddition of NBI and cyclopentene vs the reciprocal of cyclopentene concentration

used directly. Hence the fraction of the biradical leading to products,

$$\frac{k_2}{k_1+k_2}$$

is equal to $0.160 \pm .008$, which indicates that only 16% of the biradicals formed lead to products.

The quantum yield of cycloaddition of NBI to cyclopentene in benzene at room temperature (which varies with cyclopentene concentration) therefore is $0.062 \pm .003$ at infinite alkene concentration. Under this condition (i.e. at infinite alkene concentration), of the various routes for decay of the triplet excited state, processes k_p , k_d and process k_{-8} are non-competitive. The discrepancy between the quantum yield of product formation and the quantum yield of intersystem crossing ($\Phi_{i.s.c.}$ which gives the yield of triplet excited states, and which is determined as 0.39 ± 0.06) is exclusively due to collapse of the intermediate biradical to the starting materials. Thus, only 16% of the biradical intermediates proceed to adduct, while 84% revert to the ground state NBI and alkene molecules.

The proportion of the biradicals formed which goes back to the starting materials as compared with that proceeding to products with the formation of the cyclobutane ring depends on the activation energy for each

process. If only 16% of the biradicals go to the products then the activation energy for the cyclobutane formation should be greater than for the activation energy for the biradical going to the starting materials. Although there is evidently a quite large (5-fold) difference between the rates of the two processes the same cannot be said regarding the activation energies. Studies of variation of quantum yield of cyclobutane formation of cyclohexenone with various alkenes as a function of temperature^{34,87-89} have indicated that the difference in activation energies for the two processes is less than 1 kcal/mol and that approximately half of the biradicals formed proceed to products with the rest collapsing to starting materials.

The relationship between the relative rate and difference of activation parameters between the two reactions is given by

$$\Delta E_A = 1.37 \log \frac{k_a}{k_b}$$

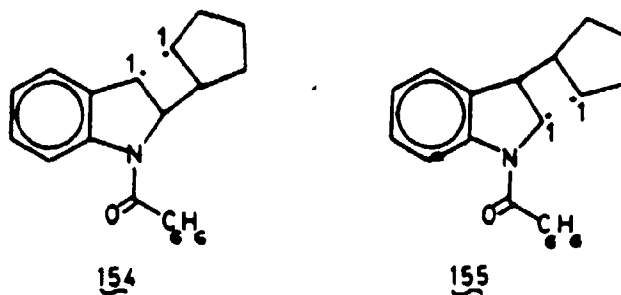
where ΔE_A is the difference in activation energy between the two reactions and k_a and k_b are the rates of the two processes.

$$\frac{k_2}{k_1+k_2} = 0.16 \quad , \quad \text{therefore} \quad \frac{k_1}{k_2} = 6.142$$

hence $\Delta E_A = 1.37 \log 6.142$
 $= 1.08 \text{ kcal/mol and } 298 \text{ K.}$

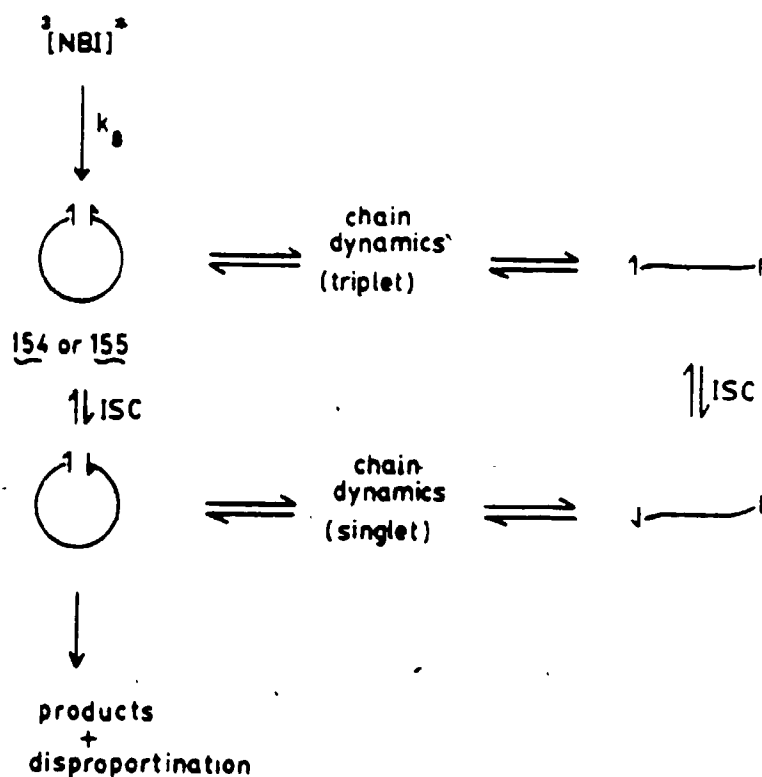
This indicates that even though there is a relatively large difference in the rates of reaction of the biradical, the activation parameters that correspond are rather small. Hence a small change in activation energy, which could easily result from a minor change in the structure, temperature or solvent, could easily change the percentage of biradicals reacting to yield products rather than reverting to the starting materials.

In the photochemical annelation reaction of NBI and cyclopentene two biradical intermediates are possible, and have the structures shown in (154) and (155).



As mentioned earlier, the cycloaddition occurs from the triplet excited state of NBI; hence the multiplicity of the initial biradical formed is triplet. This triplet biradical could take part in several processes:

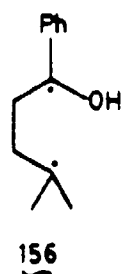
- (a) intersystem crossing to the singlet biradical;
 (b) interconversion among biradical chain conformers;
 (c) product formation from singlet biradical (Scheme 49).



SCHEME 49

At room temperature, intersystem crossing (I.S.C.) is the rate determining step in the decay of small, flexible triplet biradicals in fluid solutions.⁹⁰⁻⁹² It has also been found that there is a change in the rate-determining step for biradical decay from I.S.C. at high temperature to chain dynamics at low temperature.⁹³ At 25°C in fluid

solution, I.S.C. is typically the rate determining step for biradical decay, chain dynamics is faster and product formation from the singlet biradical is fastest of all. J.C. Scaiano et al⁹⁴ have found the lifetime of the 1,4-biradical (156), which has a similar biradical structure to that of (155).



The lifetime of (156) was found to be 97 ns in methanol and in benzene it was estimated to be 42 ns. Hence it is reasonable to assume the indole biradical (155) to have a lifetime of the order of 42 ns, and the rate of decay of the biradical should be in the order of 10^7 s^{-1} . It was estimated above that the minimum rate of biradical formation from triplet excited NBI and cyclopentene is $6.4 \times 10^6 \text{ s}^{-1}$, which is similar to the rate for decay of the biradical.

5.9 EVALUATION OF THE RATE CONSTANT FOR SELF-QUENCHING

As noted above, the photochemical dimerization of indole derivatives such as 1,3-diacetylidole has been

observed,⁷³ but no such reactions were detected for N-acetylindoles, N-benzenesulfonylindole or N-benzoylindole. The quantum yield of cycloaddition of NBI with cyclopentene (Φ°) was found in this work to change with NBI concentration; this was ascribed to a self-quenching process, with a rate constant k_{sq} , which was incorporated into Scheme 48 and which was used to derive Equation 11. Inversion of this equation gives:

$$\frac{1}{\Phi^\circ} = \frac{(k_1+k_2+k_{-8})}{k_2} \frac{(k_d+k_p+k_{sq}[NBI])}{k_8} \frac{1}{\Phi_{i.s.c.}[O]} + \frac{(k_1+k_2)}{k_2} \frac{1}{\Phi_{i.s.c.}} \quad 12$$

i.e.

$$\frac{1}{\Phi^\circ} = \frac{(k_1+k_2+k_{-8})k_{sq}}{k_2k_8[O]\Phi_{i.s.c.}} [NBI] + \text{const} \quad X$$

If it is assumed that the biradical intermediate does not reverse back to the NBI excited state (i.e. $k_{-8} = 0$) then Equation X becomes

$$\frac{1}{\Phi^\circ} = \frac{(k_1+k_2) \cdot k_{sq}}{k_2k_8[O]\Phi_{i.s.c.}} [NBI] + \text{const} \quad Y$$

The quantum yield of cycloaddition (Φ°) of NBI with cyclopentene was measured for a variety of [NBI]. A plot of $1/\Phi^{\circ}$ vs [NBI] (Fig. 8) gave a straight line whose gradient was calculated to be $13.6 \pm 1.6 \text{ M}^{-1}$. Thus from Equation Y,

$$\frac{(k_1+k_2)}{k_2k_8[O]\Phi_{I.S.C.}} \cdot k_{sq} = 13.6 \pm 1.6$$

Using the assumption that there is no reversal of the biradical intermediate (i.e. $k_{-8} = 0$) k_8 was determined above to be $(6.4 \pm 0.5) \times 10^6 \text{ s}^{-1}$, and the value $(k_1+k_2)/k_2\Phi_{I.S.C.}$ was estimated to be 16.0 ± 0.8 (Equation 12); hence $k_{sq} = (1.2 \pm 0.8) \times 10^7 \text{ s}^{-1}$.

The value of k_{sq} determined is inaccurate, and this reflects the shallowness of the gradient of the plot $1/\Phi^{\circ}$ vs [NBI]. Also, it could be argued that the change in quantum yield of cycloaddition with changing [NBI] does not arise from self-quenching but could be attributed instead to the presence of an impurity in NBI which would also produce the data obtained. The important conclusions, however, are that the process which results in a diminished Φ as [NBI] increase, is relatively inefficient, and that the product of k_{sq} and [NBI] is small relative to k_8 and k_p in Equation 12. Thus, in the work described in this thesis, it can be assumed that the self-quenching process is negligible and can be ignored for the purposes of

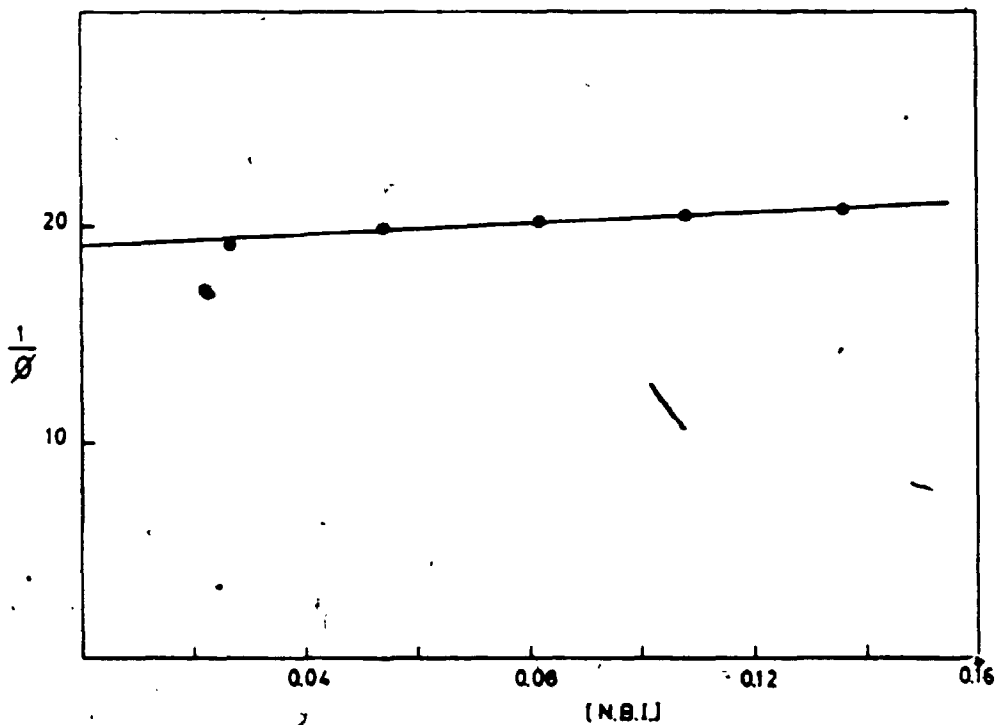


FIGURE 8: Plot of the reciprocal of quantum yield of photoaddition of NBI and cyclopentene vs the NBI concentration

determining the rate constants for the decay and reaction processes of the triplet excited state of NBI.

5.10 CONSIDERATION OF THE POSSIBILITY OF INVOLVEMENT OF AN EXCIPIEX IN THE CYCLOADDITION MECHANISM

The rate constant for reaction of the N-benzoylindole triplet excited state with cyclopentene (k_8 in Equation 7) was determined to be $6.4 \times 10^6 \text{ s}^{-1}$.

Comparison of reactivity of radicals with alkenes indicate a much slower reaction rate⁹⁵⁻⁹⁷ (Table VII).

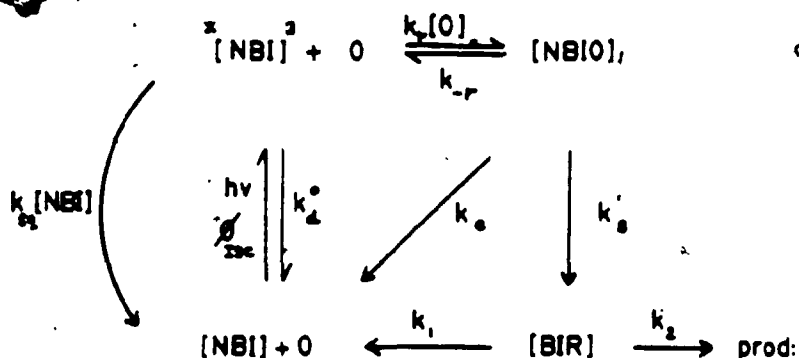
	<u>Rate Constant (s^{-1})</u>
$\cdot\text{CH}_3 + \text{ethylene}$	4.5×10^4
$\cdot\text{CH}_2\cdot\text{CH}_3 + \text{ethylene}$	3.5×10^4
$\cdot\text{CH}(\text{CH}_3)_2 + \text{ethylene}$	2.2×10^4
$\cdot\text{C}(\text{CH}_3)_3 + \text{ethylene}$	8.9×10^3
$\cdot\text{C}(\text{Ph})\text{CH}_2 + \text{CH}_2 = \text{CHPh}$	5.5×10^1
$\cdot\text{CH}(\text{OAc})\cdot\text{CH}_2 + \text{CH}_2 = \text{CH}(\text{OAc})$	1.01×10^3

TABLE VII: Rate constant for the reactivity of radicals with alkenes

The rate of formation of the biradical intermediate from the triplet excited state of NBI with cyclopentene is at least 3 orders of magnitude larger than that observed in the reaction of radicals with alkenes. If it is assumed that the NBI triplet excited state should have a reactivity

comparable with that of a radical, then the cycloaddition of NBI and cyclopentene must involve an excited state complex or an exciplex in order to explain the observed rapid rate. This reasoning has been used previously to explain the observed rapid rate in enone (2+2) photocycloaddition reactions and the Paterno-Buchi reaction of ketones with alkenes.

A revised mechanism for the photochemical cycloaddition of NBI and cyclopentene which allows for the possibility of exciplex formation is given in Scheme 50.



SCHEME 50

The exciplex is proposed to be formed from the interaction of excited NBI with the ground state alkene, O. The exciplex subsequently collapses to the biradical which can then result in the formation of the product. In the scheme, [NBI], [O], [NBIO], [BIR], are NBI, olefin, the exciplex and biradical concentrations, respectively. The

rate constant k_d^* , which describes the decay process of the 163 triplet excited state of NBI , is equal to $k_p + k_d + k_q[Q]$ where

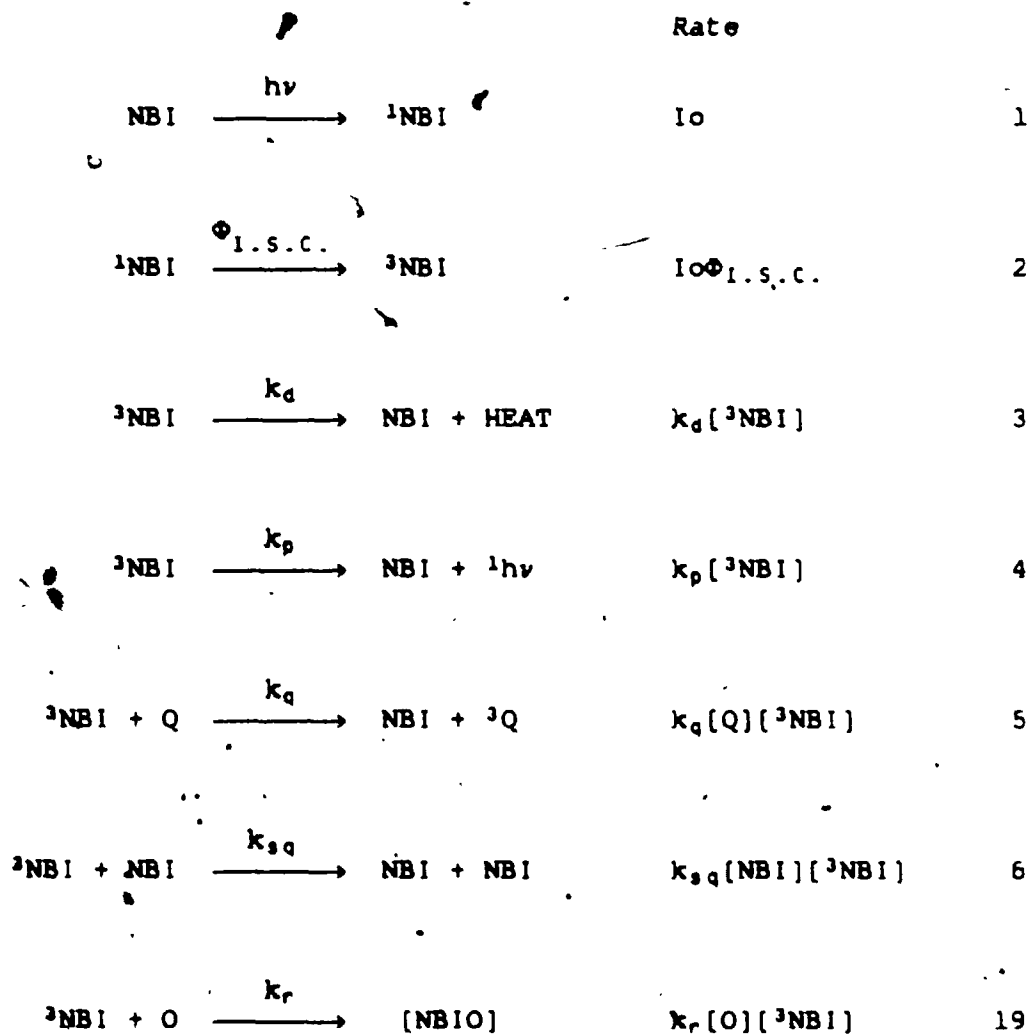
k_p = the rate constant for phosphorescence

k_d = the rate constant for radiationless decay

k_q = the rate constant for quenching by a quencher Q

k_{sq} = the rate constant for bimolecular

self-quenching. The kinetic scheme for cycloaddition which indicates an exciplex can be written as





If it is assumed that [${}^3\text{NBI}$] and [NBIO] achieve a steady state concentration then an expression for the quantum yield of product formation (Φ_p°) in the absence of quencher can be written as

$$\Phi_p^\circ = \frac{k_2}{k_1+k_2} \frac{k_g k_r [\text{O}] \Phi_{\text{I.S.C.}}}{(k_{-r}+k_e+k^1_g)(k_d+k_p+k_{gq}[\text{NBI}]) + k_r[\text{O}](k_e+k^1_g)} \quad 23$$

inversion of the equation results in

$$\frac{1}{\Phi_p^0} = \frac{(k_1+k_2)}{k_2} \frac{(k_{-r}+k_e+k_B)(k_d+k_p+k_{sq}[NBI])}{k^1_B k_r \Phi_{I.S.C.}} + \frac{1}{[O]}$$

$$\frac{(k_1+k_2)}{k_2} \frac{(k_e+k^1_B)}{k^1_B} + \frac{1}{\Phi_{I.S.C.}}$$

24

The expression for the quantum yield in the presence of quencher can be written as

$$\Phi_p =$$

25

$$\frac{k_2}{k_1+k_2} \frac{k^1_B k_r [O] \Phi_{I.S.C.}}{(k_{-r}+k_e+k^1_B)(k_d+k_p+k_{sq}[NBI] + k_q[Q]) + k_r[O](k_e+k^1_B)}$$

Division of Equation 23 by Equation 25 leads to the Stern-Volmer expression:

$$\frac{\Phi_p^0}{\Phi_p} = 1 + \frac{k_q[Q]}{(k_d+k_p+k_{sq}[NBI]) + \frac{(k_e+k^1_B)k_r[O]}{(k_e+k^1_B+k_{-r})}}$$

26

The reciprocal of the slope (M^1) of the Stern-Volmer plot is given by:

$$\frac{1}{M^1} = \frac{(k_d+k_p+k_{sq}[NBI])}{k_q} + \frac{(k_e+k^1_B)k_r[O]}{(k_e+k^1_B+k_{-r})k_q}$$

27

Earlier in this chapter, Stern-Volmer quenching experiments were described in which the relative quantum yields of adduct formation between NBI and cyclopentene were measured at various alkene concentrations in the absence and presence of various concentrations of a quencher (1,3-pentadiene). The data was analyzed assuming the applicability of Scheme 48, which committed an exciplex intermediate, and was plotted according to Equations 15 and 17 as shown in Figures 4 and 5. This data was now plotted according to Equation 26; no deviation from linearity of Stern-Volmer plots was observed. In fact the plots were identical with those shown in Figure 4 since the only difference in form between Equations 26 and 15 is in the definition of the rate constants in the intercept and gradient. Similarly the plot of reciprocal of the Stern-Volmer gradients, M^1 , against $[O]$ gave a plot identical to that shown in Figure 5 where $1/M$, rather than $1/M^1$, is plotted against $[O]$. However, the gradient (measured to be $(5.8 \pm 0.5) \times 10^{-4}$) now corresponds to

$$\frac{(k_0 + k^1_0)k_r}{(k_0 + k^1_0 + k_{-r})k_q}$$

Assuming k_q to be $1.1 \times 10^{10} \text{ M}^{-1} \text{ s}^{-1}$ in benzene at room temperature (Equation 18), then the minimum rate of exciplex formation (k_r) is calculated to be $(6.4 \pm 0.5) \times 10^6 \text{ M}^{-1} \text{ s}^{-1}$ if it is also assumed that no

reversal of the exciplex to the triplet indole occurs (i.e. $k_{-r} = 0$). The intercept of the data plotted to Equation 27 was determined as $(5.5 \pm 0.5) \times 10^{-6}$ M and this corresponds to

$$\frac{(k_d + k_p + k_{sq}[\text{NBI}])}{k_q}$$

$(k_d + k_p + k_{sq}[\text{NBI}])$ is the sum of rate constants for decay of the triplet state, which is only a function of $[\text{NBI}]$.

Division of the intercept by the gradient of Equation 27 gives:

$$\frac{(k_d + k_p + k_{sq}[\text{NBI}])(k_{-r} + k_e + k^1_B)}{k_r(k_e + k^1_B)} = (0.94 \pm 0.17 \text{ M}) \quad 28$$

$$\text{if } \frac{k_{-r}}{k^1_B + k_e} = C \quad 29$$

then Equation 28 becomes

$$\frac{(k_d + k_p + k_{sq}[\text{NBI}])(1+C)}{k_r} = (0.94 \pm 0.17 \text{ M}) \quad 30$$

Figure 7 shows the data obtained when the quantum yield of formation of cycloadduct was measured as a function of cyclopentene concentration. If it is assumed

that Equation 24 now describes this data, rather than Equation 12 which did not take into account the possibility of exciplex formation, then the slope and intercept are given by

$$\text{slope} = 149 \pm 2 M = \frac{(k_1+k_2)}{k_1} \frac{(k_{-r}+k_e+k^1_B)(k_d+k_p+k_{sq}[NBI])}{k^1_B k_r \Phi_{I.S.C.}}$$

$$\text{intercept} = 16.0 \pm 0.8 = \frac{k_1+k_2}{k_1} \frac{k_e+k^1_B}{k^1_B} \frac{1}{\Phi_{I.S.C.}}$$

$$\text{If } p = \frac{k_2}{(k_1+k_2)} \frac{k^1_B}{k_e+k^1_B} \quad 31$$

where p is the fraction of the exciplex leading to products, then

$$\text{slope} = \frac{1}{p \Phi_{I.S.C.}} \frac{(k_{sq}[NBI] + k_d+k_p)}{k_r} \left(1 + \frac{k_{-r}}{k_e+k^1_B}\right) \quad 32$$

$$= \frac{1}{p \Phi_{I.S.C.}} \frac{(k_{sq}[NBI] + k_d+k_p)(1+\epsilon)}{k_r}$$

$$\text{and intercept} = \frac{1}{p \Phi_{I.S.C.}} = 16.0 \pm 0.8$$

Using the value of $\Phi_{I.s.c.}$ determined by triplet counting (this is described below), the fraction of the reaction intermediates leading to products is calculated to be (0.16 ± 0.008) , which indicates that only 16% of the reaction intermediates (i.e. the exciplex and biradical) lead to products. Division of the slope by the intercept of Equation 24 gives

$$\frac{(k_d + k_p + k_{sq}[NBI])(1+C)}{k_r} = 9.3 \pm 0.5 M \quad 34$$

The ratio of the gradient to the intercept of Equations 27 and 24 should be identical. However, comparison of Equations 30 and 34 shows that a large discrepancy exists. The numerical value in Equation 30 was obtained from experimental data arising from Stern-Volmer quenching experiments in which the relative quantum yield of cycloadduct formation was obtained as a function of added quencher concentration, whereas the numerical value in Equation 34 was obtained from data from experiments in which the absolute quantum yield of cycloadduct formation was determined at various alkene concentrations, no quencher being added.

Possible explanations for the discrepancy between Equations 30 and 34 is that there is another mode of decay of the triplet excited state of NBI which is also effected

by the presence of a quencher. For example, if the triplet excited state of NBI is in equilibrium with another state, which is unreactive with alkene, but which is quenchable, then in the Stern-Volmer experiments the triplet excited state has another mode of decay, making the numerator in Equation 30 larger and so resulting in a larger numerical value as compared with Equation 34. This possibility, along with others, will be examined in the next section.

5.11 POSSIBILITY OF THE EXISTENCE OF A CHARGE-TRANSFER TRIPLET STATE

In the previous section it was shown that the data obtained from the two different sets of experiments were in qualitative agreement with the mechanism proposed in Scheme 50 for the photocycloaddition of NBI with cyclopentene. Thus linear Stern-Volmer plots were obtained when the relative quantum yield of adduct formation was measured as a function of added quencher, and the expected linear dependency of the reciprocal of the absolute quantum yield of adduct formation upon the reciprocal of alkene concentration was observed. However, the values of

$$\frac{(k_d + k_p + k_{sq}[NBI]) (1+C)}{k_r}$$

calculated from the results of each set of experiments were substantially different, apparently indicating that some other process is open to the triplet excited

N-benzoylindole molecule which is affected by the presence of a quencher.

Scheme 50 shows only one mode of decay of the triplet excited state of NBI which is affected by the quencher. In addition there are two other obvious possibilities:

- (a) the quenching of the singlet excited NBI
- (b) the quenching of the proposed exciplex
) intermediate

As will be discussed below, the initially formed singlet-excited state of NBI is non-fluorescent, but relaxes to a charge transfer (C.T.) state which does fluoresce. The NBI C.T. fluorescence was found to be unaffected by the presence of the triplet quenchers cyclohexadiene, 1,3-pentadiene or the alkene, cyclopentene, indicating the absence of NBI C.T. singlet state quenching by these triplet quenchers. The fluorescent lifetime of the C.T. singlet state was found to be 0.5 ns using the single photon counting technique, and it can be expected that the initially formed singlet excited state will have a lifetime of 0.5 ns or lower. For the quencher concentration range used in the Stern-Volmer experiments, these lifetimes mean that no singlet state quenching would be expected and so possibility (a) above can be discounted.

The triplet exciplex energy, while not known, is expected to be close to and slightly lower, than that of the NBI triplet excited state. The repulsion in the ground

state between NBI and cyclopentene is unlikely to be large, and hence the exciplex vertical excitation energy is not expected to drop below that of a diene quencher's triplet energy. Therefore, the exciplex should in principle be quenchable.⁹⁸ The Stern-Volmer expression for the quenching of two sequential species has the general form:

$$\frac{\Phi_0}{\Phi} = (1+k_q[Q]\tau_1)(1+k_q[Q]\tau_2) \quad 35$$

where in this case τ_1 and τ_2 are the NBI triplet and exciplex lifetimes, respectively, and are given by

$$\tau_1 = 1/(k_a+k_b+k_r), \quad \tau_2 = 1/k_d + k_r[O]$$

Since k_q is near diffusion controlled and essentially identical in both processes,³⁴ then at high quencher concentrations the Stern-Volmer plots should be non-linear. However the Stern-Volmer plots obtained for the cycloaddition of NBI and cyclopentene showed linearity (Fig. 4), which suggests the absence of quenching of the exciplex within the concentration range of the triplet quencher used (cyclohexadiene). Thus the second possibility to explain the discrepancy outlined at the start of this section can be discounted.

A third possibility to explain the observed discrepancy is that the triplet excited state of N-benzoylindole is in equilibrium with another state, which

is also quenchable, but which is unreactive with cyclopentene. This would serve to provide another mode of decay of the triplet excited state, which requires the presence of a quencher. Thus in the Stern-Volmer experiments described above the numerator of Equation 26 would be increased relative to that in Equation 24 which refers to the experiments in which the quantum yield of cycloaddition was measured in the absence of a quencher. This simple-minded approach would explain the larger numerical value of the expression in Equation 26 relative to Equation 24. If this explanation is correct, then the new quenchable, unreactive state must be identified; a good candidate is a triplet charge transfer corresponding to the singlet charge transfer state of N-benzoylindole which has been identified in this work and which is discussed in Chapter 6.

The results described in Chapter 6 demonstrate the presence of a singlet charge transfer (C.T.) state ($S_1(\text{C.T.})$) which is lower in energy than the normal singlet excited state (S_1).

As will be discussed in detail, the position of the absorption maxima of NBI does not change with changing solvent polarity, suggesting that the initially formed excited state possesses a similar degree of charge separation to the ground state molecule; in contrast the fluorescence emission shows a large Stokes' shift and a marked solvent dependence of the emission wavelength was

observed, suggesting an emitting singlet excited state possessing a large degree of C.T. character⁹⁹ (Fig. 9).

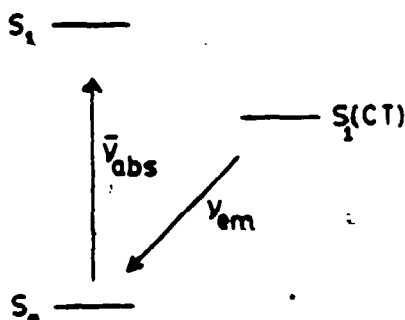


FIGURE 9: Energy levels of the singlet excited states of NBI

Given the presence of a singlet C.T. state, it is reasonable to propose the existence of a triplet C.T. state [$T_1(\text{C.T.})$] in addition to the normal triplet excited state (T_1). The energy of the $T_1(\text{C.T.})$ state would be expected to be close in energy to that of the $S_1(\text{C.T.})$ state and would also be expected to show solvent dependence (Fig. 10).

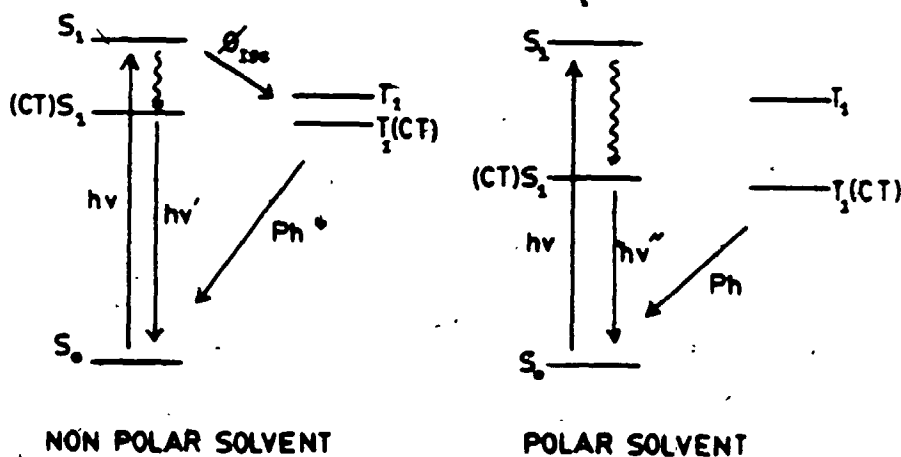


















FIGURE 10: Energy levels of excited states of NBI in polar and non-polar solvents

3

3



MICROCOPY RESOLUTION TEST CHART
NBS 1010a
ANSI and ISO TEST CHART No. 2

	1.0		2.8		2.5
	1.1		3.2		2.2
	1.25		3.6		2.0
			4.0		1.8
			4.5		1.6
			5.0		
			5.6		
			6.3		

In hexane at 77 K NBI showed a phosphorescence emission at 425 nm (Fig. 3) and the C.T. fluorescence was at 440 nm at room temperature, indicating that NBI has a triplet state slightly higher in energy than the C.T. singlet state. The proposed charge transfer triplet state would then be expected to be slightly lower in energy than the triplet state (T_1). Since the C.T. fluorescence of NBI showed a marked dependence of emission wavelength on the polarity of the solvent, indicating the lowering of the energy of the S_1 (C.T.) state with increase in polarity, a similar shift in the energy of the T_1 (C.T.) state with changing solvent polarity should be observed. The phosphorescence emission of NBI showed no significant change of emission wavelength with respect to increase in polarity of the solvent. Thus in hexane NBI showed a phosphorescence maxima at 423 nm, and when the solvent was changed to acetonitrile a bathochromic shift of only 2 nm was observed. This indicates that the phosphorescence emission arises from a transition between states which do not change much in relative energy in different solvents at 77 K.

The existence of a charge-transfer triplet state whose energy would be expected to decrease with increasing polarity of the solvent gives rise to the possibility of a change in triplet lifetime, and intersystem crossing quantum yield ($\Phi_{i.s.c.}$) as the solvent polarity is changed. Triplet counting experiments (described later in this chapter) enabled the determination of the triplet

excited state lifetimes and values of $(\Phi_{I.S.C.})$ for NBI in different solvents (Table VIII) and the results are consistent with the existence of a charge-transfer triplet state. Table VIII shows that an apparent shortening of the triplet excited state lifetime and a lowering of the value of $(\Phi_{I.S.C.})$ for NBI occurs when the polarity of the solvent is increased, as determined by triplet counting. 1,3-pentadiene ($E_T = 58$ kcal/mol) was used as the triplet quencher. This quencher was chosen because it possessed a lower triplet energy than N-benzoylindole (the phosphorescence spectra of NBI indicated that it possessed a triplet energy of 67 kcal/mol). However, the presence of a charge-transfer triplet state whose energy is solvent dependent may mean that 1,3-pentadiene quencher will only be of low enough energy to quench both the normal triplet and the C.T. triplet in non-polar solvents, whereas in polar solvents the energy of the proposed C.T. triplet state may drop below that of the quencher and so not be quenched, thus yielding a changed value of $(\Phi_{I.S.C.})$ in polar solvents.

Comparison of $E_T(30)$ values^{100,101} (a measure of solvent polarity) shows diethyl ether ($E_T(30) = 34.6$) to have a $E_T(30)$ value only slightly higher than that of benzene ($E_T(30) = 34.5$), which indicates that diethyl ether and benzene have similar polarities. The C.T. fluorescence spectrum of NBI in benzene could not be obtained due to complications arising from the absorption by benzene

Compound	Solvent	λ_{abs} nm	λ_{phos} nm	E_T kcal/mol	$\Phi_{I.S.C.}$	τ_S
(142A)	benzene	302	---	---	0.39 ± 0.01	(3.4 ± 0.3) × 10 ⁻⁸
	hexane	302	422	67.7	---	---
	MeCN	302	424	67.4	0.169 ± 0.002	(3.25 ± .06) × 10 ⁻⁹
	CH ₂ Cl ₂	303	424	67.4	0.155 ± .004	(1.22 ± .03) × 10 ⁻⁸
(157)	benzene	299	---	---	0.549 ± .008	(3.11 ± 0.1) × 10 ⁻⁸
	hexane	299	422	67.7	---	---
	MeCN	299	423	67.6	---	---
	CH ₂ Cl ₂	299	423	67.6	---	---
(158)	benzene	302	---	---	0.64 ± 0.02	1.61 ± .08 × 10 ⁻⁸
	hexane	302	---	---	---	---
	MeCN	301	---	---	---	---
	CH ₂ Cl ₂	302	---	---	---	---
(159)	benzene	288	---	---	0.021 ± .001	(3.9 ± .3) × 10 ⁻⁹
	hexane	289	---	---	---	---
	MeCN	289	---	---	---	---
	CH ₂ Cl ₂	289	---	---	---	---
(160)	benzene	314	---	---	0.47 ± 0.01	2.29 ± .04 × 10 ⁻⁸
	hexane	314	428	66.8	---	---
	MeCN	314	432	66.2	---	---
	CH ₂ Cl ₂	315	430	66.5	---	---

TABLE VIII: Photophysical properties of compounds (142a) and (157-162)

TABLE VIII (Cont'd):

Compound	Solvent	λ_{abs} nm	λ_{phos} nm	E_T kcal/mol	$\Phi_{\text{I.S.C.}}$	τ 75
(161)	benzene	---	---	---	0.050 ± 0.005	(3.2 ± 0.4) × 10 ⁻⁹
	hexane	290	---	---		
	MeCN	290	440	---		
	CH ₂ Cl ₂	290	440	65.0		
(162)	benzene	359	---	---		
	hexane	359	---	---		
	MeCN	357	---	---		
	CH ₂ Cl ₂	360	---	---		

Notes:

1. Absorption and emission spectra were recorded on solutions of ca 10⁻⁵ M concentrations.
2. λ_{abs} is the wavelength of the lowest absorption maxima.
3. λ_{phos} is the wavelength of maximum phosphorescence emission.
4. E_T is the energy of the lowest excited triplet state.
5. $\Phi_{\text{I.S.C.}}$ is the intersystem crossing quantum yield.
6. τ is the lifetime.

itself. However in diethyl ether, NBI C.T. fluorescence was observed at 480 nm which corresponds to an energy of 50 kcal/mol for the C.T. singlet state.

Based upon this result the energy of the proposed charge transfer triplet state can be estimated to be of the order of 60 kcal/mol in benzene or ether. Using the values of the energy of the singlet charge transfer state in benzene, methylene chloride and acetonitrile (obtained from the position of the fluorescence C.T. emission as described in Chapter 6) the energy of the proposed charge transfer triplet state can be estimated to be circa 60, 55 and 53 kcal/mol, respectively, in these solvents.

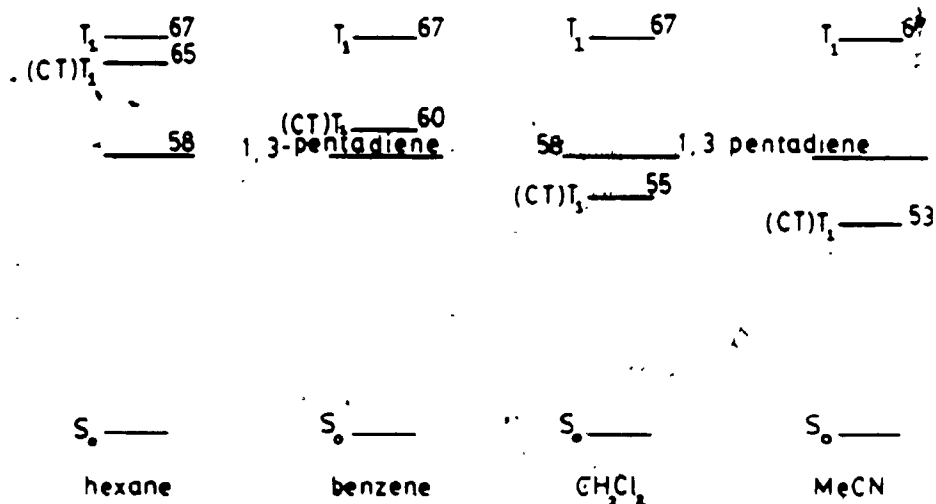


FIGURE 11: Variation of the $T_1(C.T.)$ state of NBI in solvents of different polarity

Of the three solvents for which triplet lifetimes and $\Phi_{I.S.C.}$ of NBI were obtained, only in benzene would

1,3-pentadiene be expected to quench both the T_1 and $T_1(\text{C.T.})$ states, and in both CH_2Cl_2 and MeCN only the T_1 state will be quenched. Thus the $(\Phi_{\text{I.S.C.}})$ values obtained for NBI in the solvents CH_2Cl_2 and MeCN should be different from that obtained in benzene, and this is what is observed as shown in Table VIII.

It would be possible to confirm these conclusions by using stilbene as the triplet quencher instead of 1,3-pentadiene in the triplet counting experiments. The triplet energy of cis and trans-stilbene are 57 and 50 kcal/mol, respectively. Hence the use of trans-stilbene as the triplet quencher will ensure complete quenching of both T_1 and $T_1(\text{C.T.})$ states of NBI in the solvents benzene, CH_2Cl_2 and MeCN, and should give the similar values for intersystem crossing quantum yields in all three solvents.

In addition to the effect upon $(\Phi_{\text{I.S.C.}})$, changing the solvent from benzene to MeCN results in a ten-fold reduction of the NBI triplet lifetime. The lifetimes of triplet excited state are quite susceptible to impurities present, and one can reason that the quenching in lifetime may be due to different levels of impurities in the solvents. On the other hand, an increase in polarity of the solvent will decrease the energy of the $T_1(\text{C.T.})$ state, reducing the energy gap between the $T_1(\text{C.T.})$ and the ground state and increasing the energy separation of the two triplet states; this could possibly enhance the rate of

decay of the triplets to the ground state and so shorten the triplet lifetimes.

Population of the S_1 (C.T.) state by the T_1 state could also account for the observed shortening of the NBI triplet lifetime (Fig. 12). In polar solvents the S_1 (C.T.) state is stabilized and its energy is lowered. Hence by increasing the polarity of the solvent the energy of the S_1 (C.T.) state could drop below that of the normal triplet state and population of the S_1 (C.T.) state by the T_1 state through intersystem crossing could occur. This would provide an extra mode of decay for the T_1 state and reduce its lifetime in more polar solvents, as is observed in Table VIII. The C.T. fluorescence of NBI in CH_2Cl_2 is observed at 550 nm whereas the phosphorescence is observed at 425 nm.

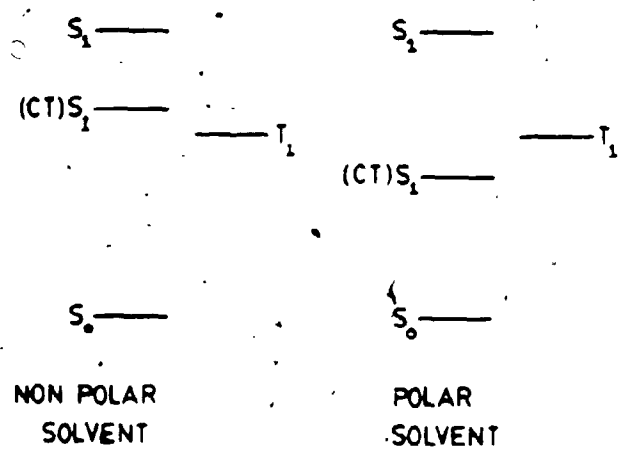


FIGURE 12: Variation of S_1 (C.T.) state of NBI in polar and non-polar solvents

If the C.T. singlet and C.T. triplet states are of similar energy then the triplet C.T. state should have an energy well below that of the T_1 state. If the decay of T_1 is accelerated by energy transfer from T_1 to S_1 (C.T.), then it should be possible to quench the C.T. fluorescence using the same concentration of 1,3-pentadiene as was used in the triplet counting experiment to quench the triplet. However quenching studies using the same concentrations of trans-piperylene as were used in the triplet counting procedure showed no effect on the C.T. fluorescence, indicating the absence of I.S.C. from T_1 to the S_1 (C.T.) state. Thus this can be ruled out as an explanation for the reduced triplet lifetime in polar solvents.

The shortening of the triplet lifetime of NBI, as observed by the triplet counting procedure, as the solvent polarity was increased could also arise from intersystem crossing from the triplet excited state to the charge-transfer singlet state. As was noted above, the triplet state is slightly higher in energy than the C.T. singlet state in non-polar solvents, but the energy of the latter drops below the triplet state in polar solvents.

If this process is operating then it would be expected to lead to delayed fluorescence from the singlet C.T. state; thus time-resolved observation of the fluorescent emission of NBI would be expected to reveal normal fluorescent emission from the C.T. state populated directly from S_1 , and a delayed emission resulting from the

C.T. state populated from the triplet. The fluorescence would be delayed by a time comparable to the triplet lifetime, which for NBI is of the order 50 ns. from the triplet counting and Stern-Volmer quenching studies.

Attempts to observe delayed fluorescence were, however, unsuccessful. The time resolved fluorescence of NBI was measured by the single photon counting technique indicating a single decaying species only, with a lifetime of 0.5 ns. Also, attempted measurement of the fluorescence spectrum of NBI using a chopper to eliminate the normal, non-delayed fluorescence did not reveal any emission. Thus the reduction of the triplet excited state lifetime with increasing solvent polarity cannot be attributed to enhanced intersystem crossing from the triplet to the charge-transfer singlet in the more polar solvents.

5.12 MEASUREMENT OF THE INTERSYSTEM CROSSING QUANTUM YIELDS OF N-BENZOYLINDOLES

Lamola and Hammond¹⁰² have developed an elegant, simple method for determining quantum yields of triplet formation (i.e. quantum yields of intersystem crossing) in solution by measuring the quantum yields of photosensitized trans \rightarrow cis isomerization of piperylene and other olefins in which analytical measurements were made with high accuracy using vapour-phase chromatography. They found that with piperylene as the acceptor $\Phi_{c \rightarrow t} / \Phi_{t \rightarrow c} = 1.24$ for different, high-energy sensitizers, where $\Phi_{c \rightarrow t}$ is the quantum yield of photosensitized cis \rightarrow trans isomerization

of piperylene and $\Phi_{t \rightarrow c}$ is the quantum yield of photosensitized trans \rightarrow cis isomerization. When a piperylene solution containing a suitable triplet energy donor is continuously irradiated, a photostationary state (p.s.s.) is eventually reached, in which

$$\frac{[\text{trans}]_{\text{p.s.s.}}}{[\text{cis}]_{\text{p.s.s.}}} = 1.22 \pm 0.05$$

Using the assumption that the I.S.C. efficiency of benzophenone was unity, ($\Phi_{t \rightarrow c}$) for 1,3-pentadiene in benzene at room temperature was evaluated as 0.44. The intersystem crossing yield of a variety of compounds were then determined, by measuring the efficiency with which they sensitized the trans to cis isomerization of 1,3-pentadiene ($\Phi_{t \rightarrow c}$).

The sensitization of the isomerization by NBI, or any other sensitizer, may be represented by an equation of the form

$$\frac{c}{\Phi_{t \rightarrow c}^{\text{obs}}} = \frac{1}{\Phi_{\text{I.S.C.}}} \left(1 + \frac{1}{k_q \tau [Q]} \right) \quad 36$$

where τ is the NBI triplet lifetime, $[Q]$ is the piperylene concentration, k_q is the rate constant for energy transfer, c is the quantum yield of formation of cis piperylene from

piperylene triplet (found to be 0.44 in benzene), and $\Phi_{I.S.C.}$ is the intersystem crossing quantum yield for the sensitizer (in this case NBI).

Solutions of NBI in benzene containing varying concentrations of trans-piperylene were irradiated in a manner such that all received the same number of photons. The amount of cis-piperylene formed in each solution was then determined and the value of c/Φ_{t-c}^{obs} calculated. The parameters of c/Φ_{t-c}^{obs} were then plotted against the reciprocal of trans-piperylene concentration (Figs. 13, 14, 15 and 16). The plot gave an intercept equal to $1/\Phi_{I.S.C.}$ as predicted in Equation 36. From the slope the triplet lifetime of NBI may be derived using the assumption that the quenching rate k_q can be approximated by the diffusion rate constant k_{diff} . This rate constant is calculated by means of the Debye equation (Equation 18). The values of the triplet lifetime and $\Phi_{I.S.C.}$ for NBI, and also for several other N-substituted indoles, are given in Table VIII. The values of $\Phi_{I.S.C.}$ and triplet lifetime of NBI are solvent dependent, and this was discussed above in relation to the possible existence of a triplet charge-transfer state. The values of $\Phi_{I.S.C.}$ for the other compounds shown in Table VIII are quite variable. This variation of $\Phi_{I.S.C.}$ with structure will be discussed in Chapter 6 since it is of relevance to the efficiency of population of the singlet C.T. state discussed there.

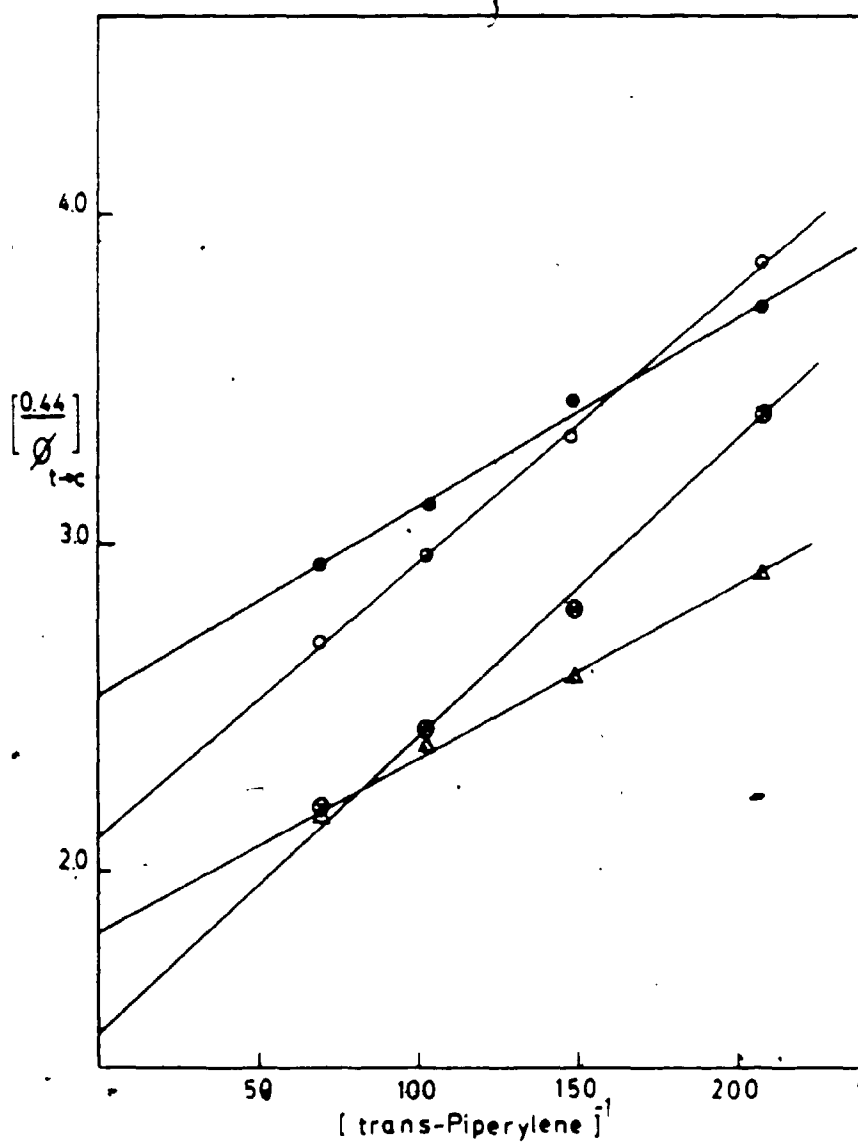


FIGURE 13: Variation in quantum yield of sensitized trans-cis isomerization of piperlyene as a function of pentadiene concentration for sensitizers (142a) - ●, (157) - ▲, (158) - ○ and (160) - ●

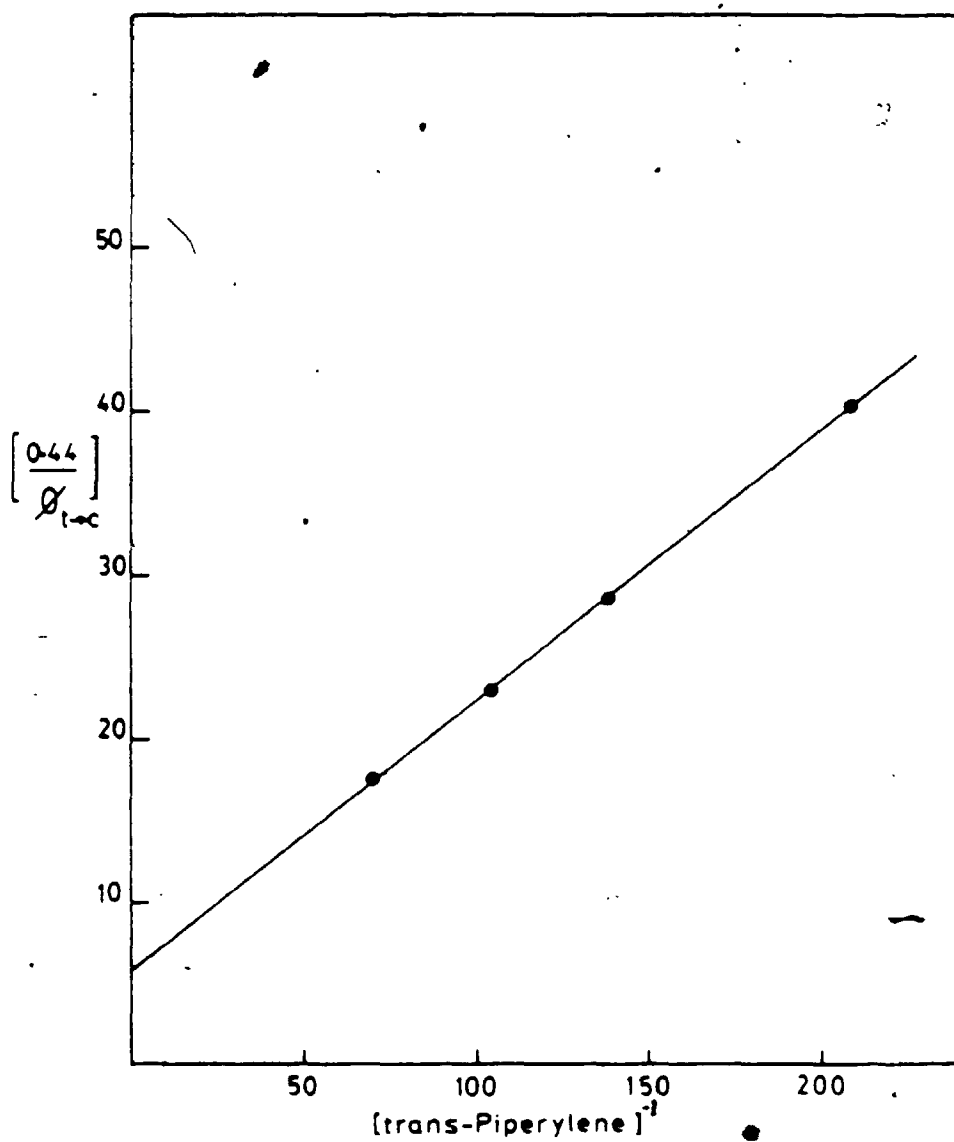


FIGURE 14: Variation in quantum yield of 0.027 M NBI sensitized trans-cis isomerization of piperlyene in acetonitrile as a function of pentadiene concentration

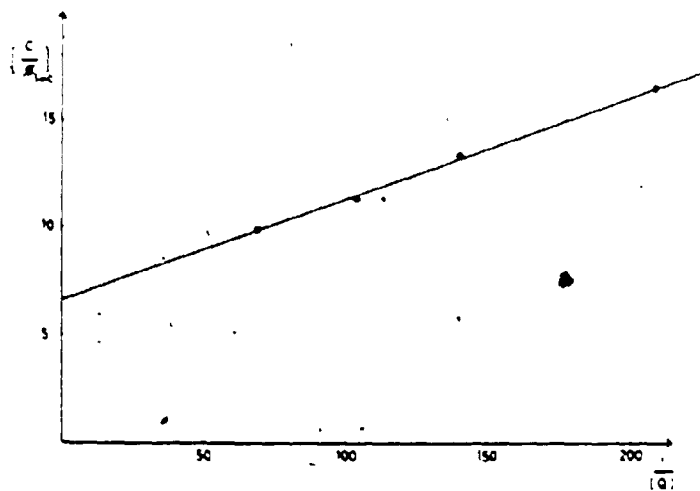


FIGURE 15: Variation in quantum yield of 0.027 M NBI sensitized trans-cis isomerization of piperylene in methylene chloride as a function of pentadiene concentration

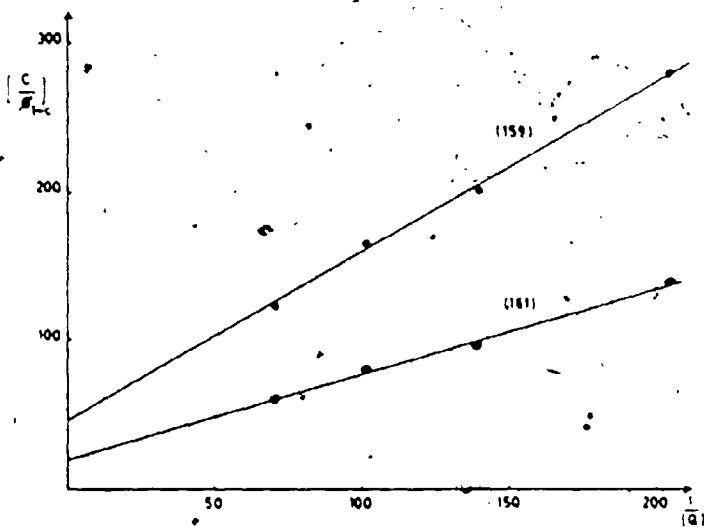
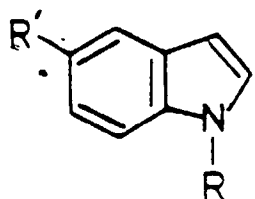
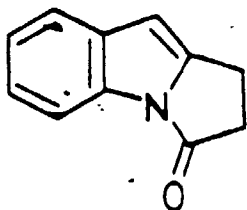


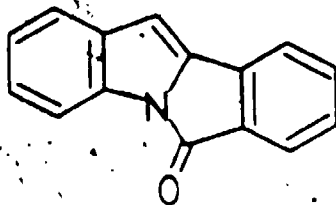
FIGURE 16: Variation in quantum yield of sensitized trans-cis isomerization of piperylene in benzene as a function of pentadiene concentration for sensitizers (159) and (161)



	R'	R
142a	H	C ₆ H ₅ CO
157	H	MeCO
158	H	p-MeO-C ₆ H ₅ CO
159	H	p-NO ₂ -C ₆ H ₅ CO
160	MeO	C ₆ H ₅ CO



161



162

The positions of the maxima in the phosphorescence spectra of NBI and related compounds are also shown in Table VIII. The phosphorescence of NBI exhibited vibrational structure; the difference between the (0-0) and (0-1) bands corresponded to 1509 cm^{-1} , which is less than the carbonyl stretching frequency of NBI which occurs at 1650 cm^{-1} . Thus the triplet state of NBI would not appear to possess simple $n \rightarrow \pi^*$ character. The position of the phosphorescence of NBI was not very solvent dependent; an increase in solvent polarity shifted the phosphorescence wavelength maxima (λ_{phos}) of NBI to the longer wavelength from 422 nm in hexane to 424 nm in acetonitrile at 77 K. This also argues against the NBI triplet state having $n \rightarrow \pi^*$ character since an opposite shift in the wavelength maximum is expected for an $n \rightarrow \pi^*$ transition.

Compound (159) did not show a detectable phosphorescence emission, nor did compound (162). Although (159) did show C.T. fluorescence, the fluorescence emission quantum yield was calculated to be small (0.06), and since $\Phi_{\text{I.S.C.}}$ is also low for this compound the singlet excited state must be deactivated mainly by means other than emission and intersystem crossing. Rotation of the benzoyl group is one of the possible modes of decay for this molecule and the possible importance of this is made clear by a comparison of (157) and the cyclic analogue (162). In the case of this pair it would be expected that (157) would be more able to decay by rotation of the acetyl group and

hence to have a low $\Phi_{1.s.c.}$ value relative to (161). However, contrary to expectations, (157) was found to have a much higher value of $\Phi_{1.s.c.}$ (0.56) than the rigid compound (161) (0.05).

It should be noted that if the postulated C.T. triplet state described in this work exists then the observed phosphorescing triplet state represents an upper triplet excited state. If this is so then the lifetime of the phosphorescing state measured in this work by triplet counting is exceptionally and unprecedentedly long for a T_2 state.

CHAPTER 6

CHARGE-TRANSFER FLUORESCENCE OF SOME N-BENZOYLINDOLES

6.1 INTRODUCTION

In the preceding chapter the photochemical cycloaddition reaction between N-benzoylindole and cyclopentene was examined. In an attempt to determine whether or not the singlet excited state of the indole derivative was involved in the reaction, its fluorescence emission was examined in the presence of alkenes. No quenching of the fluorescence intensity by the alkene was observed, which indicated that the emitting state was not apparently involved in the reaction. However, it was noticed that the fluorescence occurred at very long wavelength and with an unusually large Stokes' shift. Furthermore, the magnitude of the shift was found to be highly sensitive to the polarity of the solvent. It was decided to examine this further, and the results are presented and discussed in this chapter.

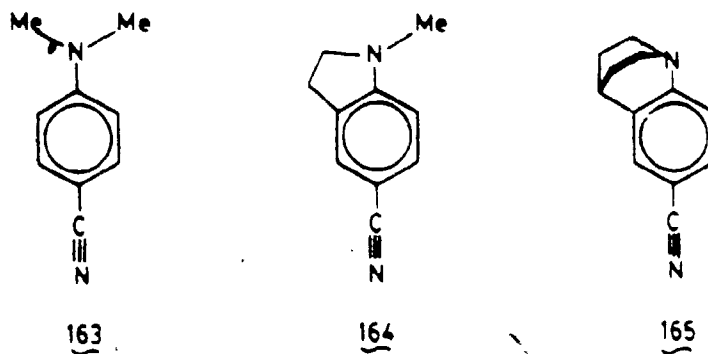
Indole itself shows principal absorption maxima at 225 nm ($\epsilon = 25000$) and 270 nm ($\epsilon = 6000$); vibrational structure is also observed (Fig. 1). It is relatively unreactive photochemically and the major route for decay of the excited state produced by uv light irradiation is through fluorescence. The electronic absorption spectrum

of indole is quite sensitive to changes in solvent. Solvent effects are also observed in the fluorescence spectra of indoles and unusually large Stokes' shifts have been observed,^{103,104} particularly for indole-5-carboxylic acid, in polar solvents. These solvent effects have been the subject of many investigations. Walker et al¹⁰⁵ suggested that the large Stokes' shift of indole in polar solvents, particularly in ethanol, methanol and n-butyl alcohol, is due to a specific solute-solvent excited state complex (exciplex). Donket et al¹⁰⁶ reported a poor correlation between the magnitude of the Stokes' shift and the dielectric constants of the solvents and proposed this as evidence for a specific, as opposed to a general, solvent effect. He also estimated the stabilization energy of the excited state due to H-bonding with water to be of the order 1800 cm^{-1} . Lippert et al¹⁰⁷ proposed that a reversal of the 1L_a and 1L_b states of indole can occur and suggested that this could be responsible for the increased Stokes' shift on going from non-polar to polar media. Mataga et al¹⁰⁸ and Suzuki et al¹⁰⁸ proposed a similar mechanism, and suggested that the initially formed second excited singlet state of indole (1L_a) becomes the fluorescent state in polar media because it is more strongly stabilized by the solvent-solute relaxation than the S_1 (1L_b) state; in non-polar solvents the 1L_b state of indole derivatives is usually a few hundred wave numbers

below the 1L_a state, the precise energy gap being dependent on the nature and position of the substituents.¹⁰⁹

A number of variable temperature studies have been reported. For example, Lakowicz and Bulter¹¹⁰ have measured the time-resolved fluorescence spectra of N-acetyltryptophanamide in propylene glycol from 205 to 313 K. Lam¹¹¹ has measured the fluorescence lifetime of indole and 2,3-dimethylindole in glycerol down to 213 K, and Meech et al¹¹² have observed the time-resolved fluorescence spectra and fluorescence decay of 1,3-dimethyl-indole in 1-butanol from 85 to 280 K. In all of these cases, the fluorescence spectrum was observed to be blue shifted as the temperature was lowered. They concluded that the fluorescence in fluid polar solvents at high temperature arises not from the pure 1L_a state but from a state with significant intramolecular charge-transfer character.

Large changes in the polarity of molecules on electronic excitation had been predicted by Forster¹¹³ and observed in charge-transfer (C.T.) complexes by Mulliken¹¹⁴ and in compounds forming intramolecular charge-transfer species (I.C.T.) by Nagakura.¹¹⁵ Support for the charge-transfer nature of these transitions came from measurements of excited-state dipole moments, either using the theory of solvent shifts (Lippert)¹⁰⁷ or by means of electro-optical methods.¹⁰⁶



p-Cyano-dimethylaniline (163), as well as a number of analogues possessing other substituents on the nitrogen-atom (164, 165), or substituents in the ring,¹¹³ exhibit two fluorescent bands in fluid solvents (Fig. 17) of medium or high polarity. Using a theory based on solvent induced shifts in the positions of the emission bands Lippert et al¹⁰⁷ ascribed the lower energy emission to a polar state.

The double luminescence of (163) has been satisfactorily explained in terms of rotation of the $N(CH_3)_2$ group in the excited state to a perpendicular conformation in which the nitrogen non-bonding pair is no longer in conjugation with the benzene ring. It has been proposed that the twisted conformer of (163) is responsible for the lower energy polar emission and has some degree of charge transfer character, whereas the higher energy fluorescence arises from the untwisted precursor. This hypothesis is known as the "twisted intramolecular charge-transfer"¹¹⁸ model (TICT).

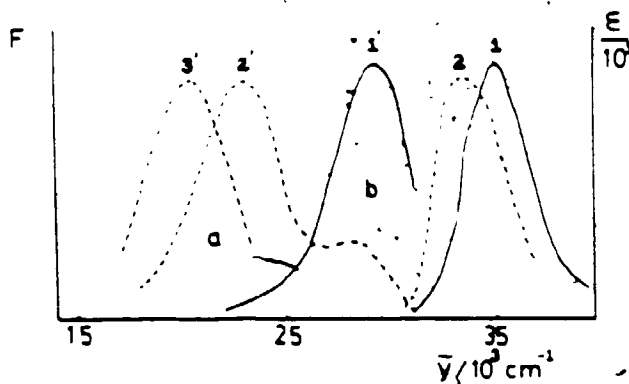


FIGURE 17: Absorption and double fluorescence of 3-methyl-4-cyano-N,N-dimethylaniline in several solvents: (a) in more polar solvents; (b) less polar ones. 1) methyl-cyclohexane; 2) CH_2Cl_2 ; 3) CH_3CN , primed-fluorescences. Absorption spectrum in CH_3CN is not shown as it is very close to curve 2.

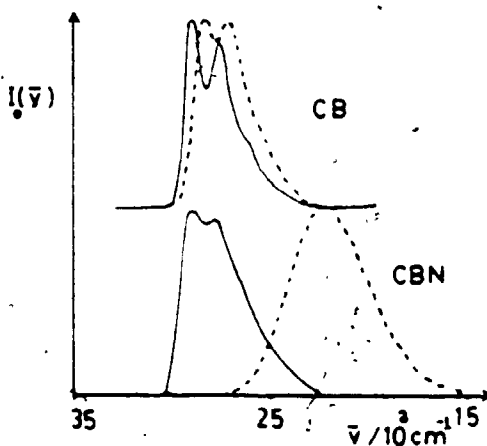
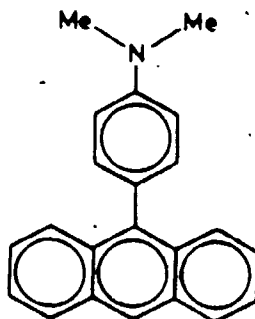


FIGURE 18: Corrected and normalized fluorescence quantum spectra of (167) and (168) in n-hexane (—) and acetonitrile (---)

The TICT model seems to be applicable to various classes of intramolecular donor-acceptor molecules (D-A) exhibiting a nearly full electron transfer from D to A in sufficiently polar solvents. The TICT model predicts that in some cases, where D and A are linked together by a formally single bond, the most favourable conformation for the charge-transfer excited state is one in which the π -systems of D and A are perpendicular, so minimizing their overlap.

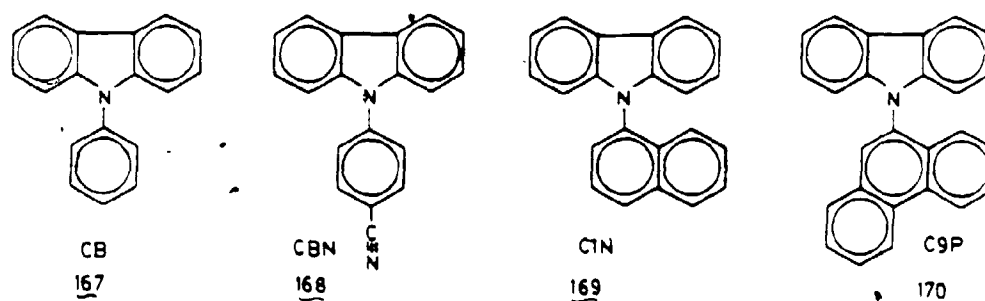
The compound 4-(9-anthryl)-N,N-dimethylaniline (ADMA) (166) also undergoes a solvent-assisted rapid relaxation¹¹⁹ of its initially formed excited singlet state to a more polar, lower energy fluorescent state.



ADMA 166

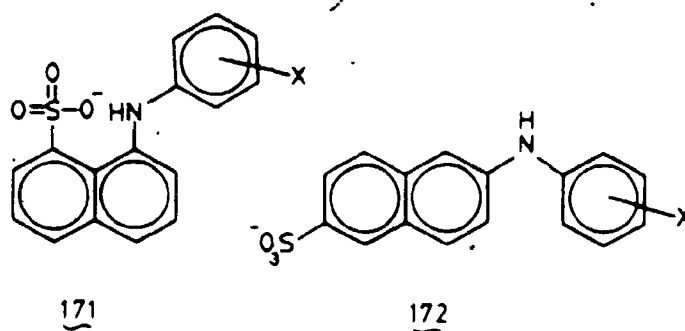
This phenomenon has also been explained by the "twisted intramolecular charge-transfer" (TICT) model, which requires that the anthryl and dimethylaniline components rotate to a mutually perpendicular conformation in order to stabilize the charge separation. An alternative explanation proposes that enhanced polarizability in the excited state enables the solvent to induce the electronic charge flow without any structural changes of the solute molecule.¹²⁰

The fluorescence behaviour of carbazole derivatives has also been investigated.¹²¹



Compounds (167), (168), (169) and (170) have been studied. In this series the donor moiety is held constant and only the acceptor properties were changed. These compounds show only one fluorescence band, whereas the other compounds discussed earlier exhibited dual fluorescence. The fluorescence spectra of (167) and (168) in polar and non-polar aprotic solvents are compared in Figure 18.

For (167) there is only a slight red shift and loss of vibrational structure in the emission when the solvent is changed from hexane to acetonitrile; however, a large red shift is observed for (168) and the loss of vibrational structure is complete when the solvent is changed from hexane to acetonitrile. For (167), TICT states are not yet energetically favourable but their formation can be switched on by changing the acceptor part of the biaromatic system. This is achieved in (168) by introducing an electron attracting substituent into the acceptor part, and in (166) and (167) by replacing the phenyl acceptor moiety with an aromatic system with better accepting properties. In the case of (167) only locally excited state fluorescence is observed because the TICT state is higher in energy and thus efficiently depopulated to S_1 according to Kasha's rule.



In water the naphthalene derivatives (171) and (172) are almost non-fluorescent but in non-polar organic

emission compounds (157, 158, 159, 160, 161 and 162) were synthesized and their photophysical properties examined.

The absorption spectrum of NBI was found to be different from that of indole and exhibited a strong band at 250 nm ($\epsilon = 5 \times 10^5$) along with a weaker band at 300 nm ($\epsilon = 8000$) which showed some possible evidence of vibrational structure (Fig. 1). The absorption spectra of (157-162) were also changed from that of indole in an analogous manner.

The emission spectra of compounds (157-162) were also examined. At room temperature N-acetylindole (157) and the cyclic analogue (161) did not emit detectably whereas compounds (NBI, 158, 159 and 160) fluoresced weakly and with very large Stokes' shifts. Compound (162) fluoresced strongly but with a much smaller Stokes' shift than the other compounds. The wavelength and intensity of the emission of NBI, and (158-160) was highly solvent dependent. Generally, the more polar the solvent, the broader and weaker was the emission and the longer the wavelength of maximum intensity. The position of the emission maxima and some quantum yields of emission were determined and are given in Tables IX and XI. The normalized fluorescence spectrum of NBI in solvents of different polarity is illustrated in Figure 19. The position of the fluorescence maxima were not concentration dependent and the excitation spectra in all cases were in agreement with the emission being derived from the compound

Compound	Solvent	λ_{abs} nm	λ_{em} nm	$\nu_{\text{abs}} - \nu_{\text{em}}$ cm^{-1}	$E_T(30)$ kcal/mol	Δf_n
142a	n-pentane	302	440	10390	32.4	.0101
"	n-hexane	302	440	10390	33.1	.0000
"	Et ₂ O	302	480	12280	34.6	.1671
"	1,4-dioxane	303	504	13270	36.0	.0203
"	THF	302	506	13350	37.4	.2097
"	CH ₃ CO ₂ Et	301	504	13270	38.1	.1997
"	HCO ₂ Et	302	503	13230	40.9	.2205
"	(i-Pr) ₂ O	302	476	12100	34.4	.1450
"	(MeOCH ₂) ₂	302	504	13270	38.6	.2141
"	(n-Bu) ₂ O	302	468	11750	34.0	.0959
"	n-PrCN	302	521	13920	43.1	.2751
"	MeCN	302	540	14590	46.0	.3055
"	CHCl ₃	303	519	13850	39.1	.1492
"	CCl ₄	304	466	11650	33.6	.0119
"	CH ₂ Cl ₂	303	518	13800	41.1	.2171
"	ClCH ₂ CH ₂ Cl	303	520	13880	41.9	.2208
"	MeCCl ₃	303	490	12700	36.2	.1982
157	n-hexane	299	-	-	-	-
160	n-hexane	314	452	9723	33.1	.0000
"	Et ₂ O	314	496	11690	34.6	.1671
"	THF	314	518	12540	37.4	.2097
"	MeCN	314	560	13990	46.0	.3055
"	CH ₂ Cl ₂	315	540	13230	41.1	.2171
159	n-hexane	288	518	15420	33.1	.0000
"	Et ₂ O	288	-	-	-	-
"	MeCN	289	-	-	-	-
"	CH ₂ Cl ₂	289	-	-	-	-
158	n-hexane	302	418	9189	33.1	.0000
"	Et ₂ O	301	456	11290	34.6	.1671
"	THF	302	474	12020	37.4	.2097
"	MeCN	301	514	13770	46.0	.3055
"	CH ₂ Cl ₂	302	496	12950	41.1	.2171
161	n-hexane	290	-	-	-	-
162	n-hexane	359	460	6116	33.1	.0000
"	MeCN	357	494	7768	46.0	.3055
"	CH ₂ Cl ₂	360	492	7453	41.1	.2171

NOTES:

Absorption and emission spectra were recorded on solutions of ca 10^{-5} M concentration.

λ_{abs} is the wavelength of the lowest absorption maximum.

λ_{em} is the wavelength of maximum emission

$\nu_{\text{abs}} - \nu_{\text{em}}$ is $(1/\lambda_{\text{abs}} - 1/\lambda_{\text{em}})$ expressed in cm^{-1} .

$E_T(30)$ is the Kosower solvent polarity parameter (see Text)

Δf_n is: $\frac{\epsilon - 1}{2\epsilon + 1} \frac{n^2 - 1}{2n^2 + 1}$

TABLE IX: Wavelengths of Absorption and Fluorescence Emission for Compounds 142a and 157-162 in Various Solvents

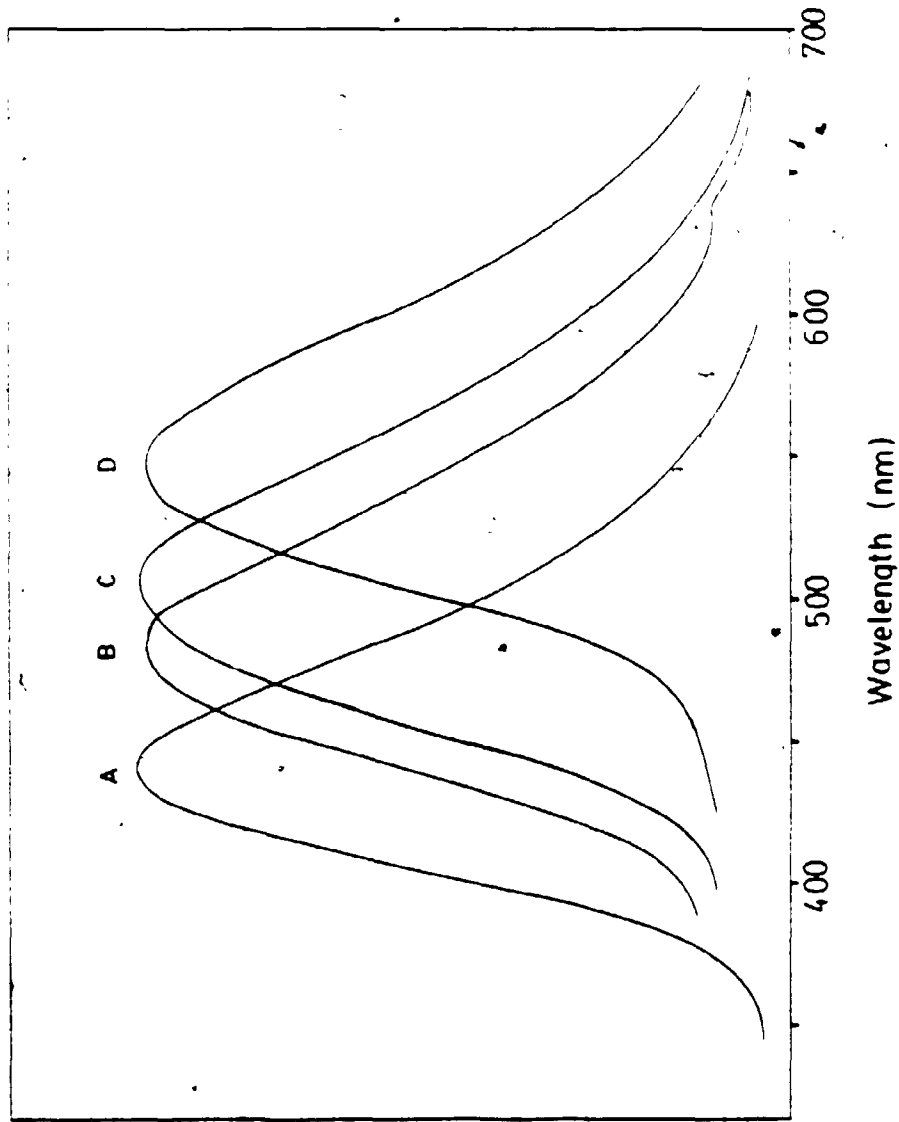


FIGURE 19: Normalized fluorescence spectra of compound (142a) (10^{-5} M). Curve A: hexane; B: diethyl ether; C: THF; D: MeCN

Normalised Fluorescence Intensity

under study, and not from any strongly emitting impurity. The phosphorescence emission spectrum of NBI (Fig. 2) at 77 K was different from that of the fluorescence and did not change with the variation of the solvent polarity.

6.2 CHARGE-TRANSFER FLUORESCENCE

The absorption spectrum of NBI showed no dependence on the solvent polarity. This suggests that the absorption does not correspond to an $n \rightarrow \pi^*$ transition since this would be expected to produce a blue shift of the absorption maximum with increased solvent polarity. The phosphorescence emission at 77 K showed a small (2 nm) shift of the wavelength of maximum emission when the solvent was changed from hexane to acetonitrile (Table VIII). This contrasts with the fluorescence emission at room temperature; for example, in the case of N-benzoylindole the position of maximum fluorescence emission intensity shifted 100 nm when the solvent was changed from hexane to acetonitrile. The possibility that the emission is due to an excimer species was considered, and can be excluded since at the concentrations of the N-benzoylindole used (10^{-5} M) the singlet excited state would have insufficient time to form an exciplex with a ground state molecule. (The lifetime of NBI fluorescence was measured to be 0.5 ns).

The fact that for NBI the positions of the absorption maxima do not change with solvent polarity

suggests that the initially formed excited state possesses a similar degree of charge separation as the ground state molecule. In contrast, the large Stokes' shift of the fluorescent emission, along with the marked solvent dependence of the emission wavelength suggests that the emitting species is a singlet state possessing a large degree of charge-transfer character, which is formed from the initially formed singlet excited state. Hence as the solvent polarity increases the charge-transfer state becomes more stabilized relative to the non-polar ground state, and therefore emits to longer wavelength. This type of long wavelength fluorescence has been observed previously in systems where potential electron donating systems are conjugated with chromophores capable of accepting charge. Examples of such systems were discussed earlier in this chapter.

6.3 INTRAMOLECULAR CHARGE-TRANSFER MODEL

Long wavelength fluorescence occurring from a charge-transfer state has been observed in various classes of intramolecular donor-acceptor molecules (D-A). In the case of NBI the indole and the benzoyl group can be identified as the donor and the acceptor, respectively. In order to confirm this the effect of the structural changes in compounds NBI and (157-162) were examined.

NBI fluoresces at 440 nm in hexane which corresponds to emission from a state 65.0 kcal/mol above the ground

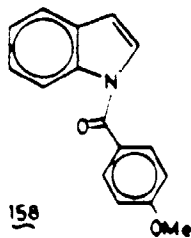
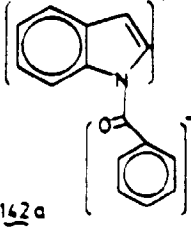
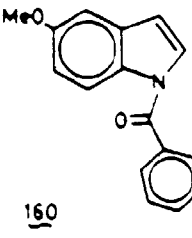
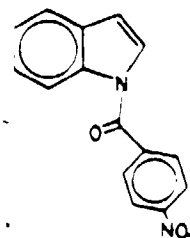
				
λ_{fl}	418 nm	440 nm	452 nm	518 nm
$E_{s,CT}^s$	68.4 kcal/mol	65.0 kcal/mol	63.3 kcal/mol	55.2 kcal/mol

TABLE X: Substitution effect on N-benzoylindole charge separation

state (Table X). By having a methoxy group at the para position of the benzoyl group of NBI (compound 158) a hypsochromic shift of the fluorescence emission maxima was observed whereas the presence of a methoxy group at the 5-position of the indole group of NBI (160), or presence of an electron withdrawing nitro group at the para position of the benzoyl group of NBI (159), results in a bathochromic shift of the fluorescence emission. The hypsochromic shift of the fluorescence maxima indicates destabilization of the fluorescing charge-transfer singlet state (increase in the singlet state energy) by the electron donating methoxy group present at the para position of the benzoyl group. The bathochromic shift induced by the presence of a methoxy group at the 5-position of indole indicates a stabilization of the charge-transfer singlet excited state (lowering in energy). These observations are consistent with the indole group acting as the electron donor in the charge-transfer

state. The stabilization of the charge-transfer singlet state induced by the presence of an electron withdrawing nitro group at the para position of the benzoyl group supports the acceptor character of the benzoyl group in the formation of the charge separated molecule.

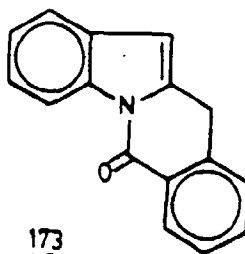
This rationalization is also consistent with the failure of N-acetylindole (157) and its cyclic analogue (161) to fluoresce since no charge-transfer would be expected if the delocalized π -system of the benzoyl group is necessary to accept the charge.

6.4 FLUORESCENCE PROPERTIES OF 6H-ISOINDOLE[2,1-a]

The cyclic analogue of the N-benzoylindole compound (162), showed longer wavelength absorption (359 nm in hexane) than the other compounds studied. This compound was also found to be very highly fluorescent, with a fluorescent quantum yield of 0.9 in hexane. This is vastly greater than the quantum yields of fluorescence of the other compounds studied, as will be discussed below. The Stokes' shift of (162) was much smaller than the other fluorescing compounds; also, a 32 nm shift occurred on changing the solvent from hexane (λ_{f1} = 450 nm) to acetonitrile (λ_{f1} = 492 nm). Thus it is much less solvent sensitive than NBI, and more reminiscent of indole itself.

The different fluorescence properties of (162), as compared with N-benzoylindole, may arise from two factors. One explanation is that the benzoyl group of (162) is held

planar and this may prevent stabilization of a charge-transfer state of a perpendicular orientation of the indole and benzoyl group required in this state. Alternatively, the conjugation of the phenyl ring through the 2-position of the indole may cause the excited state properties to resemble those of a 2-phenylindole and lessen the importance of the nitrogen carbonyl substituent.



Several different synthetic approaches were examined for the preparation of compound (173) in which the benzoyl group is held relatively planar with respect to the indole ring, but in which the phenyl group is not conjugated through the indole 2-position. This would have distinguished between the two alternatives given above. Unfortunately, all attempts to synthesize (173) were unsuccessful.

6.5 FLUORESCENCE QUANTUM YIELDS

The quantum yields of fluorescent emission for compounds (142a, 159, 160 and 163) (Table XI) indicate that

the efficiency of emission drops with increasing solvent polarity. This effect can be explained as being due to a lowering of the energy of the charge-transfer singlet state with increasing solvent polarity. This will decrease the energy gap between the charge-transfer excited state and the relatively non-polar ground state. The energy gap law which dominates transitions between electronic states of like multiplicity predicts that this should accelerate the rate of internal conversion to the ground state so that emission from the charge-transfer state competes less effectively (Fig. 20).

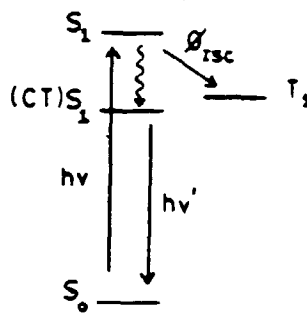


FIGURE 20: Energy levels of excited NBI

Another explanation for the decreased fluorescence yield with increasing solvent polarity is that as the charge-transfer state is stabilized by increasingly polar solvents the energy gap between it and the initially formed and non-polar S_1 state will be increased. Again, because of the energy gap law, this will slow down the rate of formation of the charge-transfer state, and the charge-

transfer process will become less competitive with intersystem crossing to the triplet state. Thus less of the charge-transfer state will be formed and the quantum yield of fluorescence from it will be reduced. This explanation assumes that the triplet state is non-polar and so its energy is not solvent dependent. Since the position of the phosphorescence emission of N-benzoylindole was found not to change with solvent polarity, this would appear to be a correct assumption. In addition, the triplet excited state cannot be populated from the charge-transfer state because in all the solvents examined the latter is lower in energy than the triplet state (Table VIII). Thus the variation in fluorescence quantum yield with solvent does not arise from intersystem crossing from the charge-transfer state to the triplet state being more favourable in solvents where, say, the two states become close in energy.

6.6 CORRELATION OF THE FLUORESCENCE EMISSION WITH THE LIPPERT EQUATION

The fluorescence emission spectra of many compounds are quite sensitive to the polarity of their environment although they are usually not as sensitive a compound as N-benzoylindole. The emission from singlet excited states generally occurs at wavelengths which are longer than those of light absorption. The loss of energy between absorption and emission of light, called the Stokes' shift, is due to several processes. These processes include energy loss due

Compound	Solvent	Φ_{em}
142a	n-hexane	.041
"	MeCN	.018
"	CH ₂ Cl ₂	.028
157	n-hexane	0.0 <u>a</u>
158	n-hexane	.13
"	CH ₂ Cl ₂	.15
159	n-hexane	.06
160	n-hexane	.07
"	MeCN	<10 ⁻² <u>b</u>
"	CH ₂ Cl ₂	.03
161	n-hexane	0.0 <u>a</u>
162	n-hexane	.9
"	MeCN	.44
"	CH ₂ Cl ₂	.62

aNo emission was observed.

bThe emission was too weak to be quantified.

TABLE XI: Quantum Yields of Fluorescence (Φ_{em}) for Compounds (142a) and (157-162) in Various Solvents

to dissipation of vibrational energy, redistribution of electrons in the surrounding solvent molecules induced by the change of dipole moment of the excited species, reorientation of the solvent molecules around the excited state dipole and, finally, specific interactions between the fluorophore and the solvent. For the fluorescent charge-transfer states which have been observed previously for molecules capable of intramolecular electron transfer between conjugated groups, the effect of solvent interactions upon the energy, and hence the wavelength of emission have been classified into specific solvent interactions (e.g. hydrogen bonding, etc.) and general solvent effects, which refers to the way in which the solvent reorganizes to stabilize the charge separated state. Absorption of light occurs in about 10^{-15} s, a time too short for significant displacement of nuclei (Frank-Condon principle). Often the electronically excited states of aromatic compounds possess dipole moments (μ^*) which are different than in the ground state (μ). As a result the absorption of a photon by the molecule results in the formation of a new dipole, which perturbs the environment of the excited species and the solvent responds by a reorganization of the solvent cage. For non-hydrogen bonding solvents, the stabilization of the charge-transfer state is presumed to arise from the general type of solvent interactions, and Lippert^{123,124} has derived an equation in which the energy difference between the ground and the

excited charge-transfer states (in cm^{-1}) is a property of the refractive index (n) and dielectric constant (ϵ) of the solvent. The Lippert equation^{123,124} takes the form shown in Equation 38.

$$\bar{\nu}_{\text{abs}} - \bar{\nu}_{\text{em}} = \frac{2}{hc} \left[\frac{\epsilon - 1}{2\epsilon + 1} - \frac{n^2 - 1}{2n^2 + 1} \right] \frac{(\mu^* - \mu)^2}{v^3} + \text{const}$$

or

$$\bar{\nu}_{\text{abs}} - \bar{\nu}_{\text{em}} = \frac{2}{hc} \cdot \Delta f_n \cdot \frac{(\mu^* - \mu)^2}{v^3} + \text{const} \quad 38$$

where $\bar{\nu}_{\text{abs}}$ and $\bar{\nu}_{\text{em}}$ represent the absorption and emission energies in cm^{-1} , respectively, h is Plank's constant, c is the speed of light, ϵ is the solvent dielectric constant, n is the solvent refractive index, v is the Onsager radius, which is the radius of the sphere occupied by the molecule in the solvent, and μ and μ^* are the dipole moments of the ground state and emitting excited state, respectively.

By plotting the degree of solvent stabilization of the excited state (i.e. $\bar{\nu}_{\text{abs}} - \bar{\nu}_{\text{em}}$) against the solvent polarizability function Δf_n it is possible to obtain a value of the change in dipole moment in going from the initially formed excited state of the charge-transfer state if a value of the Onsager radius, v , can be estimated.

Such a plot is shown for N-benzoylindole in Figure 21, and similar plots were obtained for the substituted derivatives (158) and (160). The data point corresponding to dioxane was found to be off the line. This has been observed¹²⁵ in other systems and it has been proposed that the dioxane molecule may alter its conformation and hence its effective dielectric effect in

Compound	$(\mu^* - \mu) / r^3$ ^a	$(\mu^* - \mu)$ ^b
142a	13700 ± 500	15 D
158	14800 ± 800	20 D
160	13900 ± 700	20 D

^aFrom the gradient of the Lippert plot, omitting dioxane and chlorinated solvents.

^bAssuming values of the Onsager radius, r , of 5.5 Å (142a) and 6.5 Å for (158) and (160).

TABLE XII: Dipole Moment Changes Derived from the Lippert Plots for Compounds (142a), (158) and (160).

the process of solvation of the charge-transfer complexes. From other solvent polarizability-fluorescence wavelength correlations it has been found¹²⁵ that the effective dielectric constant of dioxane is 6 or 7. Hence by using a value of this order, the dioxane point also falls onto the line in Fig. 21. In addition to dioxane, the data points for the chlorinated solvents examined did not fall on the

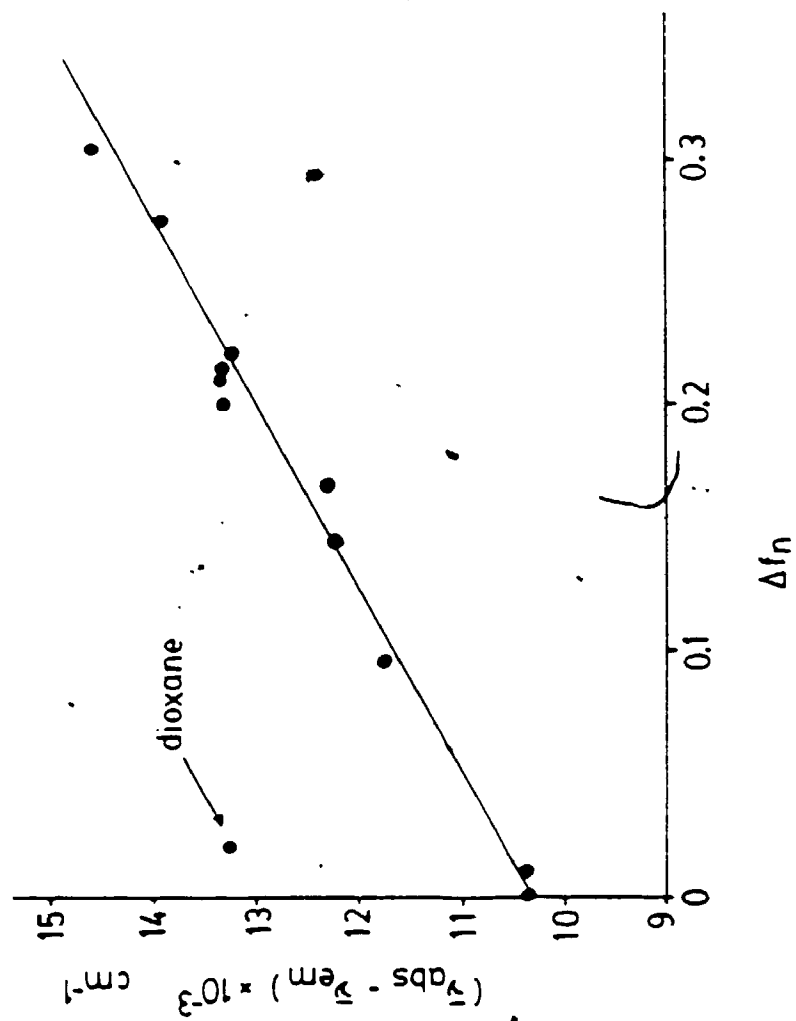


FIGURE 21: Lippert plot for compound (142a) in non-chlorinated solvents: a) plot of $(\nu_{\text{obs}} - \nu_{\text{em}})$ against the solvent polarizability function Δf_n .

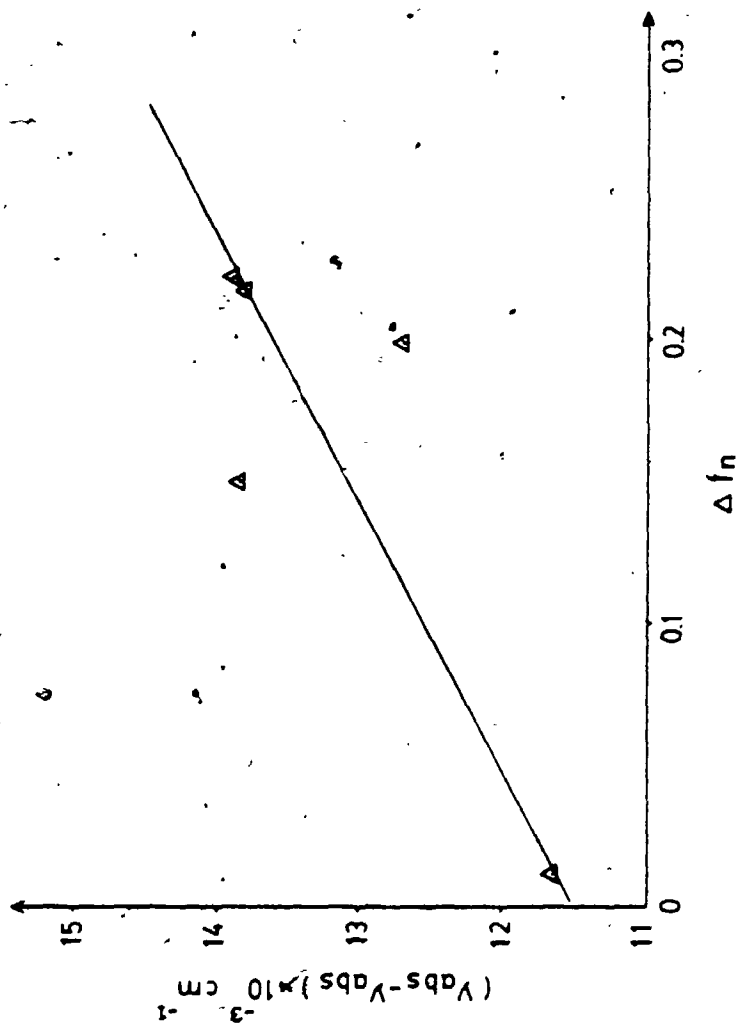


FIGURE 22: Lippert plot for compound (142a) in chlorinated solvents: a plot of $(\bar{\nu}_{obs} - \bar{\nu}_{obs}^0)$ against the solvent polarizability function Δf_n

line and were not included in Figure 21. When they were plotted separately (Fig. 22) a correlation was also observed. Presumably these solvents stabilize the charge-transfer state of a slightly different solvent interaction.

With the exception of dioxane, the data obtained in the 12 non-chlorinated solvents examined give a good fit to the Lippert equation. This supports the assignment of a charge-transfer state to the fluorescence emission of compounds (142a) and (158-160). The change in dipole moment in going from the initially formed singlet excited state to the charge-transfer state was calculated and is given in Table XII. The Onsager radius, ν , used was estimated from models to be approximately 5.5 Å for NBI and 6.5 Å for (158) and (160). The change in dipole moment is thus calculated to be of the order of 15 Debye for (142a) and 20 Debye for (158) and (160). Since 4.8 Debye corresponds to the separation of a unit charge by one Å, these values of the change in dipole moment correspond to a movement across the molecule of 3 Å in (142a) and 4 Å in (158) and (160). These distances are of the order of the separation of the major chromophores in the N-benzoylindoles and are consistent with the conclusion that the charge-transfer occurs between the indole nucleus and the benzoyl ring.

6.7 CORRELATION OF FLUORESCENCE EMISSION OF NBI WITH $E_T(30)$ VALUES

Attempted correlations between the fluorescence maxima of compounds and various parameters of solvent polarity such as the Richard-Dimroth $E_T(30)$ parameter¹²⁶ and Kosower Z value¹²⁷ have been met with varying degrees of success. These parameters are derived from the solvent dependence of the electronic spectra of dyes whose absorption maxima shift to lower energy in solvents of increasing polarity. Correlations have been made between the energy of the emitting states of charge-transfer fluorescing compounds, as determined from the position of the fluorescence maximum, and the empirical solvent polarity parameter $E_T(30)$. The $E_T(30)$ parameter for a solvent is obtained by measuring the position of the absorption maximum of the charge-transfer transition of a pyridinium betaine dissolved in the solvent. In some cases these correlations are linear and in others the correlation takes the form of two intersecting lines, which has been interpreted as being due to two emitting states,^{122b} one charge-transfer in nature and the other relatively non-polar. Correlation of the charge-transfer fluorescence maxima of NBI with $E_T(30)$ values indicated a non-linear plot. Thus, it was thought that, in principle, the existence of more than one emitting state could also apply to the NBI system described here.

The plot of energy of the emitting state of NBI against the solvent $E_T(30)$ values is given in Fig. 23. It

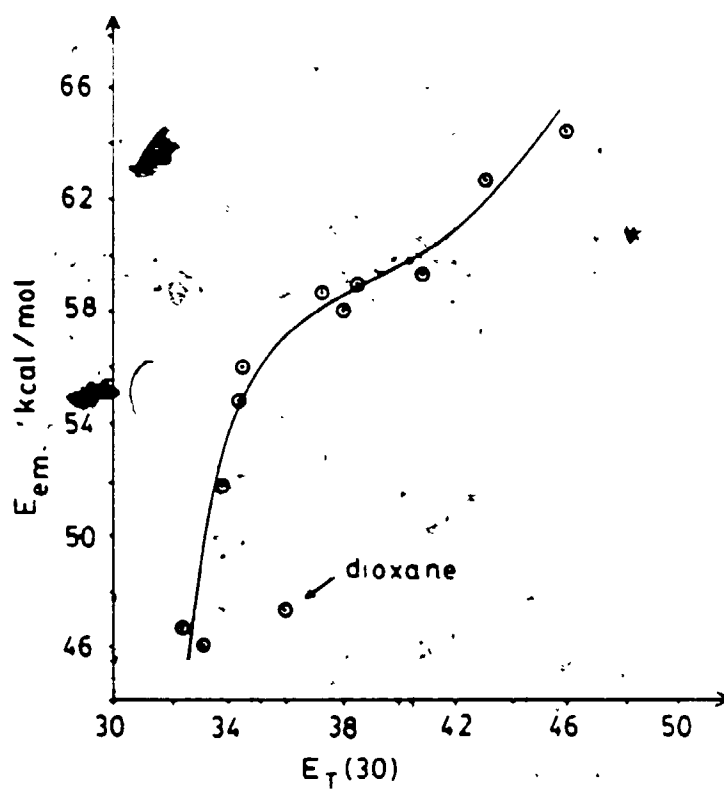


FIGURE 23: Plot of energy of the $S_0 \rightarrow S_1$ transition in kcal/mol of NBI against the solvent $E_T(30)$ value

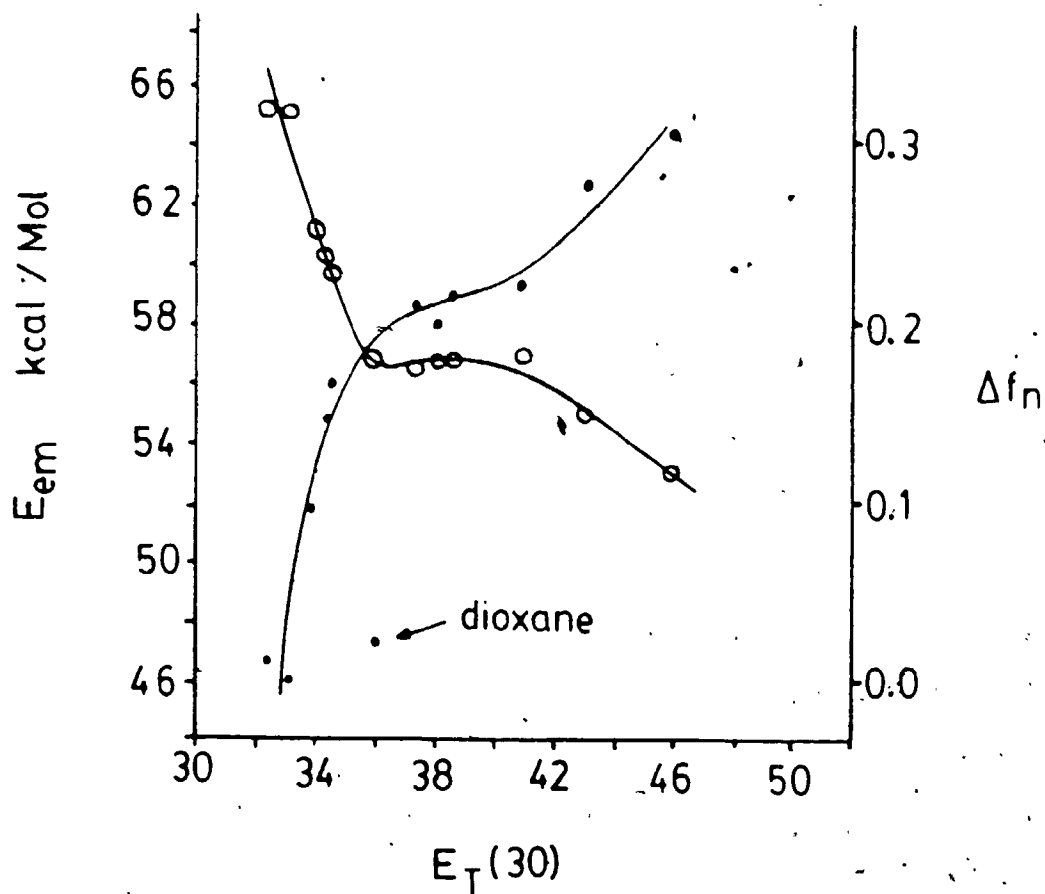


FIGURE 24: Plots of energy of the $S_0 \rightarrow S_1$ transition in kcal/mol of NBI against the solvent $E_T(30)$ value (full circles) and solvent $E_T(30)$ value against the Lippert Δf_n (open circles)

would appear that at low solvent polarities the position of the fluorescence is highly sensitive to the changing solvent polarity, and that at high polarity the position of the emission band is less dependent. This is the reverse of the trend which would be expected and would correspond to an unidentified non-polar, low-lying electronic state of the NBI molecule.

According to the model outlined earlier in this chapter (Fig. 20), in non-polar solvents the charge-transfer state will be highly destabilized and it is possible for this state to lie near or above the singlet excited state (S_1). With increasing polarity the charge-transfer singlet state will be stabilized (lowered in energy) and drop lower in energy than the initially formed singlet excited state. Hence the wavelength of the emission observed from the non-polar singlet excited state will be relatively insensitive to solvent polarity. However, in high polarity solvents the emission will be derived from the charge-transfer state and the wavelength maximum will be highly dependent on the changing solvent polarity. Therefore, in a plot of solvent $E_T(30)$ values against the emission wavelength, it would be expected that, if the charge-transfer state is above the initially formed singlet state in non-polar solvents, then a line would be obtained which would be near horizontal in low polarity solvents and of greater slope for high polarities, corresponding to solvation of the charge-transfer state.

Since the plot of $E_T(30)$ vs emission wavelength indicated the reverse trend to that expected, it was decided to examine the reliability of the $E_T(30)$ parameter by plotting it against the polarizability function Δf_n (Fig. 24). This showed a curve which mirrors that for the $E_T(30)$ vs emission plot for NBI. This would suggest that the curvature seen in the $E_T(30)$ vs emission energy plot is an artifact of the $E_T(30)$ parameter and does not relate to a change in the emitting state. These observations suggest that care should be exercised in correlating the $E_T(30)$ parameter with the emission energy when large solvent polarity ranges and solvents of widely varying chemical structure are used.

CHAPTER 7

EXPERIMENTAL

Melting points and boiling points are uncorrected. Melting points were determined on a Koffler hot stage melting point apparatus. Ir spectra were recorded with a Beckmann 4250 spectrometer. Ultra-violet spectra were recorded on a Cary 118 uv visible spectrometer and on a Hewlett Packard 8450A diode array spectrophotometer. Steady state fluorescence spectra were recorded on a Perkin-Elmer 650-40 fluorescence spectrometer and quantum yields of fluorescence were measured on this instrument relative to indole. Phosphorescence spectra were recorded on a Perkin-Elmer MPF-4 emission spectrometer. Time-resolved fluorescence measurements were conducted with a PRA single photon counting instrument using a coherent picosecond laser system consisting of a Model CR-8 argon ion laser pump, and a Model 590 dye laser equipped with a Model 7210 cavity dumper. The laser pulses were frequency-doubled and the resulting wavelength of 287 nm was used for excitation. The effective time width of the laser pulses, including the instrument response, was below 300 ps. Mass spectra were obtained on a Varian MAT-311A spectrometer at 70 eV (direct inlet). Routine proton magnetic resonance spectrum (^1H nmr) were obtained on Varian XL-200 and -300

spectrometers. Both instruments were used to obtain the ^{13}C nmr spectra. Methyl, methylene, methine and quaternary signals were identified by comparing the fully decoupled spectra with the APT^{63a} and DEPT^{63b} spectra. The chemical shifts are given in parts per million (ppm) downfield from tetramethylsilane (Me_4Si) in δ units and coupling constants are given in cycles per second (Hz). The data is reported as: chemical shift, multiplicity (δ = singlet, d = doublet, t = triplet, q = quartet, m = multiplet, ddz = double doublet, dtz = double triplet, etc.), number of protons, coupling constants and assignments.

Gas-liquid chromatography (glc) analysis was performed using 0.2" x 6' glass and copper columns packed with 5% S.E. 30 on Chemisorb W and 20% diethyleneglycol succinate on Chemisorb W columns with Varian 2400, Varian 90-P and Aerograph A90-P3 instruments equipped with a Hewlett Packard 3390A integrator. All retention times were recorded with a flowrate of 30 mL/min. Thin layer chromatography (tlc) was done on Kiesel gel 60 F₂₅₄ plates. Thick layer chromatography (plc) was performed using Kiesel gel F₂₅₄ on glass plates. Open-column chromatography was performed using Kiesel gel. Solutions were degassed with dry nitrogen gas before irradiation and were irradiated in Pyrex tubes using a medium pressure mercury lamp as the light source. The course of the reaction was followed by gas-liquid chromatography (glc).

Reagent grade solvents were used for all reactions. Anhydrous ethyl ether was Baker reagent grade and was used without further purification. All the solvents used for fluorescence and phosphorescence measurements were glass distilled spectral grade solvents. The solutions were generally 10^{-5} M in indole derivative for fluorescence and phosphorescence measurements.

N-Benzoylindole (142a)

To a stirred solution of indole (5 g, 0.043 mol), powdered NaOH (5 g, 0.125 mol) and $(\text{Bu})_4\text{NBr}$ (0.2 g) in dry methylene chloride (150 mL), a solution of benzoyl chloride (9.25 g, 0.088 mol) in methylene chloride (25 mL) was added via a dropping funnel over 15 min. The reaction was cooled with ice during the reaction. After 1.5 h water was added (50 mL) to quench the excess benzoyl chloride, and the N-benzoylindole was extracted into methylene chloride. The extracts were washed with water, dried over K_2CO_3 , filtered and the methylene chloride removed under reduced pressure to give a red oil, which was recrystallized from ether/hexane to give 142 as a white crystalline solid: 8.6 g, 91% yield.

For 142a; M.p. 63-64°C.¹²³ ^1H nmr (CDCl_3): 6.7 ppm (d, 1H, $J = 3.5$ Hz, 3H), 8.5 ppm (m, 1H, 2H), 7.3-7.9 ppm (m; 9H); exact mass m/e 221.0840. ^{13}C nmr (CDCl_3): 131.9, 129.1, 129.1, 128.6, 128.6, 127.6, 124.9, 123.9, 120.8,

116.4 and 108.5 ppm (CH), 136.0, 134.6 and 130.7 ppm (C),
168.7 ppm (C = O).

N-(p-Methoxybenzoyl)-indole (158)

The synthesis of N-(p-methoxybenzoyl)-indole was performed using the same procedure as described for the synthesis of N-benzoylindole, except for the use of p-anisoylchloride instead of benzoyl chloride. 158 was obtained as a crystalline white solid (recrystallized from diethyl ether).

For 158; M.p. 134-137°C. ^1H nmr (CDCl_3): 6.7 ppm (d, 1H, $J = 3.5$ Hz, 3H), 4.0 ppm (s, 3H, $-\text{OCH}_3$), 8.4 ppm (m, 1H, 2H), 7.0-7.9 ppm (m, 8H); exact mass m/e 251.0947.
 ^{13}C nmr (CDCl_3): 55.5 ppm (OCH_3), 131.6, 131.6, 127.7, 124.6, 123.6, 120.8, 116.2, 113.8, 113.8 and 108.0 ppm (CH), 162.6, 136.1, 130.6 and 126.5 ppm (C), 168.2 ppm (C = O).

N-(p-Nitrobenzoyl)-indole (159)

The synthesis of N-(p-nitrobenzoyl)-indole was conducted using the same procedure as described for the synthesis of NBI except for the use of p-nitrobenzoyl chloride instead of benzoyl chloride. A yellow oil was obtained. The products were separated by column chromatography using 50 g of silica gel (60-200 mesh, Baker

Analyzed reagent) and ether/ CH_2Cl_2 as the eluting solvent to give 159 as a yellow crystalline solid.

For 156: M.p. 165-167°C (n-hexane/ CH_2Cl_2). ^1H nmr (CDCl_3): 6.7 ppm (m, H, ^3H), 7.1-8.5 ppm (m, 9H); exact mass $m/e = 266.0689$; ^{13}C nmr (CDCl_3): 129.99, 129.99, 126.5, 125.5, 124.6, 123.9, 123.9, 121.2, 116.4 and 110.0 ppm (CH), 149.5, 140.2, 135.8 and 130.8 ppm (C), 166.4 (C = O).

N-Benzoyl-5-methoxyindole (160)

The synthesis of N-benzoyl-5-methoxyindole was carried out using the same procedure as described for the synthesis of NBI, except for the use of 5-methoxyindole instead of indole, to yield a white crystalline solid.

For 160: M.p. 107-109°C (diethyl ether/hexane). ^1H nmr (CDCl_3): 6.6 ppm (d, 1H, $J = 3.5$ Hz, ^3H), 8.4 ppm (m, 1H, ^2H), 3.9 ppm (s, 3H, OCH_3), 7.0-7.9 ppm (m, 8H); exact mass $m/e = 251.0436$. ^{13}C nmr (CDCl_3): 131.7, 129.1, 129.1, 128.5, 128.5, 128.2, 117.2, 113.3, 108.5 and 103.5 ppm (CH), 156.6, 134.5, 130.6 and 128.1 ppm (C), 55.6 (OCH_3), 169.1 (C = O).

N-Acetylindole (157)

The synthesis of N-acetylindole 157 was performed using the same procedure as described for the synthesis of

NBI except for the use of acetyl chloride instead of benzoyl chloride to yield a brown oil which was distilled at reduced pressure to yield a viscous liquid.

For 157; B.p. 128°C/1.8 mm¹²⁸ of Hg. ¹H nmr (CDCl₃): 2.65 ppm (s, 3H), 6.65 ppm (d, 1H, J = 3.5 Hz), 7.13-7.67 ppm (m, 4H), 8.53 ppm (m, 1H); exact mass m/e = 159.0685.

6H-Isoindolo[2.1-a]indol-6-one (162)

Compound 162 was synthesized according to the procedure described by Zimmer et al.¹²⁸

For 162; M.p. 152-153°C (EtOH). ¹H nmr (CDCl₃): 6.55 ppm (s, 1H), 7.1-8.0 ppm (m, 8H); exact mass m/e = 219.0684. ¹³C nmr (CDCl₃): 133.7, 128.8, 126.3, 125.3, 123.9, 122.3, 121.2, 113.3 and 103.5 ppm (CH), 138.9, 134.7, 134.5, 133.4 and 133.4 (C), 162.6 (C = O).

N-(O-Hydroxymethylphenyl)-2-succinimide (161a)

O-Aminobenzyl alcohol (0.065 mol) and succinic anhydride (0.065 mol) were refluxed in 250 mL of chloroform for 3 h during which time a white precipitate formed. The reaction mixture was cooled and filtered to give 161a as a white solid (yield = 63.3%).

For 161a; (CD_3COCD_3): 2.6 ppm (s, 1H, OH), 2.7 ppm (s, 4H, CH_2CH_2), 4.7 ppm (s, 2H, CH_2OH), 7.0-7.4 ppm (m, 3H), 7.9 ppm (m, 1H), 9.0 ppm (1H, NH), 11.6 ppm (s, 1H).
 ^{13}C nmr (CD_3COCD_3): 53.3, 53.4, 62.8 ppm (CH_2), 129.8, 130.0, 130.3 and 131.4 ppm (CH), 131.3 and 133.5 ppm (C), 171.9 and 176.7 ppm (C = O); exact mass m/e = 223.0399.

N-[2-(Chloromethyl)phenyl]succinimide (161b)

Compound 161a (0.04 mol) in a 250 mL flask fitted with a refluxing condenser, was treated with thionyl chloride (2 eq) at room temperature. After 30 min CHCl_3 (100 mL) was added and the solution was refluxed for 10 min. The major portion of the CHCl_3 was distilled out and more CHCl_3 was added. This was repeated several times to ensure removal of excess thionylchloride. The reaction mixture was extracted with saturated potassium bicarbonate solution, dried over potassium carbonate and concentrated to give a yellow semi-solid. This was purified using 50 g of silica gel (60-200 mesh, Baker Analyzed reagent) and $\text{CHCl}_3/\text{CCl}_4$ as the solvent to give a yellow solid (yield = 83%).

For 161b; ^1H nmr (CDCl_3): 2.8-3.0 ppm (bs, 4H), 4.4 ppm (s, 2H), 7.1-7.7 ppm (m, 4H). ^{13}C nmr (CDCl_3): 28.6, 28.6 and 43.0 ppm (CH_2), 130.7, 129.8, 129.8 and 129.2 ppm (CH), 134.6 and 131.3 ppm (C), 176.1 and 176.1 (C = O); exact mass m/e = 223.0399.

1,2-Dihydro-3H-pyrrolo-[1,2-a]-idol-3-one (161)

A chloroform solution of N-[2(chloromethyl)phenylsuccinimide and triphenylphosphine (1.1 eq) was refluxed overnight. The volume was reduced, ethyl ether added, and the resulting precipitate (2-succinimidobenzyl)-triphenylphosphonium chloride was collected, yield 85%. t-Butyllithium (1.1 eq) was added to a tetrahydrofuran solution of (2-succinimidobenzoyl)triphenylphosphonium chloride under a nitrogen atmosphere and the reaction mixture was heated to reflux for 18 h. The product was separated by liquid chromatography using 40 g of silica gel (60-200 mesh, Baker Analyzed reagent) and CHCl_3 as the solvent to yield 61% as a crystalline solid.

For 161; M.p. 150-151°C (recrystallized from MeOH). ^1H nmr (CDCl_3): 3.2 ppm (bs, 4H), 6.3 ppm (s, 1H), 7.3-7.6 ppm (m, 3H), 8.0-8.1 ppm (m, 1H); exact mass m/e = 171.069. ^{13}C nmr (CDCl_3): 124.0, 123.3, 120.5, 113.6 and 100.4 ppm (CH), 34.9 and 19.7 ppm (CH_2), 143.6, 135.3 and 130.7 (C), 189.5 (C = O).

Photoaddition of N-benzoylindole and Cyclopentene

N-benzoylindole (2.5 g, 0.011 mol) was dissolved in benzene (250 mL) previously purged with nitrogen. To this solution distilled cyclopentene (8.5 g, 0.125 mol) was added and the solution was irradiated using Pyrex and water filtered light from an Hanovia Medium Pressure Hg lamp.

After 22 h gas chromatographic analysis indicated 55% conversion of the indole to products. The benzene solution was concentrated under reduced pressure to yield 2.7 g of yellow oil. This was purified using 100 g of silica gel (60-200 Mesh, Baker Analyzed reagent) and 30/70, diethyl ether/hexane as the solvent to give 152 as a white solid which was crystallized from ether (yield 21.1%).

For 152; M.p. 124-126°C. ^1H nmr (CDCl_3): 1.1-1.9 ppm (m, 6H), 2.7 ppm (m, 1H, $J = 3, 7$ Hz), 2.84 ppm (m, 1H, $J = 3, 7$ Hz), 3.35 ppm (dd, 1H, $J = 7.5$ and 3 Hz), 4.0 ppm (bs, 1H, $J = 7.5, 3.0$ Hz), 7.1-7.7 ppm (m, 9H); exact mass $m/e = 289.1465$. ^{13}C nmr (CDCl_3): 30.9, 32.3 and 25.3 (CH_2), 129.9, 128.3, 127.1, 127.5, 126.8, 124.7, 124.6, 124.5, 118.2, 63.6, 47.8, 46.0 and 45.0 (CH), 137.4, 136.6 and 130.0 (C), 169.8 (C=O).

153; Examination of the mother liquors later revealed the presence of an equal quantity of the oily *cis-syn-cis* adduct 153. This compound was characterized by Mr. D. Hastings and was shown to have the same gas chromatographic retention time as the stereoisomer 152.

Stern-Volmer Plots

Quenching of NBI-cyclopentene Cycloaddition Reaction with Cyclohexadiene

The following solutions were prepared:

(i) 2.5×10^{-2} M cyclohexadiene in benzene; and (ii) 136.8 mg of octacosane in 100 mL in benzene.

All the solutions used were purged with nitrogen gas, and mixing and transferring of solutions was performed under a nitrogen atmosphere. NBI (225 mg), octacosane standard solution (8 mL), and 1.2 g of cyclopentene were mixed and made up to 40.0 mL with benzene. For quenching experiments 4.0 mL of this solution and samples of the cyclohexadiene solution (0, 0.2, 0.4, 0.6, 0.8, 0.9 and 1.0 mL) were pipetted into each of seven Pyrex Merry-Go-Round tubes. Benzene was added to make the volume in each tube up to 5.0 mL. The solutions were degassed and irradiated using light from a Pyrex and water filtered Hanovia Medium Pressure Hg lamp in a Merry-Go-Round apparatus at $20 \pm 1^\circ\text{C}$. The irradiation was stopped at less than 3% conversion. For each tube the amount of adduct formed relative to the amount of octacosane was determined using gas-liquid chromatography (5% S.E. 30 on Chemisorb W). The amount of adduct in tube 1 (where no cyclohexadiene was present) was divided by the amount of adduct formed in each tube containing a quencher. This ratio, designated Φ^0/Φ , was calculated for each of the tubes and was plotted against the quencher concentration, [Q]. A linear Stern-Volmer plot was thereby obtained.

Stern-Volmer plots were also obtained for cyclopentene concentrations of 0.35 M, 0.53 M, 0.82 M, 1.12 M and 1.41 M. The slope and intercept of each plot are given in Table XIII (Figs. 4 and 5). The whole experiment was repeated and the results were found to be reproducible. Similar Stern-Volmer plots were also obtained when isoprene was used as the quencher instead of cyclohexadiene.

Dilution of NBI and Cyclopentene in Benzene at 20°C

The following solutions were prepared: (1) 590 mg of NBI in 10 mL of benzene and (11) 136.8 mg of octacosane in 100 mL of benzene. 1 mL of the NBI solution, 2 mL of the standard octacosane solution and different volumes of cyclopentene (1.0, 2.0, 3.0, 4.0 and 5.0 mL) were added into a 10 mL volumetric flask. Benzene was added to make the volumes up to the mark. All solutions were purged with nitrogen before mixing, and 3 mL of each sample were irradiated in a quartz cuvette (1.00 cm path) at 313 nm using a Photon Technologies Inc. Quantacount quantum counter instrument for 3 h. After irradiation the amount of adduct formed was determined using gas-liquid chromatography (10% S.E. 30 on Chemisorb W). The photon flux absorbed by the solution in these experiments was determined by actinometry using potassium ferrioxalate, and using this value the quantum yield of adduct formation was calculated for each of the cyclopentene concentrations.

[Quencher]	$[C]_0^a = 0.39 \text{ M}$ ϕ/ϕ_0	$[C]_0^a = 0.53 \text{ M}$ ϕ/ϕ_0	$[C]_0^a = 0.82 \text{ M}$ ϕ/ϕ_0	$[C]_0^a = 1.12 \text{ M}$ ϕ/ϕ_0	$[C]_0^a = 1.41 \text{ M}$ ϕ/ϕ_0
0.0005 M	1.4	1.5	1.66	1.41	1.27
0.001 M	2.48	2.19	2.15	1.81	1.67
0.002 M	3.42	3.21	2.84	2.5	2.51
0.003 M	4.92	4.55	3.7	3.45	3.26
0.004 M	6.35	5.6	4.64	4.18	4.03
0.005 M	7.87	6.75	5.61	5.01	4.66
slope ^b	1389.1 ± 36.6	1164.8 ± 14.6	919.6 ± 179.6	797.3 ± 13.4	761.1 ± 13.3
intercept ^b	0.83 ± 0.11	0.95 ± 0.04	1.39 ± 0.54	1.01 ± 0.04	0.93 ± 0.04
coefficient of correlation	0.9979	0.9995	0.9020	0.9991	0.9990
^a cyclopentene concentration					
^b from least square calculations					

TABLE XIII: Stern-Volmer quenching data for the NBI-cyclopentene reaction

The results are plotted in Figures 6 and 7 and summarized in Table XIV.

[CYCLOPENTENE]	Φ_p
5.69 M	3.31×10^{-2}
4.55 M	1.97×10^{-2}
3.41 M	1.70×10^{-2}
2.28 M	1.24×10^{-2}
1.14 M	0.67×10^{-2}

TABLE XIV: Quantum yields of photoaddition of NBI at various cyclopentene concentrations

Φ_p - quantum yield of product formation.

Fig. 7;

Slope = 148.8 ± 1.6 M

Intercept = 16.0 ± 0.8

Coefficient of Correlation = 0.9996

Rate of Self-Quenching

The following solutions were prepared: (i) 1.50 g of NBI in 25 mL of benzene, and (ii) 136.8 mg of octacosane in 100 mL of benzene. A sample of the octacosane standard solution (2.0 mL), cyclopentene (2.0 mL) and different volumes of the NBI solutions (1.0, 2.0, 3.0, 4.0 and 5.0 mL) were added into a 10 mL volumetric flask. Benzene was added to make the volumes up to the mark. All solutions were purged with nitrogen gas and 3 mL of each sample were irradiated in a quartz cuvette at 313 nm in Photon Technologies Inc. Quantacount (PTI) quantum counter

instrument for 2500 counts so that each solution received the same number of photons. After irradiation, the amount of adduct formed was determined using gas-liquid chromatography (10% S.E. 30 on Chemisorb W) and the quantum yield of adduct formation was calculated using the known photon flux of the PTI Quantacount. A plot of $1/\Phi$ vs NBI concentration was obtained, where Φ is the quantum yield of cycloaddition of NBI and cyclopentene (Fig. 8).

$$\text{Intercept} = 19.1 \pm 0.15 \text{ M}^{-1}$$

$$\text{slope} = 13.6 \pm 1.7$$

$$\text{Coefficient of Correlation} = 0.9642$$

Quantum Yield of Triplet Formation.

Quantum Yield of Sensitized Isomerization of Piperlyne with Benzophenone in Benzene at 20°C

1.5 mL of a 2.4×10^{-1} M solution of trans-piperlyne in benzene, 1.0 mL of a 3.53×10^{-1} M solution of cycloheptane in benzene and 1.0 mL of a 6.18×10^{-1} M solution of benzophenone in benzene were mixed in a 25.0 mL volumetric flask which was then made up to the mark with benzene. All the solutions were purged with nitrogen gas. 3 mL of the mixture were transferred to a quartz cuvette and were irradiated at 313 nm in a Photon Technologies Inc. Quantacount quantum counter instrument. The irradiation was carried out at about 4% conversion to cis-piperlyne. The amount of cis-piperlyne formed from trans-piperlyne was determined using gas liquid chromatography. (15% β, β -oxydipropionitrile on Diatoport-S

column, 25' x 1/8", at 20°C) from which $\Phi_{t \rightarrow c} = 0.44 \pm 0.003$ was calculated. Using the same procedure as described above the quantum yield of sensitized isomerization of trans-piperylene was calculated to be 0.44 ± 0.003 and 0.40 ± 0.003 in acetonitrile and CCl_4 solvents, respectively.

Measurement of the Quantum Yield of Triplet Formed from Direct Irradiation of NBI in Benzene

1.0 mL of a $2.67 \times 10^{-1} \text{ M}$ solution of NBI in hexane, 0.4 mL of $3.53 \times 10^{-1} \text{ M}$ cycloheptane standard benzene solution and different volumes of $2.4 \times 10^{-1} \text{ M}$ trans-piperylene benzene solutions (0.2, 0.3, 0.4 and 0.6 mL) were added into a 10 mL volumetric flask. Benzene was added to make the volumes up to the mark. All solutions were purged with nitrogen gas. 3 mL of each sample were irradiated in a quartz cuvette at 313 nm using a Photon Technologies Inc. Quantacount quantum counter instrument. All the irradiations were carried out at less than 5% conversion. After irradiation the amount of cis-piperylene formed from trans-piperylene was determined using gas-liquid chromatography (15% *B,B*-oxydipropionitrile on Diatoport S at 20°C). $\Phi_{t \rightarrow c}$ was determined using the expression

$$\Phi_{t \rightarrow c} = \frac{\text{moles of cis-piperylene formed}}{\text{photon flux}}$$

Compound	Solvent	Intercept	Gradient/M	Coefficient of Correlation
142a	benzene	2.55 ± 0.06	(5.80 ± 0.46) × 10 ⁻³	0.9874
142a	CH ₂ Cl ₂	6.47 ± 0.18	(4.81 ± 0.13) × 10 ⁻²	0.9984
142a	MeCH	5.9 ± 0.1	0.65 ± 0.001	0.9999
157	benzene	1.82 ± 0.03	(5.32 ± 0.19) × 10 ⁻³	0.9971
159	benzene	1.56 ± 0.03	(8.80 ± 0.24) × 10 ⁻³	0.9984
160	benzene	2.11 ± 0.02	(8.44 ± 0.1) × 10 ⁻³	0.9995
161	benzene	20.1 ± 2.5	0.56 ± 0.02	0.9979

TABLE XV: Triplet counting experimental data for the compounds (142a) and (157-161)

Plots of $C/\Phi_{t \rightarrow c}$ vs $1/[Q]$ were obtained (Figs. 13, 14, 15 and 16), from which the quantum yield of triplet formation of NBI in benzene was calculated (Table VIII). The above procedure was used to determine the $\Phi_{I.S.C.}$ of compounds 157, 158 and 160 in benzene and NBI in CH_2Cl_2 solution (Figs. 13 and 15, Tables VIII and XV).

Quantum Yield of Triplet Formation of NBI in Acetonitrile

0.1 mL of a 2.67×10^{-1} M solution of NBI in acetonitrile, 0.4 mL of a 3.53×10^{-1} M cycloheptane standard acetonitrile solution and different volumes of 2.4×10^{-1} M solution of trans-piperylene in acetonitrile (0.2, 0.3, 0.4 and 0.6 mL) were added into a 10 mL volumetric flask. Acetonitrile was added to make the volumes up to the mark. All solutions were purged with nitrogen gas. 3 mL of each sample were irradiated on an optical bench using a Pyrex filter, in a quartz cuvette at $20^\circ C$ for 40 min. The amount of cis-piperylene formed from trans-piperylene was determined using gas-liquid chromatography at $20^\circ C$. A plot of $C/\Phi_{I.S.C.}$ of NBI in acetonitrile was determined (Tables VIII and XV, Fig. 14). The above procedure was utilized to determine the $\Phi_{I.S.C.}$ of compounds 159, 161 and NBI, all in benzene solution. The time of irradiation was 120 min for compounds 159 and 161 and 3 min for NBI (Fig. 16, Tables VIII and XV). The $\Phi_{I.S.C.}$ value for NBI in benzene obtained in both procedures agreed to within the experimental error.

Measurement of Emission Spectra

NBI and compound 160 were recrystallized three times from diethyl ether/hexane; 158 three times from diethyl ether; 159 five times from n-hexane/CH₂Cl₂; 162 three times from ethanol, and 161 five times from methanol.

All solvents used were distilled and shown to be non-fluorescent at the wavelengths used. Solvents n-pentane, n-hexane (Fisher, spectroscopic grade), acetonitrile (Aldrich, Spectroscopic grade) were used without further purification. Solvents anhydrous diethyl ether, 1,4-dioxane, n-propionitrile (Baker Analyzed, spectroscopic grade), chloroform, carbontetrachloride, methylene chloride (Fisher, Spectroscopic grade), ClCH₂-CH₂-Cl, CH₃-CCl₃ (B.D.H., Spectroscopic grade), ethyl acetate, ethylformate, di-isopropyl ether, di-n-butyl ether and glyme (B.D.H. reagent grade) were distilled before use to ensure the absence of fluorescing impurities. Tetrahydrofuran was freshly distilled before use from sodium and benzophenone.

The absorption and fluorescence spectra were recorded on solutions of ca 10⁻⁵ M concentrations, and were prepared immediately before use. Oxygen-free solutions were prepared by purging nitrogen gas through the sample, immediately before the measurement. The lifetime measurements were performed on oxygen-free solutions. All measurements were performed at 20°C unless otherwise noted.

The quantum yield of fluorescence for each compound was measured relative to indole. This was done by preparing a solution of indole in the same solvent, such that it had the same absorption (to within 2%) of that of the solution of N-benzoylindole (10^{-5} M) at 287 nm. Both solutions were irradiated at 287 nm and the areas under the corrected emission spectra were compared in order to calculate the quantum yield of fluorescence.

The phosphorescence spectra were recorded on solutions of ca 10^{-5} M concentrations in quartz nmr tube at 77 K and were prepared immediately before use. All solutions were purged with nitrogen gas immediately before the measurement.

Possible Quenching of Charge-Transfer Fluorescence of NBI

1.0 mL of a 2.5×10^{-4} M solution of NBI in n-hexane and different volumes of 2.4×10^{-1} M trans-piperylene solutions (0.2, 0.3, 0.4 and 0.6 mL) were placed in a 10 mL volumetric flask. Hexane was added to make the volumes up to the mark. All solutions were purged with nitrogen gas. The absorption and the emission spectra of each sample in the presence and absence of trans-piperylene were then measured and compared. The fluorescence quantum yield of NBI in the presence of the quencher was calculated for each sample, and was found to be identical, indicating the absence of fluorescence quenching. The above procedure was also performed for NBI in acetonitrile, diethyl ether and

methylene chloride, and was repeated with the use of
1,3-cyclohexadiene and cyclopentene as the quencher.

REFERENCES

1. W.A. Ayer and L.M. Browne, *Tetrahedron* 37, 2199-2248 (1981).
2. N.G. Heatley, M.A. Jennings and H.W. Florey, *Br. J. Exp. Pathology* 28, 35 (1947).
3. (a) F.W. Comer, F. McCapra, I.H. Qureshi, J. Trotter and A.I. Scott, *J. Chem. Soc. Chem. Commun.*, 310 (1965); (b) F.W. Comer, F. McCapra, I.H. Qureshi and A.I. Scott, *Tetrahedron* 23, 4761 (1967); (b) F.W. Comer and J. Trotter, *J. Chem. Soc. Chem. Commun. (B)*, 11 (1966).
4. T. Takeuchi, H. Inuma, J. Iwanaga, S. Takahashi, T. Takita and H. Umezawa, *J. Antibiotics* 22, 215 (1969).
5. T. Takeuchi, S. Takahashi, H. Inuma and H. Umezawa, *J. Antibiotics* 24, 631 (1971).
6. S. Nozoe, J. Furukawa, U. Sankawa and S. Shibata, *Tetrahedron Lett.*, 195 (1976).
7. P.G. Mantle and G. Mellows, *Trans. Br. Mycol. Soc.* 61, 513 (1973).
8. W.B. Turner, *Fungal Metabolites*, Academic Press, New York, 1971.
9. Y. Ohtsue, H. Shirahama and T. Matsumoto, *Tetrahedron Lett.*, 2795 (1976).

10. K. Hayano, Y. Ohtune, H. Shirahama and T. Matsumoto, *Tetrahedron Lett.*, 1991 (1978).
11. G. Mellows, P.G. Mantle, T.C. Feline and D.J. Williams, *Photochemistry* 12, 2717 (1973).
12. S. Takahashi, H. Naganawa, H. Inuma, T. Takita, K. Maeda and H. Umezawa, *Tetrahedron Lett.*, 1955 (1971).
13. F.W. Comer, F. McCapra, T.H. Qureshi and A.I. Scbutt, *Tetrahedron* 23, 4761 (1967).
14. T.C. Feline, G. Mellows, R.J. Jones and L. Phillips, *J. Chem. Soc. Chem. Commun.*, 63 (1974).
15. T.C. McMorris, M.S.R. Nair, P. Singh and M. Anchell, *Phytochemistry* 10, 1611, 3341.
16. S. Nozoe, H. Kobayashi, S. Urano and J. Furukawa, *Tetrahedron Lett.*, 1381 (1977).
17. M. Tanabe, K.T. Suzuki and W.C. Jankowski, *Tetrahedron Lett.*, 2271 (1974).
18. P.T. Lansbury, N.Y. Wang and J.E. Rhodes, *Tetrahedron Lett.*, 1829 (1971).
19. P.T. Lansbury, N.Y. Wang and J.E. Rhodes, *Tetrahedron Lett.*, 2053 (1972).
20. (a) B.A. Dawson, A.K. Ghosh, J.L. Jurlina, A.J. Ragauskas and J.B. Stothers, *Can. J. Chem.* 62, 2521 (1984); (b) B.A. Dawson, A.K. Ghosh, J.L. Jurlina and J.B. Stothers, *J. Chem. Soc. Chem. Commun.*, 204 (1983).

21. (a) R.D. Little, A. Bukhari and M.G. Venegas, *Tetrahedron Lett.*, 305 (1979); (b) R.D. Little and G.W. Muller, *J. Am. Chem. Soc.* 103, 3744 (1981); (c) R.D. Little, G.W. Muller, M.G. Venegas, G.L. Carroll, A. Bukhari, L. Patton and K. Stone, *Tetrahedron* 37, 4371 (1981).
22. (a) T. Hudlicky, T.M. Kutchan, S.R. Wilson and D.T. Mao, *J. Am. Chem. Soc.* 102, 6353 (1980); (b) T. Hudlicky, F.T. Koszyk, T.M. Kutchan and J.P. Sheth, *J. Org. Chem.* 45, 5020 (1980).
23. (a) K. Tatsuta, K. Akimoto and M. Kinoshita, *J. Am. Chem. Soc.* 101, 6116 (1979); (b) K. Tatsuta, K. Akimoto and M. Kinoshita, *J. Antibiotics* 33, 100 (1980).
24. (a) P.A. Wender and J.J. Howbert, *Tetrahedron Lett.* 23, 3983 (1982); (b) P.A. Wender and J.J. Howbert, *Tetrahedron Lett.* 24, 5325 (1983).
25. (a) G. Mehta and A.V. Reedy, *J. Chem. Soc. Chem. Commun.*, 756 (1981); (b) G. Mehta, A.N. Murthy, D.S. Reddy and A.V. Reddy, *J. Am. Chem. Soc.* 108, 3443 (1986).
26. A.E. Greene, *Tetrahedron Lett.* 21, 3059 (1980).
27. (a) R.L. Funk and K.P.C. Vollhardt, *Synthesis*, 118 (1980); and references therein; (b) D.H. Hua, G. Sinai-Zingdi and S. Venkataraman, *J. Am. Chem. Soc.* 107, 4088 (1985).

28. S.V. Ley and P.J. Murray, *J. Chem. Soc. Chem. Commun.*, 1252 (1982).
29. D.P. Curran and D.M. Rakiewicz, *J. Am. Chem. Soc.* 107, 1448 (1985).
30. (a) P.D. Magnus and D.A. Quagliato, *Organometallics* 1, 1243 (1982); (b) P.D. Magnus and D.A. Quagliato, *J. Org. Chem.* 50, 1621 (1985).
31. P.E. Eaton, *Accounts of Chem. Res.* 1, 50 (1968)
32. (a) H. Hikino and P. de Mayo, *J. Am. Chem. Soc.* 84, 2454 (1962); (b) B.D. Challand, G. Kornis, G.L. Lange and P. de Mayo, *J. Chem. Soc. Chem. Commun.*, 704 (1967); B.D. Challand, H. Hikino, G. Kornis, G. Lange and P. de Mayo, *J. Org. Chem.* 34, 794 (1969); (c) G. Buchi, T.A. Carlson, J.E. Powell and L.P. Tietze, *J. Am. Chem. Soc.* 92, 2165 (1970).
33. P.E. Eaton and W.S. Hart, *J. Am. Chem. Soc.* 88, 5038 (1966).
34. R.O. Loutfy and P. de Mayo, *J. Am. Chem. Soc.* 99, 3559 (1977).
35. M.C. Yang and M.J. Jorgenson, *Tet. Lett.*, 1203 (1964).
36. P.G. Bauslaugh, *Synthesis*, 288 (1970)
37. (a) P. de Mayo, H. Takeshita and A.B.M.A. Sattar, *Proc. Chem. Soc. London*, 119 (1962); P. de Mayo and H. Takeshita, *Can. J. Chem.* 41, 440 (1963); (b) P. de Mayo, *Acc. of Chem. Res.* 4, 2, 41 (1971).
38. E.J. Corey, J.D. Bass, R. Le Mahieu and R.B. Mitra, *J. Am. Chem. Soc.* 86, 5570 (1964).

39. (a) J.E. McMurray, *Acc. Chem. Res.* 7, 281 (1974);
(b) J.E. McMurray, M.P. Fleming, K.L. Kees and L.R. Krepski, *J. Org. Chem.* 43, 3255 (1978).
40. J.E. McMurray, *Acc. Chem. Res.* 16, 405 (1983).
41. T. Mukalyama, T. Sato and J. Hanna, *Chem. Lett.*, 1041 (1973).
42. S. Tyrlik and I. Wolochowicz, *Bull. Soc. Chim. Fr.*, 2147 (1973).
43. W.A. Benjamin, *Modern Synthetic Reactions*, 2nd Ed., New York, New York, 1972, pp. 167.
44. E. Block, *Organic Reactions* 30, 457 (1984).
45. J.E. Pauw and A.C. Weedon, *Tetrahedron Lett.* 23, 5485 (1982).
46. M.J. Begley, M. Mellor and G. Mahenden, *J. Chem. Soc. Chem. Commun.*, 235 (1979).
47. T.S. Cantrell, W.S. Haller and J.C. Williams, *J. Am. Chem. Soc.* 91, 4494, (1969).
48. M. Umehara, T. Oda, Y. Ikeka and S. Hishida, *Bull. Chem. Soc. Japan* 49, 1075 (1976).
49. A.C. Weedon, *Enone Photochemical Cycloaddition in Synthesis in Synthetic Organic Photochemistry*, (ed.) W.M. Horspool, Plenum, New York, 1984, p. 61.
50. M.J. Begley, M. Mellor and G. Pattender, *J. Chem. Soc. Chem. Commun.*, 235 (1979).
51. J.B. Stothers, *Carbon-13 N.M.R. Spectroscopy*, Academic Press, New York.

52. E. Koh, M.D. Sinha, P. Sandra, P.J. De Clercq and M.E. Vandewelle, *Tetrahedron* 38, 2279 (1982).
53. R.B. Woodward, K. Heusler, J. Gostelli, P. Nageli, W. Oppolzer, R. Ramage, S. Ranganathan and H. Vorburgeen, *J. Am. Chem. Soc.* 88, 852 (1966); E.J. Corey and A. Venkateswarlu, *J. Am. Chem. Soc.* 94, 6190, (1972); E.J. Corey and R.K. Varma, *J. Am. Chem. Soc.* 93, 7319 (1971).
54. L.H. Sommer, *Stereochemistry, Mechanism and Silicon*, McGraw-Hill, New York, New York, 1965, p. 132.
55. A.E. Pierce, *Silylation of Organic Compounds*, Pierce Chemical Co., Rockford, Illinois, 1968; B. Arkles, *Techniques for Silylation in Silicon Compounds, Register and Review*, Detrarch Systems, Lewitton, Pennsylvania, 1979.
56. T. Veysoglu and L.A. Mitscher, *Tetrahedron Lett.* 22, 1303 (1981); K.K. Ogilvie, *Can. J. Chem.* 51, 3799, 1973.
57. T.-L. Ho and S.H. Liu, *Chem. Ind. (London)*, 371 (1982).
58. P.G. Cassman and M. Pascone, *J. Am. Chem. Soc.* 95, 7801 (1973).
59. (a) C.W. Jefford and A.P. Boschung, *Helv. Chem. Act.* 57, 2257 (1974); (b) E.D. Mihelich and D.J. Eickhoff, *J. Org. Chem.* 48, 4135 (1983).
60. B.W. Disanayaka and A.C. Weedon, *Synthesis* 11, 952 (1983).
61. J.L. Gras, *Tetrahedron Lett.*, 2111, 2955 (1978).

62. J. Andrieux, D.H.R. Barton and H. Patin, *J. Chem. Soc. Perkin Trans. 1*, 359 (1977).
63. (a) S.L. Patt and J.N. Shoolery, *J. Magn. Reson.* 46, 535 (1982); (b) G.A. Morris and R. Freeman, *J. Am. Chem. Soc.* 107, 760 (1979).
64. D.R. Julian and G.D. Tringham, *J. Chem. Soc. Chem. Commun.*, 13 (1973).
65. (a) G.O. Schenck, W. Hartman and R. Steinmetz, *Chem. Ber.* 96, 498 (1962); (b) D.R. Arnold, *Adv. Photochem.* 6, 301 (1968).
66. C. Rivas, M. Velez and O. Crescente, *J. Chem. Soc. Chem. Commun.*, 1474 (1970).
67. G.R. Evanega and E.B. Whipple, *Tetrahedron Lett.*, 2163 (1967).
68. K. Yamasaki, T. Matsuura and I. Saito, *J. Chem. Soc. Chem. Commun.*, 944 (1974).
69. S. Narato and O. Yonemitsu, *Tetrahedron Lett.*, 2297 (1971).
70. D.R. Julian and R. Foster, *J. Chem. Soc. Chem. Commun.*, 311 (1973).
71. T. Hino, M. Taniguchi, T. Date and Y. Iidaka, *Heterocycles* 7, 105 (1977).
72. (a) D.J. Trecker, *Organic Photochemistry*, Marcel Dekker Inc., New York, 1969, Vol. 2, pp. 63; (b) D.N. Harpp and C. Heitner, *J. Org. Chem.* 35, 3256 (1970); (c) D.H. Harpp and C. Heitner, *J. Am. Chem. Soc.* 94, 8179 (1972).

73. M. Ikeda, K. Ohao, T. Uno and Y. Tamura, *Tetrahedron Lett.* 21, 3403 (1980).
74. M. Ikeda, T. Uno, K. Homma, K. Ohao and Y. Tamura, *Synthetic Comm.* 10(6), 437 (1980).
75. M. Ikeda, K. Ohao, M. Takahashi, T. Uno and Y. Tamura, *J. Chem. Soc. Perkin I*, 3741 (1982).
76. M. Ikeda, K. Ohao, S. Mohri, M. Takahashi and Y. Tamura, *J. Chem. Soc. Perkin I*, 405 (1984).
77. G.R. Evanega and D.L. Fabing, *J. Org. Chem.* 85, 1757 (1970).
78. (a) G.R. Evanega and D.L. Fabing, *Tetrahedron Lett.*, 1749 (1971); (b) T. Naito and C. Kaneko, *Tetrahedron Lett.* 22, 2671 (1981).
79. T. Naito, N. Nakayama and C. Kaneko, *Chem. Lett.*, 423 (1981).
80. (a) W. Metzner and W. Hartmann, *Chem. Ber.* 101, 4099 (1968); (b) T.T. McCullough and C.W. Huang, *Can. J. Chem.* 47, 757 (1969).
81. D.N. Harpp and C. Heitner, *J. Org. Chem.* 38, 4184 (1973).
82. S.W. Baldwin In *Organic Photochemistry*, A. Padwa (Ed.), Marcel Dekker, New York, 1981, 46, 651.
83. P.D. Davis and D.C. Neckers, *J. Org. Chem.* 42, 2374 (1977).
84. D.C. Neckers in "Synthetic Organic Photochemistry", (ed.) W.M. Horspool, Plenum, New York, 1984, p. 285.

85. T.S. Cantrell, *J. Chem. Soc. Chem. Commun.*, 1656 (1970).
86. T.S. Cantrell, *J. Org. Chem.* 39, 3063 (1974).
87. G. Jones, Jr. and B.R. Ramachandran, *J. Photochem.* 5, 341 (1976).
88. P. Margaretha, *Liebigs Ann. Chem.*, 727 (1973).
89. J.J. McCulloch, B.R. Ramachandran, F.P. Synder and G.M. Taylor, *J. Am. Chem. Soc.* 97, 6767 (1975).
90. (a) J.C. Scaiano, *Acc. Chem. Res.* 15, 252 (1982); (b) J.C. Scaiano, *Tetrahedron* 38, 819 (1982).
91. (a) R.A. Caldwell, T. Majima and C. Pac, *J. Am. Chem. Soc.* 104, 629 (1982); (b) R.A. Caldwell and D. Creed, *J. Phys. Chem.* 82, 2644 (1978); (c) R.A. Caldwell, H. Sakuragi and T. Majima, *J. Am. Chem. Soc.* 106, 2471 (1984).
92. (a) G. Closs and C. Doubleday, *J. Am. Chem. Soc.* 95, 2735 (1973); (b) G. Closs, *Adv. Magn. Reson.* 7, 1 (1975).
93. M.B. Zimmt, C. Doubleday, Jr. and N.J. Turro, *J. Am. Chem. Soc.* 108, 3618 (1986).
94. (a) R.D. Small, Jr. and J.C. Scaiano, *Chem. Phys. Lett.* 48, 354 (1977); (b) L.J. Johnston and J.C. Scaiano, *J. Am. Chem. Soc.* 108, 2349 (1986).
95. C. Walling, *Free Radicals in Solution*, Wiley, New York, 1957, Chap. 6.
96. T.H. Lowry and K.S. Richardson, "Mechanism on Theory in Organic Chemistry", Harper and Row, New York, 1981.

97. J.M. Tedder and J.C. Walton, *Adv. Phys. Org. Chem.* 16, 51 (1978).
98. A. Gupta and G.S. Hammond, *J. Am. Chem. Soc.* 98, 1218 (1976).
99. E.P.G. Templeton and W.R. Ware, *J. Phys. Chem.* 88, 4626 (1984).
100. C. Reichardt and E. Harbusch-Gornert, *Liebigs Ann. Chem.*, 721 (1983).
101. E.M. Kosower and H. Kanety, *J. Am. Chem. Soc.* 105, 6232 (1983).
102. A.A. Lamola and G.S. Hammond, *J. Chem. Phys.* 43, 2129 (1965).
103. P.S. Song and W.E. Kurtin, *Photochem. Photobiol.* 9, 175 (1969).
104. P.S. Song and W.E. Kurtin, *J. Am. Chem. Soc.* 91, 4892 (1969).
105. M.S. Walker, T.W. Bednan and R.W. Lumry, *J. Chem. Phys.* 45, 3455 (1966).
106. E. Donket, *Bull. Soc. Chim. Belges* 78, 69 (1969).
107. E. Lippert, W. Luder and H. Boos In *Advanced Molecular Spectroscopy*, A. Mangini (Ed.), Pergamon Press, Oxford, 1962, 443.
108. N. Mataga, Y. Torihaski and K. Ezumi, *Theoret. Chem. Acta* 2, 158 (1964); S. Suzuki, T. Fujii, A. Imai and H. Akatori, *J. Phys. Chem.* 81, 1592 (1977).
109. E.H. Strickland and C. Billups, *Biopolymers* 12, 1989 (1973).

110. J.R. Lakowicz and A. Bulter, Photochem. Photobiol. 36, 125 (1982).
111. H. Lami, II, Nuova Cimento Soc. Ital. Fis. 63B, 241 (1981).
112. S.R. Neech, D. Philips and A.G. Lee, Chem. Phys. Lett. 92, 523 (1982).
113. T. Forster, Z. Electrochem. 45, 548 (1939).
114. R.S. Mulliken, J. Am. Chem. Soc. 72, 600 (1950).
115. S. Nagakara and J. Tanaka, J. Chem. Phys. 22, 236 (1954).
116. W. Liptay and J. Czekalla, Z. Naturforsch 15a, 1072 (1960); *ibid* 18a, 705 (1963); *ibid*, 20a, 272 (1965).
117. K. Rofkiewicz, K.H. Grellmann and Z.R. Grabowski, Chem. Phys. Lett. 19, 315 (1973).
118. Z.R. Grabowski, K. Rofkiewicz, A. Siemiarczuk, D.J. Cowley and W. Baumann, Nouveau Jour. De Chimie 3, 443 (1979).
119. A. Siemiarczuk, Chem. Phys. Lett. 110, 437 (1984).
120. W. Baumann, F. Petzke and K.D. Loosen, Z. Naturforsch 34, 1070 (1979).
121. W. Rettig and M. Zander, Chem. Phys. Lett. 87, 229 (1982).
122. (a) E.M. Kosower, H. Dodiuk, K. Tanizawa, M. Ohlenghi and N. Orbach, J. Am. Chem. Soc. 97, 2167 (1975); (b) E.M. Kosower and H. Kanety, J. Am. Chem. Soc. 105, 6236 (1983) and references therein.

123. J.R.⁴ Lakowicz, Principles of Fluorescence Spectroscopy, Plenum Press, New York, 1983, Chapter 7.
124. E. von Lippert, Z. Electrochem. 61, 962 (1957).
125. T.R. Griffiths and T.C. Rugh, Coord. Chem. Rev. 29, 129 (1979).
126. K. Dimroth and C. Reichardt, Fortschr. Org. Forsch. 1, 11 (1968); Z.B. Maksimovic, C. Reichardt and A. Spiric, Z. Anal. Chem. 270, 100 (1974).
127. E.M. Kosower, An Introduction to Physical Organic Chemistry, Wiley, New York, 1968, p. 293.
128. M.D. Crenshaw and H. Zimmer, J. Heterocyclic Chem. 21, 623 (1984).